GEOSCIENCE CANADA

JOURNAL OF THE GEOLOGICAL ASSOCIATION OF CANADA
JOURNAL DE L'ASSOCIATION GÉOLOGIQUE DU CANADA

The Tooth of Time: J. O. Wheeler remembered

A Cordilleran Mountain High: Consequences of a hot backarc

Evolving metamorphic core complexes of the Western Grenville Province

Greenstones and granites constrain the Archean World

Book Review: Four Billion Years and Counting…

Educating the educators on mining

2015 VOLUME 42

Publisher/Éditeur
Geological Association of Canada
c/o Department of Earth Sciences
Memorial University of Newfoundland
St. John's NL Canada A1B 3X5
Tel: (709) 864-7660
Fax: (709) 864-2532
gacpub@mun.ca
gac@mun.ca
www.gac.ca

Print Edition: ISSN 0315-0941
Online Edition: ISSN 1911-4850

Volume 42

A journal published quarterly by the Geological Association of Canada, incorporating the Proceedings.
Une revue trimestrielle publiée par l'Association géologique du Canada et qui en diffuse les actes.

Subscriptions: Receiving four issues of Geoscience Canada per year for $50 is one of the benefits of being a GAC member. To obtain institutional subscriptions, please contact Érudit: www.erudit.org

Abonnement: Recevoir quatre numéros par année pour 50,00 $ du magazine Geoscience est l'un des avantages réservés aux membres de l'AGC. Pour les abonnements institutionnels, s'il vous plaît contacter Érudit: www.erudit.org

Those wishing to submit material for publication in Geoscience Canada should refer to the Instructions to Authors on the GAC® Web site, www.gac.ca

AUTHORS PLEASE NOTE:
Please use the web address http://journals.hil.unb.ca/index.php/GC/index for submissions; please do not submit articles directly to the editor.

The Mission of the Geological Association of Canada is to facilitate the scientific well-being and professional development of its members, the learned discussion of geoscience in Canada, and the advancement, dissemination and wise use of geosciences in public, professional and academic life.

Opinions expressed and interpretations presented are those of the authors and do not necessarily reflect those of the editors, publishers and other contributors. Your comments are welcome.

Cover Photo: The photograph, taken in 1981, is in the Cantilever Range of the southeastern Coast Mountains, west of Fraser River, and approximately 15 km SW of Lytton, British Columbia. Boulders in the foreground are of massive, clean granodiorite of latest Cretaceous age (K-Ar ages: Biotite ~64 Ma; Hornblende ~69 Ma). Just south of this locality the granodiorite intrudes highly deformed, greenschist grade rocks of Bridge River terrane and Jurassic–Cretaceous strata of Tyaughton-Methow basin. *Photo credit: Jim Monger.*

COLUMN

The Tooth of Time: J. O. Wheeler

Paul F. Hoffman

1216 Montrose Ave.
Victoria, British Columbia
V8T 2K4, Canada

This year geologists celebrate the bicentenary (1815–2015) of *A Delineation of the Strata of England and Wales, with part of Scotland*, by the English engineer and mineral surveyor, William Smith (1769–1839). Entirely self-motivated, his was not the first geological map ever made, but it was the first one to encompass an entire nation (Sharpe 2015; Sharpe and Torrens 2015). At a scale of five miles to the inch (1:316,800), it was printed on 15 sheets covering 4.68 square metres in all, individually hand-tinted with water-colours so as to show the surface extent of each stratum softly, but its base in sharp relief. Elements of Smith's colour scheme—green in the Cretaceous, blue in the Jurassic, grey in the Carboniferous—gained lasting international adherence. Ironically, there is no indication in Smith's public or private writings that he ever inferred, from the stratigraphic order he established, a depositional sequence in geologic time (Rudwick 2005). No matter, the map itself was transcendent.

This year will also be remembered for the passing of one of Smith's most successful modern map-making descendants, John O. Wheeler (1924–2015). Wheeler's crowning achievements were the *Geological Map of Canada* (Wheeler et al. 1996) and its companion, the *Geologic Map of North America* (Reed et al. 2005). Innovative in their day, they remain unsurpassed by any geological map at the classic scale of 1:5M. Earlier, his *Tectonic Assemblage Map of the Canadian Cordillera* (Wheeler and McFeely 1991) provided a common reference frame for a generation of Cordilleran geologists, analogous to Harold (Hank) Williams' *Tectonic Lithofacies Map of the Appalachian Orogen* (Williams 1978) and Phillip B. (Phil) King's *Tectonic Map of North America* (King 1969). J.O., as he was known, was a Cordilleran geologist first and foremost, based in Vancouver with the Geological Survey of Canada (GSC). But in the 1970s, my first decade with the organization, he was based in Ottawa first as Division Chief and then as Chief Geologist (Deputy Director-General). Soft-spoken and blessed with the happy ability to put anyone at ease, J.O. was especially loved by younger geologists because he habitually lingered around the poster booths at conferences, talking with them about their work. He often sought out junior research staff as sounding-boards for his ideas. J.O. rarely if ever talked about himself, so it was only during my voluntary secondment to the Vancouver office in 1973–74 that I began to piece together the history and background of the man himself. Five years later, he would seek my opinion about a pressing personnel decision. What I told him haunts me still.

J.O. came from a distinguished line of surveyors and mountaineers (Sandford 2006). His paternal grandfather (Fig. 1), the family patriarch in this country Arthur Oliver (A.O.) Wheeler (1860–1945), was author of a landmark monograph on the geography and history of the majestic Selkirk Range (Wheeler 1905), co-founder of the Alpine Club of Canada (ACC) in 1906, and commissioner on the Alberta–British Columbia interprovincial boundary survey (1913–24). Yet, his alpine experience began only at the age of 40.

A.O. Wheeler was raised near historic Kilkenny in the southeastern interior of Ireland, the son of land-owning Anglicans long prominent in the area as clergymen, military officers and political leaders. When A.O. was 16, a crash in food prices forced the family to sell their estates in Ireland and emigrate, to Georgian Bay, Ontario in 1876. Four years earlier, a Kilkenny neighbour, Major William Francis Butler (1838–1910), had published *The Great Lone Land: A Narrative of Travel and Adventure in the North-West of America* (Butler 1872). Having volunteered to collect intelligence about the Red River Métis Rebellion and American settlers pressing northward, Butler met with the Métis leader Louis Riel before guiding the British–Canadian military expedition of 1870 to the Red River settlement, where federal authority was restored. Butler stayed on after the expeditionary force departed and was authorized to travel across the Prairies in winter and report on living conditions in the newly acquired western territory. Reaching Rocky Mountain House in early December, he returned to Upper Fort Garry (Winnipeg) by dog team in mid-February, delivering his report to the Lieutenant-Governor two weeks later. Twelve-year-old A.O. Wheeler was one of the many who were captivated by Butler's sensitive and evocative descriptions of Western Canadian landscapes and people in winter. *The Great Lone Land* went through 19 editions in his lifetime. For A.O., his family's destination of Collingwood, Ontario was a gateway to Western Canada.

Geoscience Canada, v. 42, http://www.dx.doi.org/10.12789/geocanj.2015.42.079 pages 373–382

Figure 1. Arthur Oliver (A.O.) Wheeler, J.O. Wheeler's paternal grandfather, at the Alpine Club of Canada summer camp for 1912 at Vermilion Pass (1680 m), on the continental divide between Banff (Alberta) and Kootenay (British Columbia) national parks. Photograph by botanist Julia Henshaw, from Sandford (2006) courtesy of the Wheeler family.

Young A.O. Wheeler wasted no time. He worked as an apprentice surveyor on the north shore of Lake Huron in 1876 and assisted land surveyor and (later) pioneer forestry conservationist Elihu Stewart (1844–1935) in mapping the Algoma highlands north of Lake Superior by canoe in 1877. In 1878, he accompanied Stewart in a survey of Aboriginal lands around Prince Albert in the District of Saskatchewan of the (then) North West Territories (Sandford 2006). Certain of his calling, he underwent the academic grind required for Dominion Land Surveyors and joined the Department of the Interior in Ottawa in 1881. Not one to miss out on any action, A.O. along with other Dominion Land Surveyors joined the militia force hastily commissioned by the Conservative government of John A. Macdonald in the Spring of 1885 to quell the North West Rebellion of Saskatchewan Métis under Louis Riel, the Red River Resistance leader returned from exile south of the border. At the decisive Battle of Batoche (May 9-12, 1885), A.O. was grazed in the shoulder by a sniper's bullet two days before the Métis stronghold fell. Back in Ottawa, he was soon smitten by a daughter of the Dominion Botanist at GSC, the legendary Irish-Canadian plant collector John Macoun (1831–1920). Recruited by Sanford Fleming to assist in determining the best route across the Prairies for the Canadian Pacific Railway (CPR), Macoun participated in five survey expeditions between 1872 and 1881. Anomalous rainfall during this period caused him to recommend a southern route through Regina and Calgary as being more favourable for agriculture than a northern route through Saskatoon and Edmonton. The decision by CPR to bypass the northern trade route was one of the many grievances that had led to the North West Rebellion. The route chosen would become part of the Prairie dustbowl in the 1930s. Clara Macoun and A.O. Wheeler had one child, Edward (later Sir Edward) Oliver Wheeler, born in Ottawa in 1890.

After a brief fling as a private surveyor in Greater Vancouver, A.O. returned to the Topographical Branch in Ottawa in 1894, conducting topographical surveys of the irrigation lands south of Calgary and the adjacent Crowsnest Pass mining area for six years (Sandford 2006). It was his next assignment that introduced him to the high mountains. Rogers Pass (1330 m above sea level) offers a narrow route through the northern Selkirk Mountains of eastern British Columbia. It was discovered in 1882 at the behest of the CPR, who wished to shortcut the Great Loop of the Columbia River between Golden and Revelstoke. The construction of a rail line two years later was an engineering triumph, but before the first of two tunnels were bored in 1916, rail service had to be suspended in winter because extreme amounts of snow accumulation (~10 m/yr) caused frequent destructive avalanches. In 1899, an avalanche buried 8 people and destroyed the Rogers Pass train station. In response, A.O. was assigned to carry out the first photo-topographic survey of the Pass and its approaches, the Beaver and Illecillewaet river valleys. The photo-topographic method had been developed by Surveyor General Édouard-Gaston Deville (1849–1924) after the CPR line opened the mountains to miners and developers (Thomson 1967). On the westbound train in 1901, A.O. met the famous English mountaineer and author Edward Whymper (1840–1911), who had led the first ascent of the terrifying Matterhorn (Zermat, Switzerland) in 1865 at the cost of four lives. Whymper was in Canada courtesy of the CPR to drum up interest in Alpine tourism in western Canada. At Rogers Pass, A.O. learned climbing technique and culture from Swiss mountain guides hired by the CPR. This enabled him to reach higher stations for photo-topography. It also instilled in him a thirst to climb peaks for pleasure and a growing conviction that the western mountains should be a conscious part of the national identity. During this defining period of his life, A.O. was accompanied every summer on his surveys and many of his climbs by his son, starting in 1899 when the boy (Oliver to his father) was nine years old and continuing until he was twenty.

E.O. combined the strengths of both his parents (Sandford 2006). A strong climber, he was instrumental in establishing the first ACC mountaineering camps. His academic prowess was even more exceptional. He graduated with top honours

from Trinity College private school in Port Hope (Ontario) in 1907, and received the highest grades ever awarded, as well as an unprecedented number of academic and athletics prizes upon graduation from the Royal Military College (RMC) in Kingston (Ontario) in 1910. At the ACC camp that summer, E.O. met the English physician, explorer and mountaineer Tom G. Longstaff (1875–1964), already famous as the first to climb a peak above 7000 m in elevation, Trisul (7120 m) in the western Kumaun (India) Himalaya, in 1907. Together, they traversed Mount Assiniboine (3618 m), the 'Matterhorn of the Rockies,' a 21-hour ordeal that left Longstaff deeply impressed with E.O.'s strength and toughness as a climber (Davis 2012). For E.O., the lure of a region where nearly 100 peaks exceed *twice* the elevation of Mount Assiniboine would prove irresistible.

His performance at RMC qualified him to apply for service in the élite Corps of the Royal Engineers, with the aim of a posting in India. After two years of training in England, he was posted to Dehra Dun, a state capital in the Himalayan foothills north of Delhi and home to many national institutions including the Indian Military Academy and the Survey of India. During his second summer in the country, he hiked into the Gangotri Glacier basin and saw its famous granite towers, the first to appear being Shivling (6543 m), which would not be climbed for another 64 years. It was 1914 and the Great War in Europe was about to begin.

At the age of 24, Major E.O. Wheeler was placed in command of a Company of King George V's Own Bengal Sappers and Miners, attached to the first Indian Division that sailed for France in mid-September, six weeks after war was declared by Britain. Arriving at the Western Front by the end of October, the Company's orders were to protect and reinforce Allied trenches and saps (tunnels or covered trenches directed toward enemy lines), lay and defuse bombs, and destroy whenever possible enemy fortifications, trenches and saps (Davis 2012). The work was done mainly at night under hostile fire. According to dispatches, E.O.'s Indian Company moved to destroy one sap and found it full of enemy soldiers waiting to do the same. Hand-to-hand fighting ensued and when the Germans withdrew, the dead and dying were unceremoniously buried under orders to fill-in the sap. The details will never be known because E.O. never spoke in specifics about his wartime experiences. At one point, E.O.'s parents, who had moved to southern Vancouver Island before the war, heard that their son had been killed in action, just as A.O.'s own parents had been told after the Battle of Batoche (Sandford 2006). E.O. remained in France until late December of 1915, when the shattered Indian Corps was redeployed to Mesopotamia. Out of a total force of 48,000 men, 34,252 had perished including 1,525 officers (over 1,000 British). This at a time when Indian soldiers were not permitted to dine with other imperial troops or to be medically treated by white nurses (Davis 2012). For bravery and distinguished military service, E.O. was awarded the cross of the French Légion d'honneur (Chevalier 5th Class).

The remains of the Indian Corps arrived in Mesopotamia at a bad time. In late 1915, the 2nd (Poona) Division of Indian troops under British command had rashly attempted to extend their control northward to Baghdad from a stronghold in the southern oilfields near Basrah. They were repulsed by Turkish forces outside the capital and had retreated to Kut-al-Amara, where they were under siege without secure lines of supply. Buoyed by news of victory at Gallipoli, the Turks were pressing their advantage. In the early months of 1916, the Indian Corps diverted from France attempted without success to relieve the embattled garrison at Kut, which fell to the Turks on the 29th of April. E.O. was mentioned seven times in dispatches during the campaign and was awarded the Military Cross. In June, 1916, he collapsed with typhoid fever and was invalided back to India for over a year, returning to duty in Mesopotamia in the Fall of 1917, after the British had finally seized control of Baghdad. At war's end, the collapse of the Ottoman Empire created a power vacuum in Mesopotamia which the British intended to fill with the creation of modern Iraq. As part of this effort, E.O. was ordered to conduct a strategic reconnaissance of the potentially hostile Kurdish region around Sulaymaniyah in the mountainous northeast of the country. After completing this assignment, he returned to India in January 1919 as Brevet Major on the General Staff, before being seconded to the Survey of India in December of that year. He visited his parents in Canada for the first time in eight years in 1920 (Fig. 2), a man older than his 30 years but one lucky to still be alive.

E.O. returned to India from Canada in 1920 by way of England, hearing that Tom Longstaff's brother-in-law had died in action leaving Tom's sister Kate a widow with three children. All four had climbed together at Mount Assiniboine in 1910. As it turned out, Kate had arranged for E.O. to meet

Figure 2. Edward Oliver (E.O.) Wheeler (left) with his parents, Clara (Macoun) and Arthur (A.O.) Wheeler, at Banff in the summer of 1920. This was his only visit to Canada following military service in France and Mesopotamia during World War I, and before his marriage and participation in the British Everest Expedition of 1921. Photograph from Sandford (2006) courtesy of the Wheeler family.

a friend of hers who shared his enjoyment of tennis, golf and dancing (Sanford 2006). Five days later, E.O. was engaged to Dorothea (Dolly) Danielsen, whom he would marry in late March 1921 in Bombay. Simultaneously, Tom Longstaff's recommendation led to an invitation for E.O. to join the British Everest reconnaissance expedition of 1921 as a high-altitude surveyor, to map a 500 km^2 area centred on Mount Everest (8848 m) itself, using the Canadian photo-topographic method he had learned from his father. The expedition would depart on the 2700-km-long trek to the foot of Everest from Darjeeling on the 1st of May (Davis 2012). His honeymoon with Dolly would be a short one.

The British Everest expeditions of 1921, 1922 and 1924 were historic for many reasons, not all related to climbing. The strangeness of the post-war period as well as the gripping story of the expeditions and their personnel are brilliantly captured in Wade Davis' book, *Into the Silence* (Davis 2012). The expedition sponsors, the Royal Geographical Society (London) and their financial backers were of one mind: a British triumph of the human spirit was desperately needed to restore a sense of national purpose after the pointless slaughter of the Trench War. At the same time, an unbridgeable chasm existed across society between those who had witnessed the unspeakable carnage and those who had not. For those of my age, growing up 25 years later, the mere mention of mountains instantly conjured up an image of George Mallory and Sandy Irvine, seen momentarily through the swirling clouds and blowing snow, moving upward, high but late on the Northeast Ridge of Everest. It will never be known if they reached the summit. Mallory's body was found on the North Face in 1999, with rope trauma indicating that he and Irvine were roped together when they fell.

The 1921 expedition would be exploratory: Everest (8848 m), the highest mountain relative to sea level in the world, had been sighted and surveyed from a distance in 1856 during the Great Trigonometrical Survey of India (Molnar 1986; Keay 2001), but no Westerner had been closer than 60 km from the mountain, not least because Nepal to the south was closed to outsiders, requiring an approach from the north through Tibet (Fig. 3). The British government, for its part, quietly reversed a longstanding policy against arming the Tibetan government in order to gain consent for the expedition from the Dalai Lama (Bell 1924).

For the climbers (Fig. 4), the topographical survey was somewhat peripheral to the main thrust of the expedition, but during its 5.5 month duration no one was longer at high elevation nor more continuously exposed to the elements than Wheeler and his Tibetan assistants (Fig. 5), Gorang, Lagay and Ang Pasang (Davis 2012). Isolated from the main party for three months, they spent 41 days between 5500 and 6800 m in elevation, hauling 60 kg of equipment to high vantage points every morning, hoping for the one day in six that was clear and calm enough for photo-topography. In all, they obtained 240 images from precisely triangulated positions, from which a preliminary 1:100,000-scale topographic map was produced covering 730 km^2 to the north, west and east of Everest itself (Fig. 6). A month after climbers George Mallory and Guy Bullock had ascended the Rongbuk Glacier (Fig. 7), finding an unclimbable headwall on North Face of Everest, E.O. discovered that a seemingly unimportant meltwater tributary (Fig. 8) drained a hidden glacier, the East Rongbuk Glacier, that curled southward toward Everest. The source of this glacier (Fig. 9) was a climbable headwall to the North Col (Chang La) between Everest and Changtse (North Peak). The North Col itself was finally reached via the Kharta Glacier on September 25 by Mallory, Bullock, Wheeler and his three seasoned assistants. Mallory deemed the spur from the Col to the Northeast Ridge (Fig. 10) to be potentially doable in better weather (Mallory 1922). The 1921 expedition had achieved its main objective, to ascertain a route to the summit of Everest. Although Wheeler was not credited in expedition accounts (Howard-Bury 1922; Mallory 1922) as its discoverer, the East Rongbuk

Figure 3. Mount Everest (8848 m) from the north, at a distance of ~63 km and an elevation ~4500 m on the Tibetan Plateau near the village of Tingri. This was the closest any Westerner had come to Everest before 1921. The Northeast Ridge slopes down to the left of the summit. The spur projecting northward toward the camera from the Northeast shoulder descends to the North Col (Chang La), which is out of sight behind the peak of Changtse (4868 m), only the top of which is visible in front of the North East Ridge. The dark coloured rocks in the middle ground are folded Jurassic shales with tight synclines of Cretaceous and Eocene limestone (Heron 1922; Gansser 1964). The Mount Everest massif is composed mainly of Cambrian and Ordovician metasedimentary rocks (Myrow et al. 2009), exhumed in response to north-dipping extensional faulting (South Tibetan Detachment) of Early Miocene age (Burg et al. 1984; Burchfiel and Royden 1985). Photograph taken by Joe Hastings (1900 hr, 13 May 2007).

Figure 4. Members of the 1921 Mount Everest Expedition. Standing (left to right): Guy Bullock, Henry Morshead (surveyor), Oliver (E.O.) Wheeler (high-altitude surveyor) and George Mallory (lead climber). Seated (left to right): A.M. Heron (geologist), Sandy Wollaston, Charles Howard-Bury (expedition chief) and Harold Raeburn. Photograph by Sandy Wollaston courtesy of the Royal Geographical Society.

Figure 5. E.O. Wheeler and two of his three Tibetan assistants: Gorang, Lagay and Ang Pasang. Using a Canadian-designed photo-topographical survey camera with 12 x 17 cm plates, Wheeler took 240 single images and panoramas of the northern, western and eastern approaches to Everest, from which the first accurate topographical map of the area was constructed (Fig. 6). The technique required clear and relatively calm conditions, seldom encountered at elevations above 5000 m (wrt sea level) where the team worked for long periods. Photograph in 1921 by Sandy Wollaston courtesy of the Royal Geographical Society.

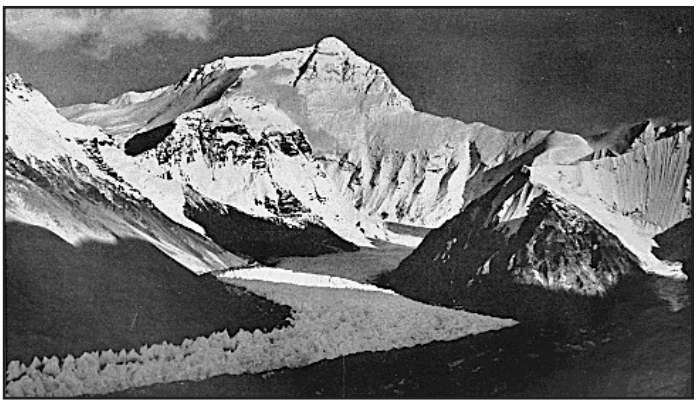

Figure 7. Mount Everest from a distance of 14.5 km on the west side of the Rongbuk valley near the confluence of the Rongbuk and West Rongbuk (hidden, lower right) glaciers. Changtse (4868 m) is the peak in front of and to the left of Everest, to which it is connected by the North Col (Chang La), the only feasible route to the summit of Everest from the north. The ascent to the North Col from the west, via the Rongbuk Glacier (foreground), was deemed to be too difficult on inspection. Photograph in 1921 by George Mallory courtesy of the Royal Geographical Society.

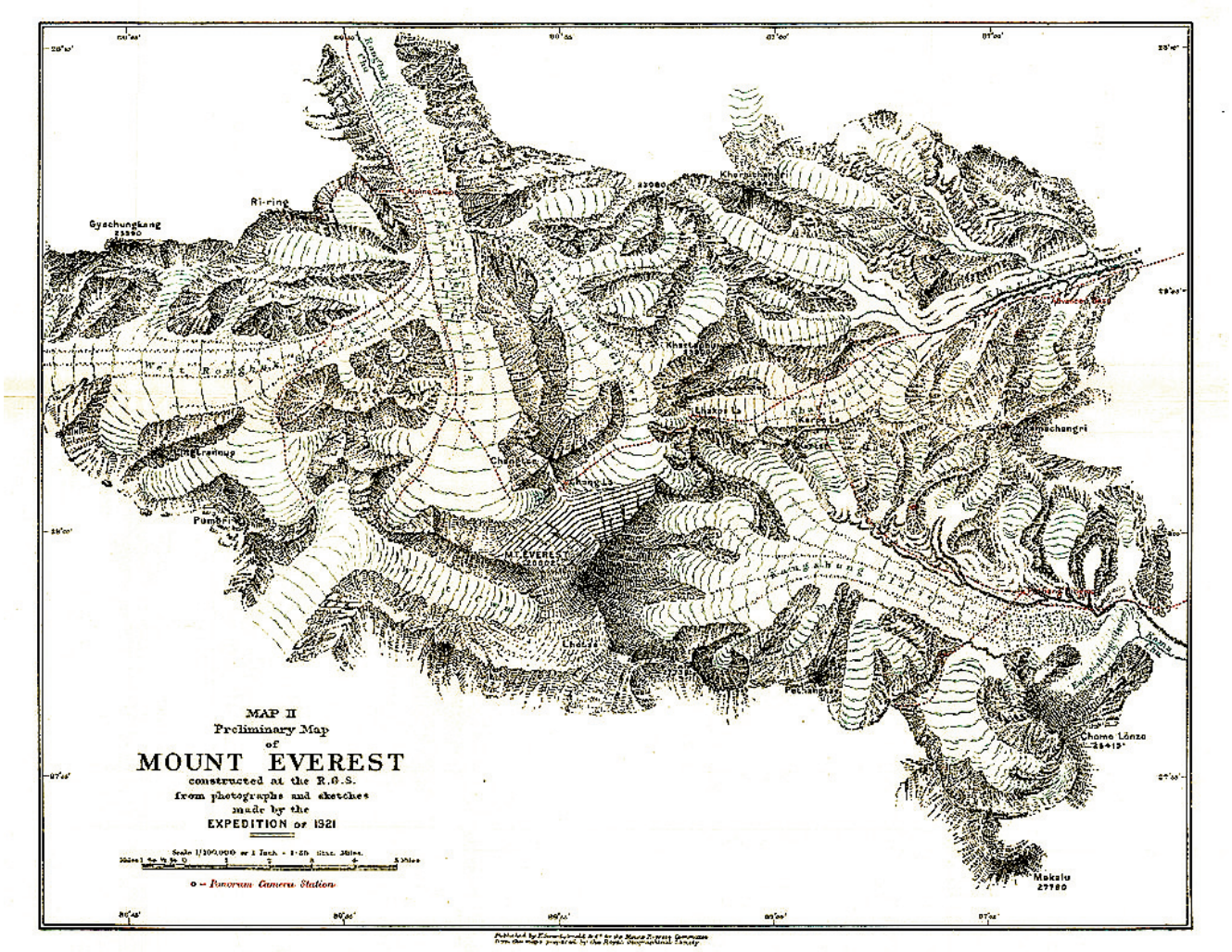

Figure 6. Preliminary Map of Mount Everest constructed at the Royal Geographical Society from photographs and sketches made by the Expedition of 1921 (Howard-Bury 1922). At a scale of 1:100,000, the map was a product of E.O. Wheeler's three-month photo-topographical survey (Davis 2012). Routes taken by the climbers during the 1921 expedition are indicated in red.

Figure 8. Meltwater drainage outlet from the East Rongbuk Glacier (hidden) onto the Rongbuk Glacier, viewed from the same location as in Figure 7. At this spot on July 5th, 1921, Mallory with Guy Bullock decided that the North Col could not be reached from the Rongbuk valley, assuming the drainage outlet shown here did not head southward toward Everest. As a result, the expedition redirected its effort to the east, via the Kharta Glacier and Windy Gap (Lhakpa La). On August 3rd, however, E.O. Wheeler in the course of his topographical survey ascended the drainage outlet and discovered the East Rongbuk Glacier as a direct route to the North Col. The significance of Wheeler's discovery was never acknowledged in expedition reports (Howard-Bury 1922; Mallory 1922). Photograph in 1921 by George Mallory courtesy of the Royal Geographical Society.

Figure 9. Headwall of the East Rongbuk Glacier, viewed from 5.5 km to the northeast at Windy Gap (Lhakpa La). The North Col (Chang La) is on the right, from which a climbable spur (Fig. 10) leads up to the shoulder of the Northeast Ridge of Everest. This was the route used in the summit attempts of 1922 and 1924. In early June, 1922, an avalanche below the North Col killed seven Sherpa porters, out of respect for whom the final expedition was delayed for a year. Photograph in 1921 by Charles Howard-Bury courtesy of the Royal Geographical Society.

Glacier was the key to the mountain from the north. It was the route used for the summit attempts of 1922 and 1924, and all subsequent Everest expeditions before 1938.

After the 1921 Everest expedition, E.O. returned to the Survey of India. In 1924 he was put in charge of the Northern Survey, based at the hilltop resort town of Mussoorie on the outskirts of Dehra Dun (Sandford 2006). It was there that Dolly and E.O.'s son John (J.O.) was born on 19 December 1924 (Fig. 11). Had they stayed, J.O. would have learned that Mussoorie lies within a doubly-plunging syncline of Ediacaran and Cambrian sedimentary rocks (Krol and Tal groups), at the base of which is a Cryogenian glacial diamictite (Blaini Formation) with a diagnostic Marinoan (635 Ma) 'cap dolomite' (Brookfield 1987; Jiang et al. 2003). The family moved, however, to Quetta in 1926, when E.O. was put in charge of the Western Survey (now Pakistan). In 1933, 8-year-old J.O. was enrolled at the Shawnigan Lake School on southern Vancouver Island (Fig. 12), where he would spend summers hiking with his grandfather who had remarried after Clara Wheeler's death the year before J.O. was born. J.O.'s father meanwhile would

Figure 10. Route to the Northeast Ridge from the North Col (lower left). The summit of Everest can be seen beyond the Ridge. The North Col (Chang La) was reached at the end of the climbing season (September 25) in 1921, but poor weather prevented further ascent. The route was used in the summit attempts of 1922 and 1924. Photograph in 1921 by George Mallory courtesy of the Royal Geographical Society.

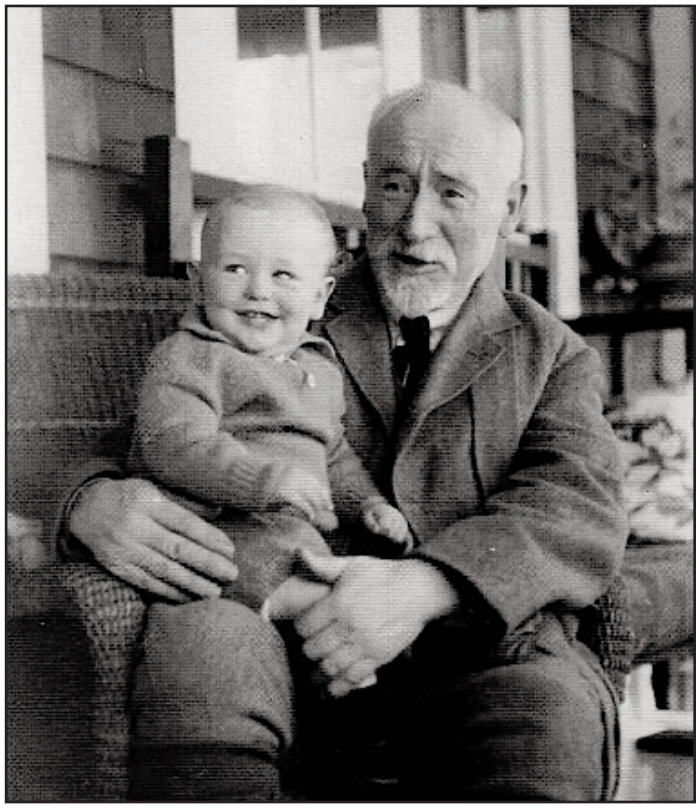

Figure 11. Arthur (A.O.) Wheeler and his only grandson, John (J.O.), aged one and a half, on his first visit to Canada in 1926. Photograph from Sandford (2006) courtesy of the Wheeler family.

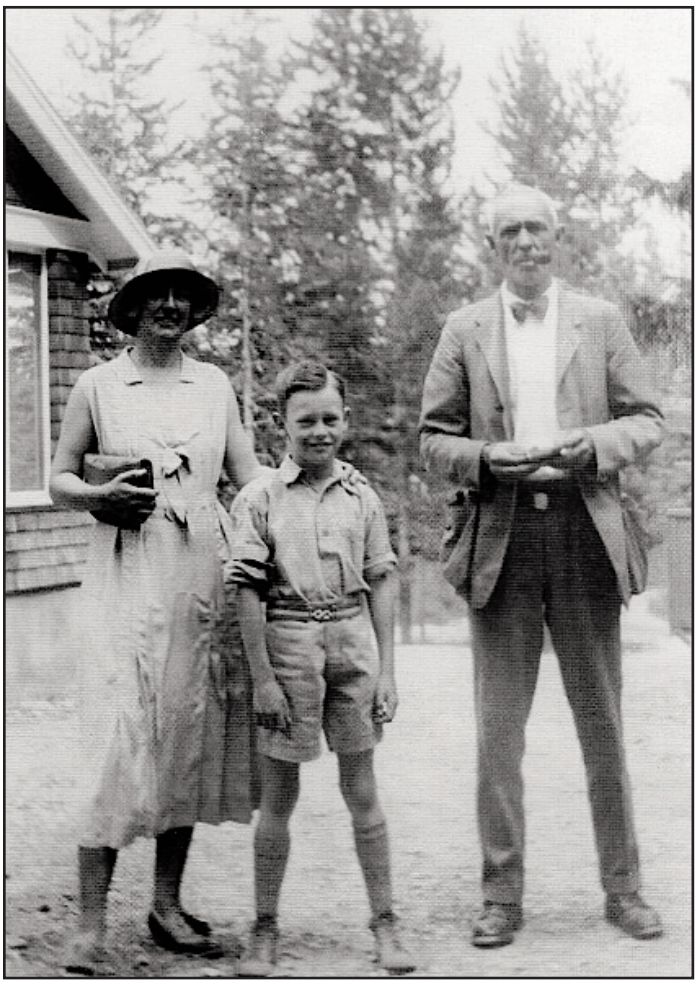

Figure 12. Eight year old John (J.O.) Wheeler with his parents, Dorothea (Dolly) Danielsen and Oliver (E.O.) Wheeler, at Banff prior to his parents' departure for India in August, 1933. J.O. was about to be enrolled at the Shawnigan Lake School on southern Vancouver Island. Photograph from Sandford (2006) courtesy of the Wheeler family.

soon move to Shillong to head the Eastern Survey, before being seconded to Calcutta in 1934 as Assistant Surveyor General, then Director of the Geodetic Branch, and finally Surveyor General of India in 1941. On his watch, the Survey ramped up production of topographical maps (to 20,000 a year) in response to the military threat posed by the Japanese occupation of British colonial Burma in 1942. Credited with helping to stave off a Japanese invasion of eastern India, E.O. Wheeler was knighted in 1943. After retiring from the Survey in 1947, he and Dolly moved to British Columbia, where they lived near Vernon in the Okanagan region. He served as President of the ACC (1950–54), the organization he had helped his father create as a teenager. He died in Vernon in 1962 following a stroke.

J.O. saw his parents only intermittently during his nine years at Shawnigan Lake School (1933–42) and four years at the University of British Columbia (UBC) in Vancouver (1943–47), where he graduated in geological engineering, with the encouragement of his grandparents, the year his parents returned from India (Sandford 2006). Like his father, J.O. was a gifted athlete and climber, and he worked for exceptional men as a student assistant with GSC for three summers. In southwestern Yukon, he assisted Hugh S. Bostock (1901–94), the 'father of Yukon geology' and grandfather of current UBC seismologist Michael Bostock. In the Omineca Mountains of northern British Columbia, he assisted his near-contemporary Fred Roots (1923–), who would soon be senior geologist on the first multi-national (Norwegian–British–Swedish) Antarctic Expedition (1949–52), later co-leader and leader respectively of major GSC projects in the High Arctic (Operation Franklin 1955) and northern Cordillera (Operation Stikine, 1956–58), and founding coordinator of the Polar Continental Shelf Project (1958–71).

J.O.'s PhD thesis project at Columbia University was on the geology of the Whitehorse (1:125,000 scale) map-area of southern Yukon, a project begun by Quaternary geologist John G. Fyles (1923–2005) and completed by J.O. during the summers of 1948–51 (Wheeler 1952). J.O. joined the permanent staff of GSC in Vancouver in 1951 (Zaslow 1975), but completion of his thesis was delayed by two new GSC projects for which very few were qualified in terms of strength, experience and temperament. The first was a geological reconnaissance of the remote northern Selwyn Mountains of eastern Yukon in 1952. Embarking soon after his marriage to Nora Jean Hughes in Vancouver, this four-month 800-km long expedition was described by no less than Hugh Bostock as *"perhaps the longest and loneliest packhorse journey for the Survey ever in the Yukon if not anywhere in the Cordillera"* (Bostock 1990). The second project, even more challenging physically, involved geological mapping in the heavily glaciated eastern St. Elias Mountains of southwestern Yukon in 1953–55. By the time of his thesis defence in 1956, J.O. had logged 10 long field seasons in the northern Canadian Cordillera, at a time when camp moves were done by packhorse train.

Over the next 13 years (1956–69), J.O. would devote another 10 field seasons to geological mapping, split between the southern Yukon and eastern British Columbia (Sandford 2006). He became Head of the Cordillera and Pacific Margin Section of GSC in Vancouver in 1967, by which time he was personally familiar with both the eastern and western Cordilleras, in the Yukon and in British Columbia. The geographical range of his knowledge was vital because a transect approach at the scale of the orogen is unrewarding (or worse) in the Canadian Cordillera due to large-magnitude, orogen-parallel, strike-slip faults, the displacement histories of which remain controversial. Jack Oliver (1923–2011), the Columbia (later Cornell) University seismologist who tested the transform fault concept as a corollory of sea-floor spreading (Isacks et al. 1968), used to joke that the challenge in geophysics is *analysis*, because data are too few, whereas the challenge in geology is *synthesis*, because data are too many (Oliver 1996).

In 1969, GSC had the foresight to send five of its Vancouver-based geologists (Hu Gabrielse, Bill Hutchison, Jim Roddick, Jack Souther and John Wheeler) to the 2nd Penrose Conference at Asilomar (California) on *"The Meaning of the New Global Tectonics for Geology*," convened by William R. (Bill) Dickinson (1931–2015). Out of the blue, a vision had arisen that unified the major features of the Earth's crust—passive and active continental margins, oceanic trenches and ridges, great faults, volcanic arcs and rifts—a vision that validated continental drift and provided an entirely new way of interpreting orogenic systems like the North and South American

Cordilleras. This was not a paradigm shift as envisioned by Thomas Kuhn (1922–1996), one that resolved a growing crisis of confidence in existing theory (Kuhn 1962), for no sense of crisis existed in geology or geophysics before the plate tectonics revolution. Only afterwards was it apparent that we had been stuck in neutral. Given the potential to interpret the Cordillera genetically for the first time, it cannot have been easy for J.O. to accept a senior management position in 1970 (Fig. 13), and one so far from an active plate boundary as Ottawa.

J.O.'s decade in Ottawa (1970–79) was one in which I lay low. Having identified the Coronation 'geosyncline' as a 1.9 Ga west-facing rifted continental margin, from reconnaissance (Fraser et al. 1971), taking the next step—determining how the margin had been destroyed—required six seasons of 1:250,000-scale mapping, first in the Great Bear magmatic zone assisted by Ian Bell, Mike Cecile and Rein Tirrul, and then in the Hepburn metamorphic-plutonic belt assisted by Mike Easton and Marc St-Onge. Moreover, I was away from Ottawa for half the years that J.O. was there.

At a conference in 1980, J.O. came over after my talk and asked if he could have a word with me privately, in his hotel room the next morning. I hadn't the slightest idea why he wanted to see me, except that it wouldn't be about my talk. When I came to his room, he motioned for me to sit down and, perfunctories exchanged, asked me point-blank what I thought about promoting John McGlynn, then a Section Head and my longtime mentor at GSC, to Chief of the Precambrian Division. GSC at this time had a 'flat' management structure. Division Chief was the key operational position: Division Chiefs did the hiring and set the programs and budgets. They reported directly to the Director General, and because there were many Divisions, each Chief had considerable autonomy.

John C. McGlynn (1926–99) had joined GSC in 1950 with a PhD in geology from the University of Chicago. He had been Resident Geologist in Yellowknife before I worked as his field assistant, in 1963 on the medial zone of Wopmay orogen and 1965 on the Nonacho basin of the Rae craton. It was through his recommendation that my thesis proposal for a sedimentological study of the Great Slave Supergroup was approved and funded by GSC. It was at the home of John, his wife Lillian (MacDougal) and their four sons that I stayed on my frequent visits to Ottawa as a graduate student in Baltimore, and where I enjoyed many a Sunday dinner after I moved to Ottawa. It was there also that I met my future wife, Jean (Erica) Westbrook.

Of Irish descent from London (Ontario), John McGlynn was funny and irreverent. A Trudeau Liberal (*"Alberta in fact did well by his oil pricing policy*."), he was fascinated by politics and politicians. He was attracted to exceptional people, his then ongoing collaboration with geologist-paleomagnetist Edward (Ted) Irving (1927–2014) being a fruitful example (Fig. 14). He was a gifted story teller who relished the absurdities of life, but he was also a magnetic listener (Fig. 15), a person people opened themselves up to. I loved John like a father, but in my innocence I had doubts about his suitability as a Division Chief. He was a nervous type, and most of his normal day was spent chatting with people around the office. When it came to writing, he didn't have a lot to show for 30 years at GSC. I was afraid he would be crushed by the job, and that's what I told J.O.

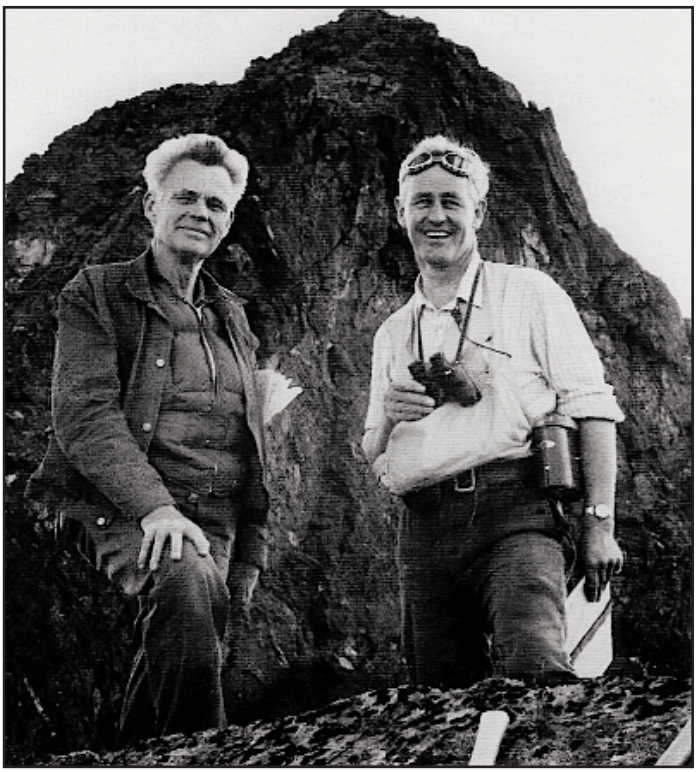

Figure 13. Appalachian structural geologist John Rodgers (1914–2004) of Yale University, President of the Geological Society of America, and John (J.O.) Wheeler (1924–2015), President-Elect of the Geological Survey of Canada, in Mount Revelstoke National Park, August 1970. Photograph from Sandford (2006) courtesy of the Wheeler family.

Figure 14. John McGlynn (left) and Edward (Ted) Irving, drilling paleomagnetic samples on the Slave craton in 1973. In the 1950's, Irving was the first geologist to demonstrate continental drift paleomagnetically (Irving 1956; Frankel 2012, 2014), thereby setting the stage for the New Global Tectonics (aka plate tectonics) of the 1960's. In the 1970's, Irving directed most of his research to paleomagnetic studies in the Canadian Shield, and McGlynn was his most frequent collaborator. GSC photograph courtesy of Lillian McGlynn.

I never heard anything more about it for several months, when it was officially announced that John McGlynn would

Figure 15. Edward (Ted) Irving (second from left) and John McGlynn (right), planning sampling strategy for Paleoproterozoic mafic dykes on Slave craton, at a GSC camp on Indin Lake (NWT) in 1973. Assistant geologists Rosaline Goodz (left) and unidentified (second from right) listen in. Mafic dykes are excellent targets for paleomagnetism, but in the 1970's they could not be accurately or precisely dated radiometrically. GSC photograph courtesy of Lillian McGlynn.

replace Ira Stevenson, then (acting) Division Chief, a position he would hold with distinction until GSC was restructured in 1987. John turned out to be a brilliant research manager and the Division flourished under Directors General Bill Hutchison and Ray Price. Among the geologists John McGlynn hired were Jean Bédard, Rob Berman, Simon Hanmer, Robert Hildebrand, Janet King, Bruce Kjarsgard, Steve Lucas, Randy Parrish, John Percival, Tony Peterson, Chris Roddick, Marc St-Onge, Rein Tirrul, Otto van Breemen, Cees van Staal and Joe Whalen. John was shrewd as a manager. Never one to suppress freedom of expression normally, he absolutely forbade any negative talk by us at periodic weekend 'retreats,' where GSC senior managers met with research scientists from every Division. Senior management got the impression that we were a pretty agreeable and positive bunch. Meanwhile, other Division Chiefs would often confide in John (chronically underestimated) their plans to outmaneuver their main competitors. In politics as in poker, it helps to know the others' cards in advance. As Division Chief, John created the strictly unofficial positions of Division geophysicist (seismologist Alan G. Green) and geologist (me). We were to advise him on technical matters and recruitment. He would of course have sought our views in any case, as he did nearly everyone's. More often than not, John did not follow my advice (I can't speak for Alan), but most others thought he did. Those who didn't agree with his decisions tended to blame me or Alan for them, which didn't bother either of us in the slightest.

During John's tenure as Chief, a state-of-the-art U–Pb geochronology facility was established in the Division by Otto van Breemen, Chris Roddick and Randy Parrish. LITHOPROBE, the multidisciplinary brainchild of J.O., who chaired its first steering committee, was established in 1984 with major involvement by Division scientists. Arguably John's greatest achievement was the smooth merger of the Earth Physics Branch with GSC in 1986. This was a potentially explosive situation in which, in effect, Earth Physics was demoted from an independent Branch to a Section within his Division. Doubtless, John's earlier successful collaboration with Ted Irving gave Earth Physics Branch scientists reassurance. In 1987, GSC was one of the few geological surveys in the world that was far stronger than it had been a decade earlier, fully able to take advantage of the conceptual breakthroughs of the New Global Tectonics.

I have often thought about my meeting with J.O. in his hotel room 35 years ago. I think about how J.O. saw in John McGlynn what I did not. I have tried to learn from his example, to see a person for what they *could* do, rather than what they could not.

There is a revealing passage in Wade Davis' book (Davis 2012) on the Mallory expeditions to Everest. Davis describes interviewing J.O. in Vancouver in 2000 (Fig. 16), noting that his own father had attended Shawnigan Lake School on Vancouver Island around the time that J.O. did, and that he (Wade) had climbed several peaks in the Yukon first surveyed by J.O. *"We met for a long afternoon,"* he writes, *"at the end of which he produced a remarkable treasure. According to Everest historians, only Guy Bullock kept a complete journal during the 1921 expedition, curt notes that were published in two parts in the Alpine Journal* [in 1962]. *Mallory wrote letters and Howard-Bury official dispatches, but neither kept a daily account. E.O. Wheeler, as it turned out, did—two complete volumes that had never been seen by anyone outside of his immediate family."*

Figure 16. Nora Jean (Hughes) and John (J.O.) Wheeler with their dog Mike on a hiking trip in the Rockies. Undated photograph from Sandford (2006) courtesy of the Wheeler family.

"I was so astonished," Davis continues, *"that I could not bring myself to ask that they be copied. But as we departed late in the day, John Wheeler handed me the two journals, saying simply that he thought I would find them useful*."

It is so characteristic of J.O. that I suspect it was at his insistence that the reader only learns of this exchange on page 584, well into the Annotated Bibliography.

REFERENCES

Bell, Sir C., 1924, The Dalai Lama; Lhasa, 1921: Journal of the Royal Central Asian Society, v. 11, p. 36–50, http://dx.doi.org/10.1080/03068372408724858.

Bostock, H.S., 1990, Pack Horse Tracks: Yukon Geoscience Forum, Whitehorse, YT, 313 p.

Brookfield, M.E., 1987, Lithostratigraphic correlation of Blaini Formation (late Proterozoic, Lesser Himalaya, India) with other late Proterozoic tillite sequences: Geologische Rundschau, v. 76, p. 477–484, http://dx.doi.org/10.1007/BF01821087.

Burchfiel, B.C., and Royden, L.H., 1985, Noth-south extension within the convergent Himalayan region: Geology, v. 13, p. 679–682, http://dx.doi.org/10.1130/0091-7613(1985)13<679:NEWTCH>2.0.CO;2.

Burg, J.P., Brunel, M., Gapais, D., Chen, G.M., and Liu, G.H., 1984, Deformation of leucogranites of the crystalline Main Central Sheet in southern Tibet (China): Journal of Structural Geology, v. 6, p. 535–542.

Butler, W.F., 1872, The Great Lone Land, a Narrative of Travel and Adventure in the North-West of America: Sampson Low, Marston, Low & Searle, London, 388 p.

Davis, W., 2012, Into the Silence, the Great War, Mallory, and the Conquest of Everest: Vintage Books, New York, 655 p., ISBN: 978-0-375-70815-2.

Frankel, H.R., 2012, The Continental Drift Controversy, Volume 2: Paleomagnetism and Confirmation of Drift: Cambridge University Press, 525 p.

Frankel, H.R., 2014, Edward Irving's palaeomagnetic evidence for continental drift (1956): Episodes, v. 37, p. 59–70.

Fraser, J.A., Hoffman, P.F., Irvine, T.N., and Mursky, G., 1971, The Bear Province, *in* Price, R.A., and Douglas, R.J.W., *eds.*, Variations in Tectonic Styles in Canada: Geological Association of Canada, Special Publication 11, p. 453–504.

Gansser, A., 1964, Geology of the Himalayas: Interscience (John Wiley & Sons), New York, 289 p., with geological map (scale 1:2M) and sections.

Heron, A.M., 1922, Geological results of the Mount Everest Expedition, 1921: The Geographical Journal, v. 59, p. 418–431, http://dx.doi.org/10.2307/1780634.

Howard-Bury, C.K., 1922, The Mount Everest Expedition: The Geographical Journal, v. 59, p. 81–99, http://dx.doi.org/10.2307/1781386.

Irving, E., 1956, Palaeomagnetic and palaeoclimatatological aspects of polar wandering: Geofisica Pura e Applicata, v. 33, p. 23–41, http://dx.doi.org/10.1007/BF02629944.

Isacks, B., Oliver, J., and Sykes, L.R., 1968, Seismology and the new global tectonics: Journal of Geophysical Research, v. 73, p. 5855–5899, http://dx.doi.org/10.1029/JB073i018p05855.

Jiang Ganqing, Sohl, L.E., and Christie-Blick, N., 2003, Neoproterozoic stratigraphic comparison of the Lesser Himalaya (India) and Yangtze block (south China): Paleogeographic implications: Geology, v. 31, p. 917–920, http://dx.doi.org/10.1130/G19790.1.

Keay, J., 2001, The Great Arc, the Dramatic Tale of How India was Mapped and Everest was Named: Perennial (HarperCollins), New York, 182 p., ISBN: 0-06-093295-3.

King, P.B., *compiler*, 1969, Tectonic map of North America: United States Geological Survey, Washington, scale: 1:5M.

Kuhn, T., 1962, The Structure of Scientific Revolutions: University of Chicago Press, 172 p.

Mallory, G.L., 1922, Mount Everest: The reconnaissance: The Geographical Journal, v. 59, p. 100–109, http://www.jstor.org/stable/1781387, http://dx.doi.org/10.2307/1781387.

Molnar, P., 1986, The structure of mountain ranges: Scientific American, v. 255, p. 70–79, http://dx.doi.org/10.1038/scientificamerican0786-70.

Myrow, P.M., Hughes, N.C., Searle, M.P., Fanning, C.M., Peng, S.-C., Parcha, S.K., 2009, Stratigraphic correlation of Cambrian–Ordovician deposits along the Himalaya: Implications for the age and nature of rocks in the Mount Everest region: Geological Society of America Bulletin, v. 121, p. 323–332, http://dx.doi.org/10.1130/B26384.1.

Oliver, J., 1996, Shocks and Rocks, Seismology in the Plate Tectonics Revolution: American Geophysical Union, Special Publications, v. 6, 5899 p., http://dx.doi.org/10.1029/SP043.

Reed, Jr., J.C., Wheeler, J.O., and Thucholke, B.E., 2005, Geologic Map of North America: Geological Society of America, Boulder, scale: 1:5M.

Rudwick, M.J.S., 2005, Bursting the Limits of Time, the Reconstruction of Geohistory in the Age of Revolution: University of Chicago Press, 708 p., http://dx.doi.org/10.7208/chicago/9780226731148.001.0001.

Sandford, R.W., 2006, Among the Great Hills, Three Generations of Wheelers and Their Contribution to the Mapping of Mountains: The Alpine Club of Canada, Canmore, Alberta, 32 p., ISBN: 0-920330-54-1.

Sharpe, T., 2015, The birth of the geological map: Science, v. 347, p. 230–232, http://dx.doi.org/10.1126/science.aaa2330.

Sharpe, T., and Torrens, H., 2015, Introduction to *A Memoir to the Map and Delineation of the Strata of England and Wales, with part of Scotland* by William Smith: Geological Society, London, 26 p.

Thomson, D.W., 1967, Men and Meridians, the History of Surveying and Mapping in Canada, Volume 2, 1867 to 1917: Queen's Printer, Ottawa, 342 p.

Wheeler, A.O., 1905, The Selkirk Range: Government Printing Bureau, Department of the Interior, Ottawa, 459 p.

Wheeler, J.O., 1952, Geology and mineral deposits of Whitehorse map-area, Yukon Territory (preliminary account): Geological Survey of Canada, Paper 52-30, 16 p. and map, scale: one inch to two miles.

Wheeler, J.O., Hoffman, P.F., Card, K.D., Davison, A., Sandford, B.V., Okulitch, A.V., and Roest, W.R., *compilers*, 1996, Geological Map of Canada/Carte Géologique du Canada: Geological Survey of Canada, Map 1860, scale: 1:5M.

Wheeler, J.O., and McFeely, P., 1991, Tectonic assemblage map of the Canadian Cordillera: Geological Survey of Canada, Map 1712A, scale: 1:2M.

Williams, H., 1978, Tectonic lithofacies map of the Appalachian Orogen: Memorial University of Newfoundland, St. John's, scale: 1:1M.

Zaslow, M., 1975, Reading the Rocks, the Story of the Geological Survey of Canada, 1842–1972: Macmillon (Canada), Toronto, 509 p., ISBN: 0-7705-1303-4.

ACKNOWLEDGEMENTS

I am endebted to R.W. (Bob) Sandford and Wade Davis for most of the information contained in this article. I thank Jim Monger for his *"Personal perspective on some GSC Vancouver office history,"* Chris Yorath for encouraging me to write the article, Tony LeCheminant and Robert Hildebrand for the chronology of GSC management changes, Hildebrand and Brendan Murphy for editorial suggestions, and Carol Evenchick, Hu Gabrielse and Roger Macqueen for the opportunity to see J.O. for the last time in January 2015.

CORRECTION

In my column on James Smith (Geoscience Canada, 2015, v. 42(1), p. 7–26), I intimated that Charles Darwin was the only English-speaking geologist who seriously referred to Jens Esmark's 1826 glacial theory during the glacial controversy of 1837 to 1865. Although not strictly a geologist, glaciologist James David Forbes discussed Esmark's theory with approval in his book, *Norway and Its Glaciers, Visited in 1851*, published in 1853 in Edinburgh. Forbes is the subject of an exceptionally erudite biography written by former Simon Fraser University historian, Frank F. Cunningham. *James David Forbes, Pioneer Scottish Glaciologist* was published in 1990 by Scottish Academic Press, Edinburgh.

ANDREW HYNES SERIES: TECTONIC PROCESSES

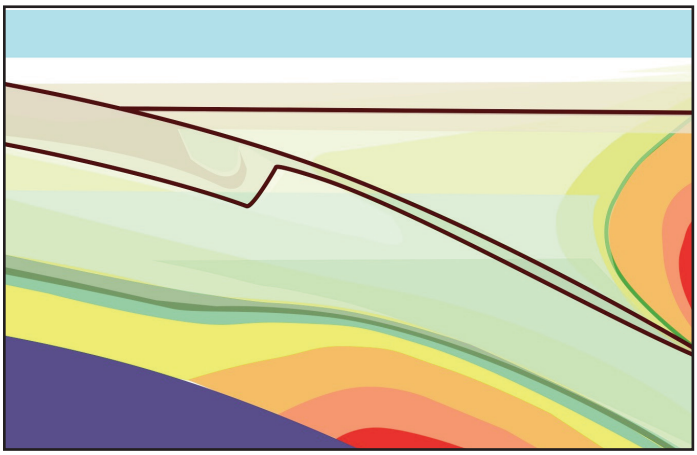

Tectonic Consequences of a Uniformly Hot Backarc and Why is the Cordilleran Mountain Belt High?

R.D. Hyndman

Pacific Geoscience Centre, Geological Survey of Canada and
School of Earth and Ocean Sciences
University of Victoria
9860 W. Saanich Road, Sidney
British Columbia, V8L 4B2, Canada
Email: rhyndman@nrcan.gc.ca

SUMMARY

Why is the North American Cordilleran mountain belt high? We expect a thick crust to support high elevations by isostasy but, remarkably, the Cordilleran crust is thin. There is no crustal root. An important recent recognition is that the high elevation is supported by thermal expansion rather than by thickened crust. The elevation of the Cordillera is only one consequence of the Cordillera being uniformly hot and having a thin lithosphere, in common with most current or recent backarcs. Some other consequences of the high temperatures compared to the adjacent cool craton include: (1) The Cordillera and other backarcs are hot, weak mobile belts that can be deformed by available plate-tectonic forces, in contrast to stable cratons that cannot; (2) Most continental seismicity is concentrated in backarcs; (3) In the Cordillera there is widespread sporadic 'backarc' volcanism; (4) The high temperatures result in very low strength in the lower crust that allows lower-crust detachment; (5) The lower crust weakness facilitates large-scale crustal oroclines that may be independent of the upper mantle; (6) The lower crust in the Cordillera and other backarcs is in amphibolite- to granulite-facies conditions, ~800–900°C at the Moho; (7) In ancient backarcs globally, regional Barrovian metamorphism is concluded to be the result of high temperatures that predate the orogenic collision and deformation. No "heat of orogeny" is required. Following the termination of subduction, backarcs cool with a time constant of 300–500 m.y.

RÉSUMÉ

Pourquoi la chaîne de montagnes de la Cordillère nord-américaine est-elle si haute? On comprend qu'une croûte sur-épaisse puisse expliquer une grande élévation, mais voilà, la croûte de la Cordillère est mince. Il n'existe pas de racine crustale. Or, récemment, une conclusion importante s'est imposée, soit que cette haute élévation s'explique par l'expansion thermique plutôt que par l'existence d'une croûte sur-épaisse. L'élévation de la Cordillère n'est qu'une des conséquences d'une Cordillère uniformément chaude flottant sur une lithosphère mince, caractéristiques communes aux zones d'arrière-arc actuelles ou récentes. Quelques unes des autres conséquences de cette haute température, par opposition aux froids cratons adjacents, comprennent: (1) La Cordillère et d'autres zones d'arrières-arcs sont des zones chaudes et facilement déformables par les forces tectoniques ambiantes, contrairement aux cratons stables; (2) La majorité de l'activité sismique continentale est concentrée dans le zones d'arrière-arc; (3) Dans la Cordillère l'activité volcanique sporadique est généralisé; (4) Ces températures élevées explique la très faible rigidité de la croûte inférieure et les décollements qu'elle subit; (5) La flaccidité de la croûte inférieure facilite la formation d'oroclinaux de grandes magnitudes qui peuvent être indépendants du manteau supérieur; (6) La croûte inférieure de la Cordillère et d'autres zones d'arrière-arc sont dans la zone de faciès amphibolite à granulite, soit 800 à 900oC à la discontinuité Moho; (7) Globalement dans les anciennes zones d'arrière-arc, le métamorphisme régional barrovien s'explique alors comme étant le résultat des hautes températures antérieures à la collision et à la déformation orogénique. Aucune « chaleur orogénique » n'est nécessaire. Après la période de subduction, les zones d'ar-

rière-arc se refroidissent à l'intérieur d'un intervalle de temps de 300 à 500 millions d'années.

Traduit par le Traducteur

INTRODUCTION

In the past few years there have been important developments in our understanding of the processes that control the large-scale tectonics of the Cordillera and other continental subduction zone backarcs, and also their ancient analogues, mainly based on geophysical data. My aim in this article is to communicate this new tentative understanding to the geological community, and to encourage the regional geological studies, analyses and interpretations that are needed to test our conclusions.

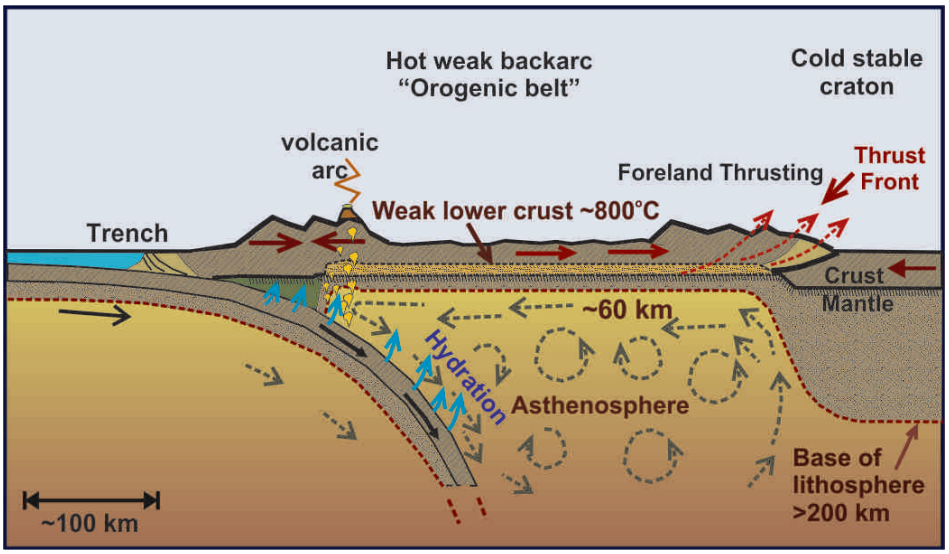

Figure 1. Cross-section of a subduction zone and backarc illustrating the hot and thin lithosphere and the inferred small-scale asthenosphere convection.

As I discuss later in more detail, I define 'backarc' thermally, as the well-defined region of uniformly high crustal and upper-mantle temperatures now recognized landward of continental-arc volcanic chains, but backarcs generally also correspond to tectonic 'mobile belts' and to high-elevation 'mountain belts.' In the geological record, we interpret the main parts of most 'orogenic belts' as ancient backarcs. For the Cordillera, the backarc hinterland defined this way extends from the Cascadia volcanic arc (and recent arcs to the north and south) to the western edge of the foreland belt (Fig. 1). The thermal decay time for the high temperatures of backarcs is 300–500 m.y., so the backarcs of the former subduction zones cut off by the Queen Charlotte and San Andreas transform faults in the Cenozoic still have the characteristic high temperatures. In contrast, most of the Cordilleran foreland belt lies over the cold and thick cratonic lithosphere. Many of my examples come from the southern Canadian Cordillera; in southern British Columbia the backarc extends to the Rocky Mountain Trench which is located over the thermal and lithosphere thickness boundary.

In the first part of this article I discuss problems with the continent/terrane collision model for the Cordilleran mountain belt. I then present evidence that the North American Cordilleran backarc is uniformly hot in contrast to the cold adjacent craton, the Canadian Shield. For our purposes here, 'craton' refers to regions with thermotectonic ages (i.e. the most recent widespread igneous activity, crustal deformation, and metamorphism) greater than about 500 Ma (most of the Canadian Shield is much older), and 'current' backarcs include those where subduction is active or has terminated within the past ~50 m.y., and which are still hot. Although there are resolvable lateral variations in current crust and upper-mantle temperatures within the Cordillera and within the craton, they are very much smaller than the contrast between the Cordillera and the craton and other stable areas. In the second part of the article I discuss some of the important consequences of the high temperatures in the Cordillera and other backarcs, including the origin of their high elevations. Many important conclusions can be reached based on the simple first-order approximation of bimodal continental thermal regimes. Later in the article I provide a short discussion of the thermal regime and its tectonic consequences in ancient backarcs with intermediate thermotectonic ages between the Cordillera and the craton, such as the Appalachian Orogenic Belt. Most of the discussion is for the North American Cordillera but many of the conclusions apply to other backarc mobile belts globally, and the study of modern backarcs such as the Cordillera gives us important insights into past processes in ancient backarc orogenic belts.

An important recent conclusion is that the lithosphere beneath the Cordillera is hot and thin (~60 km). The region has a lithosphere thickness and thermal regime that are remarkably uniform in spite of its complex surface geology and geological history. The uniformly high temperatures and thin lithosphere are in common with most other backarc mobile belts, in contrast to the cold and thick (200–250 km) lithosphere of cratons (Fig. 1). Based especially on work by Claire Currie (e.g. Hyndman et al. 2005; Currie and Hyndman 2006), we think we know why backarcs are hot. There is inferred shallow small-scale asthenosphere convection, as modelled by Currie et al. (2004). The convection likely results from viscosity reduction by water produced and driven upward from the dehydrating subducting oceanic plate as temperature and pressure increase downdip. Only a very small amount of water (~ 50 ppm) is required (e.g. Karato and Wu 1993). Rippe et al. (2013) and Arcay et al. (2006) discuss how the fluid content strongly reduces the viscosity of the mantle. In any case, independent of the causes, the evidence for high temperatures and thin lithosphere in backarcs compared to cratons is quite clear and we can discuss some of the important tectonic consequences (e.g. Hyndman 2010). These include:

(1) The average elevation of the Cordillera is high even though there is no crustal root. The crust is thin, so there is a violation of simple Airy isostasy. The high elevation compared to the craton is instead supported mainly by the density reduction due to thermal expansion.

(2) Because they are hot, the Cordillera and other backarcs are tectonically weak. They are active

mobile belts that can be deformed by plate-boundary and high elevation gravitational forces, in contrast to cold cratons that cannot easily be deformed, so remain stable for long periods of geological time. An indication of the weak Cordillera backarc lithosphere is that much of the North American seismicity is in the Cordillera where most current deformation is occurring. Another indication of backarcs being weak is that globally, continental collision deformation occurs mostly in the weak backarc side of the suture.

(3) There is widespread sporadic 'backarc' volcanism across the Cordillera, because temperatures are close to the solidus at shallow depths in the mantle. Melting may be fluxed locally by subduction water input or result from extensional stresses.

(4) The lower crust is very weak in the Cordillera and other backarcs. This weak layer allows the upper crust to detach from the mantle over large areas. Detachment of the lower crust allows the upper crust to be thrust over adjacent stable lithosphere in foreland fold and thrust belts, and also may facilitate the development of large-scale crustal oroclines that involve horizontal plane crustal bending. Many if not most oroclines may involve only the upper crust.

(5) The lower crust of the Cordillera and other backarcs are in amphibolite- to granulite-facies conditions (800–900°C) at the Moho. Such high temperatures in ancient backarcs can explain the evidence that regional Barrovian metamorphism in deeply-exhumed terranes predated orogenic deformation (e.g. Thompson et al. 2001; Collins 2002); there is no "heat of orogeny". Also, the thermal contrast between backarcs and adjacent stable areas provides an explanation for some types of paired metamorphic belts.

THE CONTINENTAL COLLISION MODEL FOR MOUNTAIN BELTS

Let us start with the puzzle of the elevation of the Cordillera.

Geologists have puzzled over the elevation of mountain belts (e.g. Fig. 2) since the earliest days of scientific geology when marine fossils were found high in the mountains of Europe. How did they get there, and what lifted them up? How did they persist when erosion was recognized as an effective levelling process? There were many theories that now appear fantastic, with some quite perceptive analyses such as by the Swiss geologist Émile Argand (Argand 1924), but a simple elegant mechanism was provided only in the 1960's with the development of the theories of continental drift and plate tectonics. The formation of mountain belts was explained through continental collision (Fig. 3) (e.g. Dewey and Bird 1970). Oceanic lithosphere can subduct beneath continents because it is cold and dense compared to the warmer asthenosphere into which it penetrates. Also, oceanic crust that might resist subduction may be transformed into dense eclogite, and so is no longer buoyant relative to the mantle. When an ocean between continents (or thick-crust oceanic terranes) closes completely, the continental crust is too thick and too low a

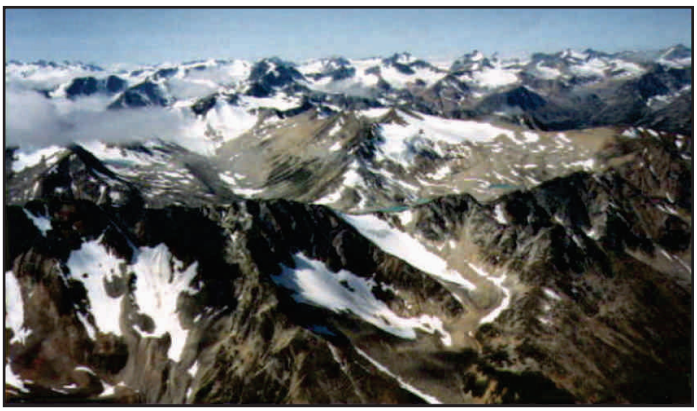

Figure 2. Aerial photo of the North American Cordilleran mountain belt. The average elevation of the belt is about 1500 m, but the crust is thin.

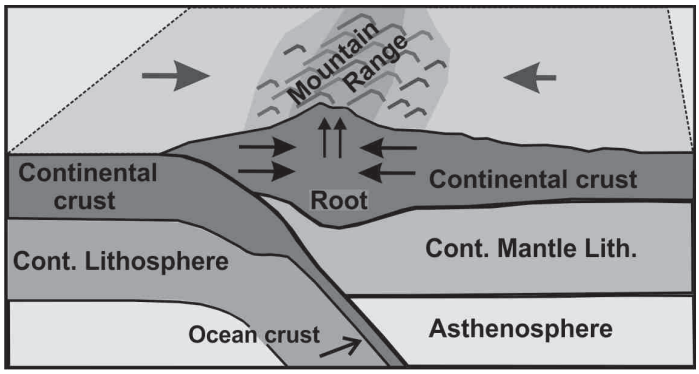

Figure 3. Model of continental collision and crustal thickening for mountain-belt formation. For the Cordillera there is no crustal root, so this is not a valid model for the high elevation.

density to subduct and there is no phase change that can increase the density of felsic materials to approach that of the mantle. Neither of the bounding crustal blocks can subduct, and the result is continental collision, crustal shortening and thickening. Ancient collisions are evident in the geological record as orogenic belts, defined by strong deformation, associated igneous activity and crustal high-temperature metamorphism. This is a very simple, elegant, and persuasive mechanism and is given in many textbooks, but let us look at this explanation for mountain belt high elevations in more detail.

In this model, the high elevations of mountain belts are supported by a thickened crustal root, similar to the deep keels of icebergs that support the height of the ice above the ocean. This is Airy Isostasy, after the English mathematician and astronomer Sir George Biddell Airy. For my discussion below, there are two primary predictions of the collision model for high mountain-belt elevations: (1) Continental (or thick-crust oceanic terrane) collision, and (2) A thick crustal root that supports the elevation. The ongoing collision of India against Asia resulting in the Himalaya Mountains and the high plateau of Tibet is the type example of this mountain-belt formation model.

First, the northward motion of India toward Asia is well recorded in paleomagnetic data, as initially shown by Edward (Ted) Irving in his Cambridge University thesis (Irving 1954) and plate models (e.g. summary by Aitchison et al. 2007). Ongoing collision, deformation and regional Himalaya–Tibet uplift are clear in high-resolution GPS position data (e.g. Bil-

ham et al. 1997; Zhang et al. 2004), and in earthquake activity at the thrust front and to the north (e.g. Feldl and Bilham 2006). Second, a 70 km thick crustal root that supports the Himalayas and Tibet through Airy isostasy is well determined through seismic structure techniques (e.g. Kind et al. 2002). Total crustal thickness is almost double the global average of about 40 km (e.g. Christensen and Mooney 1995). This thickening is approximately enough to support the high elevations, although there is another factor, thermal expansion, that is second order for this mountain belt but is the first-order cause for the Cordillera elevation, as I discuss below. For the Himalayas and Tibet, the collisional model is convincing, but we should not be too quick to apply it globally. Are these two predictions of continental collision and unusually thick crust verified for other mountain belts?

The Collision Model Applied to South and North American Mountain Belts

The continental collision and crustal thickening model for mountain-belt formation seems so reasonable and fits the largest currently active mountain belt, the Himalayas and Tibet, so well, it has not generally been appreciated that this model is not in universal agreement with observations elsewhere. There are serious problems for each of the two other largest mountain belts, the North American and South American Cordilleras. Let us first look briefly at the South American Cordillera, the Andes. Indeed there is thick crust under the highest-elevation central portion, reaching 70 km (e.g. McGlashan et al. 2008), a depth similar to that in the Himalayas–Tibet, although there is much thinner crust in the northern and southern Andes (e.g. Mooney et al. 1998). Also there is current shortening and uplift evident in GPS data, in earthquake activity, and in a variety of geological data (e.g. Khazaradze and Klotz 2003). The principal problem with the Andes is that there is no current collision and there has been none for more than 100 m.y. (e.g. Beck 1988; Ramos 2010). The ongoing shortening and crustal thickening in the central region must have resulted from unusually strong stress transmission across the South American subduction thrust. I will not dwell on that collision-model problem here, but move on to the main focus of this article, the North America Cordillera.

The North American Cordillera does not have elevations as high as those of the Himalyas–Tibet or the central Andes but the region is a mountain belt, averaging about 1500 m above sea level (Fig. 2). As for South America, the first prediction of the continental collision model encounters problems in North America. Although there have been several past terrane-accretion events, there is no current or recent widespread collision or continental accretion along most of the Pacific margin, aside from current collision of the Yakatat terrane in a small restricted area of the Gulf of Alaska, which I discuss later. The last collision event along a significant part of the west coast was the Eocene accretion of thickened oceanic crust of the narrow Crescent-Siletz Terrane at 40–50 Ma (e.g. McCrory and Wilson 2013, and references therein). Even this terrane-accretion event occurred only along the central part of the coast from Oregon to central Vancouver Island, whereas the mountain belt extends from Mexico to Alaska.

Even more serious for the applicability of the collision and crustal thickening model is the lack of thickened crust to support the Cordilleran elevation. Although the crust may have been thick in the past, it is thin now. The thin crust is the main point of my discussion below. The crust and upper-mantle structure of the Cordillera is complex, especially in the United States part, with a number of special structural and tectonic areas such as the Basin and Range extensional province, the Yellowstone hotspot (mantle plume), the quite recent Colorado Plateau uplift that resulted in the Grand Canyon, and the unusual Sierra Nevada mountains. This complexity has resulted in a tendency to focus on smaller-scale crustal variations within the Cordillera without appreciating the regional first-order picture of thin crust compared to the adjacent central North American Canadian Shield.

CRUSTAL THICKNESSES IN NORTH AMERICA AND THE ISOSTASY PROBLEM

My appreciation that there was a problem with the crustal-thickening model for the Cordillera elevation came some 20 years ago from the Canadian Lithoprobe Program, an exceptionally successful multidisciplinary geoscience effort involving academia, Federal and Provincial geological surveys, and industry geologists and geophysicists. The program was directed at the geophysically-defined deep-crustal structure and its associations with surface geological structure. There are two primary techniques for crustal and upper-mantle seismic structure that usually gave good estimates of the depth to the base of the crust, the Moho. They are deep seismic reflection (mainly 'Vibroseis,' as used in the petroleum industry) and wide-angle or refraction seismic surveys. The reflection times from subsurface layers give the depth, providing the seismic velocity of the section is known. In some areas the Moho is seen as a strong reflector, and in others the base of the crust may be defined by a change in the reflection character with depth, as the crust commonly has complex reflections from composition inhomogeneities, whereas the upper mantle is more uniform and seismically transparent. The second method, wide-angle or seismic refraction, generally uses large explosion sources with ground motion recorded at considerable distances. This method gives seismic velocities with depth, as well as defining layering within the earth, but it has low spatial resolution. These methods, as well as more recent work using receiver functions (e.g. Cassidy 1995) and surface-wave tomography (e.g. Kao et al. 2013), generally give consistent crustal thicknesses.

Figure 4 shows results from two areas where there are well-defined crustal thicknesses, the central Cordillera just north of the U.S. border and an area in the craton of the central Canadian Shield (e.g. Clowes et al. 1995; Cook et al. 2010, and references therein). The craton immediately adjacent to the Cordillera is covered by a thick layer of sediments which complicates isostasy calculation, so I have used an example from the exposed craton further to the east. However, in the Western Canada Sedimentary Basin, correcting for the sediment load and thickness gives an elevation and crustal thickness in agreement with the exposed craton. The Cordillera has an average surface elevation of about 1500 m and the Shield has an average elevation just above sea level. The surprising result is that the high-elevation Cordillera site has a thinner crust (about 32 km average), compared to the shield site (about 40 km), which is a clear violation of simple Airy Isostasy. There is no Cordilleran mountain root.

These sites are not local anomalies. The averages from a compilation of crustal thickness and surface elevation data for North America by Hasterok and Chapman (2007) are 33 ± 5 km for the Cordillera and 40 ± 4 km for the stable Canadian Shield. Similar crustal thicknesses in the region of the sections in Figure 4 have been obtained from receiver functions that use phase conversions at the Moho from distant earthquake sources (e.g. Cassidy 1995), and noise tomography surface wave inversions that use a range of frequencies to resolve velocities at different depths (e.g. Kao et al. 2013). The crustal thickness contrast in the western U.S.A. is very well resolved from USArray closely-spaced seismic stations (Levandowski et al. 2014) that indicate a clear division between the Cordillera (30–35 km) and the stable area to the east (40–45 km) (Fig. 5).

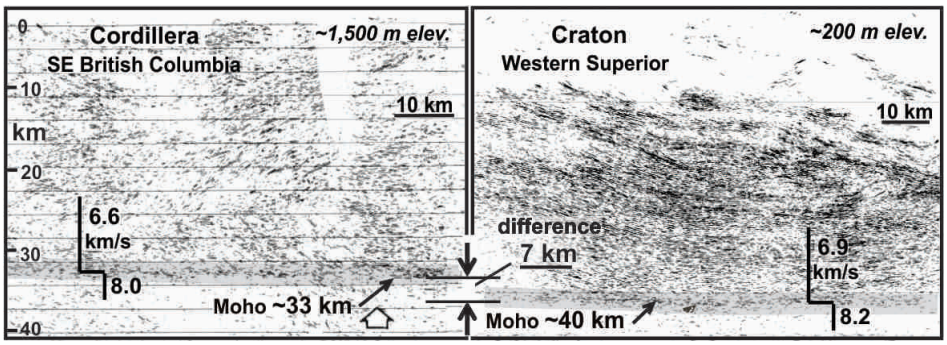

Figure 4. Seismic reflection and simplified wide-angle seismic structure estimates of crustal thickness; examples from the southern Canadian Cordillera and the adjacent craton (after Cook et al. 2010). The high elevation Cordillera has a 7 km thinner crust than the near sea level craton.

Most of the Cordilleran Belt has crustal thicknesses of 30–35 km but there are significant variations in a few areas which can be used to illustrate the difference in buoyancy between the Cordillera and Shield more graphically. Figure 6 shows the relation between crustal thickness and elevation using data from the Hasterok and Chapman (2007) compilation (Hyndman and Currie 2011). The data have been corrected for the usually small effect of differences in crustal density (i.e. Pratt Isostasy), using average crustal seismic velocities and the general relation between density and velocity. Within the Cordillera and within the Shield, there is a good linear relation between crustal thickness and elevation, just as predicted by Airy Isostasy. The slope of the line defines the density contrast at the Moho, which is similar for both areas and close to the value predicted for the expected main rock types, i.e. gabbroic lower crust and peridotite upper mantle.

Surprisingly the two lines are systematically offset by 1600 m (Fig. 6). Elevation in North America is remarkably bimodal. The Cordillera is about 1600 m higher than the Canadian Shield for the same crustal thickness. The variations from the best-fit line relating elevation and crustal thickness within each of the two areas are quite small in spite of the geological complexities. The locations shown in the figure were partly chosen to give a wide elevation range to define the lines. The variability in crustal thickness is generally quite low. I emphasize that these data are for current crustal thicknesses. The Cordillera may have had greater thicknesses and elevations at times of shortening, such as during the Laramide Orogeny when the foreland thrust belt was active (see Bao et al. 2014). To illustrate the abrupt contrast in crustal thickness between the Cordillera and the craton, Figure 7 shows the crustal transition across southeastern British Columbia and western Alberta (Hyndman and Lewis 1999; see also Burianyk et al. 1997; Cook et al. 2010). The transition is centred at about the Rocky Mountain Trench (e.g. van der Velden and Cook 1996). The Moho beneath the Cordillera to the west is at 32–34 km. Because of the load of the overthrusted upper Cordilleran crust and sedimentary thrust sheets, the lithosphere of the adjacent craton is depressed to a Moho depth of about 50 km (see Stockmal and Beaumont 1987, for models of such overthrusting). This thickness is made up of a normal-thickness

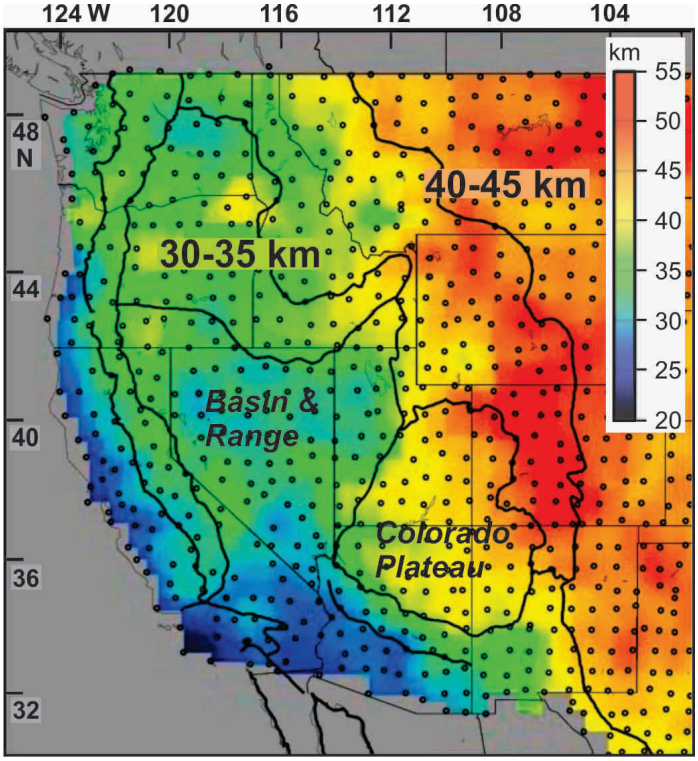

Figure 5. Crustal thickness in western United States showing the remarkably uniformly thin Cordilleran crust and thicker craton crust based on US Array seismic data (after Levandowski et al. 2014).

craton crust of about 40 km, overlain by the about 10 km thick Western Canada Sedimentary Basin section. In spite of the more than 15 km contrast in crustal thickness, there is almost no change in elevation or in Bouguer gravity. The crustal thickness contrast is balanced by the thermal contrast, as I discuss below. The figure also shows the predicted elevation for the Cordillera using the crustal thickness-elevation relationship for the cold craton in Figure 6. The predicted elevation for the 32–34 km thick Cordilleran crust, if it had a cold craton thermal regime, would be below sea level. The sharpness of the transition is indicated in a detailed shear wave tomography study of the area by Bao et al. (2014). As they illustrate, there is a sharp velocity contrast and a sharp truncation of magnetic anomalies at the Rocky Mountain Trench.

There is an interesting related comparison between the hot, thin lithosphere beneath western Europe (crustal thicknesses

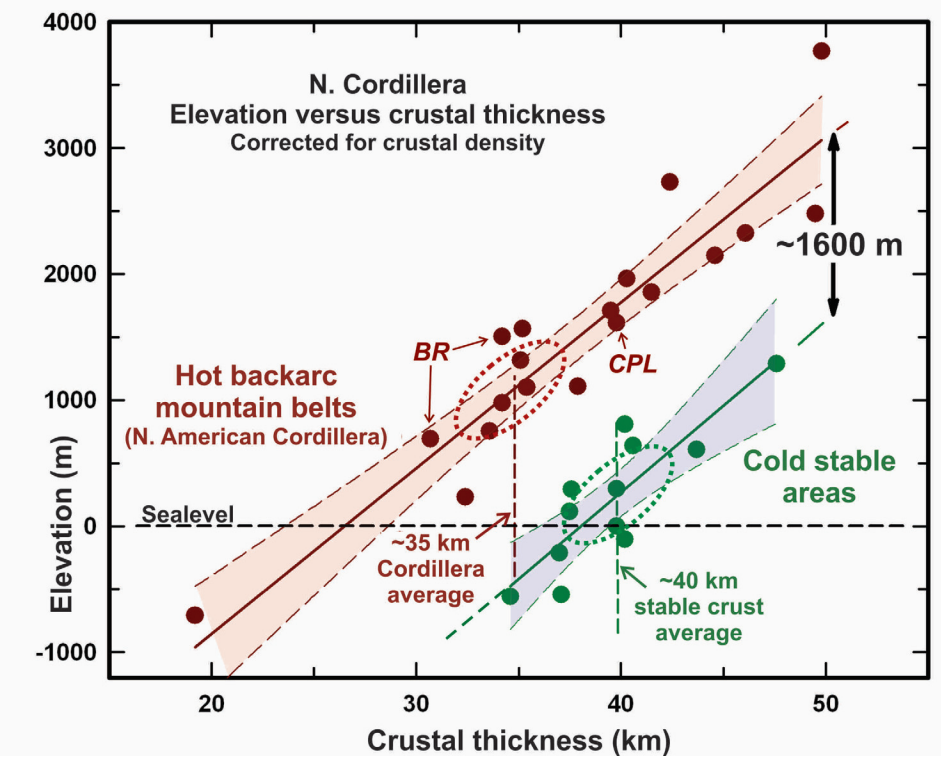

Figure 6. Elevation *versus* crustal thickness for the Cordillera and craton showing the 1600 m difference in elevation for the same crustal thickness (BR= Basin and Range; CPL= Colorado Plateau) (after Hyndman and Currie 2011).

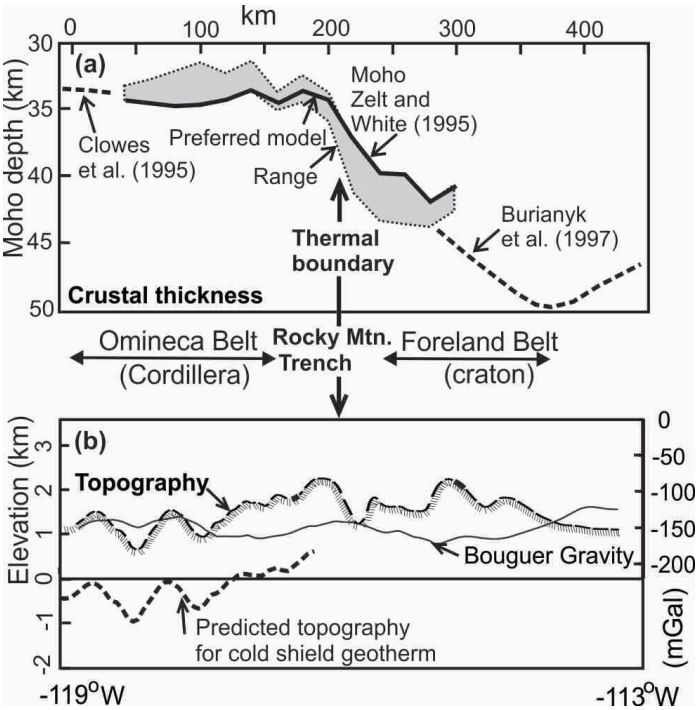

Figure 7. (a) The abrupt eastward increase in crustal thickness at the lithosphere thermal boundary beneath the Rocky Mountain Trench. (b) The small associated change in elevation and Bouguer Gravity across the crustal thickness boundary (after Hyndman and Lewis 1999). See also Cook et al. (2010), and Bao et al. (2014).

of about 30 km), compared to the cold Fennoscandian Shield to the northeast (crustal thicknesses of 40–45 km). The crust is generally somewhat thinner in western Europe compared to the North American Cordillera so the elevation is lower and there is little difference in elevation beneath western Europe and the adjacent shield (see figure 2 of Tesauro et al. 2008). Although corrections for variations in crustal density have not been applied, the averages for these two regions agree very well with our plots of crustal thickness *versus* elevation for North America. Western Europe, most of which is a current or thermally recent backarc, is equivalent to the Cordillera, and the Fennoscandian Shield is equivalent to the Canadian Shield (Fig. 6). The elevation difference between the two regions for the same crustal thickness is again about 1600 m.

CRUST AND UPPER MANTLE TEMPERATURES, AND THERMAL ISOSTASY

I now turn to the origin of these differences in crustal thickness and elevation.

The controls of continental elevation have been an important discussion for many years. There are two well-recognized factors, i.e. crustal thickness (Airy Isostasy) and crustal density (Pratt Isostasy). In addition, there has been much work on the role of mantle flow traction and mantle dynamics (e.g. reviews by Braun 2010; Flament et al. 2013; Becker et al. 2013). Although the latter may be important, as I show below it must be subordinate to the effect of thermal isostasy in generating the elevation difference between the Cordillera and adjacent craton. Also, for the Cordillera and other hot backarcs, the estimated asthenosphere viscosities appear to be too low to allow significant lithosphere basal traction and for convective buoyancy forces for that area (see also Levandowski et al. 2014).

It has been recognized for many years that the temperature in the crust and upper mantle can significantly affect the rock densities through thermal expansion, and therefore affect surface elevation. Hotter crust and upper mantle rocks will have lower densities, and so float higher. Much of the credit for elegant mathematical modelling and rigorous data analysis of the thermal effect is due to Art Lachenbruch from the U.S. Geological Survey (e.g. Lachenbruch and Morgan 1990). Many conceptual models of subduction zones have regional high temperatures near the volcanic arc, but we now recognize that there is only a small high-temperature thermal anomaly associated with the arc (e.g. Hyndman et al. 2009) except immediately around the volcanic centres. The high temperatures extend uniformly across the entire backarc, including the volcanic arc. In the next sections, I first describe the principal constraints on temperature in the crust and upper mantle, and then the effects of these temperatures in terms of elevation and other consequences.

Surface Heat Flow Temperature Estimates

Until recently the main constraint on deep-crustal and upper-mantle temperatures was the surface heat flux from the earth,

commonly estimated from temperatures measured down deep boreholes and the thermal properties of core samples of the rocks penetrated, as measured in the laboratory. These heat-flux estimates can be used to estimate lithosphere thickness (e.g. Chapman and Pollack 1977). Using this constraint on deep temperatures, Hasterok and Chapman (2007) showed that elevation is related to surface heat flow in the way expected for thermal isostasy. However, extrapolating surface heat flow to deep temperatures has a large uncertainty, especially due to variations in near-surface radioactive heat generation, which result in a considerable scatter in the relationship. The heat generation from the natural radioactivity of the unstable isotopes of uranium, thorium and potassium is commonly concentrated in the upper crust, so contributes directly to the measured surface heat flux but has only a small effect on the deep temperatures. This uncertainty can be much reduced if we have measurements of radioactive element abundance, and can allow for variations in radioactive heat generation in upper crust rocks.

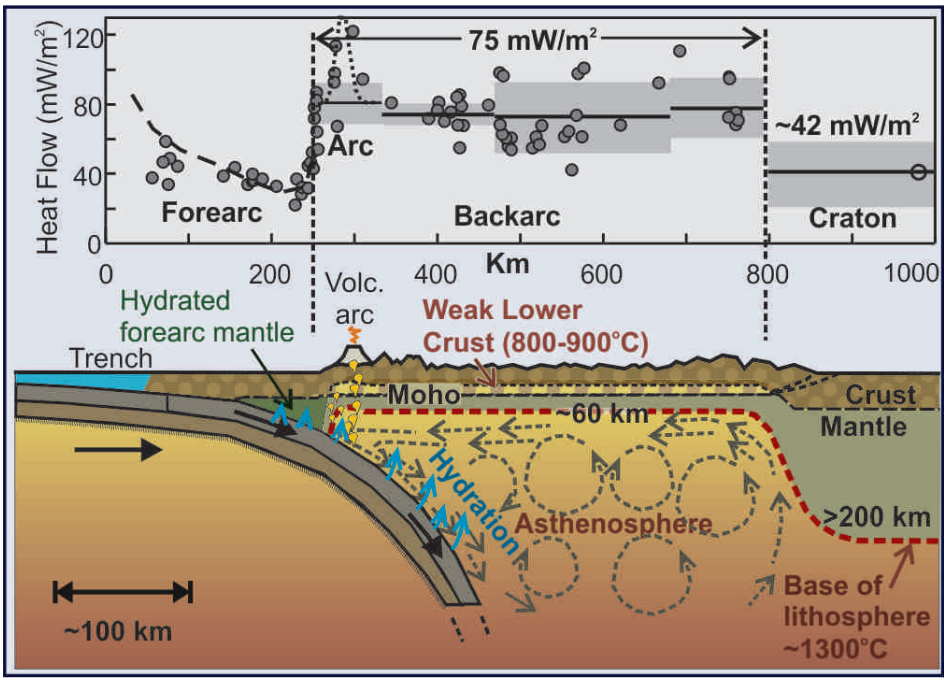

Figure 8. Heat flux data across the southern Canadian Cordillera showing the consistently high values relative to the adjacent craton, (e.g. Lewis et al. 1992). Corrections have been made for variations in upper crust radioactive heat generation that affect surface heat flow but have little effect on deep temperatures.

One area where we have good radioactive heat generation measurements, as well as detailed heat flux data, is across the southern Canadian Cordillera, especially by Trevor Lewis (e.g. Lewis et al. 1992; Hyndman and Lewis 1995; also see Lewis et al. 2003, for the northern Canadian Cordillera). David Blackwell and colleagues showed similar high heat flow in Washington and Oregon (e.g. Blackwell et al. 1990). Figure 8 shows the heat flux with a first-order correction for the effect of variations in near-surface radioactive heat generation, in a profile across the Cordillera. Considerable scatter remains, but the contrast between the nearly laterally uniform high heat flow across the Cordillera and the low heat flow for the Shield is clear. Heat flow in the Cordillera is almost twice that of the shield. The Western Canada Sedimentary Basin to the east of this Cordillera profile overlies the shield and the thick sedimentary section, coupled with fluid-advection effects, makes reliable measurements difficult (see discussion by Majorowicz et al. 2014), so I show an average heat flux for the crystalline rocks of the shield exposed further to the east. Majorowicz et al. (2014) reported one high-quality heat flow from a 2.2 km deep hole into the basement rocks beneath the Basin that gave a heat generation-corrected heat flow close to the average for the exposed shield. Mareschal and Jaupart (2004) have shown that most of the surface heat-flow variation in the shield is due to variations in upper-crustal heat generation, so there are only small lateral variations in its deep temperatures (also see Artemieva and Mooney 2001).

Other temperature constraints in our toolbox include two that I illustrate: seismic velocity in the upper mantle (especially *Vs* mantle tomography), and temperatures from mantle xenoliths at their depth of origin. Others that give consistent results are: *Te*, the mainly temperature-controlled effective elastic lithosphere thickness from gravity-topography coherence (e.g. Hyndman et al. 2009); the seismic and electrical thickness of the lithosphere, which are mainly thermally controlled (e.g. Eaton et al. 2009); low effective viscosities in the shallow mantle; the mainly thermally-controlled maximum depth of seismicity; and the depth of the Curie temperature estimated from magnetic surveys. Only the first two constraints are discussed in the following section.

Temperature Control of Seismic Velocity in the Upper Mantle

Within the continental crust, seismic velocities are mainly controlled by rock composition. However, in the upper mantle the velocity is mainly controlled by temperature and the effect of temperature on velocity from laboratory data can be used to estimate upper mantle temperatures. Higher temperatures give lower velocities. The second-order effect of lateral variations in upper-mantle composition can be corrected, especially using mantle compositions from xenoliths. A sometimes complicating factor is the presence of partial melt, especially in parts of the U.S. Cordillera, such as beneath the Yellowstone region, so I show mainly the temperatures for the Canadian Cordillera where partial melt appears generally not to be sufficiently wide spread to be important.

Temperatures can be estimated from both compressional wave velocities, *Vp*, and shear wave velocities, *Vs*. I give temperature-depth results only from shear-wave seismic tomography that uses ground surface waves moving across an area. This method generally has used earthquake-generated waves but has recently been extended to use 'noise' signals moving across an array of recording stations, with the 'noise' usually interpreted to be generated in the ocean basins. Many intersecting wave paths give velocity maps over large areas, and the depth of penetration depends on the frequency, which allows estimation of velocity-depth profiles and 3D temperatures.

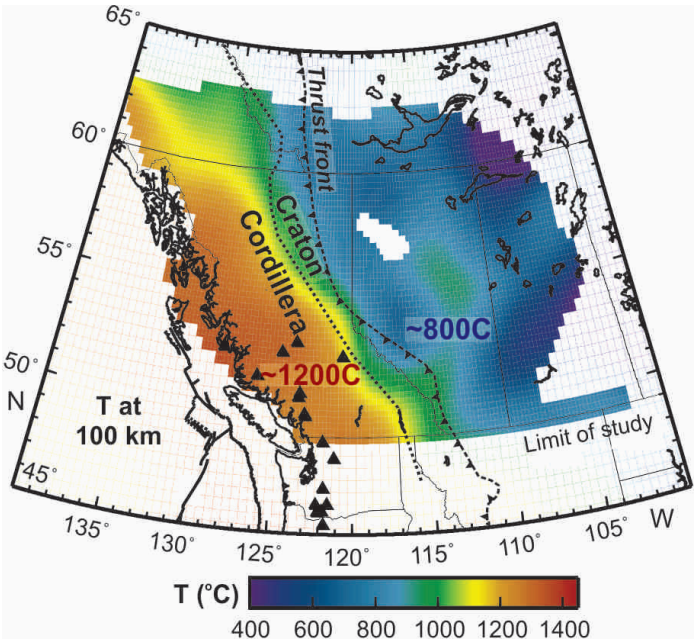

Figure 9. Temperatures at 100 km depth across the southern Canadian Cordillera (about 1200°C) and adjacent craton (about 800°C) estimated from mantle seismic velocities (after Hyndman et al. 2009).

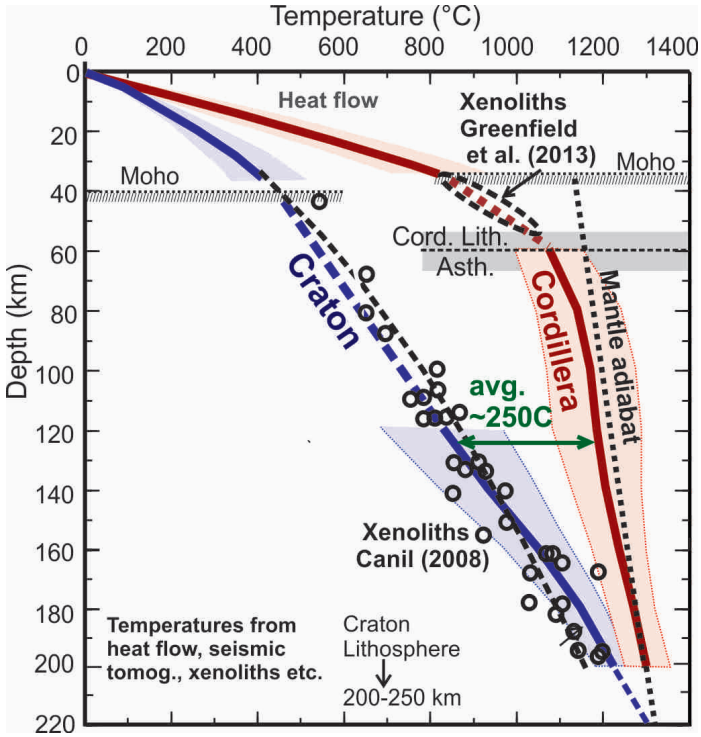

Figure 10. Average temperature-depth profile for the Canadian Cordillera and adjacent craton from heat flow, seismic tomography velocities (red and blue lines; variability, shaded areas), and xenoliths (black circles and dashed lines) (after Hyndman et al. 2009). There is a maximum difference between the Cordillera and the craton of about 400°C at 100 km and an average temperature difference to 220 km of about 250°C.

Figure 9 illustrates the temperatures at a depth of 100 km for western Canada, based on a velocity study led by Andrew Frederiksen, University of Manitoba, and temperatures calculated by Claire Currie, at the University of Alberta (e.g. Hyndman et al. 2005). The inferred temperatures are remarkably high and laterally uniform across the Cordillera and much lower and quite uniform in the adjacent craton (e.g. Hyndman et al. 2009). Bao et al. (2014) show that the Cordillera-craton mantle velocity contrast (and therefore temperature contrast) in the mantle is very sharp at the Rocky Mountain Trench. Figure 10 shows the average and variability of the temperature-depths for the Canadian Cordillera and for the western craton. Some of the variability in the results represents real temperature variation and some comes from measurement uncertainty. In any case, the variability within each region is much smaller than the difference between the two regions.

Xenolith Temperature-Pressure (Depth)

Small samples of rocks from the deep crust and upper mantle occasionally are carried to the surface through kimberlite pipe eruptions ('diamond pipes') in the craton, or entrained in volcanic magmas in the Cordillera. Commonly the exhumation rates are rapid enough that chilling retains the mineral equilibria representative of the temperature and pressure (depth) at their source, allowing calculation of temperature-depth profiles at the time of emplacement. Depth calculations are much more reliable for the xenoliths from cratonic regions, which have minerals with pressure-sensitive equilibria than for the Cordillera where the depths usually must be estimated indirectly.

Upper-mantle xenoliths have been recovered from numerous localities in the Cascadia backarc and the adjacent craton. An early study yielded 1000°C at 40 km depth, increasing to 1300°C at 60–70 km (Ross 1983), so the very high temperatures and thin lithosphere in parts of the Cordillera were inferred over 30 years ago by this method. Subsequently, Saruwatari et al. (2001) found 900–1040°C at 1.2–1.6 GPa (35–50 km depth) for southern British Columbia to Alaska. Harder and Russell (2006) studied the Llangorse/Edziza volcanic field (northwest British Columbia) and found a minimum temperature of 800–850°C which provides an estimate for the Moho and a maximum of 1050–1100°C which gives an estimate for the base of the lithosphere. They produced model geotherms that are in good agreement with those from our seismic velocity estimates; they estimated the base of the lithosphere at 52–66 km (Fig. 10). For southern British Columbia, Greenfield et al. (2013) estimated a Moho temperature at 33 km of 825 ±25°C, with 1060°C at 48 km. For all the Cordillera studies, high temperatures are inferred, with the convective adiabat at about 60 km, where rocks are weak enough for small-scale convection, close to first melting.

For the craton and stable platform, numerous studies give temperatures from mantle xenoliths (e.g. MacKenzie and Canil 1999; Canil 2008, and references therein) that are very consistent with temperatures from *Vs* (Fig. 10). There are well-resolved lateral variations but they are small compared to the contrast with the Cordillera. Other cratons globally give similar temperatures (e.g. Griffin et al. 2004), i.e. the base of the thermal lithosphere is usually at 200–250 km. This depth is similar to that obtained for the base of the lithosphere from seismic and magnetotelluric data (e.g. Eaton et al. 2009).

These results show that there is a large difference in the temperatures at the base of the crust for the cold shield (400–500°C) compared to the hot Cordilleran backarc (800–850°C); approximately a 400°C difference. I discuss only

the coolest case of the older cratons here, mainly the Archean from North America. However, Paleozoic stable areas are only slightly warmer than older regions. I discuss them briefly later. The degree to which the thermal regimes of the continents are bimodal is quite impressive, leading to some important consequences.

ORIGIN OF CORDILLERA BACKARC HIGH TEMPERATURES

The high temperatures in backarcs like the Cordillera have been explained by rapid upward convective heat transfer beneath a thin lithosphere (see Hyndman et al. 2005, for discussion). The first suggestion of this process I have found was by Hasebe et al. (1970) who were concerned with the high heat flow in the Japan Sea backarc. Based on high heat flow, high electrical conductivity and other results that presented strong evidence for high temperatures and partial melting beneath the Canadian Cordillera, Gough (1986) proposed "mantle upflow tectonics." Many models of backarc convection have assumed one large-scale circulation cell driven by the downward traction and thermal effects of the cold downgoing oceanic plate. This model is conceptually reasonable but it has proved difficult to produce the observed uniform high heat flow across the backarc with such models (e.g. Kukačka and Matyska 2008). Heat should be lost from the top of the cell such that temperatures and surface heat flow decrease toward the arc, unless the convection speed is much faster than plate motion rates. This decrease is not observed. Regional small-scale convection that maintains adiabatic temperatures below about 60 km seems to be required, with flow rates faster than relative plate-motion rates (e.g. Nyblade and Pollack 1993; Currie et al. 2004; Arcay et al. 2006). Figure 8 shows a schematic convection model along with the southern Canadian Cordilleran heat flow. In a few areas such as the Basin and Range province, present or recent crustal extension has an additional thermal effect (e.g. Lachenbruch and Sass 1978). Similarly, in oceanic backarcs where extension is occurring, it is difficult to separate the thermal effect of extension from that of convective heat transport in the underlying shallow asthenosphere. However, Watanabe et al. (1977) suggested that even in these basins, small-scale convection is needed to explain the thin lithospheres and the high heat flow that has been maintained for long times after the basins opened.

An explanation for shallow vigorous convection beneath backarc lithospheres is that the mantle viscosity is substantially lowered by incorporation of water and other volatiles expelled from the underlying subducting oceanic plate. The backarc convection system is poorly understood, but vigorous convection may mix the water throughout the whole backarc asthenosphere wedge. Another possibility is that episodes of flat-slab subduction carry water far inland and initiate small-scale convection. Mantle rocks containing even quite small amounts of water in the mineral structure (>50 ppm), have a substantially lower effective viscosity than dry mantle rocks (e.g. Karato and Wu 1993). Dixon et al. (2004) summarized the evidence for very low mantle viscosity beneath the Cordillera current and recent backarc of the western U.S.A. and concluded that such low viscosities require significant water in the upper mantle, as well as high temperatures that are close to the solidus. In areas where the landward boundary of the backarc is a craton or an old platform, such as western North America, the asthenosphere convection may be limited landward by thick, refractory lithosphere. The original craton rifting and associated asthenosphere upwelling may have extended and heated a considerable width of the margin of the craton or platform. This would have allowed subsequent backarc thermal convection to continue beneath the thinned region to the edge of the unextended craton lithosphere. Royden and Keen (1980) illustrate such margin lithosphere thinning and heating from craton rifting by the opening of the Labrador Sea ocean basin between Labrador and Greenland. The backarc also may be widened by the addition of accreted terranes, such as has occurred in western North America.

I note that globally there are a few cool backarcs, mainly where there is flat-slab subduction such that there is no space for small-scale convection between the backarc lithosphere and the underlying nearly-horizontal subducting slab (discussion by Currie and Hyndman 2006). These areas also are characterized by little or no arc volcanism. For the Peru example, see Gutscher et al. (2000).

DURATION OF HIGH TEMPERATURES IN FORMER BACKARCS

In the discussion and data shown above, I included the northern Canadian Cordillera in the backarc although subduction was cut off and stopped on that margin at ~40–50 Ma with the development of the transform Queen Charlotte Fault system (e.g. Engebretson et al. 1985; Hyndman and Hamilton 1993; McCrory and Wilson 2013). However, backarcs cool quite slowly following the termination of subduction such that the estimated lower-crust and upper-mantle temperatures in this area are little different from those to the south, landward of the presently-active Cascadia subduction zone. The same is true in California where subduction was cut off more recently by the San Andreas Fault system. There must be a finite life to the high temperatures in backarc mobile belts after the source of heat is removed, as most ancient mobile belts active in the Paleozoic or earlier no longer exhibit the high temperatures characteristic of modern backarc lithosphere. In the backarc convection model, the vigorous free convection should decline following the termination of subduction and the loss of water as a flux for convection. The processes involved are undoubtedly complex, including slab window and slab break-off effects, and may take tens of millions of years. However, lithosphere cooling and thickening are probably conductive following the increase in upper-mantle viscosity due to water loss through partitioning into arc and backarc melt fractions, and through upward diffusion. The cooling time constant may be estimated from compilations of heat flow and inferred lithosphere temperatures (Fig. 11a) and elevation (Fig. 11b) compared to the age of the most recent thermotectonic event (igneous activity, metamorphism, volcanism, etc.) (e.g. Pollack et al. 1993; Nyblade and Pollack 1993; Pavlenkova 1996; Artemieva and Mooney 2001). Much of the variability for similar ages comes from variable upper-crust radioactive heat generation that has only a small effect on deep temperatures. The thermotectonic age is assumed to correspond approximately to the time since termination of subduction and therefore of water input. The most rapid decrease in heat flow appears to be in the several hundred m.y. following the last thermotec-

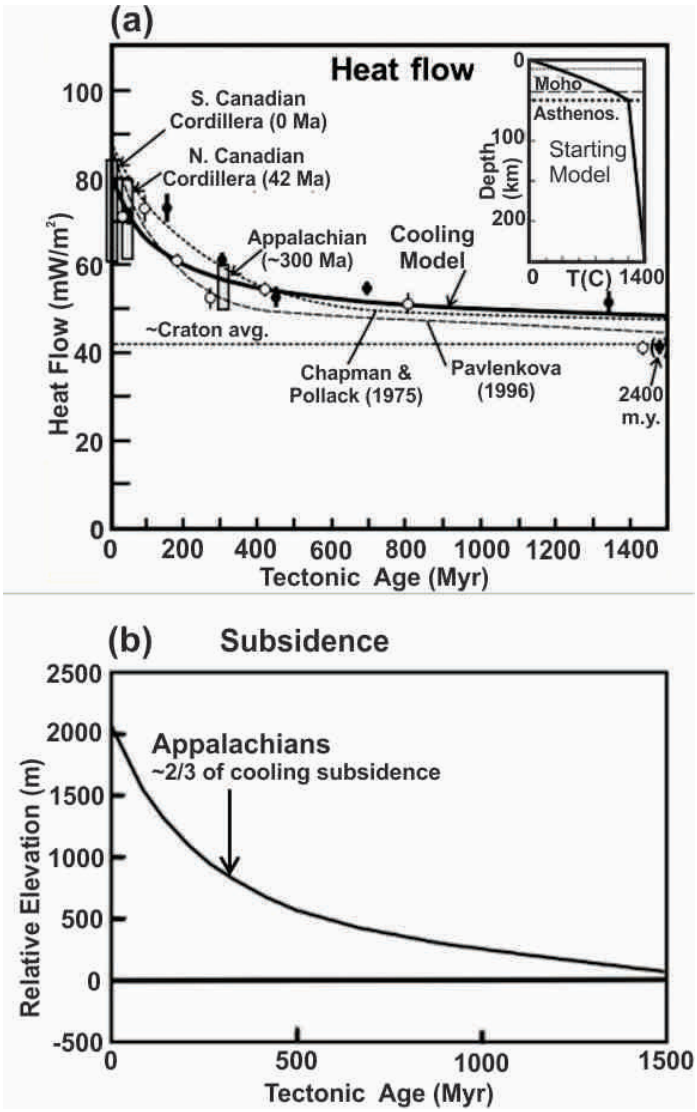

Figure 11. (a) The decay of backarc high temperatures. The heat flow from a simple cooling model is compared to heat flow *versus* thermotectonic age (after Currie and Hyndman 2006). (b) Simple model thermal elevation decay; there is general agreement for the Appalachian former backarc, with a model and current elevation of 600–800 m.

tonic event, and the data suggest a 300–500 m.y. time constant, (i.e. the time for there to be ~37% remaining of the total change) (see also Sleep 2005). A similar cooling and lithosphere thickening time is suggested by several examples.

The Appalachian former backarc mobile belt, in which the last significant deformation occurred at about 300 Ma, is now cool and stable. Although heat flow and other thermal data suggest that it is still somewhat warmer than the cratons (e.g. Pollack et al. 1993), at least some of the difference may be due to greater upper-crust heat generation (Mareschal and Jaupart 2004). The residual thermal elevation above that for the craton, however, remains quite significant at 600–800 m (Fig. 11b). In contrast, the northern Canadian Cordillera, where margin subduction was cut off by the Queen Charlotte-Fairweather transform fault zone in the Eocene, 40–50 Ma, still has high heat flow and inferred high temperatures at depth (Lewis et al. 2003), similar to currently active backarcs (Fig. 9).

Currie and Hyndman (2006) used a simple conductive model with an initial thin backarc lithosphere and an underlying adiabatic asthenosphere to illustrate these features (Fig. 11). This model is the limiting case of abrupt termination of convection to a depth of 250 km (approximate thickness of craton lithosphere) at the time of termination of subduction. The heat flow data are not corrected for variations in upper-crust heat generation, and the effect of erosion of the high-radioactivity upper crust should give a somewhat lower heat flow at longer times than the simple cooling model. The heat flow as a function of age predicted by the model is in general agreement with that observed (Fig. 11), which suggests that the termination of shallow free convection generally occurs only a few tens of millions of years after subduction stops.

CONSEQUENCES OF THE HIGH TEMPERATURES IN THE CORDILLERA AND OTHER BACKARCS

In addition to the high elevation discussed above, there are numerous other consequences of the crust and upper-mantle high temperatures in the Cordilleran backarc that I will now discuss. These have wide implications for processes in modern orogenic belts and also for their ancient analogues.

Thickness and Strength of the Lithosphere; Weak Mobile Belts and Seismicity

The Effect of Temperature on Lithosphere Strength

The weakness of the Cordillera backarc is well illustrated by its current and recent complex deformation (Fig. 12). It is a mobile belt. Most North American crustal seismicity occurs in the Cordillera, reflecting the widespread current deformation. There is oblique extension in the Gulf of California, where the crust is being rifted and extended, and new ocean crust is forming. In near-coastal California, the San Andreas Fault zone is a broad zone of shearing (at about 5 cm per year) with westernmost California moving northward as part of the Pacific Plate. To the northeast, the Basin and Range province is a broad region of block faulting, that is extending at a rate of about 1 cm/yr. Along the coast of Oregon, the Cascadia forearc sliver is moving to the northwest at about 3 mm/yr and colliding with a stronger Vancouver Island, resulting in crustal seismicity in Puget Sound and the southern Georgia Strait. In the corner of the Gulf of Alaska, the Yakutat block is colliding with North America resulting in the continent's highest elevations, the St. Elias-Chugach mountains near the coast. This collision is also concluded to result in strain transfer across the Cordillera to the current thrusting and high seismicity in the Mackenzie Mountains at the eastern foreland (Mazzotti and Hyndman 2002). The northern Cordillera example shows the concentration of North American seismicity in the Cordillera. There is much lower seismicity and earthquake hazard in eastern North America (e.g. Frankel et al. 2000; Adams and Atkinson 2003).

The Cordillera has a long history of varied past deformation, including the widespread Laramide thrusting at the Cordillera Rocky Mountain front, and strike-slip faulting in the north-central Cordillera. The complex tectonic evolution of the belt is mainly in response to changing plate-boundary forces on the west coast, where the Pacific and North American plates interact.

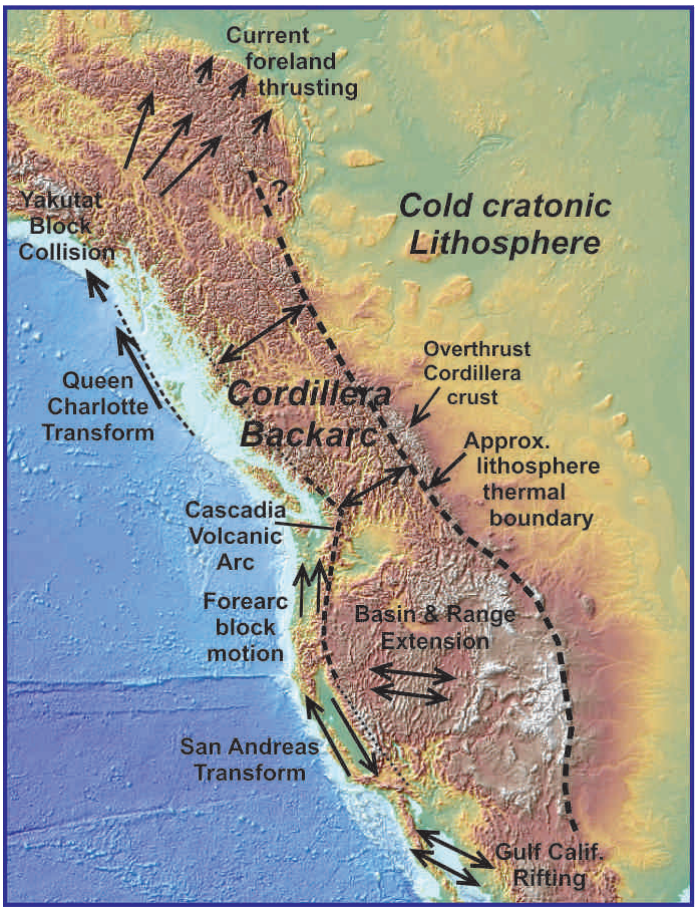

Figure 12. The Cordilleran backarc mobile belt illustrating the ongoing deformation, strike-slip faulting, normal faulting (extension), and thrust shortening (modified from Hyndman et al. 2005).

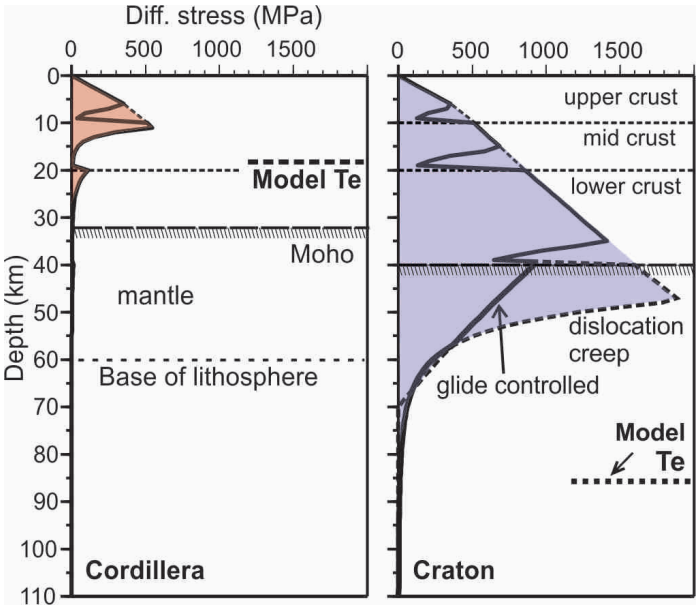

Figure 13. Strength *versus* depth estimates for the Cordilleran backarc compared to the craton (assuming in compression), based on temperature-depth estimates and laboratory rheology (modified from Hyndman et al. 2009). In the Cordillera there is significant strength only in the upper crust.

Along with deformation forces, lithosphere strength is a primary control of where tectonic deformation and seismicity occurs, and the nature of deformation processes. Lithosphere strength increases with depth in the shallow cool frictional regime because of the downward-increasing load on fault surfaces, and is not significantly related to composition or temperature. However, at greater depths where there is ductile deformation, temperature is the most important control (e.g. Ranalli 1995). Therefore, strength in the ductile regime decreases with depth, except for a downward step increase in strength at the Moho due to the change to the stronger mantle rock type. In the shallow frictional regime, the principal variable is the pore pressure, which can range from hydrostatic (i.e. porosity is connected to the surface) to lithostatic (i.e. porosity is not connected and the pore pressure is the load of the overlying rock). Townend and Zoback (2000) argued that in the frictional upper section, at least of cratons, the porosity is connected to the surface by fractures and other connected porosity, and pore pressure is generally close to hydrostatic. An estimate of the strength of the lithosphere as a function of depth in the high-temperature Canadian Cordilleran backarc and the adjacent low-temperature Canadian Shield by Stephane Mazzotti and others is shown in Figure 13 (see Flück et al. 2003; Lewis et al. 2003; Hyndman et al. 2009). In this simple model, the upper crust follows the Byerlee Law criterion for brittle fault sliding (e.g. Ranalli 1995) with hydrostatic pore pressure, and deformation at greater depths follows power law creep (Karato and Wu 1993) at a common plate-boundary deformation rate of $\sim 10^{-15} s^{-1}$. In the example shown, the upper crust is taken to have the rheology of granite, the lower crust of diabase, and the mantle of olivine (e.g. Ranalli 1995). There is considerable uncertainty in the deformation mechanisms and how laboratory data should be applied, but using our estimated backarc temperatures, most models have significant tectonic strength only in the upper 15–20 km of the crust and little strength in the lower crust. The uppermost mantle is slightly stronger but still tectonically very weak. In contrast, for cold craton regions there is a strong crust and upper mantle to at least 60 km. In all models, the much thinner and weaker lithosphere predicted for backarcs compared to cratons is clear. For large-scale deformation models we need the total strength of the lithosphere, which may be estimated by integrating the strength over depth (Fig. 14). In this figure, 'wet' and 'dry' refer to the laboratory rheologies that may apply to backarc mobile belts and cratons, respectively. The combined crustal- and mantle-lithosphere strength for backarc mobile belts is at least 10 times less and may be as much as 100 times less than that of cratons.

The above analysis indicates that the Cordilleran backarc is easily deformed. The mobile belt lithosphere strengths of $< 5 \times 10^{12}$ N/m are within the range suggested for plate-tectonic forces and the elevation gravitational potential of mountain belts of $1–10 \times 10^{12}$ N/m (e.g. Lynch and Morgan 1987; Whittakaer et al. 1992; Zoback et al. 2002). In contrast, cratonic lithospheres are too strong to be readily deformed. Some special process that weakens the cratonic lithosphere is required for deformation to occur, and these regions thus remain stable for long periods of geological time. Alternatively, if one fixes the plate-boundary forces at their estimated values, the calculated strain rates for backarcs are in the range observed for mobile belts like the Cordillera and are very small for stable

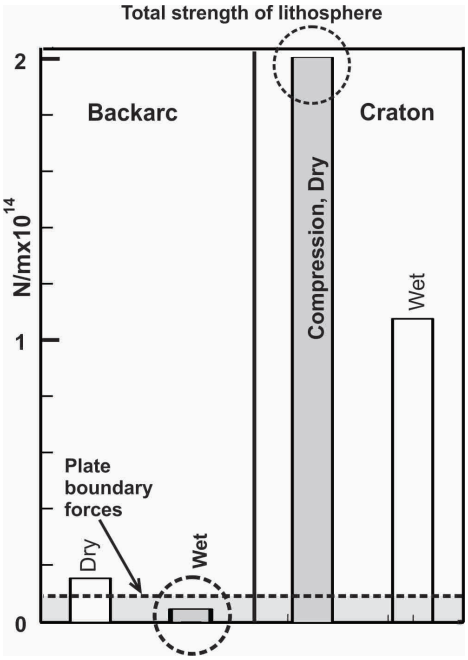

Figure 14. Total strength of the lithosphere for hot backarcs and cold cratons, compared to average plate-boundary forces. Backarcs may be deformed by plate-boundary forces; cratons cannot be deformed by such forces unless weakened by some transient process (after Hyndman et al. 2009).

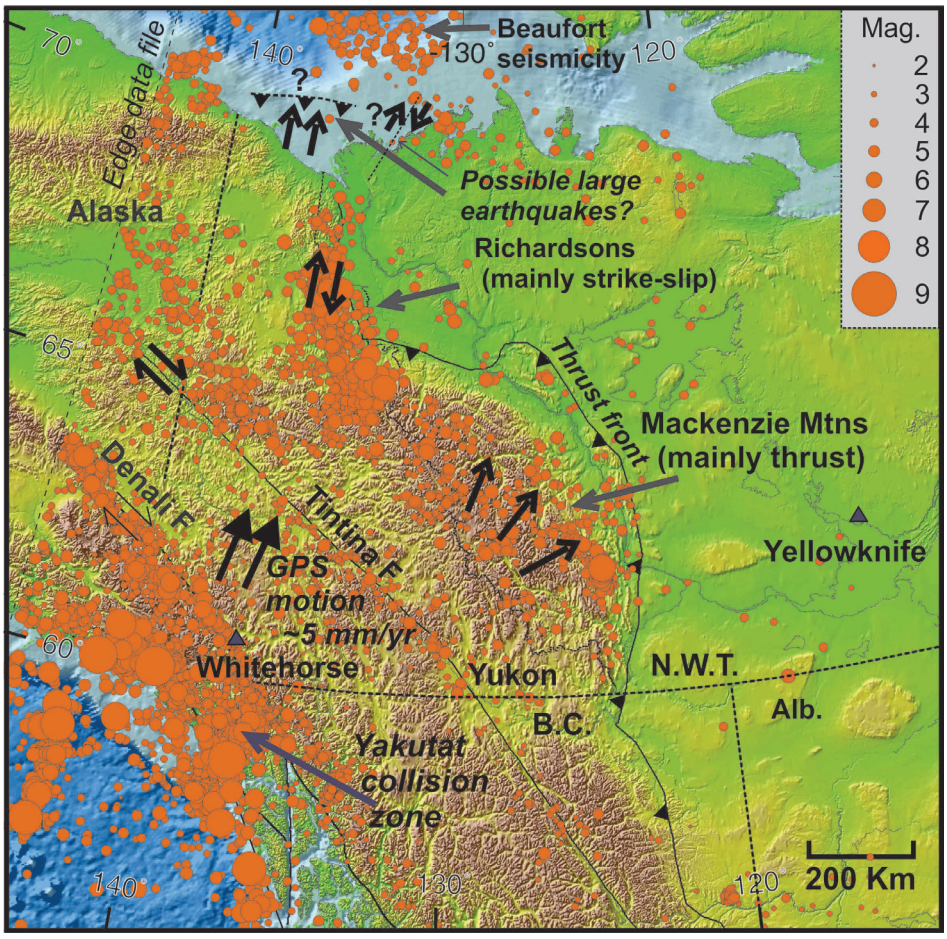

Figure 15. Seismicity across the northern Canadian Cordillera showing that the earthquakes are largely limited to the weak backarc (from the Geological Survey of Canada earthquake data base). The strong seismicity in the Mackenzie Mountains foreland belt appears to be due to the Yakutat terrane collision in the corner of the Gulf of Alaska.

cratons and platforms (e.g. Zoback et al. 2002). The seismicity across the northern Cordillera illustrates the weak backarc and the low seismicity in the adjacent strong craton (Fig. 15). This large difference in lithosphere strength between hot backarcs and cold cratons plays a major role in subsequent orogenic deformation.

Collision Deformation

In simple continental collision, one side of the suture will have been a subduction zone with a hot backarc, i.e. the hanging-wall. The other side commonly will have been a cool rifted margin, i.e. the footwall. Therefore, we expect that there will be very little deformation on the cold footwall side which has strong lithosphere. Of course, in detail, the collision zone will be complex because the former arc and forearc, and possibly accreted oceanic terranes, will lie between these bounding blocks. The type example of continental collision is that of India into Asia. As expected, almost all of the deformation has been on the Asian side, which was the former hot and weak backarc for the Tethys ocean subduction, now represented by the Himalayas and Tibet. The cratonic Indian side has hardly deformed, because its lithosphere is cool and strong. Most deformation associated with continental or terrane collision occurs in areas that formed part of the hot and weak backarc prior to collision, as concluded by Clark and Royden (2000).

Effective Elastic Thickness, Te

Two other useful indicators of the strength *versus* depth profiles that are strongly temperature-dependent are the effective elastic thickness (*Te*) and the maximum depth of earthquakes. *Te* is the thickness of the crust and upper mantle that can maintain elastic strain due to topographic and density variation loads. It may be calculated from the coherence between gravity and topography with horizontal wavelength (Fig. 16) (for the Cordillera and adjacent craton, e.g. Flück et al. 2003; Hyndman et al. 2009; for the adjacent craton, e.g. Audet and Mareschal 2007). The elastic thickness is 'effective' because it may be the combination of two or more layers, e.g. the upper crust and upper mantle with an intervening weak lower crust layer. There also is a dependence on the uncertain duration of the loads, but it provides a good first-order estimate of elastic thickness. *Te* in the Cordilleran backarc is less than 20 km, in good agreement with model predictions based on crustal temperature and composition. There is negligible strength in the upper mantle. *Te* is greater than 60 km in the craton indicating considerable strength in the uppermost mantle.

Maximum Depth of Earthquakes

The maximum depth of earthquakes in the crust depends strongly on temperature. In the Cordilleran backarc most earthquakes are shallower than 15 km, consistent with *Te* estimates. Hyndman et al. (2003) show an example for the Cascadia backarc where there is intense seismicity. The critical temperature depends somewhat on composition and strain rate, but is 350–450°C for common crustal compositions and mobile-belt strain rates. There are few areas with sufficient

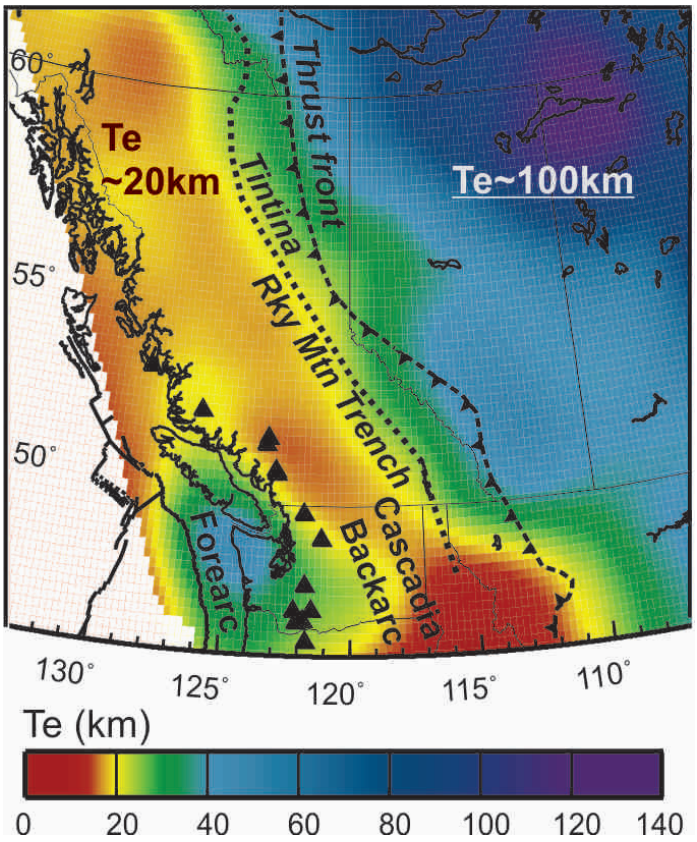

Figure 16. Effective elastic thickness *Te*, for the Cordillera and adjacent craton (after Flück et al. 2003). The average *Te* is 15–20 km for the Cordillera and over 60 km for the craton.

earthquakes to define the depth range in the craton because the strain rates are so low, and there is a strain rate dependence of the maximum temperature for seismicity. However, an area in the Cascadia forearc has a similar cool crustal thermal regime and quite rapid deformation. In that area earthquakes extend to at least 25 km in the lower crust, corresponding again to 350–450°C (Hyndman et al. 2003).

Flat Moho

An interesting related observation is that the Moho is generally quite flat in backarcs, at a depth of about 33 km in the Cordillera, in spite of a wide range of deformation structures and differences in erosion levels (see Fig. 5). This can be understood by appreciating that the high temperatures mean very low strength in the lower crust and quite low strength in the uppermost mantle. Over long geological times, i.e. tens of millions of years, the Moho can be viewed as a 'liquid-liquid' boundary that relaxes to a near-horizontal gravitational equipotential through lateral flow of the lower crust and perhaps the uppermost mantle (see Bird 1991; McKenzie et al. 2000). Cook et al. (2010) provide seismic reflection sections and discuss such 'resetting' of the Moho, among other processes.

Regional Backarc Volcanism

There is a clear association of 'backarc' volcanism with the high-temperature Cordillera and other continental backarcs, in contrast to the rare volcanism in cratons. I will not discuss this association in any detail, but simply point out the relevant

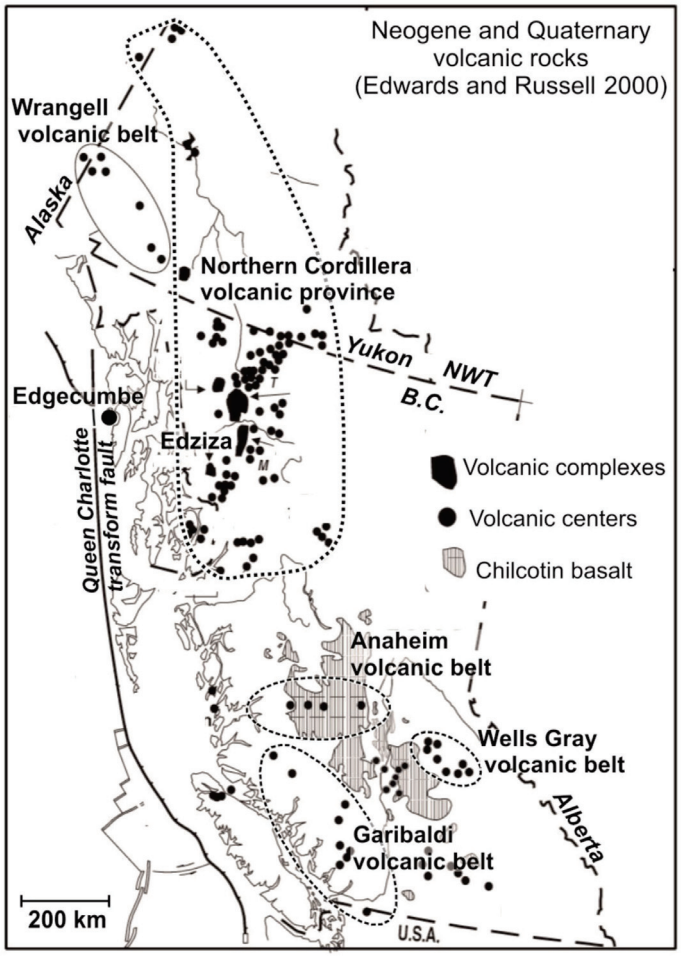

Figure 17. Distribution of the widespread Quaternary volcanic rocks that are restricted to the Cordilleran backarc (modified after Edwards and Russell 2000).

observations. Throughout most of the Cordillera there has been widespread sporadic Cenozoic volcanism as summarized by Armstrong and Ward (1991, and references therein) and Edwards and Russell (2000) (Fig. 17). The latter mapped the extent of magmatic fields between eastern Alaska and northern Mexico during the successive time intervals of 55–40, 40–25, 25–10, and 10–0 Ma. They found that some areally extensive and voluminous intermediate-composition magmatic fields coincide with extensional metamorphic core complexes that likely represent collapse of orogenically-thickened crust and high elevations. Widespread and frequent volcanism is not surprising, as temperatures are close to the upper-mantle solidus at shallow depths of ~60 km in the Cordilleran backarc mantle, and melting may be fluxed by subduction water input. A small tectonic extensional stress change can result in decompression melting. An interesting example is the Llangorse/Edziza volcanic field in northwest British Columbia (e.g. Souther et al. 1984; Armstrong and Ward 1991; Harder and Russell 2006), where the ongoing collision of the Yakutat Terrane in the corner of the Gulf of Alaska may be generating tensional tears in the adjacent lithosphere, facilitating late Cenozoic volcanism.

Lower Crust Detachment and Regional Oroclines

As I discussed earlier, the lower crust of the Cordillera and other continental backarcs must be very weak. Although it is

also tectonically weak, the uppermost mantle in most estimates has greater strength than the overlying lower crust, so the two may move independently. We therefore expect that horizontal detachment may be common (e.g. Oldow et al. 1990), allowing decoupling of the lower crust and upper mantle. Remarkably, it appears that deformational forces can be transmitted over large distances solely through the strong upper crust of backarcs. The upper mantle may not be involved or may move independently. An example of lower-crust detachment and transport across the entire northern Cordillera was given by Mazzotti and Hyndman (2002). Much credit for establishing that lower-crust detachment is common goes to German geophysicist Rolf Meissner (e.g. Meissner and Mooney 1998; Meissner et al. 2006). He seems to have convinced most of the European geoscience community, but lower-crust detachment is less accepted and appreciated in North America.

As well as the arguments for low strength based on laboratory data and estimated lower-crust temperatures that I discussed earlier (Fig. 13), we now have several indicators that widespread detachment does occur in the Cordillera and other current or thermally recent backarcs. I discuss this evidence briefly below.

Lower Crust Horizontal Reflectors

In the Cordillera and a number of other current or recent backarcs there are common horizontal seismic reflector bands in the lower crust (e.g. Matthews 1986) that may be interpreted to result from horizontal detachment shearing (for the Cordillera, e.g. Clowes and Kanasewich 1970; Parsons et al. 1992). As summarized by Meissner et al. (2006), some of the clearest densely-laminated reflectivity in the lower crust is in Phanerozoic extensional areas that we now interpret to be in current or recent backarcs. There have been many discussions of possible causes of laminated reflectivity, including compositional layering, low-velocity fluid-filled shear zones, and horizontal magmatic intrusions (e.g. Wever and Meissner 1987; Hyndman and Shearer 1989; Warner 1990). What may be an important correlation is that the estimated temperature often is where many rocks become ductile (350–450°C) at the top of the reflective layers and also at the top of the electrically-conductive layer in the lower crust of the Cordillera (Marquis et al. 1995). The conclusion of a tectonically very weak lower crust in backarcs supports the idea that lower-crust horizontal reflectivity is due to horizontal shearing.

In some areas, the horizontal seismic reflectivity extends up to the mid-crust (Fig. 18). Although the current temperatures at mid-crustal levels may be too low for ductile deformation, they may have been hotter when that level was deeper in a thickened crust in the past. Also, in a few areas the lower-crust reflectivity is 5–10 km above the base of the crust. In some hot backarcs, the lowermost crust is in granulite-facies conditions (800–900°C) and so is anhydrous. This dry mineralogy may be stronger than the overlying slightly shallower and therefore cooler amphibolite-facies regions where there is more bound water that reduces the strength.

The reflectors are interpreted to result from stretching and flow of heterogeneities such as mafic intrusions, producing long thin sub-horizontal reflecting layers with marked contrasts in seismic impedance. Such layers could be 'frozen in' and remain as temperatures decline and the crust strengthens.

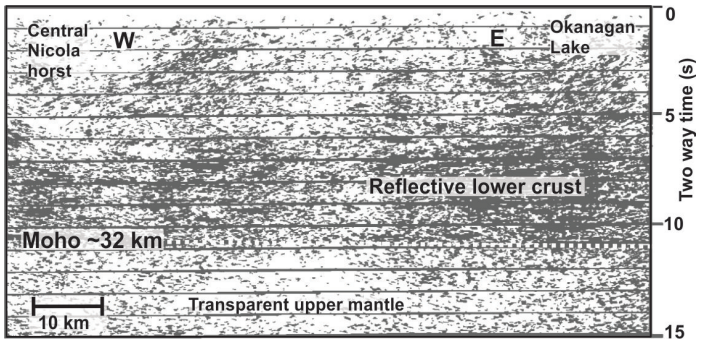

Figure 18. Seismic reflection section from the SE Canadian Cordillera Lithoprobe surveys showing pervasive lower-crust horizontal reflectors (after Cook et al. 1992).

Oueity and Clowes (2010) proposed such a development to explain seismic reflection and refraction characteristics at the base of the crust beneath the Paleoproterozic Great Bear magmatic arc in the Canadian Northwest Territories. However, lower-crust horizontal reflectors are less common in geologically older areas, so a variety of geological processes may reduce the layered impedance contrasts over long periods of time.

Important support for shearing as the origin of lower-crustal reflectors, is the observation of banding or lamination and anisotropy in amphibolite- to granulite-facies rocks formed in the lower crust, as inferred from petrological studies. In several large areas, exhumed lower-crustal rocks with strong horizontal compositional laminations are now exposed at the surface (e.g. Sandiford 1989; Dumond et al. 2010; Regan et al. 2014). Temperatures at the time of the lower-crust ductile flow were estimated to be about 800°C at 30 km depth.

In addition to these examples, there is the question of the role of lower-crust shearing in the formation of gneiss generally, especially banded gneisses (e.g. Myers 1978). The foliation of many, if not most, gneisses may result from horizontal shearing when they were in the lower crust. Where there are banded gneiss layers with strong impedance contrasts in the lower crust, they may be responsible for the observed horizontal seismic reflectivity.

Tectonic Indicators of Lower Crust Detachment

Lower-crust detachment is inferred from large-scale horizontal tectonic motions, especially the overthrusting of the upper crust of backarcs over the adjacent craton or stable platform as argued by Oldow et al. (1990). In a few places globally, where the backarc crust is especially thick, there may be extrusion of the very weak lower crust (e.g. Bird 1991; Royden et al. 1997; Beaumont et al. 2001), including under core complexes (Block and Royden 1990). Lower-crust extrusion has been discussed for an area of the SE Canadian Cordillera (e.g. Gervais and Brown 2011). In backarcs that have very thick crust, like the high Andes, it has been suggested that there may even be convection in the lower crust (e.g. Babeyko et al. 2002).

Several tectonic observations support horizontal shearing in the lower crust and horizontal transport of the upper crust in backarcs. Lower-crust detachments seem necessary to explain the common characteristics of foreland fold and thrust belts where the upper mobile belt crust is thrust over the stable craton or platform, apparently without the upper mantle moving, or moving independently. The lower-crustal detach-

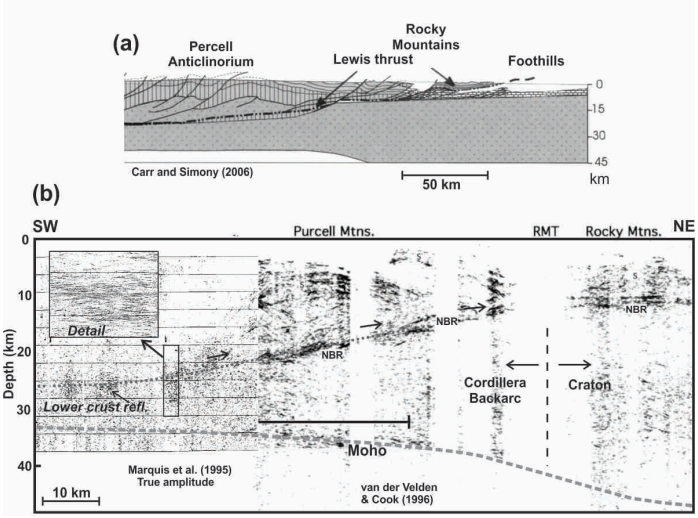

Figure 19. (a) Geological section across the Rocky Mountain Front (after Carr and Simony 2006) illustrating the thrusting of the backarc upper crust over the craton. (b) Seismic reflection section showing the lower-crust detachment in the Cordillera (after Marquis et al. 1995) rising to join the basal thrust (NBR) of the foreland sediment section (after van de Velden and Cook 1996).

ment in the backarc hinterland may connect to the basal detachment in foreland thrusting that is weakened by high fluid pressure (see seismic sections in Fig. 19). Examples are the current northern Canadian Cordillera (Mazzotti and Hyndman 2002), and Laramide-age structures in the southern Canadian Cordillera (e.g. Brown et al. 1992; van der Velden and Cook 1996; Hyndman and Lewis 1999; Carr and Simony 2006). The current Andes of central South America (Hindle et al. 2002) may be similar. As previously discussed, the Yakutat terrane collision in the corner of the Gulf of Alaska has been interpreted to be the cause of current seismically-active thrust deformation of the Mackenzie Mountains at the foreland belt 800 km to the east (Fig. 20), and for northerly crustal motion and thrusting in the Mackenzie River Delta (Mazzotti and Hyndman 2002; Leonard et al. 2008). The backarc lower-crust detachment must be sufficiently weak to transfer the stress from the plate-boundary collision and the gravitational potential of the elevation of the high coastal mountains to the weak foreland fold and thrust belt far to the east, even though only the upper Cordilleran crust has significant strength. In contractional orogens, it has been argued that a through-going basal detachment in the lower crust separates the entire crustal section from the underlying mantle lithosphere (e.g. Oldow et al. 1990; Mazzotti and Hyndman 2002) (Fig. 21). If this is correct for backarc mobile belts like the Cordillera, thrust faults, transcurrent faults, and extensional faulting commonly are restricted to the overlying detached crustal section.

Oroclines

Another geological process that may involve lower-crust detachment is the development of oroclines. The concept of large-scale crustal deformation in a horizontal plane with little vertical deformation was first described in detail by Warren Carey in Tasmania (Carey 1955). Johnston et al. (2013) provided a detailed review of this process that involves bending or buckling about a vertical axis of rotation. Several examples in backarcs are the Cordillera–Alaska orocline (e.g. Johnston

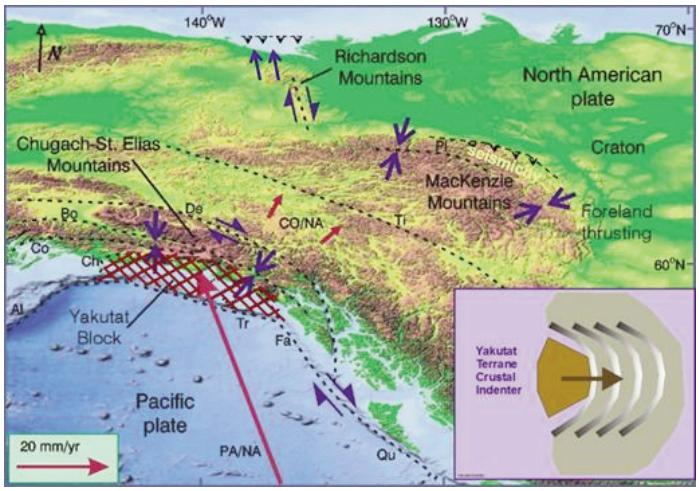

Figure 20. The Yakutat Terrane collision indenter in the Gulf of Alaska that drives the whole Cordilleran upper crust across the Cordillera to the active Mackenzie Mountains fold and thrust belt, and north to the fold and thrust belt of the Mackenzie River Delta (Mazzotti and Hyndman 2002; Leonard et al. 2008).

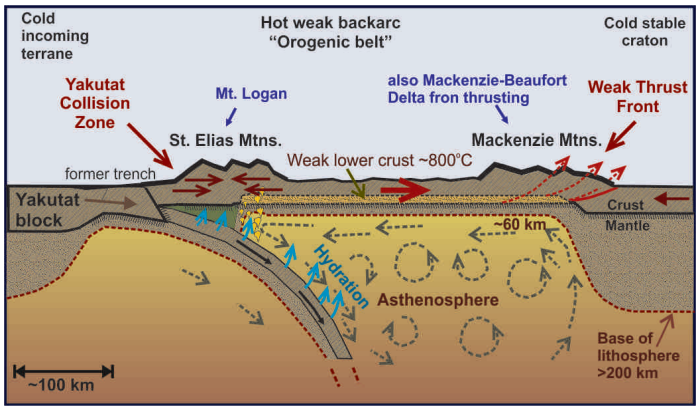

Figure 21. Model cross-section illustrating the current strain transfer across the northern Cordillera from the Yakutat collision zone to the Mackenzie Mountains that are overthrusting the craton (after Mazzotti and Hyndman 2002).

2001, 2008), and the Cantabrian of northern Spain (e.g. Weil et al. 2000). There is an important question in oroclinal bending that has not yet been well studied, i.e. what happens to the upper mantle? If the upper mantle is involved in the bending, we should expect substantial thickening and thinning of the lithosphere at bends that is not evident in topography or structure. If the upper mantle and lower crust have negligible tectonic strength, as suggested here, they can readily move out of the way as the upper crust bends, and the upper crust may move independently over the lower crust detachment. This model requires that there be translation of the upper crust over hundreds of kilometres.

Since we conclude that sufficiently high temperatures for lower-crust detachment mainly occur in hot subduction zone backarcs, the weak orogenic hinterland that hosts most large-scale oroclines must also be in the backarcs. Cratons and other tectonically old lithospheres are too strong to deform in this way. A tentative conclusion is that most oroclines involve only the upper crust. The uppermost mantle may not move or may follow a different trajectory. The physical processes involved in oroclinal deformation, especially the depth of deformation, are topics that need further study.

Continental Collision, Orogenic Heat, and Bimodal Metamorphic Belts

Barrovian Metamorphism

Another important recent conclusion that I will discuss only briefly is that the high temperatures estimated for backarcs like the Cordillera are consistent with the increasing evidence that regional 'Barrovian' metamorphism predates the deformation in orogenic belts. There is no "heat of orogeny." The most common style of regional metamorphism in time and space is the 'Barrovian' metamorphic series first defined by George Barrow (1893) who, in the late 19th century, mapped a series of zones of progressive metamorphism in a sequence exposed in the Scottish Highlands. Subsequent studies have shown peak metamorphic temperatures of 600–700°C at crustal depths of 20–30 km (e.g. Jamieson et al. 1998, and references therein). The temperature at the base of a 35 km thick crust like the Cordillera thus was about 800°C, if there was a normal downward increasing gradient. This is very similar to the temperatures that we infer at the base of the crust in the Cordillera and other current backarcs.

High paleotemperatures are a defining feature of now deeply-exhumed orogenic belts, as inferred from widespread high-temperature regional metamorphism, granitic plutonism, and ductile deformation at mid- to lower-crustal depths. However, the origin of these regional high paleotemperatures has been difficult to understand. As Jamieson et al. (1998) state, a quantitative explanation for Barrovian metamorphism in thermal-tectonic models of orogenesis has proven elusive (e.g. Loosveld and Etheridge 1990; Jamieson et al. 1998; Thompson et al. 2001; Vanderhaeghe and Teyssier 2001; Collins 2002). Commonly the heat and high temperatures are simply ascribed to 'orogenic heating' without reference to the actual mechanism. In fact, most orogenic processes should absorb heat. Orogenic belts that involve underthrusting put cool near-surface material at greater depths, resulting in decreased temperature gradients. Alternatively, the crust may be tectonically thickened, which stretches the isotherms vertically, reducing the gradient. Significant frictional strain-heating is unlikely because, if the crust is strong enough for significant frictional heating, it is too strong to be deformed by available plate-boundary and gravitational forces.

Two main sources of heat have been previously proposed. The first is the emplacement of upper crustal rocks with high radioactive heat-generation into the lower crust during the shortening (see Jamieson et al. 1998, 2007). In shortening and underthrusting models there is an evolving competition between cooling by the underthrusting and thickening, and radioactive heating within the deforming orogenic belt. Such underthrusting can produce the metamorphic temperatures (e.g. Jamieson et al. 1998). However, this explanation predicts maximum temperatures 50–100 m.y. after collision, whereas peak metamorphic assemblages are commonly argued to be earlier than, or at least synchronous with, the thickening (e.g. Thompson et al. 2001; Collins 2002). A good example where the high temperatures are concluded to originate some 100 m.y. prior to deformation is the Aracuai orogeny of Eastern Brazil (Gradim et al. 2014). The radioactive-heating model also does not explain how shortening and thickening can be initiated in cold, strong lithosphere prior to the heating. As I discussed earlier, the available plate-boundary and gravitational forces are much too small to deform stable cold strong lithosphere. The second suggested heat source is backarc extension prior to collision. This explanation requires that such extension must occur less than about 50 m.y. before the collision orogeny in order for the heat not to have decayed. As well, Thompson et al. (2001) argue that there must be thinning of the mantle lithosphere with little thinning of the crust to explain the inferred crustal thicknesses following collision. A much more satisfactory model is that hot and thin backarc lithosphere is the primary locus of shortening (Hyndman et al. 2005), such that the high temperatures predate the deformation. This explanation corresponds to the vise or inherited-weakness model (e.g. Ellis et al. 1998; Thompson et al. 2001; Collins 2002).

We argue that the heat for the metamorphism comes from the pre-existing hot backarc, not from the orogenic deformation process itself. Figure 22 illustrates the correspondence between the Cordillera backarc thermal regime as in Figure 10, and the temperature-depth profile of Barrovian metamorphic gradients, i.e. 600–700°C at 20–30 km (see summary by Jamieson et al. 1998). Recognizing that most continental- or terrane-collision orogens inherit pre-existing hot and weak backarcs may resolve the long-standing problem of the origin of the high temperatures associated with orogeny. There is no actual "heat of orogeny." The high temperatures existed in the backarc of one side of the collisional orogen prior to the collision and the shortening deformation.

For the type case of Scotland Barrovian metamorphism, the situation is well stated by Johnson and Strachan (2006):

> "*Geochronological data indicate that the Caledonian thrust sheets of NW Scotland were assembled in less than 18 Ma, yet regional Barrovian metamorphism to amphibolite facies and local melting occurred syn-thrusting. …it is clear that there is insufficient time to generate the high metamorphic temperatures during the thrusting event. …a plausible explanation for the heat source is …a 20–25 Ma period of crustal heating in a back-arc setting… Most of the orogenic heat therefore came from the pre-existing back-arc rather than the orogenic process itself.*"

Orogenic Belt One-sided Deformation

The high-temperature backarc thermal regime and inferred weak lithosphere model also provides insight into the shortening in continental collisions. As we should expect, the deformation occurs primarily on the side of the closing ocean that had the arc and the weak backarc. This one-sided deformation pattern is very clear for the India–Asia collision. Most of the deformation has been on the Asian side, which represents the former hot and weak backarc. The leading edge of the Himalayan Mountains appears to be backarc crust overthrusting the largely undeformed strong Indian lithosphere. Initial shortening and crustal thickening appear to be concentrated at the leading and trailing edges of the backarc mobile belt. In this example, shortening is mainly in the Himalayan mountain front and in several shortening zones to the north of Tibet. The Tibetan plateau has experienced little shortening, at least of its upper crust. Another example that I have worked on is the current collision of the Yakutat terrane in the Gulf of Alaska that started at about 6 Ma. Here, there has been strong

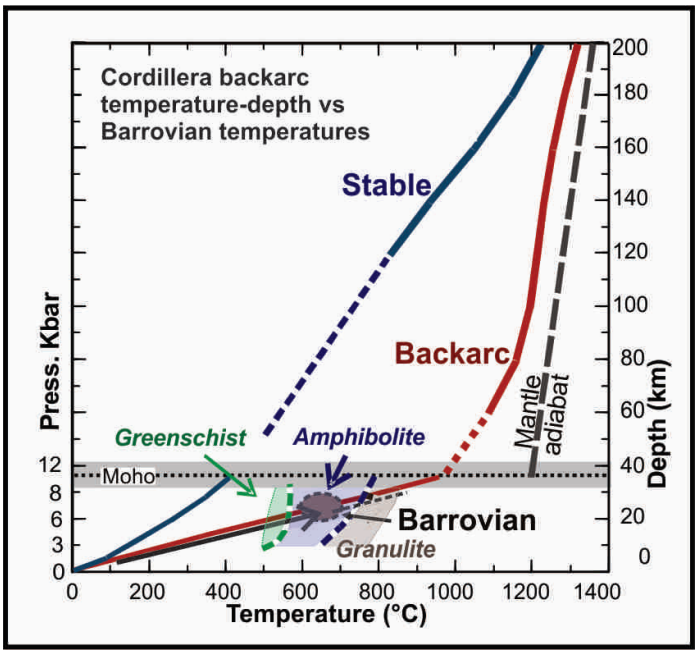

Figure 22. Barrovian metamorphic temperatures (e.g. 600–700°C at 20–30 km; see Jamieson et al. 1998) compared to temperatures estimated for the Cordillera and other backarcs. The lower crust is in granulite-facies conditions.

shortening in the coastal collision zone that was a former backarc (St. Elias Mountains area) and again in foreland thrusting of the Mackenzie Mountains of the eastern Cordillera. There is little shortening in the intervening central Cordillera as evident by the pattern of current seismicity (Fig. 15), and the crust remains thin (32–35 km) (e.g. Mazzotti and Hyndman 2002). With further shortening, the high temperatures may allow the crust of the whole backarc to be thickened to >50 km, such as for the Altiplano of the South American Andes, for Tibet, and perhaps for the Laramide orogeny of western North America, producing a broad high elevation plateau.

Bimodal Metamorphism

Another characteristic of ancient collisional orogenic belts is the presence of paired bimodal metamorphic belts, defined by contrasting high-pressure/low temperature and low-pressure/high-temperature conditions. As described by Brown (2010), "*Paired metamorphic belts are belts of contrasting... thermal gradient, one warmer and the other colder, juxtaposed by plate tectonics process, formed during or shortly after the formation of the containing rock stratum.*" This metamorphic contrast may be explained by one side (the hanging-wall side) of a suture being the former hot arc-backarc hinterland and the other being the incoming little-deformed cold continental crust (the footwall side) (e.g. Brown 2006).

CONCLUSIONS

The conclusions of the work summarized in this article are based on the now strong evidence that the North American Cordillera and most other backarcs are remarkably uniformly hot with thin (~60 km) lithospheres. They contrast with the cold Canadian Shield, and other cratons and stable platforms, (thermotectonic ages greater than 500 Ma) which have thick (200–250 km) lithospheres. The thermal structure of backarc regions has consequences for their elevations, mechanical strength and other physical properties, for regional metamorphism, and has important implications for the behaviour of the crust and mantle during collisional orogenesis.

We now have strong constraints on the temperatures in the crust and upper mantle. These include, (1) Heat flow and radioactive heat-generation data, (2) Temperature-sensitive upper-mantle seismic velocities, especially from shear-wave tomography, and (3) Kimberlite and volcanic xenoliths that constrain the temperature-depth profile in the upper mantle at the time of eruption. Several other constraints with lesser precision indicate similar thermal regimes, and support the conclusion of uniformly high temperatures in backarc regions in contrast to cold cratons and other stable areas.

Some of the numerous important consequences of the high Cordillera backarc temperatures are:

(1) The high elevation of the Cordillera is supported by thermal isostasy, in spite of the region having a thin crust.

(2) The Cordillera and other mountain belts are mainly in backarcs. These regions are mobile belts; they exhibit long-term weakness compared to adjacent cratons and stable platforms. They deform readily because they are hot and weak enough to be deformed by plate-boundary forces and gravitational forces linked to their high elevations. Most current seismicity is in weak backarcs. Backarcs may be hot because of shallow asthenosphere convection, facilitated by water driven upward from the underlying subducting plate.

(3) Most volcanism away from subduction zone volcanic arcs is located in backarcs like the Cordillera. Temperatures are close to the solidus at shallow depths in the mantle and partial melting may be fluxed by water being driven off the underlying subducting oceanic plate or by extensional stresses.

(4) Orogenic shortening during continental collision is concentrated in former backarc mobile belts that are much weaker than the adjacent stable areas. The pre-existing or inherited high temperatures of these regions provide an explanation for widespread orogenic plutonism, high-temperature regional metamorphism, and ductile crustal deformation.

(5) Backarc and subsequent orogenic belt temperatures are high enough to allow lower-crust detachment that decouples complex surface tectonics from the uppermost mantle. Such detachment allows the upper backarc crust to overthrust strong cratons in foreland belts. The detachment also may mean that most oroclines are detached in the lower crust and do not involve the mantle. In a few areas of hot and thick crust, lower-crustal flow and extrusion may occur.

(6) The "heat of orogeny" and Barrovian metamorphism may be a consequence of high backarc temperatures prior to collision, not a result of the collision process itself. Paired metamorphic belts may represent juxtaposition in a collision suture of a hot backarc against a cold craton or stable platform.

ACKNOWLEDGEMENTS

I wish to thank the many graduate students, postdoctoral fellows, and colleagues that have collaborated with me on the various aspects of the work described in this article, and that have provided stimulating and challenging discussions. Claire Currie, Stephane Mazzotti, Lucinda Leonard, Paul Flück, and Guy Marquis are especially thanked. Reviewers Ron Clowes and Andrew Hynes made very helpful comments and recommendations that significantly improved the manuscript, and a third reviewer provided some thought-provoking discussion of the concepts involved.

REFERENCES

Adams, J., and Atkinson, G., 2003, Development of seismic hazard maps for the proposed 2005 edition of the National Building Code of Canada: Canadian Journal of Civil Engineering, v. 30, p. 255–271, http://dx.doi.org/10.1139/l02-070.

Aitchison, J.C., Ali, J.R., and Davis, A.M., 2007, When and where did India and Asia collide?: Journal of Geophysical Research, v. 112, B05423, http://dx.doi.org/10.1029/2006JB004706.

Arcay, D., Doin, M.P., Tric, E., Bousquet, R., and De Capitani, C., 2006, Overriding plate thinning in subduction zones: Localized convection induced by slab dehydration: Geochemistry, Geophysics, Geosystems, v. 7, Q02007, http://dx.doi.org/10.1029/2005GC001061.

Argand, E., 1924, La tectonique de l'Asie: International Geological Congress Proceedings, v. 7, p. 171–372.

Armstrong, R.L., and Ward, P., 1991, Evolving geographic patterns of Cenozoic magmatism in the North American Cordillera: The temporal and spatial association of magmatism and metamorphic core complexes: Journal of Geophysical Research, v. 96, p. 13201–13224, http://dx.doi.org/10.1029/91JB00412.

Artemieva, I.M., and Mooney, W.D., 2001, Thermal thickness and evolution of Precambrian lithosphere: A global study: Journal of Geophysical Research, v. 106, p. 16387–16414, http://dx.doi.org/10.1029/2000JB900439.

Audet, P., and Mareschal, J-C., 2007, Wavelet analysis of the coherence between Bouguer gravity and topography: application to the elastic thickness anisotropy in the Canadian Shield: Geophysical Journal International, v. 168, p. 287–298, http://dx.doi.org/10.1111/j.1365-246X.2006.03231.x.

Babeyko, A.Y., Sobolev, S.V., Trumbull, R.B., Oncken, O., and Lavier, L.L., 2002, Numerical models of crustal scale convection and partial melting beneath the Altiplano–Puna plateau: Earth and Planetary Science Letters, v. 199, p. 373–388, http://dx.doi.org/10.1016/S0012-821X(02)00597-6.

Bao, X., Eaton, D.W., and Guest, B., 2014, Plateau uplift in western Canada caused by lithospheric delamination along a craton edge: Nature Geoscience, v. 7, p. 830–833, http://dx.doi.org/10.1038/ngeo2270.

Barrow, G., 1893, On an intrusion of muscovite-biotite gneiss in the southeastern Highlands of Scotland, and its accompanying metamorphism: Quaternary Journal of the Geological Society, v. 49, p. 330–358, http://dx.doi.org/10.1144/GSL.JGS.1893.049.01-04.52.

Beaumont, C., Jamieson, R.A., Nguyen, M.H., and Lee, B., 2001, Himalayan tectonics explained by extrusion of a low-viscosity crustal channel coupled to focused surface denudation: Nature, v. 414, p. 738–742, http://dx.doi.org/10.1038/414738a.

Beck, M.E., Jr., 1988, Analysis of late Jurassic–recent paleomagnetic data from active plate margins of South America: Journal of South American Earth Science, v. 1, p. 39–52, http://dx.doi.org/10.1016/0895-9811(88)90014-4.

Becker, T.W., Faccenna, C., Humphreys, E.D., Lowry, A.R., and Miller, M.S., 2013, Static and dynamic support of western United States topography: Earth and Planetary Science Letters, v. 402, p. 234–246, http://dx.doi.org/10.1016/j.epsl.2013.10.012.

Bilham, R., Larson, K., Freymueller, J., and Project Idylhim members, 1997, GPS measurements of present-day convergence across the Nepal Himalaya: Nature, v. 386, p. 61–64, http://dx.doi.org/10.1038/386061a0.

Bird, P., 1991, Lateral extrusion of lower crust from under high topography in the isostatic limit: Journal of Geophysical Research, v. 96, p. 10275–10286, http://dx.doi.org/10.1029/91JB00370.

Blackwell, D.D., Steele, J.L., Kelley, S., and Korosec, M.A., 1990, Heat flow in the state of Washington and thermal conditions in the Cascade Range: Journal of Geophysical Research, v. 95, p. 19495–19516, http://dx.doi.org/10.1029/JB095iB12p19495.

Block, L., and Royden, L.H., 1990, Core complex geometries and regional scale flow in the lower crust: Tectonics, v. 9, p. 557–567, http://dx.doi.org/10.1029/TC009i004p00557.

Braun, J., 2010, The many surface expressions of mantle dynamics: Nature Geoscience, v. 3, p. 825–833, http://dx.doi.org/10.1038/ngeo1020.

Brown, M., 2006, Duality of thermal regimes is the distinctive characteristic of plate tectonics since the Neoarchean: Geology, v. 34, p. 961–964, http://dx.doi.org/10.1130/G22853A.1.

Brown, M., 2010, Paired metamorphic belts revisited: Gondwana Research, v. 18, p. 46–59, http://dx.doi.org/10.1016/j.gr.2009.11.004.

Brown, R.L., Carr, S.D., Johnson, B.J., Coleman, V.J., Cook, F.A., and Varsek, J.L., 1992, The Monashee décollement of the southern Canadian Cordillera: a crustal-scale shear zone linking the Rocky Mountain Foreland belt to lower crust beneath accreted terrane, *in* McClay, K.R., *ed.*, Thrust tectonics: Springer Netherlands, p. 357–364.

Burianyk, M.J.A., Kanasewich, E.R., and Udey, N., 1997, Broadside wide-angle seismic studies and three-dimensional structure of the crust in the southeast Canadian Cordillera: Canadian Journal of Earth Sciences, v. 34, p. 1156–1166, http://dx.doi.org/10.1139/e17-093.

Canil, D., 2008, Canada's craton: A bottoms-up view: GSA Today, v. 18, p. 4–10, http://dx.doi.org/10.1130/GSAT01806A.1.

Carey, S.W., 1955, The orocline concept in geotectonics-Part I: Papers and Proceedings of the Royal Society of Tasmania, v. 89, p. 255–288.

Carr, S.D., and Simony, P.S., 2006, Ductile thrusting *versus* channel flow in the southeastern Canadian Cordillera: evolution of a coherent crystalline thrust sheet: Geological Society, London, Special Publications, v. 268, p. 561–587, http://dx.doi.org/10.1144/GSL.SP.2006.268.01.26.

Cassidy, J.F., 1995, Review: Receiver function studies in the southern Canadian Cordillera: Canadian Journal of Earth Sciences, v. 32, p. 1514–1519, http://dx.doi.org/10.1139/e95-123.

Chapman, D.S., and Pollack, H.N., 1975, Global heat flow: A new look: Earth and Planetary Science Letters, v. 28, p. 23–32, http://dx.doi.org/10.1016/0012-821X(75)90069-2.

Chapman, D.S., and Pollack, H.N., 1977, Regional geotherms and lithospheric thickness: Geology, v. 5, p. 265–268, http://dx.doi.org/10.1130/0091-7613(1977)5<265:RGALT>2.0.CO;2.

Christensen, N.I., and Mooney, W.D., 1995, Seismic velocity structure and composition of the continental crust: A global view: Journal of Geophysical Research, v. 100, p. 9761–9788, http://dx.doi.org/10.1029/95JB00259.

Clark, M.K., and Royden, L.H., 2000, Topographic ooze: Building the eastern margin of Tibet by lower crustal flow: Geology, v. 28, p. 703–706, http://dx.doi.org/10.1130/0091-7613(2000)28<703:TOBTEM>2.0.CO;2.

Clowes, R.M., and Kanasewich, E.R., 1970, Seismic attenuation and the nature of reflecting horizons within the crust: Journal of Geophysical Research, v. 75, p. 6693–6705, http://dx.doi.org/10.1029/JB075i032p06693.

Clowes, R.M., Zelt, C.A., Amor, J.R., and Ellis, R.M., 1995, Lithospheric structure in the southern Canadian Cordillera from a network of seismic refraction lines: Canadian Journal of Earth Sciences, v. 32, p. 1485–1513, http://dx.doi.org/10.1139/e95-122.

Collins, W.J., 2002, Hot orogens, tectonic switching, and creation of continental crust: Geology, v. 30, p. 535–538, http://dx.doi.org/10.1130/0091-7613(2002)030<0535:HOTSAC>2.0.CO;2.

Cook, F.A., Varsek, J.L., Clowes, R.M., Kanasewich, E.R., Spencer, C.S., Parrish, R.R., Brown, R.L., Carr, S.D., Johnson, B.J., and Price, R.A., 1992, Lithoprobe crustal reflection cross section of the southern Canadian Cordillera, 1, Foreland thrust and fold belt to Fraser River Fault: Tectonics, v. 11, p. 12–35, http://dx.doi.org/10.1029/91TC02332.

Cook, F.A., White, D.J., Jones, A.G., Eaton, D.W.S., Hall, J., and Clowes, R.M., 2010, How the crust meets the mantle: Lithoprobe perspectives on the Mohorovičić discontinuity and crust–mantle transition: Canadian Journal of Earth Sciences, v. 47, p. 315–351, http://dx.doi.org/10.1139/E09-076.

Currie, C.A., and Hyndman, R.D., 2006, The thermal structure of subduction zone back arcs: Journal of Geophysical Research, v. 111, B08404, http://dx.doi.org/10.1029/2005JB004024.

Currie, C.A., Wang, K., Hyndman, R.D., and He, J., 2004, The thermal effects of steady-state slab-driven mantle flow above a subducting plate: The Cascadia subduction zone and backarc: Earth and Planetary Science Letters, v. 223, p. 35–48, http://dx.doi.org/10.1016/j.epsl.2004.04.020.

Dewey, J.F., and Bird, J.M., 1970, Mountain belts and the new global tectonics: Journal of Geophysical Research, v. 75, p. 2625–2647, http://dx.doi.org/10.1029/JB075i014p02625.

Dixon, J.E., Dixon, T.H., Bell, D.R., and Malservisi, R., 2004, Lateral variation in upper mantle viscosity: Role of water: Earth and Planetary Science Letters, v. 222, p. 451–467, http://dx.doi.org/10.1016/j.epsl.2004.03.022.

Dumond, G., Goncalves, P., Williams, M.L., and Jercinovic, M.J., 2010, Subhorizontal fabric in exhumed continental lower crust and implications for lower crustal flow: Athabasca granulite terrane, western Canadian Shield: Tectonics, v. 29, TC2006, http://dx.doi.org/10.1029/2009TC002514.

Eaton, D.W., Darbyshire, F., Evans, R.L., Grütter, H., Jones, A.G., and Yuan, X., 2009, The elusive lithosphere–asthenosphere boundary (LAB) beneath cratons: Lithos, v. 109, p. 1–22, http://dx.doi.org/10.1016/j.lithos.2008.05.009.

Edwards, B.R., and Russell, J.K., 2000, Distribution, nature, and origin of Neogene–Quaternary magmatism in the northern Cordilleran volcanic province, Canada: Geological Society of America Bulletin, v. 112, p. 1280–1295, http://dx.doi.org/10.1130/0016-7606(2000)112<1280:DNAOON>2.0.CO;2.

Ellis, S., Beaumont, C., Jamieson, R.A., and Quinlan, G., 1998, Continental collision

including a weak zone: the vise model and its application to the Newfoundland Appalachians: Canadian Journal of Earth Sciences, v. 35, p. 1323–1346, http://dx.doi.org/10.1139/e97-100.

Engebretson, D.C., Cox, A., and Gordon, R.G., 1985, Relative motions between oceanic and continental plates in the Pacific basin: Geological Society of America Special Papers, v. 206, p. 1–60, http://dx.doi.org/10.1130/SPE206-p1.

Feldl, N., and Bilham, R., 2006, Great Himalayan earthquakes and the Tibetan plateau: Nature, v. 444, p. 165–170, http://dx.doi.org/10.1038/nature05199.

Flament, N., Gurnis, M., and Müller, R.D., 2013, A review of observations and models of dynamic topography: Lithosphere, v. 5, p. 189–210, http://dx.doi.org/10.1130/L245.1.

Flück, P., Hyndman, R.D., and Lowe, C., 2003, Effective elastic thickness T_e of the lithosphere in western Canada: Journal of Geophysical Research, v. 108, 2430, http://dx.doi.org/10.1029/2002JB002201.

Frankel, A.D., Mueller, C.S., Barnhard, T.P., Leyendecker, E.V., Wesson, R.L., Harmsen, S.C., Klein, F.W., Perkins, D.M., Dickman, N.C., Hanson, S.L., and Hopper, M.G., 2000, USGS national seismic hazard maps: Earthquake spectra, v. 16, p. 1–19, http://dx.doi.org/10.1193/1.1586079.

Gervais, F., and Brown, R.L., 2011, Testing modes of exhumation in collisional orogens: Synconvergent channel flow in the southeastern Canadian Cordillera: Lithosphere, v. 3, p. 55–75, http://dx.doi.org/10.1130/L98.1.

Gough, D.I., 1986, Mantle upflow tectonics in the Canadian Cordillera: Journal of Geophysical Research, v. 91, p. 1909–1919, http://dx.doi.org/10.1029/JB091iB02p01909.

Gradim, C., Roncato, J., Pedrosa-Soares, A.C., Cordani, U., Dussin, I., Alkmim, F.F., Queiroga, G., Jacobsohn, T., da Silva, L.C., and Babinski, M., 2014, The hot back-arc zone of the Araçuaí orogen, Eastern Brazil: from sedimentation to granite generation: Brazilian Journal of Geology, v. 44, p. 155–180, http://dx.doi.org/10.5327/Z2317-4889201400010012.

Greenfield, A.M.R., Ghent, E.D., and Russell, J.K., 2013, Geothermobarometry of spinel peridotites from southern British Columbia: implications for the thermal conditions in the upper mantle: Canadian Journal of Earth Sciences, v. 50, p. 1019–1032, http://dx.doi.org/10.1139/cjes-2013-0037.

Griffin, W.L., O'Reilly, S.Y., Doyle, B.J., Pearson, N.J., Coopersmith, H., Kivi, K., Malkovets, V., and Pokhilenko, N., 2004, Lithosphere mapping beneath the North American plate: Lithos, v. 77, p. 873–922, http://dx.doi.org/10.1016/j.lithos.2004.03.034.

Gutscher, M-A., Spakman, W., Bijwaard, H., and Engdahl, E.R., 2000, Geodynamics of flat subduction: Seismicity and tomographic constraints from the Andean margin: Tectonics, v. 19, p. 814–833, http://dx.doi.org/10.1029/1999TC001152.

Harder, M., and Russell, J.K., 2006, Thermal state of the upper mantle beneath the Northern Cordilleran Volcanic Province (NCVP), British Columbia, Canada: Lithos, v. 87, p. 1–22, http://dx.doi.org/10.1016/j.lithos.2005.05.002.

Hasebe, K., Fujii, N., and Uyeda, S., 1970, Thermal processes under island arcs: Tectonophysics, v. 10, p. 335–355, http://dx.doi.org/10.1016/0040-1951(70)90114-9.

Hasterok, D., and Chapman, D.S., 2007, Continental thermal isostasy: 2. Application to North America: Journal of Geophysical Research, v. 112, B06415, http://dx.doi.org/0.1029/2006JB004664.

Hindle, D., Kley, J., Klosko, E., Stein, S., Dixon, T., and Norabuena, E., 2002, Consistency of geologic and geodetic displacements during Andean orogenesis: Geophysical Research Letters, v. 29, p. 29-1–29-4, http://dx.doi.org/10.1029/2001GL013757.

Hyndman, R.D., 2010, The consequences of Canadian Cordillera thermal regime in recent tectonics and elevation: a review: Canadian Journal of Earth Sciences, v. 47, p. 621–632, http://dx.doi.org/10.1139/E10-016.

Hyndman, R.D., and Currie, C.A., 2011, Why is the North America Cordillera high? Hot backarcs, thermal isostasy, and mountain belts: Geology, v. 39, p. 783–786, http://dx.doi.org/10.1130/G31998.1.

Hyndman, R.D., and Hamilton, T.S., 1993, Queen Charlotte area Cenozoic tectonics and volcanism and their association with relative plate motions along the northeastern Pacific margin: Journal of Geophysical Research, v. 98, p. 14257–14277, http://dx.doi.org/10.1029/93JB00777.

Hyndman, R.D., and Lewis, T.J., 1995, Review: The thermal regime along the southern Canadian Cordillera Lithoprobe corridor: Canadian Journal of Earth Sciences, v. 32, p. 1611–1617, http://dx.doi.org/10.1139/e95-129.

Hyndman, R.D., and Lewis, T.J., 1999, Geophysical consequences of the Cordillera-craton thermal transition in southwestern Canada: Tectonophysics, v. 306, p. 397–422.

Hyndman, R.D., and Shearer, P.M., 1989, Water in the lower continental crust: modelling magnetotelluric and seismic reflection results: Geophysical Journal International, v. 98, p. 343–365.

Hyndman, R.D., Mazzotti, S., Weichert, D., and Rogers, G.C., 2003, Frequency of large crustal earthquakes in Puget Sound–Southern Georgia Strait predicted from geodetic and geological deformation rates: Journal of Geophysical Research, v. 108, 2033, http://dx.doi.org/10.1029/2001JB001710.

Hyndman, R.D., Currie, C.A., and Mazzotti, S.P., 2005, Subduction zone backarcs, mobile belts, and orogenic heat: GSA Today, v. 15, p. 4–10, http://dx.doi.org/10.1130/1052-5173(2005)15<4:SZBMBA>2.0.CO;2.

Hyndman, R.D., Currie, C.A., Mazzotti, S., and Fredricksen, A., 2009, Temperature control of continental lithosphere thickness, Te vs Vs: Earth and Planetary Science Letters, v. 277, p. 539–548, http://dx.doi.org/10.1016/j.epsl.2008.11.023.

Irving, E., 1954, The palaeomagnetism of the Torridonian sandstone series of North-Western Scotland: Unpublished PhD thesis, University of Cambridge, Cambridge, UK.

Jamieson, R.A., Beaumont, C., Fullsack, P., and Lee, B., 1998, Barrovian regional metamorphism: Where's the heat?: Geological Society, London, Special Publications, v. 138, p. 23–51, http://dx.doi.org/10.1144/GSL.SP.1996.138.01.03.

Jamieson, R.A., Beaumont, C. Nguyen, M.H., and Culshaw, N.G., 2007, Synconvergent ductile flow in variable strength continental crust: Numerical models with application to the western Grenville orogen: Tectonics, v. 26, TC5005, http://dx.doi.org/10.1029/2006TC002036.

Johnson, M.R.W., and Strachan, R.A., 2006, A discussion of possible heat sources during nappe stacking: the origin of Barrovian metamorphism within the Caledonian thrust sheets of NW Scotland: Journal of the Geological Society, v. 163, p. 579–582, http://dx.doi.org/10.1144/0016-764920-168.

Johnston, S.T., 2001, The Great Alaskan Terrane Wreck: reconciliation of paleomagnetic and geological data in the northern Cordillera: Earth and Planetary Science Letters, v. 193, p. 259–272, http://dx.doi.org/10.1016/S0012-821X(01)00516-7.

Johnston, S.T., 2008, The Cordilleran ribbon continent of North America: Annual Review of Earth and Planetary Sciences, v. 36, p. 495–530, http://dx.doi.org/10.1146/annurev.earth.36.031207.124331.

Johnston, S.T., Weil, A.B., and Gutiérrez-Alonso, G., 2013, Oroclines: Thick and thin: Geological Society of America Bulletin, v. 125, p. 643–663, http://dx.doi.org/10.1130/B30765.1.

Kao, H., Behr, Y., Currie, C.A., Hyndman, R., Townend, J., Lin, F-C., Ritzwoller, M.H., Shan, S-J., and He, J., 2013, Ambient seismic noise tomography of Canada and adjacent regions: Part I, Crustal structures: Journal of Geophysical Research, Solid Earth, v. 118, p. 5865–5887, http://dx.doi.org/10.1002/2013JB010535.

Karato, S-i., and Wu, P., 1993, Rheology of the upper mantle: a synthesis: Science, v. 260, p. 771–778, http://dx.doi.org/10.1126/science.260.5109.771.

Khazaradze, G., and Klotz, J., 2003, Short and long term effects of GPS measured crustal deformation rates along the south central Andes: Journal of Geophysical Research, v. 108, 2289, http://dx.doi.org/10.1029/2002JB001879.

Kind, R., Yuan, X., Saul, J., Nelson, D., Sobolev, S.V., Mechie, J., Zhao, W., Kosarev, G., Ni, J., Achauer, U., and Jiang, M., 2002, Seismic images of crust and upper mantle beneath Tibet: Evidence for Eurasian plate subduction: Science, v. 298, p. 1219–1221, http://dx.doi.org/10.1126/science.1078115.

Kukačka, M., and Matyska, C., 2008, Numerical model of heat flow in back-arc regions: Earth and Planetary Science Letters, v. 276, p. 243–252, http://dx.doi.org/10.1016/j.epsl.2008.07.055.

Lachenbruch, A.H., and Morgan, P., 1990, Continental extension, magmatism and elevation; formal relations and rules of thumb: Tectonophysics, v. 174, p. 39–62, http://dx.doi.org/10.1016/0040-1951(90)90383-J.

Lachenbruch, A.H., and Sass, J.H., 1978, Models of an extending lithosphere and heat flow in the Basin and Range province, *in* Smith, R.B., and Eaton, G.P., *eds.*, Cenozoic Tectonics and Regional Geophysics of the Western Cordillera: Geological Society of America Memoirs, v. 152, p. 209–250, http://dx.doi.org/10.1130/MEM152-p209.

Leonard, L.J., Mazzotti, S., and Hyndman, R.D., 2008, Deformation rates estimated from earthquakes in the northern Cordillera of Canada and eastern Alaska: Journal of Geophysical Research, v. 113, B08406, http://dx.doi.org/10.1029/2007JB005456.

Levandowski, W., Jones, C.H., Shen, W., Ritzwoller, M.H., and Schulte-Pelkum, V., 2014, Origins of topography in the western U.S.: Mapping crustal and upper mantle density variations using a uniform seismic velocity model: Journal of Geophysical Research, v. 119, p. 2375–2396, http://dx.doi.org/10.1002/2013JB010607.

Lewis, T.J., Bentkowski, W.H., and Hyndman, R.D., 1992, Crustal temperatures near the Lithoprobe southern Canadian Cordillera transect: Canadian Journal of Earth Sciences, v. 29, p. 1197–1214, http://dx.doi.org/10.1139/e92-096.

Lewis, T.J., Hyndman, R.D., and Flück, P., 2003, Heat flow, heat generation, and crustal temperatures in the northern Canadian Cordillera: Thermal control of tectonics: Journal of Geophysical Research: Solid Earth, v. 108, 2316, http://dx.doi.org/10.1029/2002JB002090.

Loosveld, R.J.H., and Etheridge, M.A., 1990, A model for low pressure facies metamorphism during crustal thickening: Journal of Metamorphic Geology, v. 8, p. 257–267, http://dx.doi.org/10.1111/j.1525-1314.1990.tb00472.x.

Lynch, H.D., and Morgan, P., 1987, The tensile strength of the lithosphere and the

localization of extension, *in* Coward, M.P., Dewey, J.F., and Hancock, P.L., *eds.,* Continental Extensional Tectonics: Geological Society, London, Special Publications, v. 28, p. 53–65, http://dx.doi.org/10.1144/GSL.SP.1987.028.01.05.

MacKenzie, J.M., and Canil, D., 1999, Composition and thermal evolution of cratonic mantle beneath the central Archean Slave Province, NWT, Canada: Contributions to Mineralogy and Petrology, v. 134, p. 313–324, http://dx.doi.org/10.1007/s004100050487.

Majorowicz, J., Chan, J., Crowell, J., Gosnold, W., Heaman, L.M., Kück, J., Nieuwenhuis, G., Schmitt, D.R., Unsworth, M., Walsh, N., and Weides, S., 2014, The first deep heat flow determination in crystalline basement rocks beneath the Western Canadian Sedimentary Basin: Geophysical Journal International, v. 197, p. 731–747, http://dx.doi.org/10.1093/gji/ggu065.

Mareschal, J-C., and Jaupart, C., 2004, Variations of surface heat flow and lithospheric thermal structure beneath the North American craton: Earth and Planetary Science Letters, v. 223, p. 65–77, http://dx.doi.org/10.1016/j.epsl.2004.04.002.

Marquis, G., Jones, A.G., and Hyndman, R.D., 1995, Coincident conductive and reflective middle and lower crust in southern British Columbia: Geophysical Journal International, v. 120, p. 111–131, http://dx.doi.org/10.1111/j.1365-246X.1995.tb05915.x.

Matthews, D.H., 1986, Seismic reflections from the lower crust around Britain, *in* Dawson, J.B., Carswell, D.A., Hall, J., and Wedepohl, K.H., *eds.,* The Nature of the Lower Continental Crust: Geological Society, London, Special Publications, v. 24, p. 11–21, http://dx.doi.org/10.1144/GSL.SP.1986.024.01.03.

Mazzotti, S., and Hyndman, R.D., 2002, Yakutat collision and strain transfer across the northern Canadian Cordillera: Geology, v. 30, p. 495–498, http://dx.doi.org/10.1130/0091-7613(2002)030<0495:YCASTA>2.0.CO;2.

McCrory, P.A., and Wilson, D.S., 2013, A kinematic model for the formation of the Siletz-Crescent terrane by capture of coherent fragments of the Farallon and Resurrection plates: Tectonics, v. 32, p. 718–726, http://dx.doi.org/10.1002/tect.20045.

McGlashan, N., Brown, L., and Kay, S., 2008, Crustal thickness in the central Andes from teleseismically recorded depth phase precursors: Geophysical Journal International, v. 175, p. 1013–1022, http://dx.doi.org/10.1111/j.1365-246X.2008.03897.x.

McKenzie, D., Nimmo, F., Jackson, J.A., Gans, P.B., and Miller, E.L., 2000, Characteristics and consequences of flow in the lower crust: Journal of Geophysical Research, v. 105, p. 11029–11046, http://dx.doi.org/10.1029/1999JB900446.

Meissner, R., and Mooney, W., 1998, Weakness of the lower continental crust: a condition for delamination, uplift, and escape: Tectonophysics, v. 296, p. 47–60, http://dx.doi.org/10.1016/S0040-1951(98)00136-X.

Meissner, R., Rabbel, W., and Kern, H., 2006, Seismic lamination and anisotropy of the Lower Continental Crust: Tectonophysics, v. 416, p. 81–99, http://dx.doi.org/10.1016/j.tecto.2005.11.013.

Mooney, W.D., Laske, G., and Masters, T.G., 1998, CRUST 5.1: A global crustal model at 5°× 5°: Journal of Geophysical Research, v. 103, p. 727–747, http://dx.doi.org/10.1029/97JB02122.

Myers, J.S., 1978, Formation of banded gneiss by deformation of igneous rocks: Precambrian Research, v. 6, p. 43–64, http://dx.doi.org/10.1016/0301-9268(78)90054-2.

Nyblade, A.A., and Pollack, H.N., 1993, A global analysis of heat flow from Precambrian terrains: Implications for the thermal structure of Archean and Proterozoic lithosphere: Journal of Geophysical Research, v. 98, p. 12207–12218, http://dx.doi.org/10.1029/93JB00521.

Oldow, J.S., Bally, A.W., and Avé Lallemant, H.G., 1990, Transpression, orogenic float, and lithospheric balance: Geology, v. 18, p. 991–994, http://dx.doi.org/10.1130/0091-7613(1990)018<0991:TOFALB>2.3.CO;2.

Oueity, J., and Clowes, R.M., 2010, Nature of the Moho transition in NW Canada from combined near-vertical and wide-angle seismic reflection studies: Lithosphere, v. 2, p. 377–396, http://dx.doi.org/10.1130/L103.1.

Parsons, T., Howie, J.M., and Thompson, G.A., 1992, Seismic constraints on the nature of lower crustal reflectors beneath the extending Southern Transition Zone of the Colorado Plateau, Arizona: Journal of Geophysical Research, v. 97, p. 12391–12407, http://dx.doi.org/10.1029/92JB00947.

Pavlenkova, N.I., 1996, Crust and upper mantle structure in northern Eurasia from seismic data: Advances in Geophysics, v. 37, p. 1–133, http://dx.doi.org/10.1016/S0065-2687(08)60269-1.

Pollack, H.N., Hurter, S.J., and Johnson, J.R., 1993, Heat flow from the Earth's interior: Analysis of the global data set: Reviews of Geophysics, v. 31, p. 267–280, http://dx.doi.org/10.1029/93RG01249.

Ramos, V.A., 2010, The tectonic regime along the Andes: Present-day and Mesozoic regimes: Geological Journal, v. 45, p. 2–25, http://dx.doi.org/10.1002/gj.1193.

Ranalli, G., 1995, Rheology of the Earth: Springer, New York, 413 p.

Regan, S.P., Williams, M.L., Leslie, S., Mahan, K.H., Jercinovic, M.J., and Holland, M.E., 2014, The Cora Lake shear zone, Athabasca granulite terrane, an intraplate response to far-field orogenic processes during the amalgamation of Laurentia: Canadian Journal of Earth Sciences, v. 51, p. 877–901, http://dx.doi.org/10.1139/cjes-2014-0015.

Rippe, D., Unsworth, M.J., and Currie, C.A., 2013, Magnetotelluric constraints on the fluid content in the upper mantle beneath the southern Canadian Cordillera: Implications for rheology: Journal of Geophysical Research, v. 118, p. 5601–5624, http://dx.doi.org/10.1002/jgrb.50255.

Ross, J.V., 1983, The nature and rheology of the Cordilleran upper mantle of British Columbia: Inferences from peridotite xenoliths: Tectonophysics, v. 100, p. 321–357, http://dx.doi.org/10.1016/0040-1951(83)90193-2.

Royden, L., and Keen, C.E., 1980, Rifting process and thermal evolution of the continental margin of eastern Canada determined from subsidence curves: Earth and Planetary Science Letters, v. 51, p. 343–361, http://dx.doi.org/10.1016/0012-821X(80)90216-2.

Royden, L.H., Burchfiel, B.C., King, R.W., Wang, E., Chen, Z., Shen, F., and Liu, Y., 1997, Surface deformation and lower crustal flow in eastern Tibet: Science, v. 276, p. 788–790, http://dx.doi.org/10.1126/science.276.5313.788.

Sandiford, M., 1989, Horizontal structures in granulite terrains: A record of mountain building or mountain collapse?: Geology, v. 17, p. 449–452, http://dx.doi.org/10.1130/0091-7613(1989)017<0449:HSIGTA>2.3.CO;2.

Saruwatari, K., Ji, S., Long, C., and Salisbury, M.H., 2001, Seismic anisotropy of mantle xenoliths and constraints on upper mantle structure beneath the southern Canadian Cordillera: Tectonophysics, v. 339, p. 403–426, http://dx.doi.org/10.1016/S0040-1951(01)00136-6.

Sleep, N.H., 2005, Evolution of the continental lithosphere: Annual Review of Earth and Planetary Sciences, v. 33, p. 369–393, http://dx.doi.org/10.1146/annurev.earth.33.092203.122643.

Souther, J.G., Armstrong, R.L., and Harakal, J., 1984, Chronology of the peralkaline, late Cenozoic Mount Edziza volcanic complex, northern British Columbia, Canada: Geological Society of America Bulletin, v. 95, p. 337–349, http://dx.doi.org/10.1130/0016-7606(1984)95<337:COTPLC>2.0.CO;2.

Stockmal, G.S., and Beaumont, C., 1987, Geodynamic models of convergent margin tectonics: The southern Canadian Cordillera and the Swiss Alps: Canadian Society of Petroleum Geology Special Publications, Memoir 12, p. 393–411.

Tesauro, M., Kaban, M.K., and Cloetingh, S.A.P.L., 2008, EuCRUST-07: A new reference model for the European crust: Geophysical Research Letters, v. 35, L05313, http://dx.doi.org/10.1029/2007GL032244.

Thompson, A.B., Schulmann, K., Jezek, J., and Tolar, V., 2001, Thermally softened continental extensional zones (arcs and rifts) as precursors to thickened orogenic belts: Tectonophysics, v. 332, p. 115–141, http://dx.doi.org/10.1016/S0040-1951(00)00252-3.

Townend, J., and Zoback, M.D., 2000, How faulting keeps the crust strong: Geology, v. 28, p. 399–402, http://dx.doi.org/10.1130/0091-7613(2000)28<399:HFKTCS>2.0.CO;2.

van der Velden, A.J., and Cook, F.A., 1996, Structure and tectonic development of the southern Rocky Mountain trench: Tectonics, v. 15, p. 517–544, http://dx.doi.org/10.1029/95TC03288.

Vanderhaeghe, O., and Teyssier, C., 2001, Partial melting and flow of orogens: Tectonophysics, v. 342, p. 451–472, http://dx.doi.org/10.1016/S0040-1951(01)00175-5.

Warner, M., 1990, Basalts, water, or shear zones in the lower continental crust?: Tectonophysics, v. 173, p. 163–174, http://dx.doi.org/10.1016/0040-1951(90)90214-S.

Watanabe, T., Langseth, M.G., and Anderson, R.N., 1977, Heat Flow in Back Arc Basins of the Western Pacific, *in* Talwani, M., and Pitman, W.C., *eds.*, Island Arcs, Deep Sea Trenches and Back-Arc Basins: American Geophysical Union, Washington, D.C., p. 137–161, http://dx.doi.org/10.1029/ME001p0137.

Weil, A.B., Van der Voo, R., van der Pluijm, B.A., and Parés, J.M., 2000, The formation of an orocline by multiphased deformation: a paleomagnetic investigation of the Cantabria-Asturias Arc Hinge-Zone (northern Spain): Journal of Structural Geology, v. 22, p. 735–756, http://dx.doi.org/10.1016/S0191-8141(99)00188-1.

Wever, T., and Meissner, R., 1987, About the nature of reflections from the lower crust: Annales Geophysicae, Series B, v. 5, p. 349–352.

Whittakaer, A., Bott, M.H.P., and Waghorn, G.D., 1992, Stresses and plate boundary forces associated with subduction: Journal of Geophysical Research, v. 97, p. 11933–11944, http://dx.doi.org/10.1029/91JB00148.

Zhang, P-Z., Shen, Z., Wang, M., Gan, W., Bürgmann, R., Molnar, P., Wang, Q., Niu, Z., Sun, J., Wu, J., Hanrong, S., and Xinzhao, Y., 2004, Continuous deformation of the Tibetan Plateau from global positioning system data: Geology, v. 32, p. 809–812, http://dx.doi.org/10.1130/G20554.1.

Zoback, M.D., Townend, J., and Grollimund, B., 2002, Steady-state failure equilibrium and deformation of intraplate lithosphere: International Geology Review, v. 44, p. 383–401, http://dx.doi.org/10.2747/0020-6814.44.5.383.

Received April 2015
Accepted as revised August 2015

ANDREW HYNES SERIES: TECTONIC PROCESSES

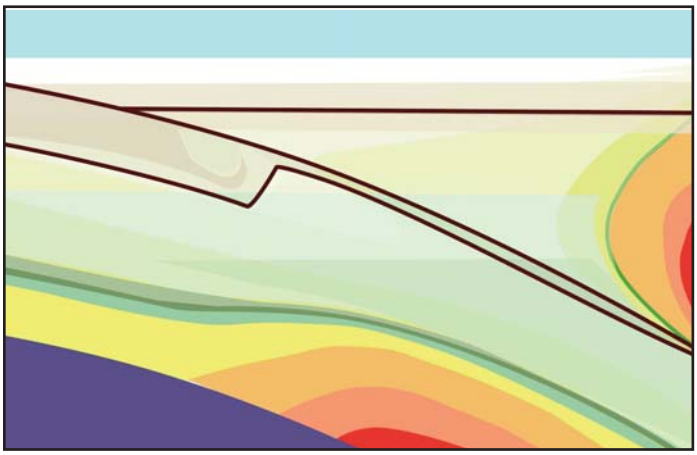

Post-peak Evolution of the Muskoka Domain, Western Grenville Province: Ductile Detachment Zone in a Crustal-scale Metamorphic Core Complex

Toby Rivers[1] and Walfried Schwerdtner[2]

[1]Department of Earth Sciences
Memorial University
St. John's, Newfoundland and Labrador, A1B 3X5, Canada
Email: trivers@mun.ca

[2]Department of Earth Sciences
University of Toronto
22 Russell Street
Toronto, Ontario, M5S 3B1, Canada

SUMMARY

The Ottawa River Gneiss Complex (ORGC) in the western Grenville Province of Ontario and Quebec is interpreted as the exhumed mid-crustal core of a large metamorphic core complex. This paper concerns the post-peak evolution of the Muskoka domain, the highest structural level in the southern ORGC that is largely composed of amphibolite-facies straight gneiss derived from retrogressed granulite-facies precursors. It is argued that retrogression and high strain occurred during orogenic collapse and that the Muskoka domain acted as the ductile detachment zone between two stronger crustal units, the underlying granulite-facies core known as the Algonquin domain and the overlying lower grade cover comprising the Composite Arc Belt. Formation of the metamorphic core complex followed Ottawan crustal thickening, peak metamorphism and possible channel flow, and took place in a regime of crustal thinning and gravitational collapse in which the cool brittle–ductile upper crust underwent megaboudinage and the underlying hot ductile mid crust flowed into the intervening megaboudin neck regions. Post-peak crustal thinning in the Muskoka domain began under suprasolidus conditions, was facilitated by widespread retrogression, and was heterogeneous, perhaps attaining ~90% locally. It was associated with a range of ductile, high-temperature extensional structures including multi-order boudinage and associated extensional bending folds, and a regional system of extension-dominated transtensional cross-folds. These ductile structures were followed by brittle–ductile fault propagation folding at higher crustal level after the gneiss complex was substantially exhumed and cooled. Collectively the data record ~60 m.y. of post-peak extension on the margin of an exceptionally large metamorphic core complex in which the ductile detachment zone has a true thickness of ~7 km. The large scale of the core complex is consistent with the deep level of erosion, and the long duration of extensional collapse is compatible with double thickness crust at the metamorphic peak, the presence of abundant leucosome in the mid crust and widespread fluid-fluxed retrogression, collectively pointing to the important role of core complexes in crustal cooling after the peak of the Grenvillian Orogeny.

RÉSUMÉ

Le complexe gneissique de la rivière des Outaouais (ORGC) dans la portion ouest de la Province de Grenville au Québec et en Ontario est interprété comme le cœur d'un grand complexe métamorphique à coeur de noyau. Le présent article porte sur l'évolution post-pic du domaine de Muskoka, soit le niveau structural le plus élevé de l'ORGC composé en grande partie d'orthogneiss au faciès amphibolite dérivés de précurseurs au faciès granulite. Nous soutenons que la rétromorphose et les grandes déformations se sont produites durant l'effondrement orogénique et que le domaine de Muskoka en a été une zone de détachement ductile entre deux unités crustales plus résistantes, le cœur au faciès granulite sous-jacent étant le domaine Algonquin, et la chapeau sus-jacent à plus faible grade de métamorphisme comprenant le Ceinture d'Arc Composite. La for-

mation du complexe métamorphique à coeur de noyau est survenue après l'épaississement crustale ottavien, le pic métamorphique et le possible flux en chenal, et s'est produit en régime d'amincissement crustal et d'effondrement gravitationnel au cours duquel la croûte supérieure refroidie a subit un mégaboudinage et où la croûte moyenne chaude et ductile sous-jacente a flué dans les régions entre les mégaboudins. L'amincissement crustale post-pic dans le domaine de Muskoka, qui a débuté en conditions suprasolidus, a été facilité par une rétromorphose généralisée, hétérogène, atteignant à peu près 90 % par endroits. Celle-ci a été associée avec une gamme de structures d'extension ductiles de haute température, incluant du boudinage de plusieurs ordres de grandeur et de plis de flexure d'extension, ainsi qu'un système régional de plis croisés d'origine transtensionnelle. À ces structures ductiles a succédé une phase de plissement de propagation de failles cassantes à ductiles à un plus haut niveau crustal, après que le complexe gneissique ait été exhumé et se soit refroidi. Prises ensemble, les données indiquent une extension post-pic sur la marge d'un complexe métamorphique à coeur de noyau exceptionnellement grand aux environs de 60 m.y. et dans laquelle la zone de détachement montre une épaisseur véritable d'environ 7 km. La grandeur de l'échelle du complexe métamorphique à coeur de noyau concorde avec le fort niveau d'érosion, et la grande durée de l'effondrement d'extension est compatible avec une croûte de double épaisseur au pic de métamorphisme, la présence de leucosomes abondants dans la croûte moyenne et d'une rétromorphose à flux fluidique généralisée, l'ensemble indiquant l'importance du rôle des complexes métamorphiques à coeur de noyau dans le refroidissement de la croûte après le pic de l'orogenèse grenvillienne.

Traduit par le Traducteur

INTRODUCTION

Metamorphic Core Complexes

Metamorphic core complexes consist of exhumed high-grade deep crust (the metamorphic core) surrounded by lower-grade or unmetamorphosed shallower crust (the cover or carapace) separated by ductile low-angle extensional detachment faults or shear zones. First recognized and defined in a continental arc setting (the North American Cordillera, e.g. Coney 1974, 1980; Lister and Davis 1989) as high-level, relatively small elliptical structures a few tens of km long by a few km wide, more recent work has led to the identification of deeper, much larger bodies (e.g. Shuswap complex; Vanderhaeghe et al. 1999, 2003) and to examples from collisional settings (e.g. the Variscan Massif Central, Malavieille et al. 1990; the Caledonian Western Gneiss Region, Krabbendam and Dewey 1998; Cycladic, Carpathian, and Anatolian segments of the Alpine Orogen, Janák et al. 2001; Whitney et al. 2007; Thomson et al. 2009; Kruckenberg et al. 2011), and the Iranian Plateau of the Arabia–Eurasia collisional orogen (Kargaranbafghi and Neubauer 2015). The original definition of a metamorphic core complex was based on Cordilleran examples, but in a recent review the definition was generalized to accommodate features of those formed at deep crustal levels and in other tectonic settings, as follows: "*A* [metamorphic] *core complex is a domal or arched geologic structure composed of ductilely deformed rocks and associated intrusions underlying a ductile-to-brittle high-strain zone that experienced tens of kilometers of normal-sense displacement in response to lithospheric extension*" (Whitney et al. 2013, p. 274). Moreover, although originally observed in continental crust, comparable structures are now also known in oceanic crust, leading to the understanding that core complexes are a signature of crustal-scale extension and thinning in a wide range of settings, and that they may have played a significant role in crustal cooling and the thermal evolution of Earth. Metamorphic core complexes are distinguished from gneiss domes, with which they may be associated, by crustal thinning resulting from the extensional setting, presence of the detachment zone, and the subordinate role of diapirically driven magmatic flow (e.g. Teyssier and Whitney 2002).

The crustal-scale architecture of core complexes, in which the hot deep crust and cool shallow crust are juxtaposed across the extensional detachment, implies important crustal attenuation and hence the transfer of material and heat from deep to shallower crustal levels, with the potential to drive enhanced fluid flow. The processes of heat and fluid transfer tend to weaken the crust, inducing a positive feedback loop that may influence the magnitude of extension (Whitney et al. 2013). In continental settings, metamorphic core complexes typically develop by collapse of overthickened crust during orogeny (e.g. Rey et al. 2001; Teyssier and Whitney 2002). Insight into the roles of factors that determine their final architecture, including the total amount of extension, the extension rate, the temperature in the mid crust, and the role of melt weakening, have been investigated in numerical modelling experiments (e.g. Rey et al. 2001, 2009; Teyssier and Whitney 2002; Vanderhaeghe 2009; Whitney et al. 2013), and in core complexes from tectonically active orogens (e.g. Kargaranbafghi and Neubauer 2015), leading to more informed interpretations in ancient examples. For instance, the detachment zones above many shallow Cordilleran metamorphic core complexes are narrow greenschist-facies mylonite zones up to a few metres wide, whereas in the larger deeper examples the detachment zones may be from several hundred metres to 2 km or more wide and composed of amphibolite-facies rocks.

This paper concerns the southwest margin of a very large Precambrian metamorphic core complex, the Ottawa River Gneiss Complex (formerly Central Gneiss Belt; Schwerdtner et al. submitted) situated in the western Grenville Province in Ontario and western Quebec, the exposed part of which has a surface area > 60,000 km^2. The identification of metamorphic core complexes in the Grenville Province is quite recent (Rivers 2012, 2015) and many details of their evolution remain poorly constrained. In this contribution, we focus on field evidence relating to the post-peak structural and metamorphic evolution of the southern part of the Ontario segment of the Ottawa River Gneiss Complex where the Muskoka domain structurally overlies the Algonquin domain, particularly the identification of the detachment zone and the manifestation, scale, and duration of extension recorded on it.

Definition and Large-scale Architecture of the Ottawa River Gneiss Complex

The new name Ottawa River Gneiss Complex (ORGC) was proposed by Schwerdtner et al. (submitted) for the large area of high-grade rocks in the western Grenville Province of Ontario and western Quebec between the Grenville Front

Tectonic Zone and the Composite Arc and Frontenac-Adirondack belts, previously termed the Central Gneiss Belt by Wynne-Edwards (1972). At the time of its original naming, the gneiss complex was not well studied and was principally defined by its gneissic character and upper amphibolite- to granulite-facies assemblages that were inferred to be the depositional basement to the non-gneissic, lower grade (greenschist- to amphibolite-facies) rocks of supracrustal origin in the adjacent 'Central Metasedimentary Belt' (later Composite Arc Belt) to the southeast. The new name is proposed in order to make a formal break with the original nomenclature and acknowledge the significant evolution in understanding since it was applied (see below and Schwerdtner et al. submitted).

The first attempts at internal subdivision of what we term the ORGC were made in the Ontario segment by Davidson and Morgan (1981), Davidson et al. (1982), and Davidson (1984) who used zones of continuous, flaggy gneissic layering or '*straight gneiss*' to delineate an imbricate stack of mostly SE-dipping domains and subdomains with distinctive lithologies, structural history and metamorphic grade (Fig. 1). Davidson et al. (1982) interpreted the stacked domains in the footwall and hanging wall of the Allochthon Boundary as Grenvillian thrust sheets or nappes, and Davidson (1984) specifically described the Muskoka and Parry Sound domains at the top of the stack as *"crustal blocks or wedges* [that have] *overridden one another in a northwesterly direction"* (p. 278). Culshaw et al. (1983, 1997) grouped the domains on both sides of the Allochthon Boundary into structural levels and their continuations at depth were subsequently verified on a LITHOPROBE deep seismic transect (White et al. 2000). The concept of structural levels was central to the comprehensive review of the structural and metamorphic evolution of the Ontario segment of the gneiss complex by Carr et al. (2000) and was also adopted in the Quebec segment where it was similarly supported by seismic data (e.g. Martignole and Calvert 1996; Nadeau and van Breemen 1998; Martignole et al. 2000).

In contrast to the view of the domains as exclusively a product of thrusting, Easton (1992) recognized that latest displacement on some domain boundaries, including those of the Muskoka domain, was extensional, and Culshaw et al. (1994) reported kinematic evidence for post-peak Ottawan extensional shear zones in the Britt domain and what is now known as the Shawanaga domain (Fig. 2). These interpretations were given concrete expression by U–Pb zircon dating of extensional reworking of the Allochthon Boundary at ~1020 Ma by Ketchum et al. (1998), and since then a range of evidence for post-peak extension has been described (e.g. Nadeau and van Breemen 1998; Carr et al. 2000; Timmermann et al. 2002; Rivers 2008, 2012; Jamieson et al. 2010; Schwerdtner et al. 2014). However, as discussed below its extent remains poorly constrained.

Since the early 1980s the subdivision of the Ontario segment of the gneiss complex has been modified many times (e.g. Culshaw et al. 1983, 1994, 1997, 2004; Carr et al. 2000; Ketchum and Davidson 2000; Dickin and Guo 2001; Jamieson et al. 2007, 2010), and as noted some progress has been made in extending the framework into the Quebec segment (e.g. summary in Martignole et al. 2000). With respect to the latter point, the largely granulite-facies Algonquin domain in the hanging wall of the Allochthon Boundary in Ontario was correlated with the Lac Dumoine domain in western Quebec by Rivers et al. (2012), but a structurally overlying unit corresponding to the Muskoka domain was not identified. Given this protracted history of changes in both the locations of domain boundaries and correlations among domains, as well as the interpretation of Rivers (2012) that the gneiss complex as a whole is a large domal metamorphic core complex, Schwerdtner et al. (submitted) proposed the new name, Ottawa River Gneiss Complex, after the river that bisects it. In describing the first-order components of the ORGC, they stated: *"the segment of the ORGC in the hanging wall of the* [Allochthon Boundary] *is composed of the remnants of a deep-crustal thrust-sheet stack that was assembled in the Ottawan phase of the Grenvillian Orogeny (~1090–1020 Ma). In contrast, the* [segment in its] *footwall* […] *is a thrust stack of parautochthonous rocks formed in the Rigolet phase at ca. 1000-980 Ma."* Moreover, as shown by recent work and emphasized in this study, the ORGC is an archive of both pre-Grenvillian and Grenvillian tectonic history, of which the post-peak Ottawan part involved important extension during exhumation and cooling.

The correlation chart of Jamieson et al. (2007, 2010) for the Ontario segment of the ORGC (Fig. 2) is used as a tectonic template in this study. In this figure, the SE-dipping allochthonous sheets in the hanging wall of the Allochthon Boundary (structural levels 2–3) were emplaced during the main Ottawan collisional phase of the Grenvillian Orogeny (~1090–1020 Ma), and overlie the parautochthon in its footwall (structural level 1) that underwent its principal deformation in the Rigolet phase (~1005–980 Ma; Rivers et al. 2012). Specifically the southeast part of structural level 3 is composed of the Muskoka domain and its Moon River and Seguin subdomains that are correlated with the Ahmic and Shawanaga subdomains farther northwest, all of which overlie the Algonquin-Lac Dumoine domain and related subdomains of structural level 2. The Wallace subdomain of the Muskoka domain was recently defined by Schwerdtner et al. (submitted).

Grade and Timing of Metamorphism in the ORGC

Structural levels 2−3 comprising most of the allochthonous part of the ORGC structurally above the Allochthon Boundary are composed almost entirely of high-grade metamorphic rocks with upper amphibolite-, granulite-, and rare relict eclogite-facies assemblages that formed during the Ottawan phase of the Grenvillian Orogeny (Carr et al. 2000; Rivers et al. 2012). Of relevance to this study is the observation of Davidson et al. (1982) that metamorphic assemblages in the Algonquin domain (structural level 2) at the base of the stack are principally granulite facies, whereas those in the overlying Muskoka domain (structural level 3) are principally amphibolite facies. Our work and that of others supports this general conclusion, but we show in this study that in detail the picture is more nuanced, with preservation of both prograde and retrograde assemblages in different parts of both domains.

In addition to a distinction based on metamorphic grade, several authors have followed Carr et al. (2000) in emphasizing that many of the gneisses in the Algonquin domain and equivalent subdomains in level 2 carry geochronological evidence for a high-grade metamorphism at ~1.5–1.45 Ga prior to Ottawan reworking during the Grenvillian Orogeny and are thus polymetamorphic (polycyclic), whereas those in the

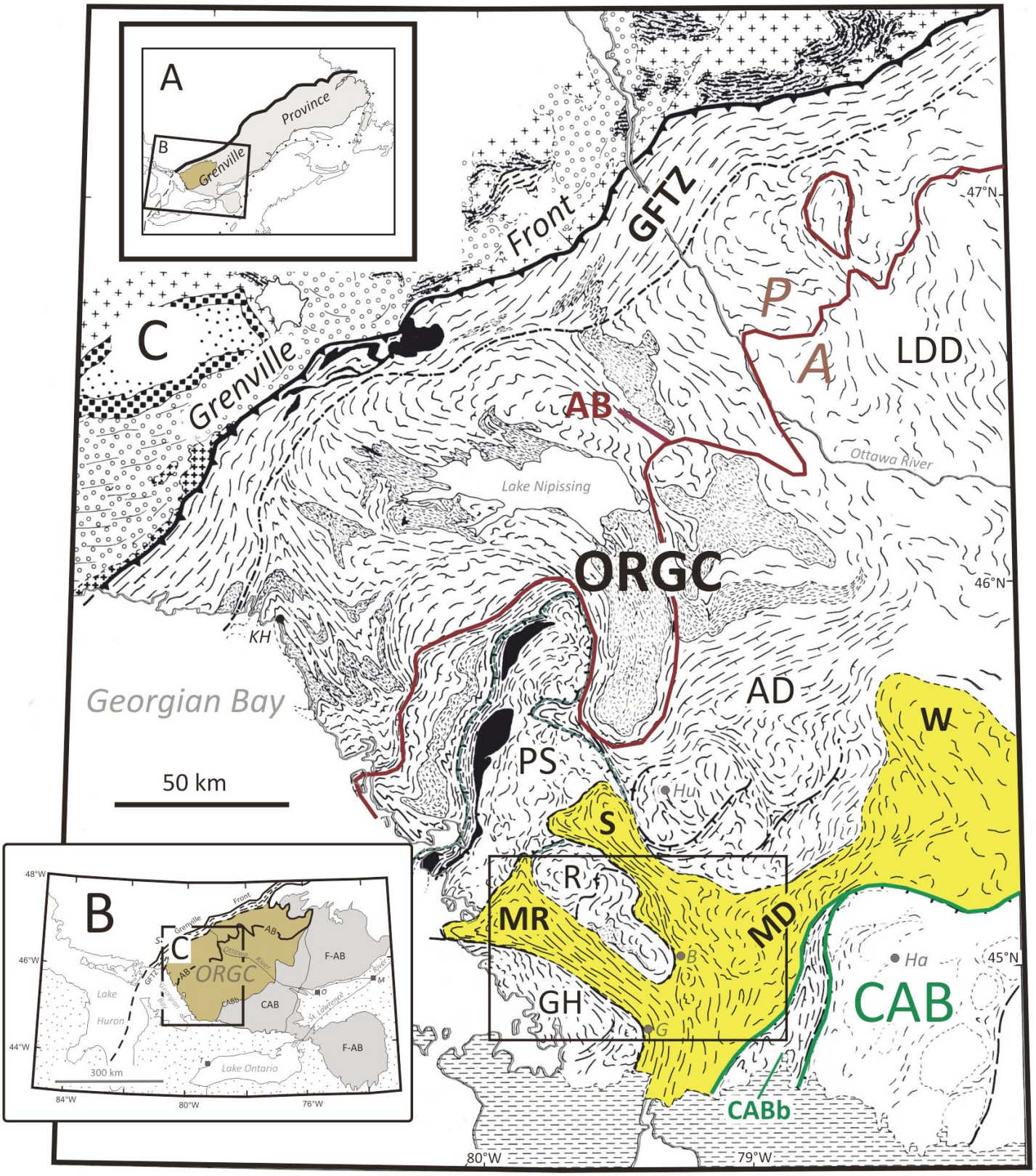

Figure 1. A–B: Location of the Ottawa River Gneiss Complex (ORGC, highlighted in brown) in the SW Grenville Province. The ORGC is bisected by the Ottawa River into Ontario and Quebec segments, and extends between the Grenville Front Tectonic Zone (GFTZ) and Composite Arc and Frontenac-Adirondack belts (CAB and F-AB). AB – Allochthon Boundary, CABb – Composite Arc Belt boundary zone; *M* – Montréal, *O* – Ottawa, *S* – Sudbury, *T* – Toronto. C: Foliation trend map of part of the Ontario segment of the ORGC, with the Muskoka domain (MD), including its NW-trending synformal Moon River (MR), Seguin (S) and Wallace (W) subdomains, highlighted. Short dashes – granitoid plutons, black – anorthosite bodies. AD – Algonquin domain, GH – Go Home subdomain, LDD – Lac Dumoine domain, PS – Parry Sound domain, R – Rosseau subdomain. The AB divides the ORGC into allochthonous (*A*) and parautochthonous (*P*) parts. Box shows approximate area of present study; *B* – Bracebridge, *G* – Gravenhurst, *Ha* – Haliburton, *Hu* – Huntsville, *KH* – Key Harbour. C modified from Davidson (1984); boundaries of Wallace subdomain are approximate; location of AB from Ketchum and Davidson (2000).

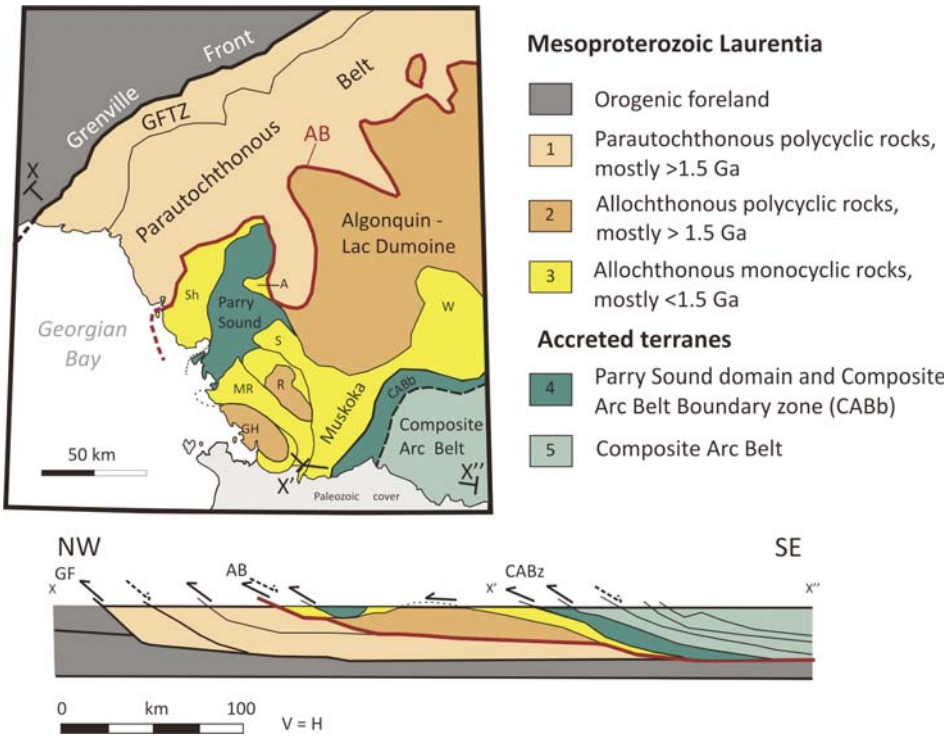

Figure 2. Tectonic map of the western Grenville Province and NW-SE crustal-scale cross-section X-X'-X" based on deep seismic data integrated with geological evidence showing division of the orogenic crust into 5 structural levels. The <1.5 Ga monocyclic rocks in the Muskoka domain and the structurally equivalent Shawanaga (Sh) and Ahmic (A) domains in structural level 3 overlie the mostly >1.5 Ga rocks in the Algonquin–Lac Dumoine domain (structural level 2) in the immediate hanging wall of the Allochthon Boundary (AB). GFTZ – Grenville Front Tectonic zone; GH, MR, R, S, W – Go Home, Moon River, Rosseau, Seguin and Wallace subdomains. Redrawn and slightly modified from Jamieson and Beaumont (2011), after Culshaw et al. (1997).

Muskoka domain and equivalent subdomains in level 3 were principally unmetamorphosed prior to the Grenvillian orogeny, and hence are monocyclic (Fig. 2).

The Large Hot Orogen (LHO) Paradigm

The term large hot orogen (LHO), introduced by Beaumont et al. (2001), was an outcome of the results of two-dimensional numerical thermal–mechanical scaled modelling of collisional orogenesis. The first applications were to the Himalaya–Tibet Orogen, but the concept quickly found application in the Grenville Province. In these models, prolonged convergence leads to the development of a wide plateau in the orogenic hinterland as crust is detached from the subducting sub-continental lithospheric mantle and shortened to double thickness. Due to the long duration of collision, and assuming reasonable values for mantle heat flow and internal heat generation in the crust, the numerical experiments predict that the mid and lower crust under the orogenic plateau will attain temperatures of > 700ºC after about 20 m.y. of collision. Partial melting of felsic lithologies under these conditions leads to the development of a 20–30 km wide crustal 'channel' of relatively low density, low-viscosity anatectic material (leucosome and ductile restite) that is transported under the plateau and may eventually be extruded at the orogenic front by one of two mechanisms depending upon its rheology: gravitational forcing of low-viscosity material due to the weight of the overlying plateau leading to '*homogeneous channel flow,*' or tectonic forcing of higher-viscosity material due to the piston effect of newly introduced strong cool crust into the orogen leading to '*inhomogeneous channel flow with formation of hot fold nappes*' (Beaumont et al. 2006).

A numerical experiment based on these principles was compared to the crustal-scale cross-section of the ORGC shown in Figure 2 (Jamieson et al. 2007; GO-3 series). In this experiment, tectonic forcing of the weak mid crust by the entry of progressively stronger crust into the orogen leads to heterogeneous channel flow and extrusion of ductile material from the channel analogous to a stack of hot crystalline nappes. In addition to the first-order similarity of the crustal-scale architecture, a feature of this experiment that resonates with present understanding is the high-strain ductile deformation of the mid crust in a sub-horizontal regime (orogenic infrastructure) beneath an upper crust that remains little deformed away from the orogenic front (orogenic superstructure). Empirical evidence for Ottawan high strain and associated high-grade metamorphism in the orogenic infrastructure and their absence in the superstructure was described by Rivers (2012).

Jamieson and co-workers subsequently published a second set of numerical experiments potentially relevant to the Grenville Province in which convergence was stopped after prolonged collision and the orogen allowed to evolve as a result of gravitational body forces (GO-ST series; Jamieson et al. 2010; Jamieson and Beaumont 2011). From the perspective of the ORGC in the orogenic hinterland, the principal difference between the results of the two sets of experiments is that in the GO-ST series the crust undergoes a gravitationally-driven attenuation after convergence ceases and zones of high strain, potentially analogous to normal faults, develop as it proceeds. However, since strain discontinuities ('faults') are not permitted by the continuum-mechanics formulation and the resolution of the experiment is low, it is difficult to compare the model results with structures observed in nature.

The Collapsed LHO Paradigm

Implicit in the GO-ST series of experiments by Jamieson et al. (2010) is the understanding that LHOs eventually undergo gravitationally driven collapse once the mid crust becomes thermally or melt-weakened beyond a critical value and/or the tectonic forces holding up the orogen decay. In the case of the western Grenville Province, the assembly of empirical evidence pointing to important post-peak ductile extensional shearing and crustal thinning, within both the ORGC and in the tectonically overlying Composite Arc Belt (CAB), has been ongoing for more than two decades. It includes a combination of structural evidence (e.g. van der Pluijm and Carlson 1989; Culshaw et al. 1994; Busch and van der Pluijm 1996; Busch et al. 1997; Schwerdtner et al. 2005, 2010b; Selleck et al. 2005), metamorphic evidence (Busch et al. 1996b; Rivers 2008), and a wide range of geochronological evidence including U–Pb

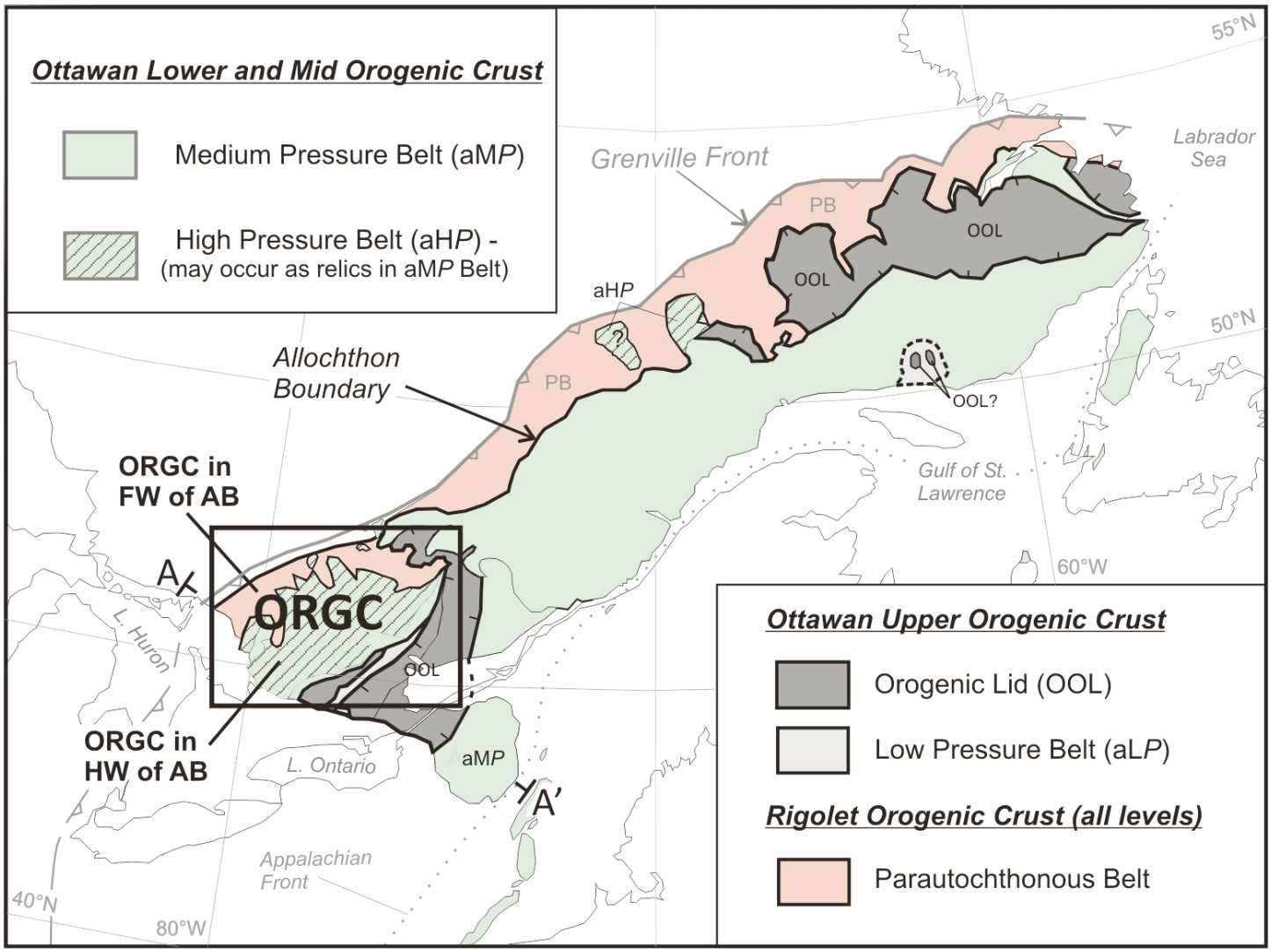

Figure 3. Tectonic sketch map of the Grenville Province showing the baric subdivision of allochthonous units in the hanging wall (HW) of the Allochthon Boundary (AB); a*HP*, a*MP*, and a*LP* are the allochthonous high, medium, and low pressure belts with Ottawan metamorphism. The orogenic lid is the preserved remnants of the orogenic superstructure lacking Ottawan metamorphism (OOL – Ottawan orogenic lid). Collapse led to juxtaposition of orogenic superstructure (OOL) against orogenic infrastructure (ORGC) along normal-sense shear zones. FW – footwall. Box shows approximate location of study area in the ORGC. Slightly modified from Rivers (2012).

data on titanite (Mezger et al. 1991), zircon (Corrigan and van Breemen 1997; Ketchum et al. 1998), and monazite (Wong et al. 2012), and $^{40}Ar/^{39}Ar$ dating on hornblende (e.g. Cosca et al. 1991, 1992, 1995; Busch et al. 1996a; Streepey et al. 2004). Initially, the evidence for extension within the upper-crustal CAB and mid-crustal ORGC (orogenic superstructure and infrastructure, respectively) was evaluated separately (e.g. Mezger et al. 1991; Culshaw et al. 1994; Streepey et al. 2004; Selleck et al. 2005). However, more recently the data from both levels have been integrated with estimates of regional peak pressure variations during the Ottawan metamorphism, leading to a more holistic picture (Fig. 3; Rivers 2008; 2012; Rivers et al. 2012; McLelland et al. 2013; Schwerdtner et al. 2014). In this interpretation, parts of the orogenic superstructure, preserved segments of which are referred to as the orogenic lid, are juxtaposed against exhumed mid-crustal gneiss terranes such as the ORGC (orogenic infrastructure), implying that after crustal thickening and peak metamorphism the orogen underwent profound orogenic collapse (also known as gravitational collapse, extensional collapse, or gravitational spreading).

Rivers (2008, 2012) proposed a conceptual model to explain the crustal architecture of the western Grenville Province that integrated empirical evidence from structural and metamorphic measurements in the ORGC and CAB with results from two-dimensional numerical experiments of orogenic collapse (e.g. Rey et al. 2001, 2009; Vanderhaeghe 2009). In this model, the mechanisms of extensional flow in the crust undergoing collapse varied with depth, such that megaboudinage of the strong upper crust was accompanied by flow of the underlying gneissic mid crust into the neck regions between adjacent megaboudins, collectively leading to the formation of large (≥ 100 km diameter) domical metamorphic core complexes (Fig. 4). In this setting, it is inferred that most major tectonic boundaries either formed or were reworked in extension, which was predominantly SE-directed in the ORGC, but both NW- and SE-directed elsewhere (Fig. 4).

Study Area and Definition of Map Units

The focus of this study is the allochthonous segment of the ORGC, to the southeast of and structurally above the

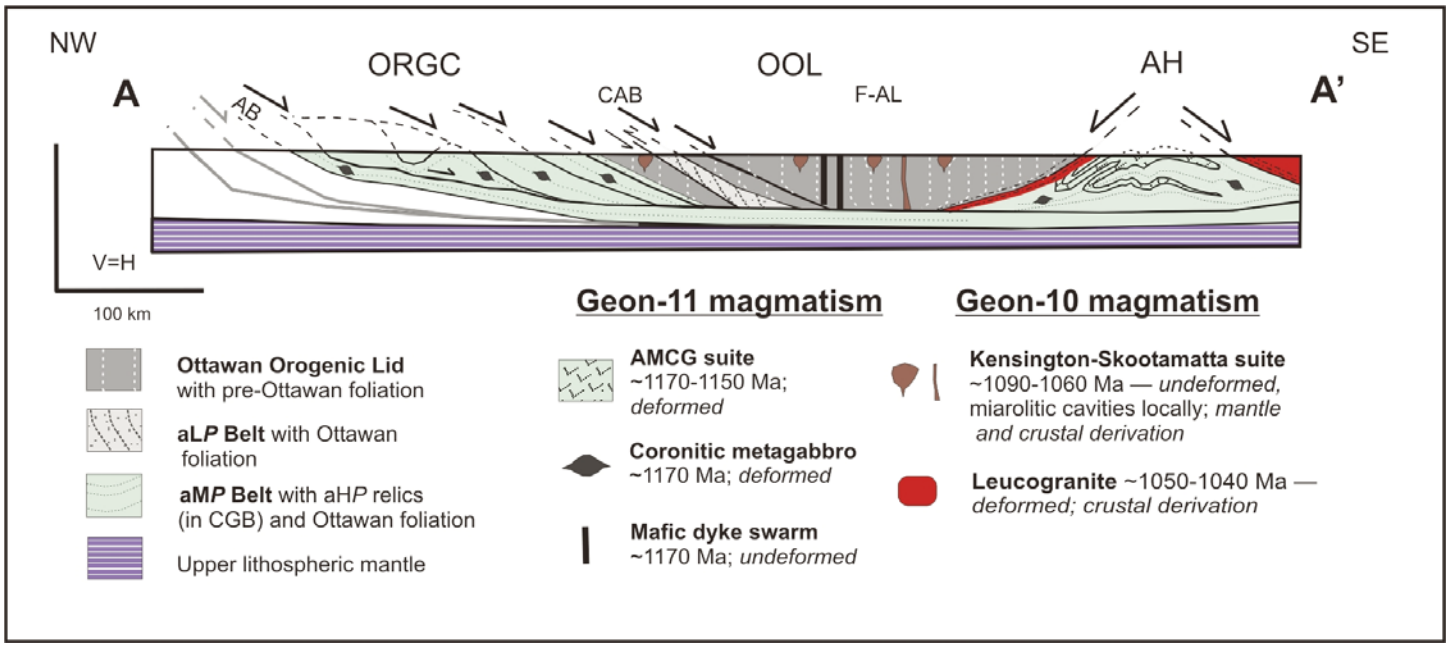

Figure 4. Schematic NW-SE crustal-scale cross-section of crust in the hanging wall of the Allochthon Boundary (AB), SW Grenville Province; for location of A-A', see Figure 3. Major boundaries are constrained by seismic data. Remnants of the orogenic superstructure with steep pre-Grenvillian fabrics and mineral assemblages are preserved in the Ottawan Origin Lid (OOL) (CAB –Composite Arc Belt, F-AL –Frontenac-Adirondack Lowlands domain), which is juxtaposed against the exhumed orogenic infrastructure (ORGC –Ottawa River Gneiss Complex, AH –Adirondack Highlands domain). Two examples of the contrasting tectonic signatures of approximately coeval pre-Grenvillian igneous bodies in the orogenic infrastructure and superstructure are illustrated schematically; (i) geon-11 mafic intrusions in the ORGC (infrastructure) are deformed lenticular coronitic metagabbro bodies with retrograde amphibolite-facies rims, whereas those in the OOL (superstructure) are undeformed mafic dykes; (ii) syn-extension geon-10 leucogranite at the margin of the AH (infrastructure) is strongly deformed (Selleck et al. 2005), whereas high-level granitoid bodies in the Kensington-Skootamatta suite (Corriveau et al. 1990; Easton 1992; Corriveau and Gorton 1993) emplaced in the OOL (superstructure) are undeformed. Modified from Rivers (2015).

Allochthon Boundary. Our specific interest is the Muskoka domain in structural level 3, a SE-dipping sheet-like body with several NW-trending synformal lobes, and its contact relationships with the structurally underlying Algonquin domain and overlying Composite Arc Belt. Although most of the data, examples and illustrations come from the area of the box in Figure 1, our observations and measurements are considerably more wide-ranging, extending beyond the eastern limit of the figure.

Geological maps of the study area show that it is principally underlain by two orthogneiss suites: (i) ≥ 1.46 Ga calc-alkaline *'grey gneiss suite'* (informal name) composed of meta-tonalite, -granodiorite and -gabbro, and (ii) 1.46–1.43 Ga A-type meta-monzonite, -monzodiorite, -gabbro and -anorthosite and related members of an '*AMCG suite'* (Lumbers and Vertolli 2000a, b; Lumbers et al. 2000). Geochemical and isotopic data indicate that both suites are juvenile, and they have been interpreted to represent remnants of a Mesoproterozoic continental-margin arc and backarc basin respectively (Dickin and McNutt 1990; Timmermann et al. 1997, 2002; Nadeau and van Breemen 1998; McMullen 1999; Carr et al. 2000; Rivers and Corrigan 2000; Slagstad et al. 2004a, b, 2009; Dickin et al. 2008, 2014). A third unit, (iii), not shown on regional geologic maps, consists of massive to weakly deformed granite pegmatite dykes up to a few metres wide that cross-cut the older gneisses.

All three units occur in both the Muskoka domain (structural level 3) and the underlying Algonquin domain (structural level 2). As elaborated below, distinction between the gneissic units in the two structural levels is principally a function of their metamorphic grade and strain intensity. Hence, although the Algonquin and Muskoka domains are clearly distinguished on tectonic maps such as those shown in Figures 1 and 2, they are less evident on the 1:50,000 lithological maps.

High-grade metamorphism in the two orthogneiss suites took place during the Ottawan phase of the Grenvillian orogeny from ~1090–1020 Ma (e.g. Timmermann et al. 1997, 2002; McMullen 1999; Slagstad et al. 2004a, 2009). Most observed contacts between gneissic units are tectonic, but relict intrusive contacts are preserved locally. On the other hand, the rectiplanar margins of the cross-cutting granite pegmatite dykes indicate that they intruded into the gneissic rocks after ductile deformation had ceased and they were exhumed and cooled, and available data suggest they crystallized at ~1000 Ma (i.e. post-Ottawan; Corrigan et al. 1994; Bussy et al. 1995).

PETROLOGIC OBSERVATIONS

Ottawan Metamorphism in the Algonquin Domain

As noted in the introduction, the initial subdivision of the southeast ORGC was in part based on metamorphic grade, with the Algonquin domain (structural level 2) being predominantly underlain by granulite-facies rocks and the Muskoka domain (structural level 3) by upper amphibolite-facies rocks (e.g. Davidson and Morgan 1981; Davidson et al. 1982; Culshaw et al. 1983). Small pods and lenses of relict eclogite-facies rocks were discovered at discrete structural levels in both domains by Davidson (1990). Subsequent work has shown that some granulite-facies assemblages in the Algonquin domain exhibit evidence of variable replacement by amphibolite-facies assemblages and the eclogite-facies assemblages are almost completely replaced by granulite- and amphibolite-facies

assemblages. Geochronological data (e.g. Ketchum and Krogh 1997, 1998; Ketchum et al. 1998), although not unequivocal, have been interpreted to indicate that the eclogite-facies metamorphism in the Algonquin domain took place at ≥ 1090 Ma, the widespread granulite-facies overprint occurred at ~1080 Ma, and was followed by variable retrogression to amphibolite-facies assemblages (see Rivers et al. 2012, p. 180 for discussion). Peak *P–T* determinations for the granulite-facies rocks of the Algonquin domain are 850–1100 MPa and 750–850°C (Anovitz and Essene 1990), the wide range probably being due to post-peak re-equilibration.

Ottawan Metamorphism in the Muskoka Domain

Assemblages, P–T Conditions and Timing

Although metamorphic mineral assemblages in the Muskoka domain and structural level 3 are principally upper amphibolite facies, patches and relics of granulite-facies assemblages are widespread (e.g. Pattison 1991; Timmermann et al. 1997, 2002) and relict eclogite has been reported from the Shawanaga subdomain (Jamieson et al. 2003). In the study area, the grey gneiss suite is extensively migmatitic in most outcrops due to the presence of leucosome, whereas the units of the AMCG suite are generally more homogeneous in appearance. Granulite-facies assemblages in both units are principally composed of *Hbl*±*Cpx*±*Opx*±*Bt*-*Qtz*-*Pl*±*Or*-*Liq* (mineral abbreviations after Whitney and Evans 2010), with *Hbl*±*Bt* commonly mantling pyroxene and contributing to the definition of the gneissic fabric and straight gneiss layering. Assemblages in amphibolite-facies gneiss are similar, but lack *Opx*±*Cpx*. Most leucosomes are strongly attenuated leading to a stromatic texture that contributes to the gneissic layering, but some are cross-cutting (see also Timmermann et al. 1997, 2002; Slagstad et al. 2005).

Estimated peak *P–T* conditions for the granulite-facies assemblages in the Muskoka domain are 800–1150 MPa and 750–850°C (Anovitz and Essene 1990; Pattison 1991; Culshaw et al. 1997; Carr et al. 2000; Timmermann et al. 2002), i.e. comparable to those in the underlying Algonquin domain. U–Pb zircon estimates for the time of peak granulite-facies metamorphism in the Muskoka domain are ~1080 Ma (lower intercepts of TIMS and SHRIMP analyses; Bussy et al. 1995; Timmermann et al. 1997; Slagstad et al. 2004a, b), again comparable to those in the Algonquin domain within uncertainties. Moreover, peak *P–T* estimates for the amphibolite-facies assemblages in the Muskoka domain are not distinctly different from those for the granulites, being in the range 1000–1100 MPa and 750–800°C, leading Timmermann et al. (2002) to deduce that the distribution of granulite- and amphibolite-facies assemblages in the transition zone was a function of the a_{H2O} in the ambient fluid. Timmermann et al. (1997) dated a *Hbl*-*Bt*-bearing, foliation-parallel leucosome in amphibolite-facies gneiss in the Muskoka domain at 1064 ±18 Ma (U–Pb zircon, TIMS), a result subsequently confirmed more precisely by the SHRIMP method (1067 ±9 Ma; Slagstad et al. 2004b), and Bussy et al. (1995) presented U–Pb TIMS data for metamorphic zircon in dykes in the Moon River subdomain that bracketed the timing of amphibolite-facies ductile deformation between ca. 1065 and 1045 Ma.

Granulite Formation and the Role of Fluids

Several petrological studies of prograde granulite formation in the Muskoka domain have highlighted the important role played by infiltration of low a_{H2O} fluid. In (i) amphibolite-facies metagabbro bodies with anastomosing diffuse *Opx*-bearing tonalitic veins in the Seguin subdomain and Muskoka domain *sensu stricto*, Pattison (1991) and Timmermann et al. (2002) respectively concluded that formation of metamorphic *Opx* in the tonalitic veins occurred by subsolidus dehydration of *Hbl* driven by infiltration of a low a_{H2O} fluid. Later coarser-grained veins with sharp margins in the example studied by Pattison (1991) were deduced to be a result of closed-system anatexis. Timmermann et al. (2002) also described two other types of granulite and granulite-formation process in felsic to intermediate gneiss in the Muskoka domain; (ii) patchy granulite, consisting of metre-scale diffuse patches overprinting the amphibolite-facies fabric that formed by *Bt*-dehydration melting; and (iii) rare, late *Opx*-bearing felsic veins that truncate the amphibolite-facies fabric and developed by infiltration of a low a_{H2O} melt ±fluid. In all three occurrences, *Opx* may display thin retrograde *Hbl* rims that were inferred to be a result of back-reaction between *Opx* and H_2O formed during melt crystallization (Timmermann et al. 2002).

In contrast to these examples of well preserved granulite, we have observed many occurrences of highly retrogressed granulite relicts in amphibolite-facies gneiss throughout the Muskoka domain, prompting us to add a fourth category, (iv) relict *Opx*±*Cpx*-bearing granulite-facies assemblages in leucosomes, porphyroclasts and boudins in which the pyroxene is rimmed to completely replaced by *Hbl*±*Bt* aggregates that are elongate in the high-strain amphibolite-facies fabric. This latter relationship is similar to the 'textbook' evidence for variably pervasive textural and mineralogical retrogression of granulite-facies rocks in an Archean terrane in West Greenland described by McGregor and Friend (1997). Examples of retrogressed granulite in the Muskoka domain are shown in Figure 5.

Recalling that amphibolite-facies assemblages typify the Muskoka domain as originally defined (Davidson et al. 1982), we interpret these observations collectively to indicate that although prograde granulite-facies assemblages and textures are locally well preserved (i–iii above), on the scale of the domain as a whole they are relict and apart from patchy remnants and preserved 'islands' they are variably overprinted by post-peak retrograde amphibolite-facies assemblages (iv above), in places to such an extent that their original granulite-facies history is essentially obliterated. In the field, evidence for progressive replacement of granulite-facies assemblages by amphibolite-facies assemblages may be indicated by the colour of the feldspar (plagioclase and/or orthoclase). In outcrops in which the feldspar has a greenish hue and greasy lustre, the mafic phases are usually aggregates of *Cpx*±*Opx* (or have cores of these minerals surrounded by *Hbl*±*Bt*) indicative of recrystallization under granulite-facies conditions, whereas in outcrops in which the feldspars are whitish to pinkish, the mafic minerals are typically aggregates of *Hbl*±*Bt* implying thorough recrystallization under amphibolite-facies conditions. On the basis of our observations, the retrograde recrystallization may have taken place under either static (weakly strained

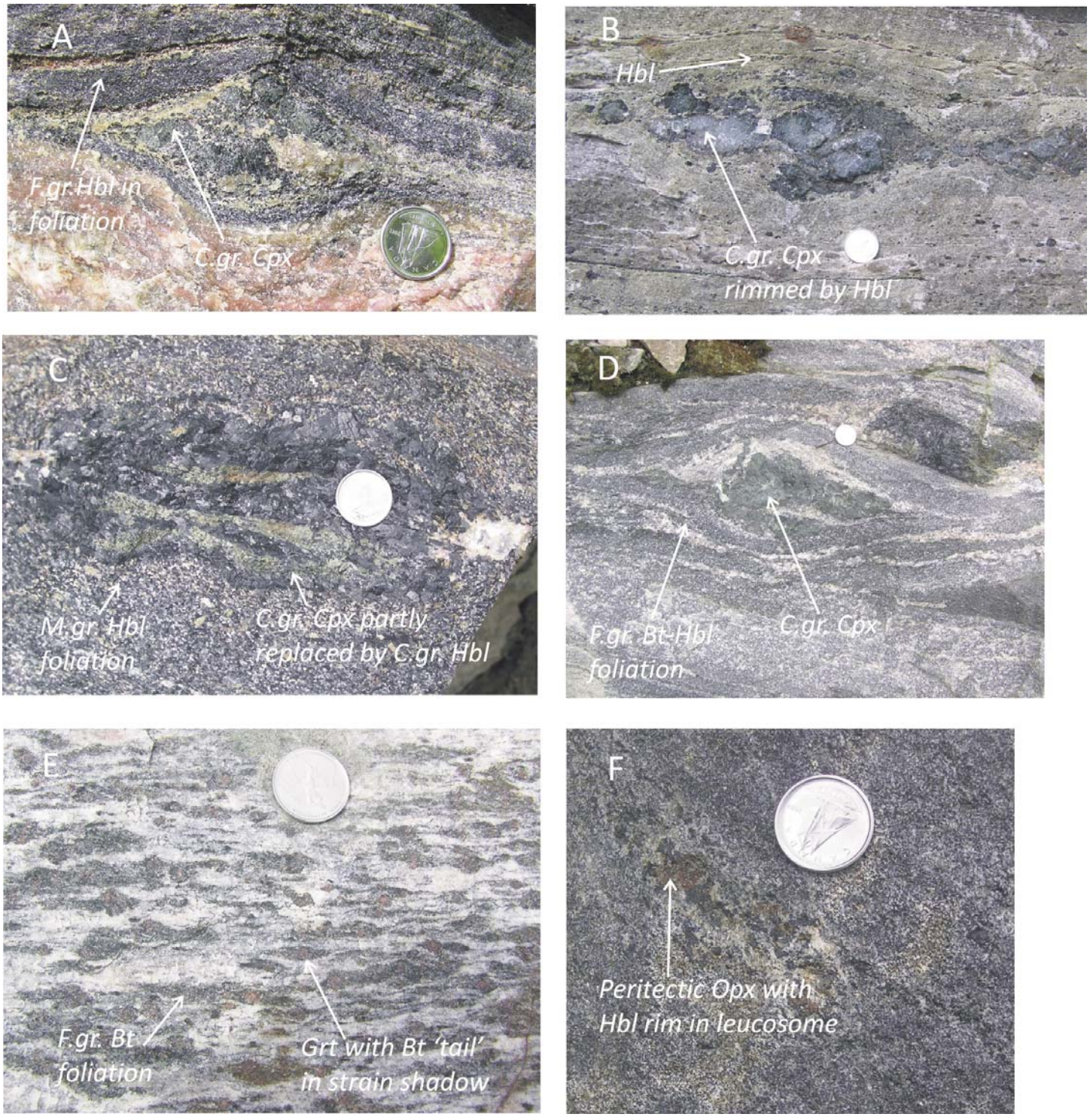

Figure 5. Photographs showing details of the high strain amphibolite-facies fabric in the Muskoka domain, its retrograde character indicated by the presence of relict anhydrous phases, remnants of the former granulite-facies assemblage, that are partially replaced by hydrous phases. A–D: Inclusions in grey gneiss in which *Cpx* is variably replaced by *Hbl* in high-strain fabric composed of *Hbl*±*Bt*; note thinning of tectonic layering above inclusion in A and B and incipient boudinage of inclusion in B and C. E: *Grt* partially replaced by elongate *Bt* aggregates in monzodioritic gneiss. F: Spidery *Opx*-bearing tonalitic leucosome in mafic gneiss in which *Opx* is partially replaced by *Hbl*. C.gr., M.gr., and F.gr. – coarse-, medium- and fine-grained.

or undeformed; rare) or dynamic (high-strain; common) conditions. We interpret this to imply that incursion of hydrous fluid into the Muskoka domain occurred after the peak of granulite-facies metamorphism when the crust was still hot and deeply buried, and was commonly accompanied by high strain. The implications of this deduction and of the spatial distribution of the relict granulite-facies rocks are discussed in a later section.

Anatexis, Migmatite Formation and the Role of Fluids

As discussed in the previous section, Timmermann et al. (2002) proposed that *Bt*-dehydration melting led to formation

of *Opx*-bearing leucosome in patchy granulite in the Muskoka domain. Specifically they proposed two leucosome-forming reactions with peritectic *Hbl* and *Opx* as follows:

$$Bt + Pl + Qtz = Hbl + Kfs + Liq \quad (1)$$

$$Bt + Pl + Qtz = Opx + Kfs + Liq \quad (2)$$

Hornblende-bearing leucosomes (1) are widespread in the Muskoka domain, whereas *Opx*-bearing leucosomes (2) are mostly restricted to areas of patch granulite. Prograde reactions (1) and (2) occur when the upper temperature stability of *Bt* in the presence of the other reactants is exceeded. No evidence for *Hbl*-dehydration melting was observed by Timmermann et al. (2002), compatible with their *T* estimates of 750–800°C. Slagstad et al. (2005) pointed out that due to the low modal abundance of *Bt* in typical granodioritic orthogneiss the amount of melt generated by (1) and (2) would have been limited (≤ 10%).

Slagstad et al. (2005) recognized two migmatite morphologies in dioritic and granodioritic gneiss they termed patch and stromatic migmatite. Melanosomes are present in both cases, supporting geochemical evidence for *in situ* derivation of leucosome in the host gneiss. The patch migmatite in dioritic gneiss is tonalitic in composition, carries prominent peritectic *Hbl* as poikiloblastic or skeletal grains, and is an irregularly distributed feature, in part fracture-related, that composes ≤ 5% of the rock by volume. The authors concluded that it developed from a sub-solidus, water-fluxed melt reaction such as:

$$Bt + Pl + Qtz + H_2O = Hbl + Liq \quad (3)$$

Although similar to (1) in terms of solid reactants, Slagstad et al. (2005) referred to experimental results indicating that formation of peritectic *Hbl* only occurs in melts with 3–4 wt.% H_2O, levels not attained by *Bt*-dehydration melting (see also Brown 2013).

Stromatic migmatite studied by Slagstad et al. (2005) is common in granodioritic gneiss and consists of concordant to subconcordant *Hbl*-bearing leucosome comprising 20–30%, up to locally 40–50% of the rock by volume. Some leucosomes are undeformed and injected along the foliation or into boudin necks and shear bands, whereas others are folded, with the presence of several generations being interpreted to indicate the volume of leucosome represents the vestiges of a cumulative record rather than the amount present at any one time. Slagstad et al. (2005, p. 899) concluded: *"The very high leucosome proportions in stromatic migmatites* […] *are inconsistent with in situ partial melting, both because granodioritic gneisses are unlikely to yield such high melt proportions and because complementary residual rocks are missing. Although the concordant melanosomes may represent residues after partial melting, the small volume of melanosomes (typically only 1-2 mm thick) cannot account for the volume of the leucosome in the rocks."* As a result, they concluded that (p. 915): *"The field, petrographic, and geochemical evidence from the stromatic migmatites suggests that in addition to in situ partial melting, a significant proportion of the leucosome present* […] *was derived from external sources."* More recently, Aranovich et al. (2013) have shown how dissolved K–Na-bearing brines in fluid-present melting drive the minimum melt towards more *Qtz*- and *Kfs*-rich compositions (so-called brine trend), which may explain the high K_2O contents in some leucosomes studied by Slagstad et al. (2005).

Collectively these studies of migmatite formation in the Muskoka domain suggest (i) in granodioritic gneiss, small quantities of leucosome (≤ 10%) were formed by *Bt*-dehydration melting during prograde metamorphism, some of which may have been lost, but (ii) a significant proportion of the 20–50% leucosome in granodioritic gneiss was derived externally. In dioritic gneiss, (iii) limited melt formation (≤ 5%) in patches and along fractures was driven by water- (±K-Na brine-) fluxed melting under subsolidus conditions; and in metagabbro (iv) the formation of a network of tonalitic leucosomes with peritectic *Opx* was driven by influx of a low a_{H2O} fluid that promoted *Bt* breakdown.

Biotite-dehydration melting implies the absence of a hydrous fluid phase (or the presence of a fluid with a low a_{H2O}), but water-fluxed melting requires the presence of a hydrous fluid phase (or a fluid phase with a high a_{H2O}), so they cannot occur at the same place and time. Moreover the drivers, melting conditions and physical effects of the two processes are different: dehydration melting is driven by *T* exceeding the solidus and results in an increase in the volume of the system ($\Delta V_{melting}$ positive) potentially leading to brittle failure and melt expulsion, whereas water-fluxed melting in a suprasolidus terrane is driven by fluid influx and leads to a reduction in volume ($\Delta V_{melting}$ negative) (Clemens and Droop 1998; Weinberg and Hasalová 2015). This suggests that if both processes took place in the same area, as indicated by the cited studies, they must have occurred sequentially, likely with dehydration melting during prograde metamorphism preceding fluid-fluxed melting at or after the metamorphic peak. Injection of melt from outside the system could have occurred at either time. Another relevant issue is that leucosomes produced by dehydration melting are H_2O-undersaturated and able to rise in the crust before reaching their solidi, whereas water-fluxed magmas are H_2O-saturated and unable to rise significantly before freezing. This difference has implications for the preservation of leucosome at its site of formation.

Metamorphism of Al-rich Mafic Rocks

Metamorphic mineral assemblages and structures in small lenses and layers of Al-rich metagabbro and mafic gneiss in the grey gneiss unit warrant special discussion because they form the basis for arguments regarding the timing and strain associated with decompression and exhumation of the gneiss complex. Prograde metamorphism of these lithologies is inferred to have led to the peak assemblage *Grt±Cpx±Opx±Hbl±Pl±FeTi oxide±Bt±Cal* and to a microstructure in which grossular-rich garnet formed porphyroblasts at the expense of calcic plagioclase (Schwerdtner et al. 1974). Consistent with this interpretation, these authors reported examples from the Moon River subdomain in which small grains of sillimanite and quartz occurred as inclusions in garnet or in plagioclase surrounding resorbed garnet, but are absent from the matrix. However, an aluminosilicate phase may not form in bulk compositions that are undersaturated in alumina, the Al instead entering solid-solution phases such as pyroxene or amphibole via the Tschermak exchange. In this case, possible reactions are:

$$Tr\text{-}Hbl + An = Ts\text{-}Hbl + Grt + Qtz \quad (4)$$

$$Tr\text{-}Hbl + An = Ts\text{-}Cpx \pm Ts\text{-}Opx + Grt + Qtz + H_2O \quad (5)$$

Both reactions are sensitive to pressure, the left-hand sides as written being the low-*P* sides (e.g. Berman 1991; Schaubs et al. 2002). Our observations suggest that some *Pl* remained as a stable phase in the peak *P*–*T* assemblage, implying the rocks were granulite rather than eclogite.

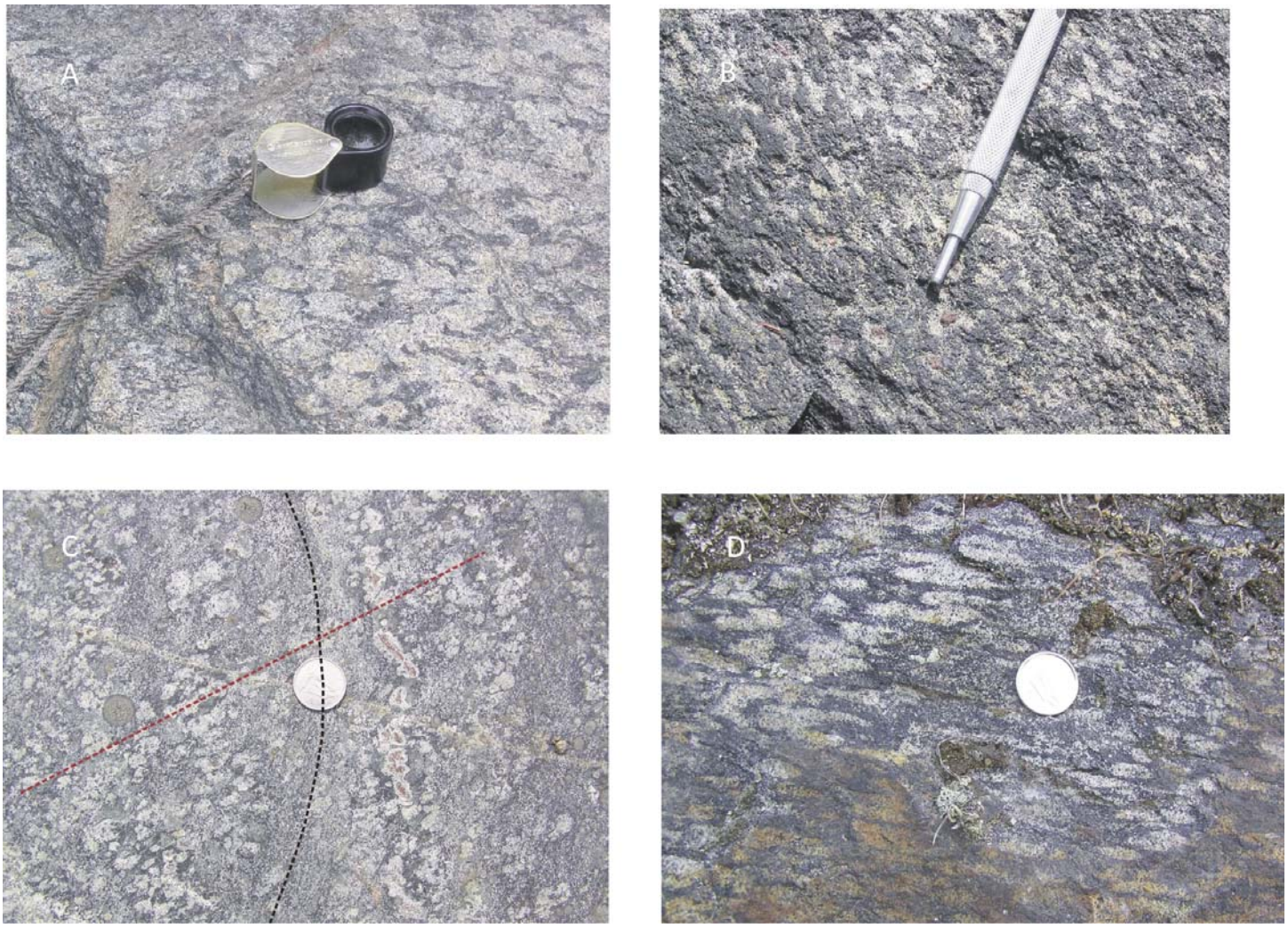

Figure 6. *An*-rich plagioclase aggregates pseudomorphing former *Grt* porphyroblasts in metagabbro and mafic gneiss, Muskoka domain (A). Relict *Grt* is present in cores of some pseudomorphs in B and C. In B, relict subophitic texture suggests the protolith was gabbro, whereas in C the presence of layering (dashed black line) overprinted by a weak tectonic fabric (dashed red line) suggests the protolith was mafic gneiss. D: Horizontal outcrop surface in the core of the Moon River synform about 20 km NW of Gravenhurst. The elliptical shapes of plagioclase pseudomorphs provide evidence for ductile strain during or after decompression. In 3-dimensions, the pseudomorphs in (D) are prolate, their long axes trending NW-SE parallel to the hinge line of the Moon River synform, implying a component of post-peak constrictional strain parallel to the axis of the cross-fold.

We deduce that during decompression and retrogression at high temperature, reactions (4) and (5) operated in reverse, resulting in the formation of *An*-rich plagioclase at the expense of *Grs*-rich garnet. This led to the formation of a distinctive replacement texture in which *Pl* aggregates pseudomorph former *Grt* porphyroblasts (Fig. 6), with relict *Grt* and *Sil* remaining in the cores of some pseudomorphs facilitating interpretation (Schwerdtner et al. 1974). Evidently decompression was accompanied by hydrous retrogression in many cases, because pyroxenes surrounding the *Pl* pseudomorphs after *Grt* are partly to completely replaced by *Hbl*±*Bt*.

Strain During Decompression

Pseudomorphs mimic the shapes of the objects they replace, so in the absence of strain it is assumed that the shapes of idioblastic *Grt* would be inherited by the *Pl* aggregates. Hence, distorted shapes of the aggregates may be used as qualitative indicators of the shape and magnitude of strain acquired after the metamorphic peak during decompression and retrogression (Waddington 1973; Schwerdtner et al. 1974, 1998, 2005, 2014). However, because idioblastic garnet grains are non-spherical the imprecision of strain estimates increases with increasing strain level (Schwerdtner et al. 1974, their fig. 5).

In the Muskoka domain, some pseudomorphic *Pl* aggregates after *Grt* are quasi-idioblastic (Fig. 6A–B), indicating that decompression of the metagabbro/mafic gneiss was not accompanied by significant finite strain at the dm-scale at those localities, whereas others are moderately to highly distorted in two- or three-dimensions and resemble prolate or oblate ellipsoids, thereby providing information on the local geometry of ductile deformation during and/or after decompression ± retrogression (Fig. 6C–D).

Extrapolating from this interpretation suggests that part of the high strain embedded in the gneissic fabric of the ORGC occurred during decompression and retrogression. Indeed, the implication is that where the gneissic fabric is composed of post-peak amphibolite-facies assemblages, as we infer to be the case throughout much of the Muskoka domain, a significant component of the strain may have occurred *after* the peak of metamorphism during decompression and retrogression.

Although this inference presently remains unquantified, it has profound implications for the interpretation of structures in the Muskoka domain of the ORGC as discussed further below.

POST-PEAK EXTENSIONAL STRUCTURES FORMED DURING DECOMPRESSION AND RETROGRESSION

Straight Gneiss Fabric

Representative images of the straight gneiss fabric that characterizes much of the Muskoka domain are shown in Figure 7. On centimetre to metre scales, the alternation of straight pink to grey granitoid and black amphibolite layers is typical (Fig. 7A–D). Features indicative of its high-strain origin include mylonitic layers, stretched *Hbl* aggregates and rotated *Hbl* porphyroclasts (Fig. 7F–H, respectively). Hornblende and biotite are the principal mafic phases, and where pyroxenes are present they are relict and rimmed or surrounded by the high-strain *Hbl*±*Bt*±*Pl*±*Kfs*±*Qtz* fabric (e.g. Figs. 5, 7E). From the shapes of deformed feldspar and hornblende aggregates we assess the strain in the straight gneiss to be S>L to S>>L; although the extension direction (L) can generally be found in most outcrops, it is not prominent or present on all foliation surfaces.

In his description of straight gneiss in the ORGC in general, Davidson (1984) noted that *"Amphibolite facies assemblages* [in straight gneiss] *occur in most* […] *boundary zones* [between domains]*"* (p. 276), which is consistent with our observations, even in cases where granulite-facies assemblages are stable within the domain itself. Thus, following the logic developed in the previous paragraphs, we deduce that the amphibolite-facies mineral assemblages defining the dominant fabric elements in the Muskoka domain, including the regional high-strain foliation that is widely expressed as a straight-gneiss fabric (Fig. 7), formed after peak metamorphism during decompression and retrogression. Moreover, we note that straight gneiss is not restricted to the margins of the Muskoka domain, but is also widespread within the interior implying the domain as a whole has undergone unusually high strain.

However, although the straight gneiss fabric in the Muskoka domain obviously has a high-strain history, it is not defined

Figure 7. Examples of amphibolite-facies straight gneiss, grey gneiss unit, Muskoka domain. In A–D note extreme attenuation, parallelism and continuity of thin amphibolite layers (black) and thicker layers of granitic, granodioritic to dioritic gneiss. Isoclinal folds outlined by amphibolite layers are common (e.g. arrow in C), the axes of which generally plunge SE parallel to the regional elongation lineation. In C, also note the diffuse white margins adjacent to several amphibolite layers, a result of fluid diffusion between layers of contrasting composition after formation of the high-strain layering. E: Amphibolite-facies high-strain foliation in grey gneiss surrounding central thicker layer of monzonitic gneiss with relict isoclinal fold in clinopyroxenite layer. F: Post-migmatization mylonite layer (arrow) illustrating heterogeneous retrograde strain on the cm scale. G-H: High-strain tectonic layering flowing around elongate and round porphyroclastic aggregates of *Hbl* (arrows).

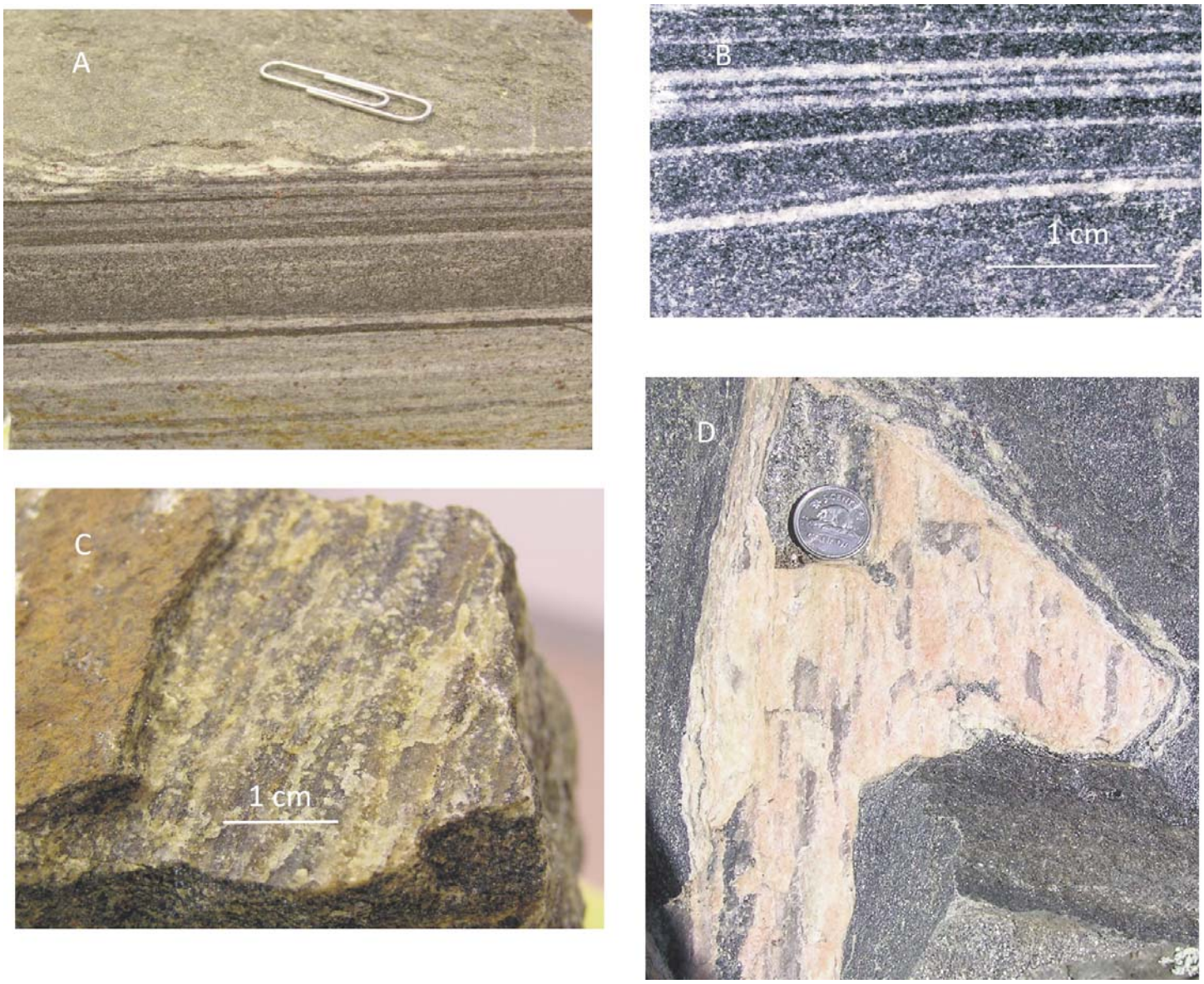

Figure 8. Fabric details in the grey gneiss, Muskoka domain. A: High-strain continuous layering in straight gneiss; the mafic mineralogy (principally *Bt*) is retrograde, small *Grt* porphyroblasts in felsic layers are partially replaced by rims of *Pl*. The upper foliation surface under paper clip is a *Bt*-rich layer composed of equant grains with their cleavage parallel to the foliation plane, but they do not define a lineation, suggesting *Bt* crystallization was late. B: Close-up of layering in mafic, amphibolite-facies straight gneiss; the foliation is principally defined by stretched leucosomes, not by a strong crystallographic preferred orientation of *Bt* and *Hbl* in the mafic layers. C: Close-up of foliation surface in monzodioritic gneiss showing development of L-fabric defined by stretched feldspar aggregates and minor *Qtz*. *Grt* is partly replaced by *Pl* and surrounded by rims and tails of *Bt*. Note greenish tint of feldspar, suggestive of a granulite-facies precursor, and variable preservation of the lineation. D: L-fabric on foliation surface in granitic gneiss defined by *Qtz* ribbons and streaky *Kfs*; other foliation surfaces in sample lack a lineation and are coated with *Bt*. Note pinkish *Kfs* and lack of evidence for granulite-facies precursor.

by a strong crystallographic- or shape-preferred orientation of inequant minerals such as *Hbl* and *Bt* on a crystalline scale. For instance, Davidson (1984) described the fabrics at the margins of domains in the ORGC as *"exhibit*[ing] *continuous planar foliation due to parallelism of streaky, dark mineral aggregates, flat hornblende-bearing quartzofeldspathic lenses, feldspar augen distributed on foliation planes, aligned amphibolitic slivers and variably developed compositional layering* […]*, features* [that] *combine to give the rocks a streaky or 'shredded' appearance. In places the gneisses are evenly fine grained and well layered* […] *straight gneisses* […, but] *usually* […] *grain size is variable and uneven, and layer boundaries are diffuse.* […]. *Gneisses with quartzofeldspathic lenses give the impression that they are the flattened equivalents of migmatites whose formerly less regular leucosomes have been attenuated"* (p. 276). This is also a fitting description of the straight gneiss fabric throughout the Muskoka domain. In addition, we emphasize that in the typical well-layered S>L and S>>L straight-gneiss tectonites, the shape and/or crystallographic preferred orientation of mineral grains contributes little to the total planar fabric. The foliation is chiefly defined by the gneissic layering and concordant flattened leucosomes (Fig. 8A–B), with the preferred orientation of mineral grains playing a subordinate role. We further note that many foliation surfaces in the straight gneiss are coated with late equant *Hbl*±*Bt* grains that exhibit only weak preferred orientation parallel to the layering, and lack shape or crystallographic expression of an L-fabric.

In interpreting the origin and evolution of the straight gneiss fabric at the grain scale, we make the following deduc-

tions: (a) from the *Qtz* ribbons and *Fsp* augen, the presence of narrow mylonite zones and the variable and uneven grain size, we deduce that the high-strain fabric developed by ductile processes such as intracrystalline gliding (*Qtz*) and sub-grain formation (*Fsp*) at high temperature; (b) from the streaky texture of mafic aggregates and the local preservation of relict *Px* rimmed and replaced by *Hbl*±*Bt,* we deduce that it is principally a retrograde fabric that developed after peak granulite-facies metamorphism; (c) from the lack of crystallographic preferred orientation of *Hbl*±*Bt* we deduce that these minerals underwent post-peak annealing after most deformation had ceased; and (d) from the *Hbl*±*Bt* coatings on some foliation surfaces we deduce there was widespread fluid influx along the foliation after cessation of intense strain. Collectively these suggest three possible origins for the straight gneiss fabric: (i) it is mimetic on the peak-metamorphic granulite-facies fabric, thereby implying that most strain was accrued during thrusting; (ii) it developed as a new high-strain fabric during post-peak amphibolite-facies retrogression/exhumation and extensional collapse; or (iii) it represents some combination of (i) and (ii) that involved variable extensional reworking of older compressional fabrics. Distinction among these possibilities is difficult due to annealing and the *Bt*±*Hbl* coatings on many foliation surfaces, and moreover is only feasible where relicts of the original fabric are preserved and post-peak strain markers are available, such as *Pl* pseudomorphs after *Grt*. Although this issue merits additional study, we conclude from the available data that (iii) is most likely, but the widespread evidence for strongly heterogeneous strain and recrystallization, noted previously, makes it difficult to quantify and generalize in practice.

Cross-folds

Cross-folds are orogen-perpendicular or orogen-oblique structures that in the Grenville Province mostly have gently SE-plunging hinge lines, i.e. approximately perpendicular to the traces of the Allochthon Boundary and the Grenville Front. In the ORGC, they are prominent on a regional scale and deform the stacked allochthons southeast of the Allochthon Boundary, including the contact between structural levels 2 and 3 in the study area, and they also extend to the parautochthon to the northwest (Fig. 9A). The northwest-trending Moon River and Seguin lobes of the Muskoka domain (structural level 3) are the sites of large synformal cross-folds separated by the conjugate Bracebridge antiform in structural level 2 – indeed it is cross-folding that causes the distinctive map pattern. Regional cross-folds have large inter-limb angles and steep axial surfaces (Fig. 9B), lack penetrative axial planar fabrics, and exhibit noncylindrical profiles due to thickness variations around their hinges and plunge variations along their hinge lines. Moreover, on a regional scale their hinge-line traces converge or diverge, exhibit irregular spacing, and vary in trend from SE (orogen-perpendicular) to ESE (orogen-oblique) (Fig. 9A).

In the Muskoka domain, the cross-folds comprise a multi-order fold system, with wavelengths ranging from metre-scale structures visible in outcrop to the ≥20 km-scale Moon River, Seguin and Wallace synforms. Moreover, although the majority of metre-scale cross-folds have steep to upright axial surfaces, examples with inclined and recumbent axial surfaces also

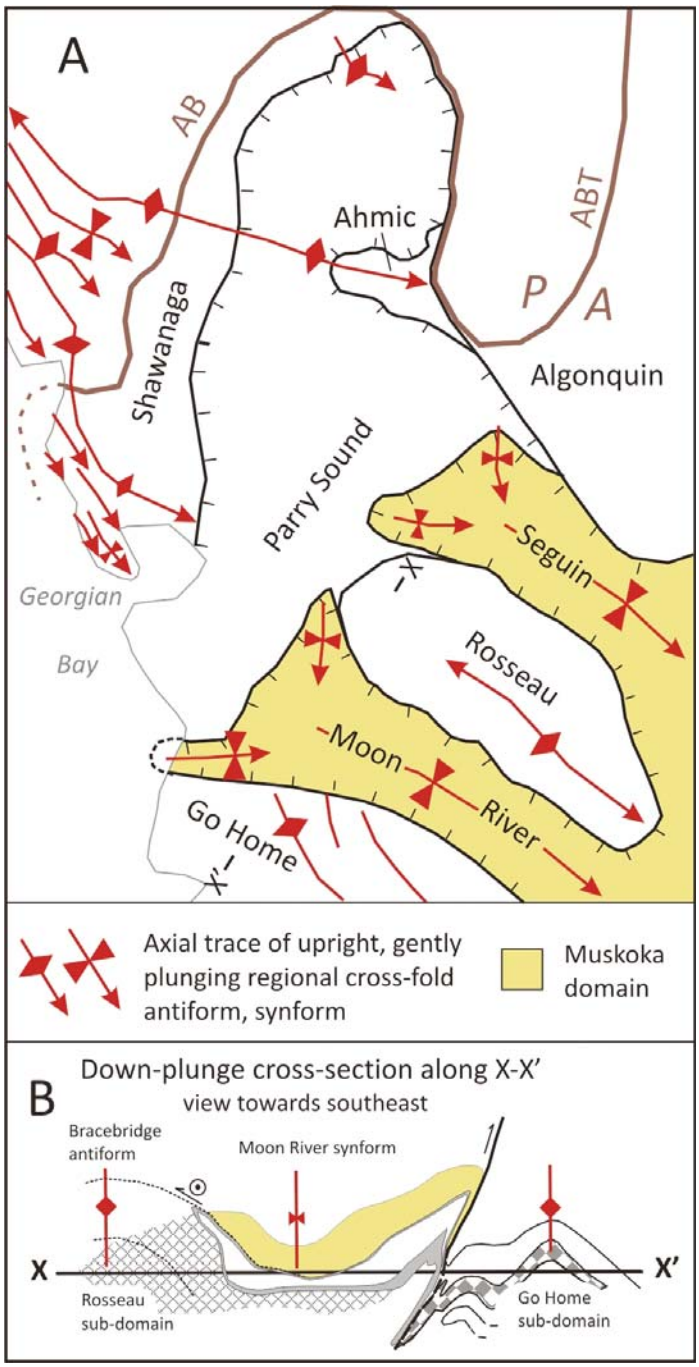

Figure 9. A: Sketch map showing regional distribution of hinge line traces of km-scale cross-folds in the western ORGC (redrawn from Davidson 1984); AB – Allochthon Boundary, *P* – parautochthonous segment, *A* – allochthonous segment; X-X' – location of cross-section; B: Cross-section along X-X' showing upright axial surfaces and large inter-limb angles of the Moon River synform, Bracebridge antiform, and unnamed antiform in the Go Home domain that are superposed on older recumbent structures. Redrawn from Gower (1992).

occur. Figure 10 illustrates outcrop-scale examples from the Muskoka domain and from the Parautochthonous Belt to the north of the Allochthon Boundary.

The origin of the cross-folds is a long-standing issue. There is agreement they are buckle folds with extension parallel to their hinge lines (Waddington 1973; Schwerdtner and van Berkel 1991; Gower 1992; Klemens 1996; Culshaw 2005; Schwerdtner and Klemens 2008; Schwerdtner et al. 2010a), but

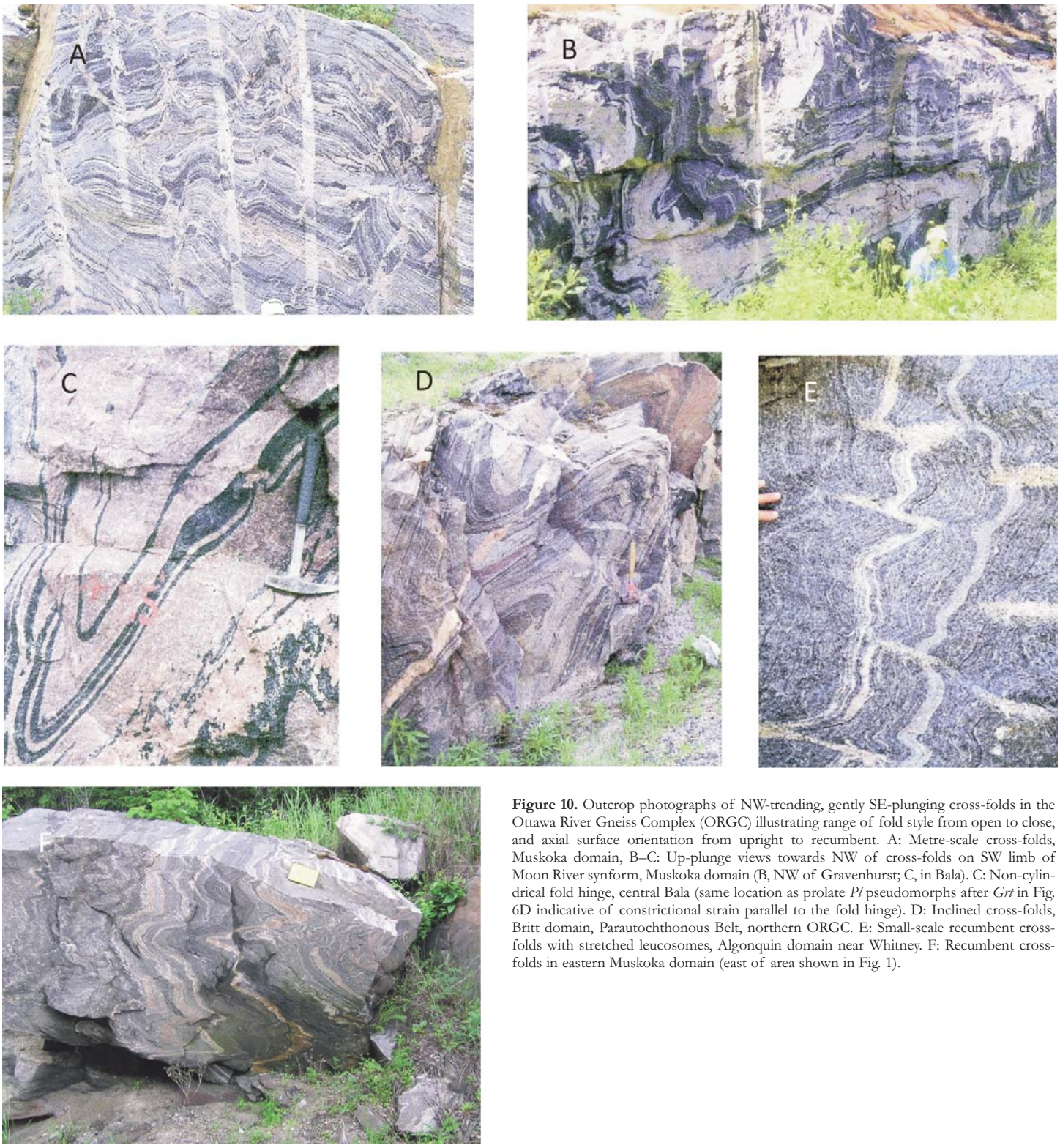

Figure 10. Outcrop photographs of NW-trending, gently SE-plunging cross-folds in the Ottawa River Gneiss Complex (ORGC) illustrating range of fold style from open to close, and axial surface orientation from upright to recumbent. A: Metre-scale cross-folds, Muskoka domain, B–C: Up-plunge views towards NW of cross-folds on SW limb of Moon River synform, Muskoka domain (B, NW of Gravenhurst; C, in Bala). C: Non-cylindrical fold hinge, central Bala (same location as prolate *Pl* pseudomorphs after *Grt* in Fig. 6D indicative of constrictional strain parallel to the fold hinge). D: Inclined cross-folds, Britt domain, Parautochthonous Belt, northern ORGC. E: Small-scale recumbent cross-folds with stretched leucosomes, Algonquin domain near Whitney. F: Recumbent cross-folds in eastern Muskoka domain (east of area shown in Fig. 1).

no consensus about the deformation regime in which they developed. Our observations throughout the western ORGC indicate the hinge zones of km-scale cross-folds are composed of strongly lineated rocks with L>>S mineral-shape fabrics, whereas the limbs are weakly lineated with S>>L mineral-shape fabrics (Schwerdtner et al. 1977; Schwerdtner 1987). This dichotomy, previously inferred to be a result of superimposed deformation, is now interpreted in terms of development in a regime of post-peak ductile transtension (Schwerdtner et al. 2014, submitted; Rivers and Schwerdtner 2014).

Since transtension has been relatively neglected in the geological literature until recently, we briefly review the geometric and kinematic principles before discussing its relevance to cross-folds in the study area. Quantitative elaboration of the

principles was developed by Sanderson and Marchini (1984) and Dewey et al. (1998), and analogue and numerical investigations of transtensional strain were performed by Teyssier and Tikoff (1999), Venkat-Ramani and Tikoff (2002), and Fossen et al. (2013). Applications to natural examples were described by Docka et al. (1998), Krabbendam and Dewey (1998), McFadden et al. (2010), and Fossen at al. (2013).

The upper part of Figure 11A is a representation of the model set-up used in most analogue and numerical experiments of ductile transtension, comprising a horizontally layered region of interest between two vertically-sided rigid blocks that diverge at angle α. Axial surfaces and hinge lines of transtensional folds developed in subhorizontal layers are steep and subhorizontal respectively, and oblique to the horizontal axes of the far-field stress system. The folds form by shortening (buckling) normal to their hinge lines and extension parallel to their hinge lines, the latter being a hallmark of transtensional folding. Figure 11B–C illustrates the development of cross-folds in rocks previously deformed into recumbent isoclinal folds, such as may occur during assembly of a thrust stack. The hinge lines of these cross-folds are parallel to those formed in horizontally layered crust, but exhibit a range of axial surface orientation from upright to recumbent depending upon the original orientation of the folded layer, another unique attribute of transtensional folding.

On the basis of the magnitude of α and the orientations of the principal far-field stresses σ_1 and σ_2, transtensional deformation is subdivided into two types: *wrench-dominated systems* ($0° < \alpha < 20°$, σ_2 vertical, σ_1 and σ_3 horizontal), and *extension-dominated systems* ($20° < \alpha < 90°$, σ_1 vertical, σ_2 and σ_3 horizontal, illustrated in Fig. 11A). An artefact of the changing orientations of σ_1 and σ_2 is that in wrench-dominated systems, transtensional folds are amplified during progressive strain, whereas in extension-dominated systems they are suppressed due to vertical shortening (flattening) with the result that open folds with large inter-limb angles develop.

Two-dimensional surface representations of the deformed region undergoing extension-dominated transtensional strain (Fig. 11D) show that hinge lines of transtensional folds rotate towards the extension direction with increasing deformation, with the result that the divergence angle after several increments of strain (θ) is larger than that for a single increment (α).

In applying these principles to the large-scale first-order cross-folds in the ORGC, we note that they are developed in highly attenuated straight gneiss (Fig. 7), preserve evidence for constrictional strain parallel to their hinge lines (L>>S; Schwerdtner et al. 1974, 1977; Schwerdtner 1987), and have large inter-limb angles (Fig. 9B), all compatible with a transtensional setting. Moreover, mesoscopic second-order cross-folds with parallel hinge lines exhibit a range of axial surface orientation from vertical through inclined to recumbent (Fig. 10), also compatible with the analysis of Fossen et al. (2013) and not readily explained by other folding regimes. In summary, the authors consider the interpretation that the cross-folds developed in a regime of post-peak, extension-dominated ductile transtension to be compelling. This conclusion, including an explanation for the L>>S fabrics in their hinges and the S>>L fabrics in their limbs, is developed in greater detail in a companion study by Schwerdtner et al. (submitted).

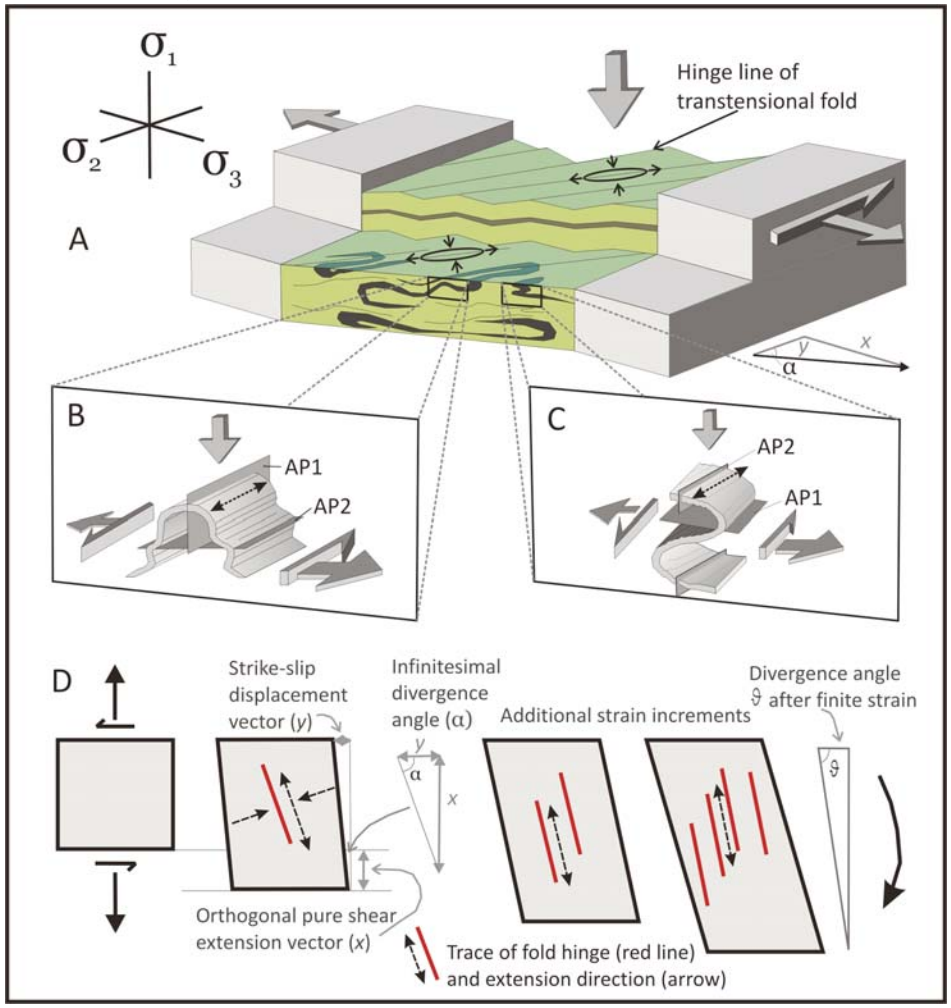

Figure 11. A: Typical model set-up for extension-dominated sinistral transtension of subhorizontally layered crust between vertically-sided rigid blocks with divergence angle α, and the extension (*x*) and wrench (*y*) parts of the transtension tensor. Upper part of figure shows development of transtensional folds with subhorizontal hinge lines, steep axial surfaces, and large inter-limb angles. B–C: Enlargements of lower part of figure showing (B) refolding of pre-existing recumbent limbs of isoclinal folds, giving rise to transtensional folds with steep axial surfaces (AP1), the steep limbs of which may later become refolded by recumbent folds (AP2); and (C) refolding in the steep hinge regions, where superimposed transtensional folds have recumbent axial surfaces (AP1) that may later be refolded by folds with steep axial surfaces (AP2). D: Two-dimensional plan-view sketches showing the extension (*x*) and wrench (*y*) parts of extension-dominated transtension, the infinitesimal divergence angle α, and the finite divergence angle θ after two additional increments of sinistral transtensional strain. Transtensional folds develop by buckling perpendicular to fold hinge lines (due to wrench part of deformation) and extension parallel to their hinge lines (due to extension part of deformation), and orientations of the shortening and extension directions after the first strain increment are shown by dashed black arrows. With successive strain increments, their hinge lines rotate towards the principal extension direction (curved black arrow at right hand side). A–C modified from Fossen et al. (2013).

Boudinage

Straight gneiss with a strongly attenuated fabric, a signature of the Muskoka domain (Fig. 7), implies very high extensional strain in the plane of the foliation and is compatible with the observed wide range of boudinage-related structures. Some general features of boudinage and associated pinch and swell structures are shown in Figure 12, and metre- to cm-scale examples from the Muskoka domain are shown in Figure 13. Since boudinage is a scale-invariant process, such structures may also be anticipated in thicker packages of multi-layers at larger scales (discussed below).

Although in principle boudinage in the Muskoka domain could have occurred during either crustal thickening or extension, cases in which the high-strain fabric surrounding the boudin is amphibolite facies, but the boudin contains evidence for relict granulite-facies assemblages (Figs. 5, 7E, 13E–F), support the interpretation that it principally occurred after the metamorphic peak during retrogression and decompression.

Foliation Boudinage

Foliation boudinage (Fig. 12C) develops when a visually homogeneous foliated or gneissic rock is extended parallel to the foliation beyond its yield strength resulting in brittle−ductile failure, the fracture porosity generated typically being filled with leucosome in high-grade rocks giving rise to pucker structures (Ward et al. 2008). Leucosome-filled pucker structures are common in the Muskoka domain and some examples are shown in Figure 14. Again, the question arises whether the structures developed during thrusting or extension. That all the leucosomes illustrated in Figure 14 are undeformed suggests they are late, an inference supported by the presence of *Hbl*±*Bt* in the attenuated fabric. Moreover, most leucosomes contain peritectic *Hbl*, implying H_2O-saturated melt formed by reaction (3) was either still present after the metamorphic peak or was generated during extension. The occurrence of *Opx*-bearing leucosomes (Fig. 14C) is relatively rare, but may indicate that some melt produced by dehydration melting by reaction (2) at the metamorphic peak was still present and migrated into dilational zones during extension.

Foliation Megaboudins

Kilometre-scale major lenticular structures, first defined and described in the Muskoka domain by Schwerdtner and Mawer (1982), were interpreted as foliation megaboudins by Schwerdtner et al. (2014). Erosion surface slices through these gently dipping elliptical structures appear as oval foliation traces with short-axis dimensions of 20–30 km and long-axis dimensions of 50-60 km; i.e. they are of crustal scale. Two examples were described by Schwerdtner et al. (2014), of which one, the Germania foliation megaboudin, is situated in the study area and illustrated in Figure 15. In 3-D, it has the shape of an inclined disc plunging shallowly to the east (Schwerdtner et al. 2014).

In addition to the implication from its disc shape of significant attenuation of the gneissic foliation on a large scale, the lithologies within the Germania foliation megaboudin also preserve evidence of the ductility contrast that gave rise to the boudinage. The core of the megaboudin is composed of granulite-facies rocks with weak strain fabrics (Fig. 16A–B), whereas the rim consists of amphibolite-facies rocks with high-strain

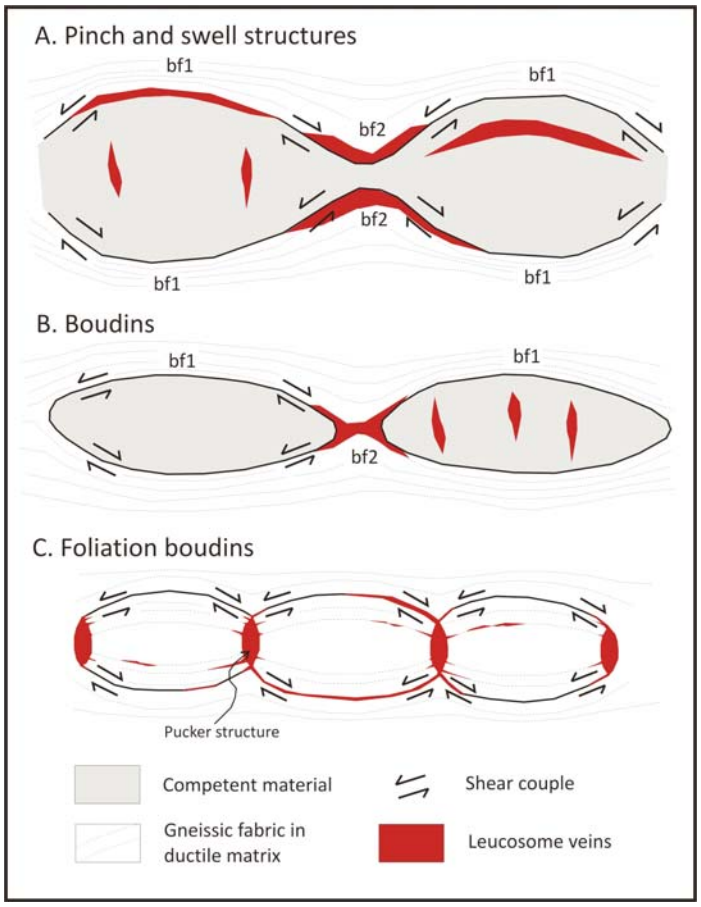

Figure 12. Sketches of (A) pinch-and-swell structures, (B) lenticular boudins, and (C) foliation boudinage. Local shear-sense reversal at opposite ends of boudins is due to differential attenuation between the relatively stiff boudin and ductile matrix. In (A–B) two types of extensional bending fold (bf) in the ductile matrix are shown. bf1 have large inter-limb angles resulting from moulding of the stretched matrix around the curved surface of the boudin, whereas bf2 are lower strain structures with smaller inter-limb angles that form in the neck regions between adjacent boudins, exhibit marked layer thickening in their hinge zones, and die out away from the boudin axis. Lateral change in layer thickness associated with bf1 and bf2 folds provides a measure of local attenuation (see text). In foliation boudinage (C), pucker structures develop despite the lack of obvious lithological or competency contrast between the material forming the boudin and the matrix. Possible locations of leucosome veins are shown in each case. Modified from Schwerdtner et al. (2014).

fabrics (Fig. 16C). This suggests the foliation megaboudin developed by reworking of a pre-existing granulite-facies fabric *during* retrogression, with reaction weakening under suprasolidus conditions reducing viscosity and permitting profound attenuation of the fabric at the margins of the structure. In this context, the weakly strained core is interpreted as a remnant of the peak-Ottawan granulite-facies fabric that escaped post-peak retrogression. Moreover, this may also provide an explanation for the preservation of other weakly strained granulite-facies features in the southwest Muskoka domain, such as those described by Timmermann et al. (2002) and illustrated in Figure 16D. From our reconnaissance work in the Algonquin and Muskoka domains we have tentatively defined several foliation megaboudins (Schwerdtner et al. 2014; Rivers and Schwerdtner 2014), and we consider them to be a signal of the coeval retrogression and attenuation of the peak Ottawan granulite-facies crust.

In contrast to the shapes of typical mesoscopic foliation boudins (e.g. Figs. 12C, 14A–C), the neck regions of the Ger-

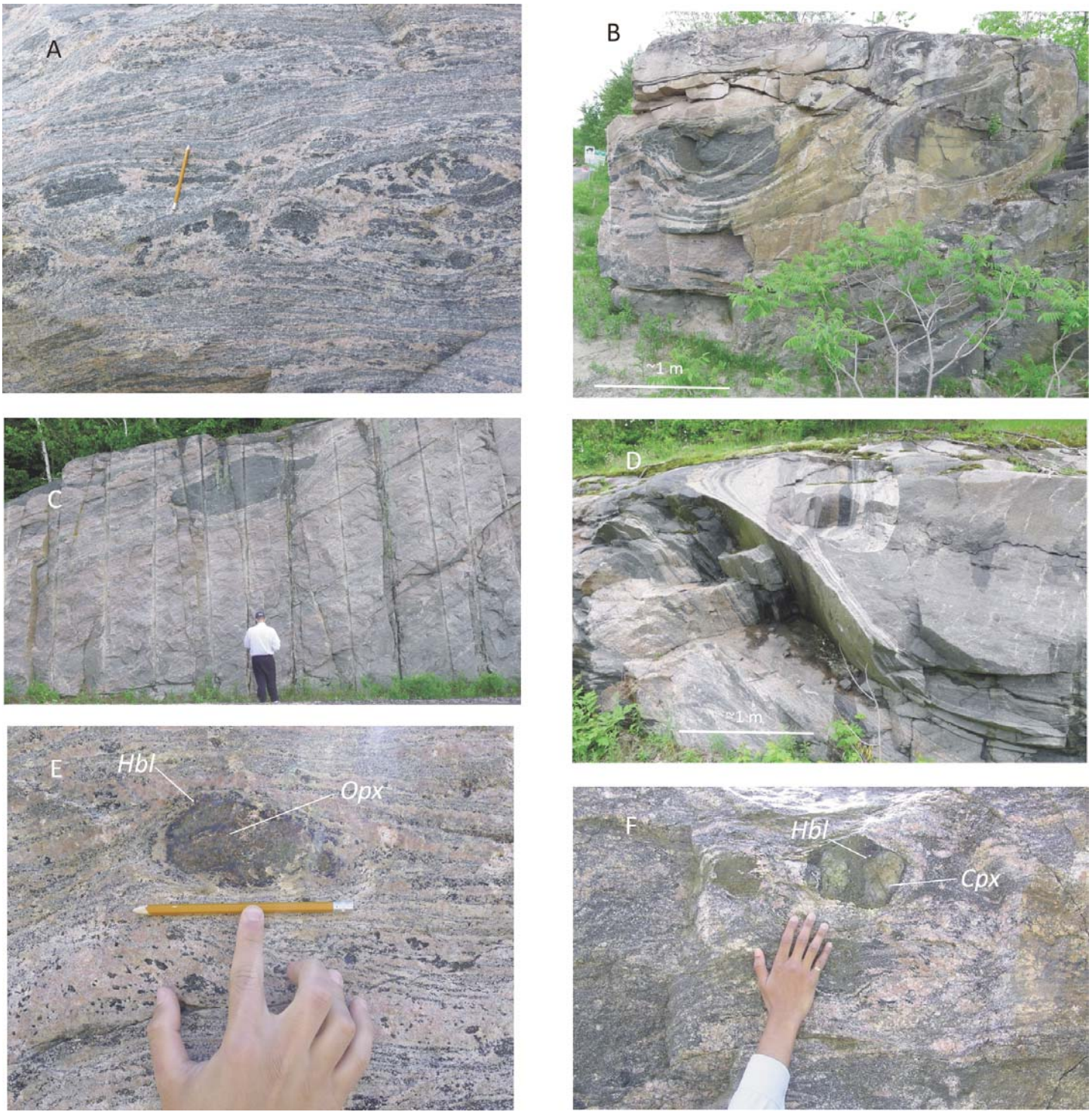

Figure 13. Metre- and centimetre-scale boudinage in amphibolite-facies grey gneiss, Muskoka domain. A: *Hbl*-bearing leucosome surrounding boudins during break-up of amphibolite layers; B–C: Differing degrees of separation between adjacent boudins; D: 'Fishmouth' boudin in which the boudin margin undergoes attenuation with adjacent matrix after formation; softening and attenuation of the boudin margin are driven by retrogression. Note thin leucosome-filled extensional fractures in boudin at high angle to the external foliation; E–F: Evidence that boudinage was associated with retrogression of the gneissic fabric surrounding the boudin, specifically relict *Opx* in the core of a small boudin with a *Hbl* rim in E, and clinopyroxenite boudin partially replaced by amphibolite along a fracture at high angle to the gneissic layering in F, implying brittle extension was accompanied by retrogression of *Cpx* to *Hbl*.

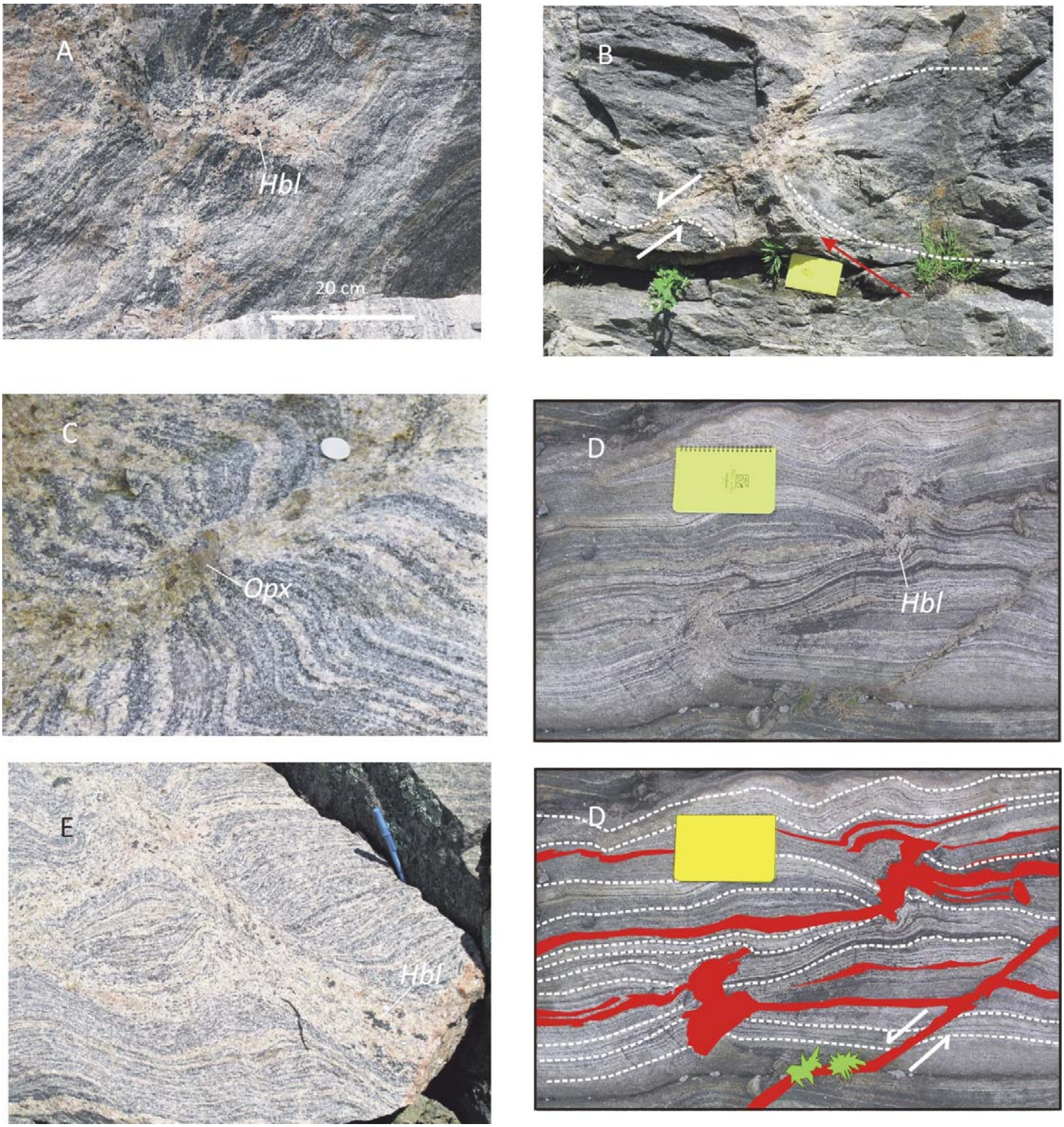

Figure 14. Field photographs of small-scale foliation boudinage showing pucker structures, A–D in grey gneiss from the Muskoka domain, E from the Parry Sound domain. A–C: Spidery cm-scale granitoid leucosomes in boudin necks are not continuous for more than a few cm suggesting local derivation, and may be sites of melt loss. In (B) foliation is enhanced with dashed white lines and minor extensional offset is shown (half arrows); localized high strain foliation (red arrow) defines margin of foliation boudin. Leucosomes in A–B have peritectic *Hbl*, those in C have peritectic *Opx*; *Hbl*±*Bt* present in foliation in all cases. D (shown without and with interpretation): Leucosome with peritectic *Hbl* in the neck regions between foliation boudins, parallel to the foliation, and along a discordant vein that exhibits normal-sense offset (half arrows). In contrast to (A–C), at least some of the leucosome was derived from outside the field of view. E: Boudin surrounded by leucosome with peritectic *Hbl*, possible small-scale analogue for an early stage of formation of foliation megaboudins (see text).

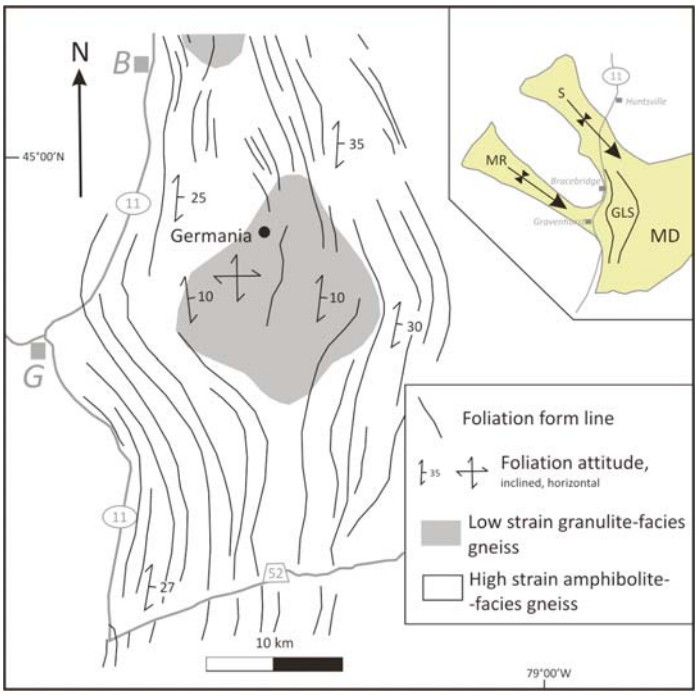

Figure 15. Sketch map of the Germania foliation megaboudin or Germania lenticular structure (GLS), showing its discoid shape in 2-dimensions defined by structural form lines, with the central area underlain by weakly strained granulite-facies rocks and the margins by high-strain amphibolite-facies gneiss. The granulite-facies core of the structure is a peak-Ottawan metamorphic relict; foliation megaboudinage and formation of the high-strain amphibolite-faces gneiss at the margins of the structure took place during post-peak exhumation and retrogression. Location of granulite at northern margin of map from Timmermann et al. (2002). *B* – Bracebridge, *G* – Gravenhurst (modified from Schwerdtner et al. 2014). Inset figure shows location of the GLS within the Muskoka domain (MD) and its relation to the Moon River (MR) and Seguin (S) synforms. Modified from Rivers and Schwerdtner (2014).

Figure 16. A–C: Comparison of structures and mineral assemblages developed in the core (A–B) and margin (C) of the Germania foliation megaboudin. The core exhibits coarse-grained granulite-facies mineral assemblages and weak strain fabrics, whereas the margin consists of high-strain amphibolite-facies gneiss. B: 1–2 cm, undeformed orthopyroxene megacrysts in metamonzonite in the core of the megaboudin. D: Undeformed granulite-facies enclave with anastomosing network of *Opx*-bearing leucosome. A and C from Schwerdtner et al. (2014), D from Timmermann et al. (2002).

mania foliation megaboudin are not the sites of spidery leucosome bodies or pucker structures at high angle to the foliation. This may suggest that leucosome at the terminations of the megaboudin formed early and became attenuated with the amphibolite-facies foliation, as seen in the mesoscopic examples illustrated in Figures 7E and 14E. In summary, the orientation, shape, size and mineral assemblages of the Germania foliation megaboudin imply post-peak, N-S stretching and ductile attenuation of crustal scale in the Muskoka domain, i.e. orogen-perpendicular extension during exhumation and orogenic collapse.

Large-scale Extensional Bending Folds

Boudinage implies the ductile layering surrounding the boudin is attenuated, forming extensional bending folds of opposing curvature surrounding the boudin itself and within the boudin neck region (bf1 and bf2; Fig. 12). Examples of large-scale ($\geq$ 10 km) extensional bending folds in the Parry Sound domain of the ORGC were given by Schwerdtner et al. (2014). We describe an example defined by the NW-trending boundary between structural levels 2 and 3 here, which separates the antiformal, granulite-facies Rosseau subdomain (structural level 2) from the synformal Seguin subdomain (structural level 3). The non-cylindrical bf2 extensional bending fold is termed the Camel Lake synform (Fig. 17). The folded foliation defining the Camel Lake synform is an

amphibolite-facies high-strain fabric, locally straight gneiss, providing qualitative support for an origin by post-peak retrogression and attenuation.

The minimum magnitude of the NW-SE ductile extension associated with the development of the Camel Lake synform and adjacent antiforms can be estimated from the map pattern and km-scale UTM grid in Figure 17 and assuming a plunge of 20°ENE (Lumbers and Vertolli 2000a). In the horizontal plane, the apparent thicknesses in the core of the synform and adjacent antiform are ~5.5 km and 0.5 km (*t* and *t'*, Fig. 17), corresponding to true thicknesses of ~1.9 and 0.2 km respectively, indicating the thickness of the antiformal hinge zone around the barrel-shaped megaboudin was reduced by ~90%. The amount of orogen-perpendicular extension on the 10 km scale implied by this attenuation (double-headed red arrow; Fig. 17) can be constrained within broad limits assuming the rock volume and thickness of the hinge zone of the Camel Lake synform remained constant during extensional bending (Schwerdtner 1970, 1977). Assuming *average* thinning of 50% on the 10 km scale, for axisymmetric biaxial boudinage NW-SE bulk extension would have been ~40%, whereas for triaxial boudinage (typical of the field area; Schwerdtner et al. 2014) NW-SE bulk extension may have exceeded 200%.

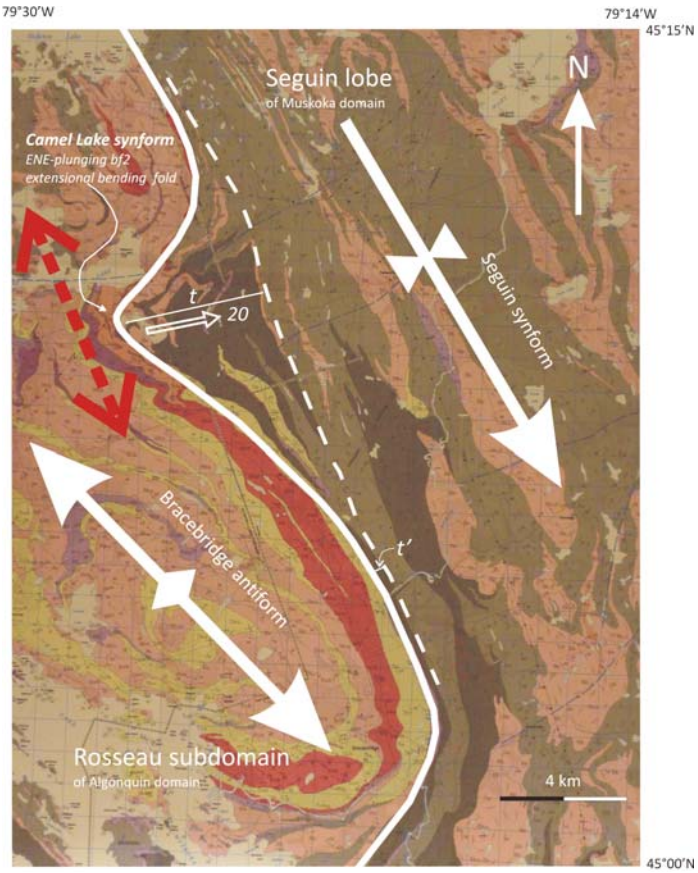

Figure 17. Photograph of part of a 1:50,000 scale geological map with overlain line-work showing the Camel Lake synform, a bf2 extensional bending fold outlined by the thick solid white line marking the contact between the granulite-facies Rosseau subdomain and amphibolite-facies Seguin subdomain (structural levels 2 and 3, respectively). The thinner dashed white line marks the approximate eastern limit of the Camel Lake synform in the Seguin subdomain, illustrating the extreme thickening in the fold hinge and non-cylindrical geometry characteristic of bf2 folds. The boundary between the Seguin and Rosseau subdomains dips ~20–30° ENE in most of the map area, and the Camel Lake synform plunges at ~20 -->070°. The hinge region of the synform is a low-strain window, preserving isoclinal folds in the mafic grey gneiss unit (dark brown) that probably developed during prograde thrusting and crustal thickening and were refolded during post-peak boudinage and formation of the Camel Lake synform. The red NW-SE-trending double-headed arrow indicates the orogen-perpendicular extension direction implied by the Camel Lake extensional bending fold. Part of the Bracebridge sheet (NTS 31 E/3; Lumbers and Vertolli 2000a; UTM km grid for scale); map reproduced by permission of the Ontario Geological Survey.

Also apparent from Figure 17 is the preservation of isoclinal folds in mafic grey gneiss in the core of the Camel Lake synform that are refolded by the synform itself. This supports our contention discussed above that the thicker crustal section in the core of the synform is a low-strain window. Hence, we infer the isoclinal folds developed during thrusting and prograde metamorphism, whereas the refolding took place during post-peak retrogression and triaxial boudinage.

In summary, we conclude the Camel Lake synform provides evidence for very substantial attenuation of the base of the Muskoka domain during formation of the regional post-peak amphibolite-facies foliation. The orientation and location of the boudinage and extensional bending fold imply the more competent, granulite-facies structural level 2 was extended in a NW-SE, orogen-perpendicular direction probably by > 200%, and the overlying more ductile Muskoka domain in structural level 3 underwent local attenuation by as much as 90% in the barrel-shaped bf1 bending folds, thereby collectively providing evidence for important post-peak orogen-perpendicular crustal extension and thinning on the 10 km scale.

Extensional Fault Propagation Folds and Granite Pegmatite Dykes

Fault propagation folds (FPFs) develop at the tips of active brittle faults (Fig. 18), and until recently, extensional FPFs were only known from unmetamorphosed sedimentary rocks (e.g. Schlische 1995; White and Crider 2006; Ferrill et al. 2012). The first report of extensional FPFs in gneissic rocks was by Schwerdtner et al. (2014) who investigated their relationship to late cross-cutting pegmatite dykes in the ORGC.

Since FPFs are brittle-ductile structures that develop in rocks with significant strength, their presence in plastically

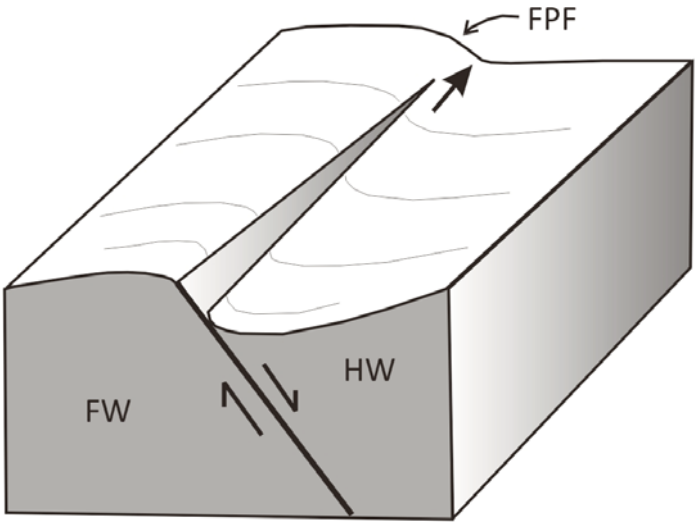

Figure 18. 3-D sketch showing the lateral propagation of an extensional fault leading to the formation of a fault propagation fold (FPF) with a subhorizontal axis. FPFs develop from the distribution of elastic stresses at the fault tip due to the scissor movement of the fault, and their formation is restricted to brittle-ductile rocks. FW – footwall, HW – hanging wall. Redrawn from White and Crider (2006).

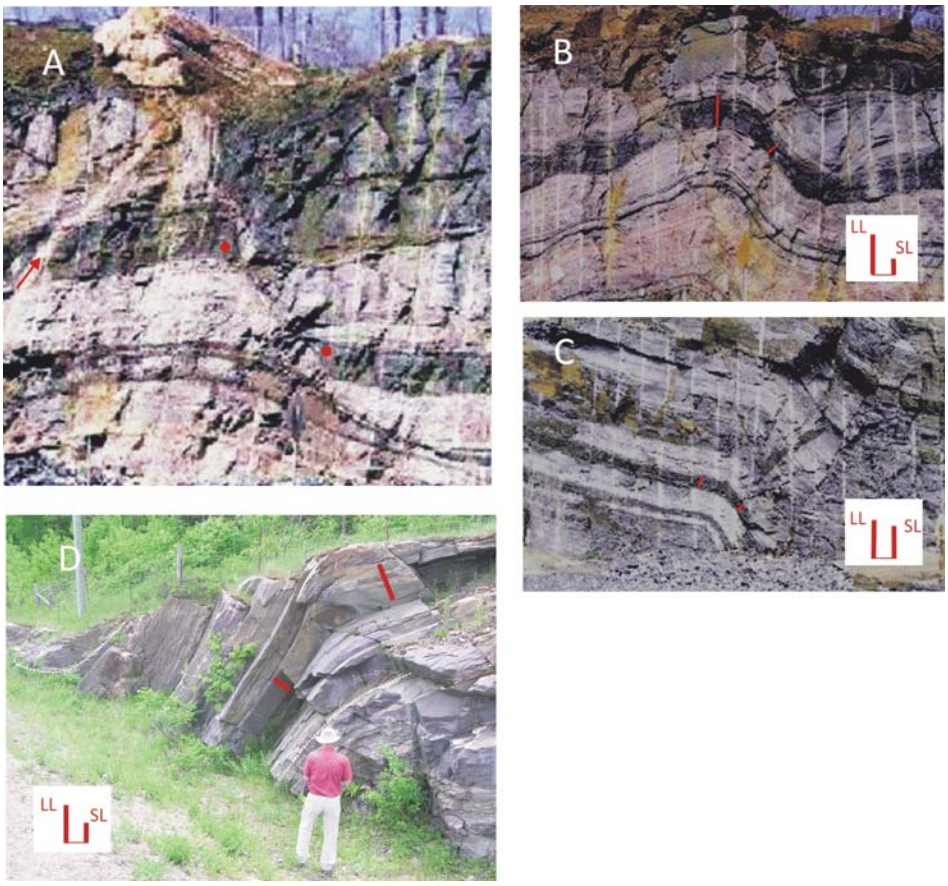

Figure 19. SE-dipping extensional fault propagation folds (FPFs) in the Ottawa River Gneiss Complex. A: FPF transected by an extensional fault parallel to the short monoclinal limb that causes visible offset of amphibolite layer (red dots mark piercing points). Red arrow points to NW-dipping granite pegmatite dyke oriented parallel to the axial surface of the FPF in the footwall. B–D: FPFs in which the short monoclinal limbs are attenuated, but there is no fault. Red bars show thicknesses of folded layers on the long limbs (LL) and short limbs (SL), and their relative lengths are compared at the bottom of each image. Attenuation in the short monoclinal limb ranges from 100% in A, ~60% in B, ~45% in D, to ~18% in C. Foliation is highlighted by dashed white line in D. A–C modified after Schwerdtner et al. (2014).

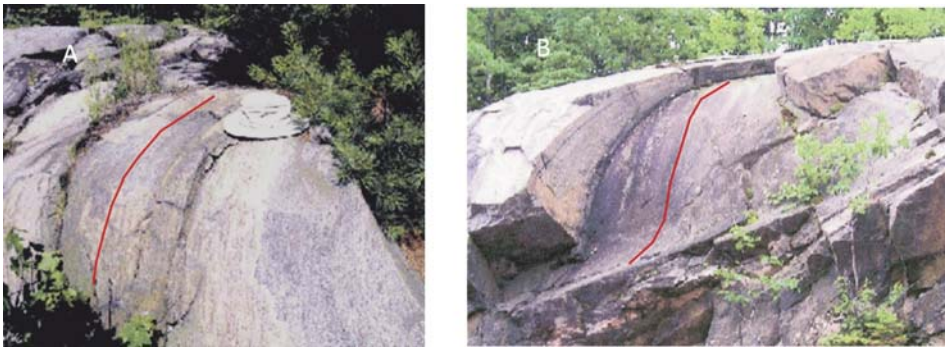

Figure 20. Fault propagation folds in the Muskoka domain showing down-dip lineations (highlighted by thin red lines) on the short monoclinal limbs. Slightly modified from Schwerdtner et al. (2014).

deformed high-grade gneiss of the ORGC implies they formed late in the history of the gneiss complex, after the high-grade rocks had undergone significant exhumation and cooled and strengthened. Our field work indicates that extensional FPFs are common in the ORGC and some examples and characteristic features are shown in Figures 19–20. In general, their hinge zones form arcs or quasi-chevron shapes and they exhibit monoclinal symmetry due to dissimilar limb lengths. The short limbs of most FPFs dip moderately to steeply to the SE, may be significantly thinned compared to the long limbs (Fig. 19), and are the sites of approximately down-dip lineations defined by fine-grained stretched mineral aggregates that are subparallel to the regional L fabric (Fig. 20). There is a visual correlation between the strength of the lineation and the degree of attenuation in the short limb of the FPFs (Fig. 19), suggesting that in some FPFs the regional extension lineation was enhanced *during* formation of the FPF by flexural shear between adjacent layers (e.g. Hobbs et al. 1976). This conclusion is compatible with their development spanning the ductile–brittle transition.

The absolute time of formation of extensional FPFs such as those illustrated in Figures 19–20 cannot be readily determined, but Schwerdtner et al. (2014) showed that the short limbs of some FPFs are the sites of cross-cutting, undeformed to weakly deformed granite pegmatite dykes from < 1–15 m wide, the emplacement of which is considered to closely approximate the time of FPF formation. They referred to these as set-1 dykes and some examples from the Muskoka domain are shown in Figure 21. A later set of granite pegmatite dykes that is undeformed and in which individual dykes are generally thinner (< 50 cm), was emplaced parallel to the NW-dipping axial surfaces of the FPFs. Examples of these set-2 dykes are illustrated in Figure 22.

Figure 23 is a sketch showing the geometric relations of set-1 and set-2 dykes and extensional FPFs and their inferred emplacement mechanisms. We envisage a regime of limited brittle-ductile extension during gravitationally-driven orogenic collapse with dyke emplacement driven by magmatic overpressure at depth. As noted previously, U–Pb zircon crystallization ages of the pegmatite dykes in the ORGC, some of which were located in the monoclinal limbs of FPFs, are ~1000–990 Ma (Corrigan et al. 1994; Bussy et al. 1995), compatible with the deduction of late-orogenic emplacement.

Schwerdtner et al. (2014) compiled orientation data for poles to > 1200 granite pegmatite dykes from the Algonquin and Muskoka domains of the ORGC and the northern margin of the CAB that yielded a maximum in the SE quadrant, implying most dykes have NE-SW strikes and NW dips respectively. From these data, they showed that the set-1 and set-2 dykes are principally SE- and NW-dipping respectively. In Figure 24A–B, we present new data for the orientations of poles to >500 mostly set-2 pegmatite dykes in the map area and adjacent parts of the Muskoka domain. These

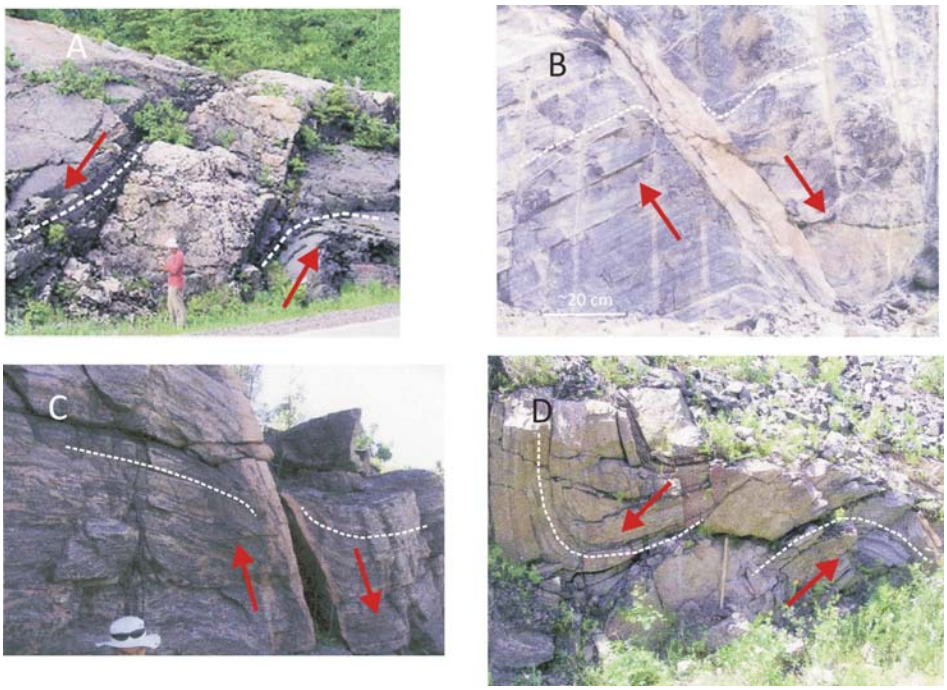

Figure 21. Set-1 SE-dipping granite pegmatite dykes emplaced in short limbs of FPFs, Muskoka domain. White dashed lines highlight curvature of gneissic layering adjacent to dykes. Sense of displacement indicated by red arrows is top-side-down to SE. A after Schwerdtner et al. (2014), B–D after Rivers and Schwerdtner (2014).

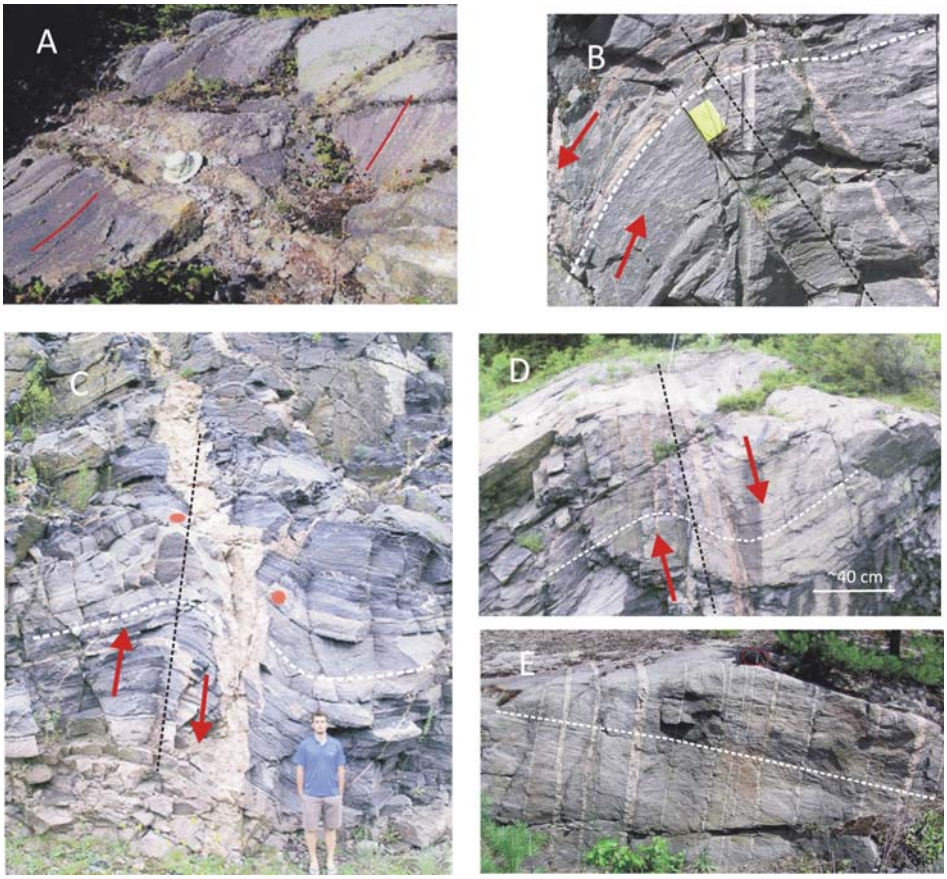

Figure 22. Set-2 granite pegmatite dykes (gneissic foliation highlighted by dashed white lines, axial surface of FPF indicated by dashed black lines; red arrows indicate sense of displacement in FPF, red dots in C are piercing points). A–D: Cross-cutting dykes parallel to steeply NW-dipping axial surfaces of FPFs (except C in which axial surface and dyke are subvertical), Muskoka domain; in A, outcrop surface exposes short monoclinal limb of FPF with down-dip lineation (highlighted by red lines) cut by pegmatite dyke (under hat). E: swarm of subvertical dykes, Algonquin domain (camera case outlined in red for scale). Displacement in FPFs is top-side-down to SE in A–B and to NW in D. A and C modified from Schwerdtner et al. 2014.

data also define a statistically significant maximum in the SE quadrant of the stereonet.

A model for emplacement of the SE-dipping set-1 dykes that form a small part of the population is shown schematically in Figure 24C. For the NW-dipping set-2 dykes, we follow the interpretation of Schwerdtner et al. (2014) in part, but also propose an additional controlling factor. On the basis of the observation that the regional SE dip of the gneissic layering is statistically perpendicular to the orientations of most set-2 dykes, Schwerdtner et al. (2014) proposed that gravitationally driven slip on incompetent layers in the mechanically active layering caused reorientation of the local principal stress from vertical to orthogonal to the layering, promoting fractures (tension gashes) in adjacent more competent layers (Fig. 24D). As with the set-1 dykes, magmatic overpressure at depth led to utilization of these fractures for emplacement of the set-2 dykes. Our new insight is that some of the set-2 dykes are preferentially oriented parallel to the axial surfaces of the FPFs (Figs. 19A, 22). These surfaces are also at high angles to the gneissic layering rendering them statistically indistinguishable to foliation normals. We speculate that the quasi-chevron style of the FPFs induced mechanical weakness parallel to the axial surfaces that was subsequently exploited by overpressured magma from depth.

DISCUSSION

In the previous paragraphs, we have presented observations pertaining to the post-peak structural and metamorphic development of the Muskoka domain in the study area. Based on our investigations elsewhere we have no reason to believe they are not representative of the domain as a whole, and in this section we draw them together, emphasizing salient points and noting any departures from previous interpretations.

Fluid-fluxed Partial Melting and Post-peak Retrogression

As discussed above, our work suggests the amphibolite-facies assemblages that characterize much of the Muskoka domain are a retrograde feature. The local preservation of Ottawan (~1085 Ma) granulite- or H*P*-granulite-facies assemblages provides insight into the peak Ottawan *P–T* metamorphic conditions and suggests they were comparable to those in the underly-

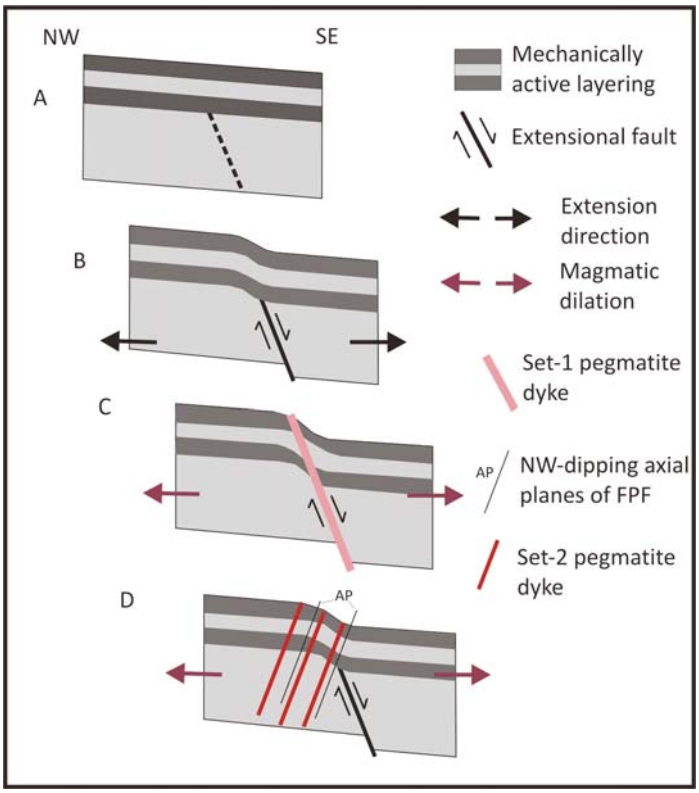

Figure 23. Sketches illustrating relationships of granite pegmatite dykes to extensional FPFs in the ORGC. Regional mechanically active gneissic layering dips gently SE. A–B: Local thinning associated with propagation of high-level extensional fault and formation of FPF. C: Emplacement of set-1 pegmatite dyke, magmatic dilation perpendicular to short limb of FPF. Subsequent displacement on fault, if any, results in brittle deformation of the dyke. D: Emplacement of set-2 dykes parallel to NW-dipping axial surface of FPF. Modified from Schwerdtner et al. (2014).

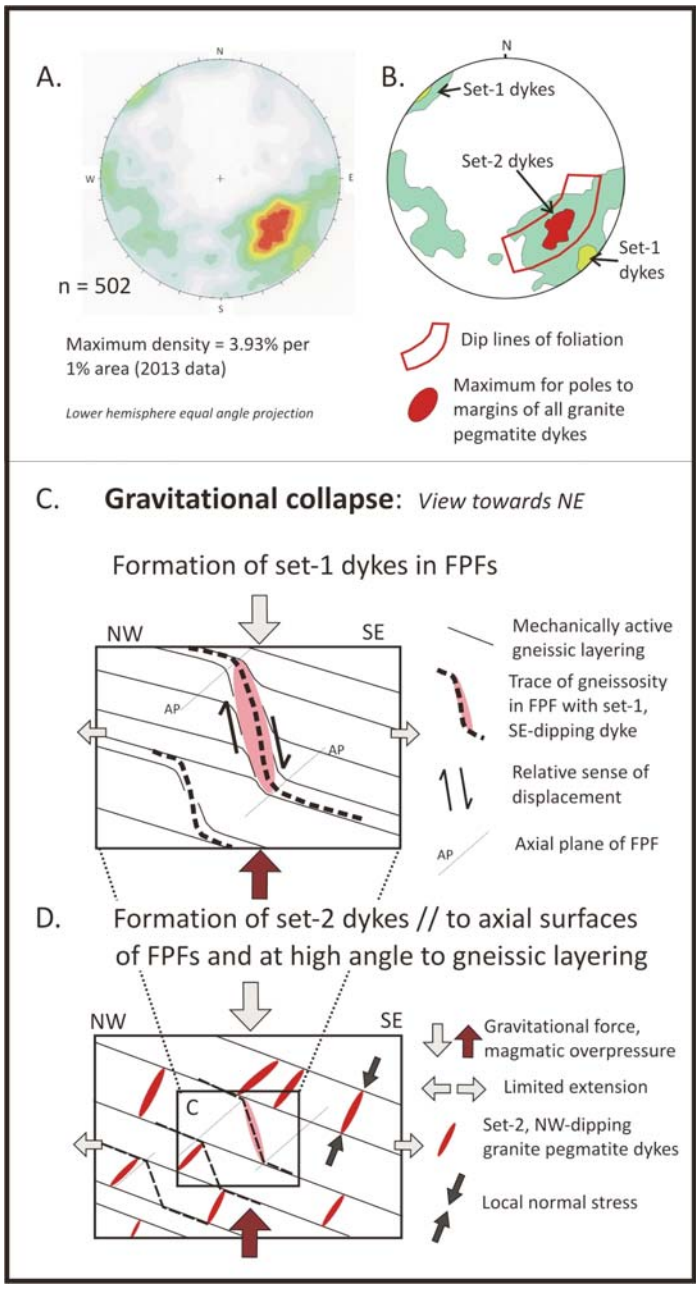

Figure 24. A: Stereographic plot of poles to margins of pegmatite dykes, Muskoka domain (2013 data). Maximum point density of 3.93% per 1% area is statistically significant. B: Summary of data in A showing the maximum point density within the arc segment defined by the dip directions of the host gneissic layering. C–D: Schematic cross-sectional model of the Muskoka domain viewed towards NE showing formation of set-1 and set-2 dykes. Intrusion of dykes is driven by a negative vertical gradient in magmatic overpressure in crust undergoing gravitational collapse, implying emplacement in an overall regime of subhorizontal crustal extension; magma plumbing system not shown. Model is scale invariant; measured dyke widths range from a few cm to 15 m and dyke lengths are generally greater than the height of outcrops, but are otherwise unconstrained. D modified from Schwerdtner et al. (2014).

ing Algonquin domain before retrogression. Thus we deduce that the reported examples of coexisting granulite and amphibolite in the Muskoka domain resulting from local variations in a_{H2O} in a H_2O–CO_2 fluid phase (Pattison 1991; Timmermann et al. 2002) are relict features that elsewhere have been so pervasively overprinted by high-strain amphibolite-facies assemblages and fabrics as to be completely or almost completely obliterated. This interpretation is reinforced by the striking visual correlation between the weak strain in the preserved granulite-facies assemblages (Fig. 16A–B, D; Pattison 1991, his figs. 3–4; Timmermann et al. 2002, their fig. 3) and the high-strain amphibolite-facies assemblages that characterize most of the Muskoka domain (Fig. 7) and are especially well developed along its basal contact with the Rosseau subdomain (Rivers and Schwerdtner 2014). Thus in a regional context, we consider the evidence supports a *sequential* evolution involving partial to almost total retrogression of a peak granulite-facies domain.

A principal conclusion of the study of migmatization in the Muskoka domain by Slagstad et al. (2005) was that although some *Opx*-bearing leucosome was formed by *Bt*-dehydration melting on the prograde metamorphic path, the large volume of *Hbl*-bearing leucosome (≥ 30–50% in many outcrops) is incompatible with both the thin melanosomes and an origin by dehydration melting, and requires that much melt was derived elsewhere by water-fluxed melting and injected into the domain. Thus both the mineralogical composition and the volume of the most abundant leucosomes indicate open-system conditions at or after the metamorphic peak.

The inference of widespread retrogression from peak granulite- to post-peak amphibolite-facies assemblages at suprasolidus conditions implies pervasive ingress of hydrous fluid at high *P–T,* and the presence of *Pl* aggregates pseudomorphing former *Grs*-rich *Grt* implies significant decompres-

sion at high *T*. Details of the *P–T–a*$_{H2O}$ retrograde path at high *T* remain poorly constrained, particularly the extent to which ingress of the hydrous fluid (± K-Na brine) fluxed suprasolidus partial melting, a process that appears likely in principle. The striking correlation between post-peak strain and retrogression in the Muskoka domain suggests these variables were intimately linked and constituted a positive feedback loop, giving rise to the characteristic straight gneiss fabric (Fig. 7) with a few 'islands' of weakly strained, largely unretrogressed granulite remaining. Concerning the timing of retrogression in the ORGC, available geochronological data indicate it may have begun as early as ~1060 Ma (Bussy et al. 1995; Timmermann et al. 1997, 2002; Slagstad et al. 2004a, b), and that it was widespread and pervasive at ~1020 Ma (Ketchum et al. 1998). Moreover, brittle-ductile extension and pegmatite emplacement were ongoing in the cooled exhumed rocks at ~1000 Ma (see Schwerdtner et al. 2014). However, geochronological data that are well constrained by field relations relevant to this issue remain few and there is scope for additional work to bracket the different stages of this process more tightly.

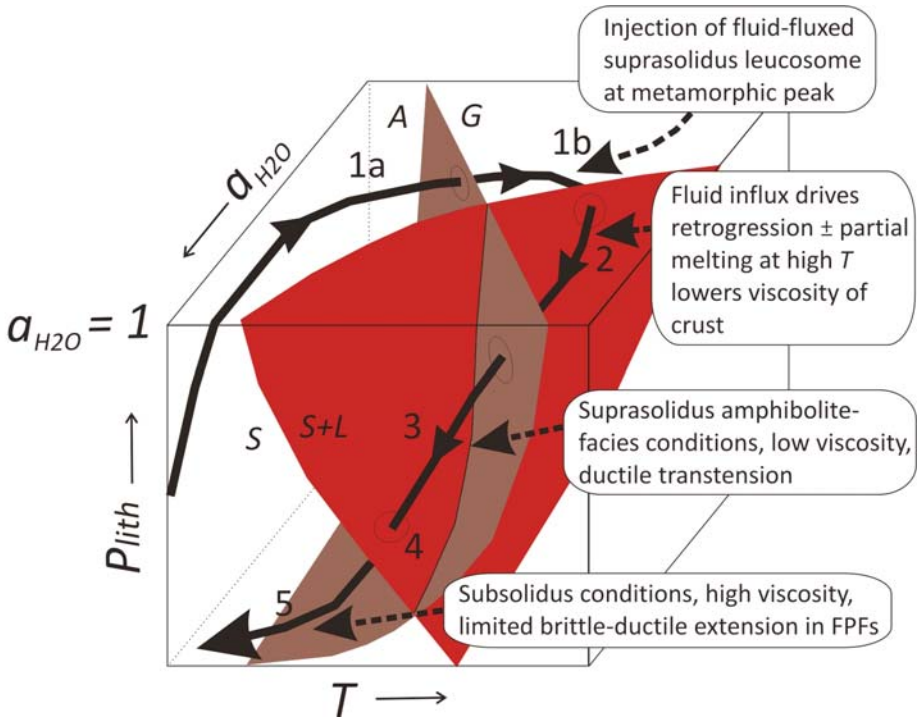

Figure 25. Schematic *P–T–a*$_{H2O}$*–t* path for the Muskoka domain; brown plane represents boundary between amphibolite–granulite (*A–G*) facies; red plane represents the granite solidus separating solid phases (*S*) from solids coexisting with silicate liquid (*S+L*). *Stage 1:* Prograde Ottawan metamorphism during formation of crustal-scale thrust stack; *1a*: amphibolite-facies path; *1b*: granulite-facies path, attainment of peak *P–T* at low *a*$_{H2O}$, limited *Bt*-dehydration melting, injection of suprasolidus leucosome (Slagstad et al. 2005). Estimated peak *P–T* conditions ~1000–11000 MPa / 800–850°C at ~1085 Ma (Timmermann et al. 2002). *Stage 2:* Initiation of gravitational collapse at ~1060 Ma(?). Influx of hydrous fluid at near-peak *P–T* drives *a*$_{H2O}$ towards unity, promoting widespread retrogression to amphibolite-facies assemblages ± fluid-present partial melting. *Stage 3:* Suprasolidus amphibolite-facies assemblages with coexisting leucosome, low viscosity crust, initiation of transtensional cross-folding, boudinage, decompression and cooling. *Stage 4:* Transition to subsolidus conditions, significant increase in crustal viscosity and diminution of ductile extensional strain. *Stage 5:* Brittle-ductile extensional fault-propagation folding and dyke injection in cooled, partly exhumed, and largely retrogressed crust (~1000 Ma).

Figure 25 is a schematic *P–T–a*$_{H2O}$*–t* loop for the Muskoka domain. Details supporting the ~100 m.y. duration of the complete *P–T–t* path, and the ~60 m.y. duration of the post-peak segment involving retrogression and decompression are summarized above and in the caption. The inferred central role of an influx of hydrous fluid in stage 2, driving retrogression and possibly also partial melting in the peak suprasolidus granulite-facies assemblages, is shown by the important increase in the *a*$_{H2O}$ variable at high *P–T*. Decompression (stage 3) principally took place under suprasolidus amphibolite-facies conditions and occurred while the rocks were undergoing extension, as witnessed by the attenuated high-strain amphibolite-facies foliation around boudins and pinch-and-swell structures, and the prolate *Pl* aggregates after *Grt* in mafic rocks. Transition to subsolidus conditions (stage 4) appears to have taken place after most penetrative strain had ceased but the *T* was still sufficiently high to anneal fabrics in straight gneiss.

The nature of the dominant melting reaction (dehydration melting *versus* water-fluxed melting) is important as it bears on the overall density of the system and whether there was a positive contribution to buoyancy and exhumation (Clemens and Droop 1998; Teyssier and Whitney 2002; Whitney et al. 2013; Yakymchuk and Brown 2014; Weinberg and Hasalová 2015). We have followed the logic of Slagstad et al. (2005) to argue from the abundance of leucosome with peritectic *Hbl* that water-fluxed melting was widespread in the Muskoka domain, thereby supporting the thesis of Weinberg and Hasalová (2015) that this can be an important process in the deep crust. Such leucosomes with high *a*$_{H2O}$ are unable to rise far in the crust before reaching their solidi and do not make a positive contribution to buoyancy. Thus, unless post-peak intrusion of voluminous low *a*$_{H2O}$ melt derived by dehydration melting in the deeper crust (i.e. Algonquin domain) was important, the ORGC as a whole would not have had positive buoyancy relative to the overlying carapace. As noted, rare occurrences of leucosome with peritectic *Opx* in post-peak extensional structures may be explained by drainage of liquid formed by *Bt*-dehydration melting on the prograde path rather than by melt formed during decompression, but their small volume suggests they would have made a negligible contribution to crustal density. Overall, these considerations lead us to conclude that exhumation of the metamorphic core of the ORGC was probably driven by regional forces rather than local buoyancy forces, i.e. it is not a gneiss dome.

Collapsed Large Hot Orogen

As noted in the introduction, following numerical modelling of LHOs by Beaumont et al. (2001), the channel flow concept was applied with some success to the hinterland of the Grenville Province (e.g. Jamieson et al. 2007, 2010; Rivers 2008, 2012; Jamieson and Beaumont 2011; Rivers et al. 2012). In this study we do not directly address the question of whether the ORGC carries a cryptic signal of channel flow at

peak metamorphic conditions, but rather focus on the post-peak history and its bearing on gravitationally driven collapse. Figure 25 shows our interpretation that post-peak retrogression and extension in the Muskoka domain began at high *P–T* in ductile suprasolidus rocks and continued to lower *P–T* in brittle-ductile subsolidus rocks, resulting in profound, but spatially heterogeneous, structural reworking, i.e. compatible with the *Collapsed LHO paradigm* discussed in the introduction. The presence of abundant leucosome, both derived *in situ* and injected from elsewhere, followed by pervasive retrogression ± fluid-present partial melting, transformed the Muskoka domain into a weak ductile detachment zone between two stronger crustal members: the underlying granulite-facies Algonquin domain, and the overlying greenschist- to amphibolite-facies Composite Arc Belt. Thus, although possibly focussed in rocks that were already weak due to grain-size reduction and the presence of leucosome at the metamorphic peak, we argue that the domain remained rheologically weak during much of its post-peak retrograde evolution.

In addition to linked dynamic retrogression and extensional strain *within* the Muskoka domain, Rivers and Schwerdtner (2014) reported field evidence from the vicinity of its lower contact with the granulite-facies Rosseau subdomain for dynamic *downward* encroachment of the domain boundary into its footwall by high-strain reworking and retrogression, a deduction that may explain the different locations of the boundary on regional maps (e.g. in Figs. 1 and 2). Moreover, there is also evidence for *upward* dynamic growth of the Muskoka domain into its hanging wall, for example where the northwest terminus of the Moon River lobe of the Muskoka domain is overlain by the Parry Sound domain. In this area, a monzogranite gneiss unit with *'augen structure and relict igneous texture'* in the hanging wall (Parry Sound domain) was pervasively reworked in the contact zone into '[monzonitic gneiss with] *laminated structure and* [amphibolite-facies] *metamorphic fabric'* in the footwall (Moon River subdomain) (descriptions from map legend, Lumbers and Vertolli 2000c). These observations imply that the high-strain amphibolite-facies character of the Muskoka domain (structural level 3) was not only progressively imposed throughout the domain itself, leaving a few remnant 'islands' of granulite-facies rocks, but also encroached into both its lower and upper contacts (structural levels 2 and 4). More generally it points to dynamic growth of high-strain extensional/ transtensional fabrics during retrogression, and incidentally suggests that not all lithologies in the Muskoka domain are monocyclic.

On the basis of seismic data (White et al. 2000), the present true thickness of the thrust stack comprising the allochthonous part of the ORGC (structural levels 2–4) is about 30 km, and that of the Muskoka domain (structural level 3) about 7 km (Fig. 2). We deduce that the thickness of gneiss comprising the Muskoka domain was substantially greater prior to collapse, and thus that it records an important, but regionally unquantified component of sub-vertical thinning and sub-horizontal extensional strain. As discussed, this strain was likely strongly heterogeneous, but on the basis of visually estimated 2-D shapes of plagioclase pseudomorphs after garnet in metagabbro and mafic gneiss of ~2:1 to 4:1 on horizontal surfaces (Fig. 6) and ~2:1 to 3:1 on vertical surfaces, it may have been on the order of 50–75% locally, and was ~90% at the base of the Muskoka domain adjacent to the contact with the boudinaged Rosseau subdomain (Fig. 17).

In summary, we consider the evidence marshalled above provides strong support for the *Collapsed LHO paradigm*. Moreover, since LHOs in the numerical models of Beaumont et al. (2001) are characterized by a mid-crustal channel under the orogenic plateau, this conclusion indirectly implies the former existence of a mid-crustal channel – which as noted in the introduction is compatible with the contrasting tectonic evolutions of contemporary units in the orogenic infrastructure and superstructure (Fig. 4). We thus tentatively conclude that collapse may have been focussed in the former mid-crustal channel, thereby explaining why the latter is not readily identified from the present map pattern.

Metamorphic Core Complex

Collectively these observations and deductions support a metamorphic core complex model for the present architecture of the ORGC (Fig. 26A), with the Muskoka domain forming the detachment zone separating the core from the cover. However, the ORGC is at least an *order of magnitude larger* in horizontal dimensions than envisaged by Whitney et al. (2013) in their review, a difference that may perhaps be explained by the large area of double thickness crust, the deep erosional level, and the unusually large amount of leucosome in the mid crust in the Grenville Orogen. Moreover, unlike the generic models of core complexes that have symmetrical dome shapes, the ORGC exhibits regional dips towards the SE and is asymmetrical, a feature we attribute to later crustal thickening of its northwestern footwall during formation of the Parautochthonous Belt in the Rigolet phase of the Grenvillian Orogeny. This asymmetry also explains why the detachment zone of the core complex is principally located along its southeastern margin.

Figure 26B emphasizes the relationship between the core and the detachment zone. In Cordilleran core complexes, the detachments range from thin (< 100 m) zones of greenschist-facies mylonite in high-level examples (e.g. Malavieille 1993), to much thicker (~2 km) zones of high-strain amphibolite-facies gneiss in deeper examples (e.g. Carr et al. 1987; Schaubs et al. 2002). In both cases, the rocks comprising the detachment zone were derived from the fluid-weakened top of the metamorphic core. In the case of the ORGC, although the detachment zone comprising the Muskoka domain is considerably thicker again (~7 km), the model remains applicable in that it was similarly derived from the metamorphic core, which we deduce in this case was weakened by both fluid infiltration driving retrogression and an abundance of leucosome. Figure 26B also illustrates the tectonic context of the foliation megaboudins within the detachment zone in which 'islands' of low-strain granulite-facies relicts are surrounded by high-strain amphibolite-facies gneiss.

We have shown that the Muskoka domain is replete with evidence of boudinage on a range of scales, consistent with our interpretation that much of the preserved structure within the domain developed under conditions of far-field extension or transtension. Boudinage is inevitable in rheologically heterogeneous material undergoing significant extension, and Figure 26C illustrates the deduction that it also occurred on a crustal scale during orogenic collapse, leading to the more

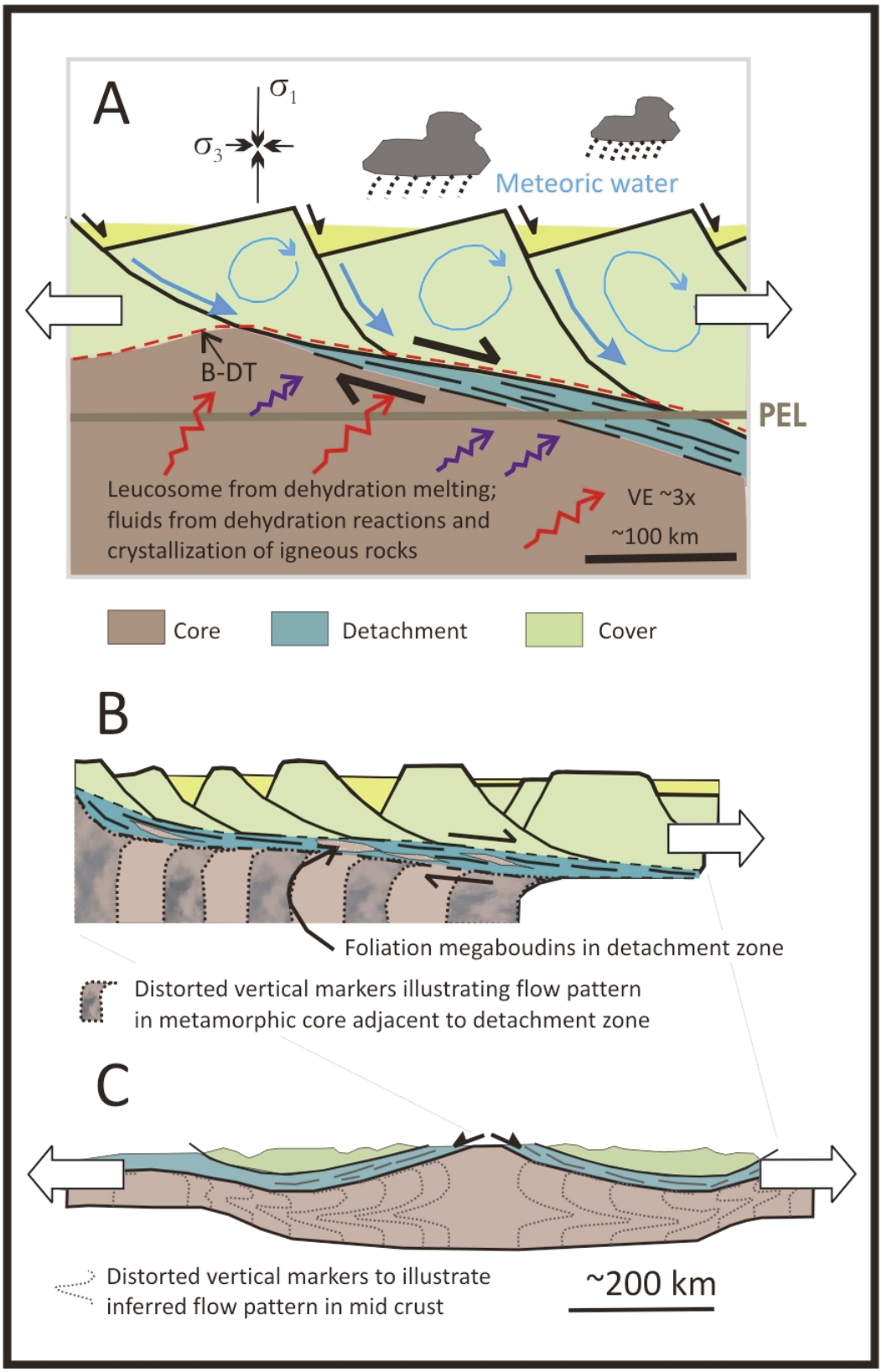

Figure 26. A: Sketch illustrating a metamorphic core complex in thickened crust with maximum far-field compression (σ_1) vertical. The extensional detachment zone separates the hot ductile core from the cool, brittle-ductile cover. Applied to the Ottawa River Gneiss Complex (ORGC) at the present erosion level (PEL) the core, detachment horizon and cover are the Algonquin domain, Muskoka domain, and Composite Arc Belt respectively. Downward flow of meteoric fluids and upward flow of igneous/metamorphic fluids ± melt results in retrogression and reaction weakening, lowering viscosity and focussing extensional strain in the detachment zone. B-DT –Brittle-ductile transition. B: Sketch illustrating the variable reworking and reorientation of gneissosity in the core adjacent to and within the detachment zone. Lozenges of high-grade core with relict structure and metamorphism surrounded by penetratively reworked and retrogressed rocks are represented by foliation megaboudins in the Muskoka domain of the ORGC. C: Regional setting of a crustal-scale core complex in a collapsed large hot orogen, showing megaboudinage of the cover and flow of the core into the neck region between megaboudins of cover rocks. A modified from Whitney et al. (2013), B modified from Malavieille (1993), C modified from Rey et al. (2001), Rivers (2012).

competent cool upper crust forming megaboudins and flow of the hot ductile mid crust into the megaboudin neck regions (Rey et al. 2001; Rivers 2012).

The origin of the fluid that fluxed post-peak retrogression ± partial melting in the Muskoka domain has not been determined. In their review Whitney et al. (2013) discussed both high-level metamorphic core complexes in which meteoric fluids were dominant and deeper-level examples, where crustal fluids were derived from metamorphic dehydration reactions and/or crystallizing igneous intrusions at depth (see Fig. 26A). In the amphibolite-facies Omineca Belt of the North American Cordillera, where this issue has been extensively evaluated, the consensus is that fluids of deep-crustal origin were dominant (e.g. Carr et al. 1987; Hinchey et al. 2006; Mulch et al. 2006; Holk and Taylor 2007; Gordon et al. 2008, 2009). Weinberg and Hasalová (2015) have pointed out that the ultimate source of crustal fluids in such deep settings may be the hydrous minerals and intergranular water in buried supracrustal rocks in the thickened orogenic crust, which is gradually released during prograde metamorphism.

As noted in the introduction, Whitney et al. (2013) stated that one of the criteria for a metamorphic core complex was that the detachment zone was the site of "…*10s of kilometers of normal-sense displacement in response to lithospheric extension*…". Although we have little doubt that the Muskoka domain was indeed the site of normal-sense displacement of at least this magnitude, we are unable to provide robust quantitative constraints. Malavieille (1993) illustrated a numerical kinematic model with a combination of non-uniform vertical thinning (flattening) and extensional shear at the top of the metamorphic core that may be relevant (see Fig. 26B), but as noted from limited strain markers (e.g. *Pl* pseudomorphs after *Grt*), flattening strain was strongly heterogeneous in the Muskoka domain and we have no robust constraints on the magnitude of shear strain. Moreover, Malavieille's (1993) study was a 2-D treatment of strain, but given the evidence for transtensional folding, a 3-D analysis is clearly called for. Hence, although we are presently unable to quantify the magnitude of strain that took place across the detachment zone between the core and the carapace of the ORGC (i.e. within the Muskoka domain), we consider the evidence is indisputable that it was large, involved both ductile strain within the detachment zone as a whole, as well as extensional displacement along internal shear zones, and hence is qualitatively compatible with the definition of Whitney et al. (2013).

Ductile Post-peak Structural Evolution — Cross-Folding and Megaboudinage

This study has revealed important details of the post-peak structural evolution of the mid crust during exhumation and orogenic collapse. Cross-fold systems composed of gentle to close, upright to moderately inclined buckle folds with hinge lines at high angles to the orogenic front occur on a range of scales in the Muskoka domain. Moreover, they also extend into other domains of the ORGC, including the footwall of the Allochthon Boundary (Fig. 9A). The larger cross-folds and some outcrop-scale examples carry evidence for constrictional strain parallel to their hinge lines (Fig. 6D), and exhibit irregular spacing and divergence of their hinge line traces (Fig. 9A), both hallmarks of buckle folding in an extension-dominated transtensional regime. The few examples of recumbent cross-folds (Fig. 10E, F) may mark locations where the initial orientation of the gneissic layering was steep (e.g. in the hinge zones of recumbent folds formed during thrusting), or they may have developed by refolding as shown in Figure 11; additional work is necessary to distinguish between these possibilities.

Figure 27 is a schematic diagram showing the inferred post-peak transtensional setting of the Muskoka domain in the ORGC in which the major Moon River, Seguin and Wallace synformal cross-folds developed. The figure is based on a conclusion of Fossen et al. (2013) that *"the direction of transtensional fold hinges, in regions of high strain, is a good indicator of the oblique divergence that generated the folds"* (p. 101). Although it is not yet possible to precisely determine the orientations and magnitudes of the wrench and extensional components of transtension in a geographic reference frame, we include the figure to show our conceptual understanding of the regional post-peak, extension-dominated sinistral transtensional regime in the hope that it may stimulate further testing and refinement.

The multi-order character of the cross-folds can be gauged from a comparison of Figures 9 and 27. Regional examples, such as the Moon River, Seguin and Wallace synforms and Bracebridge antiform, imply structural level 2 and the top of structural level 3 were buckled together as a multilayer sequence, whereas the outcrop-scale cross-folds deformed gneissic multilayers within the grey gneiss unit. Although not yet satisfactorily explained by theory and modelling, it is possible multi-order folding is a characteristic of extension-dominated transtension in exhumed high-grade terranes, as it is also a feature of the Western Gneiss Region of Norway (Krabbendam and Dewey 1988). We suspect it may be related to the suppression of fold amplification in this mode of transtension.

Formation of the regional Bracebridge antiform was accompanied by extension parallel to its axis and the development of two incipient megaboudins separated by the Camel Lake extensional bending fold that collectively provide evidence for important orogen-perpendicular extension, perhaps by as much as 200% locally on the 10 km scale. Moreover, the arrangement implies the presence of granulite-facies crust in structural level 2 underlying amphibolite-facies crust with granulite relicts in structural level 3, a relationship we attribute to encroaching retrogression and reworking along the interface between the core and the detachment zone in a core complex setting. As with cross-folds, the evidence for large-scale boudinage is supported by similar structures at the outcrop scale, suggesting pervasive post-peak thinning of the Muskoka domain. However, due to the limited 3-D exposure of most mesoscopic boudins, the local principal directions and magnitudes of extension cannot generally be estimated with confidence.

The weakly strained core of the Germania foliation megaboudin with relict granulite-facies rocks (Figs. 15–16) incorporates the granulite-facies metagabbro bodies in southern Seguin domain described by Pattison (1991) and some of the granulite locations studied by Timmermann et al. (2002). In Figure 27, we also show the locations of the Rockaway Lake structure, another megaboudin figured by Schwerdtner et al. (2014), and an area of granulite-facies rocks in SE Muskoka domain delineated by Timmermann et al. (2002). Given the small number of detailed petrologic studies of the eastern

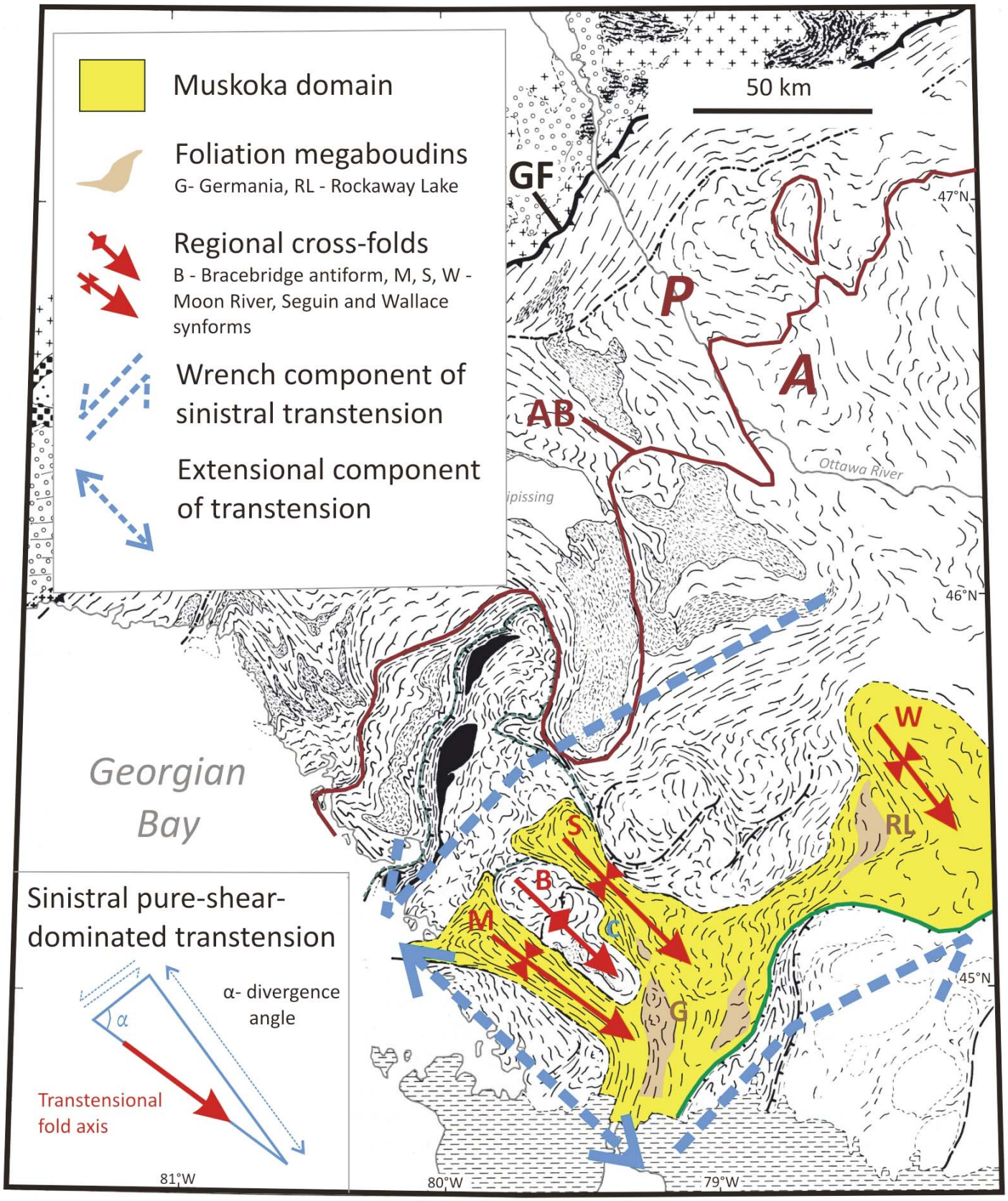

Figure 27. Sketch map of the southwestern Ottawa River Gneiss Complex (ORGC) with locations of major upright cross-folds and foliation megaboudins; B - Bracebridge antiform, M, S, W - Moon River, Seguin and Wallace synforms; G, RL - Germania and Rockaway Lake foliation megaboudins; C - Camel Lake synform (extensional bending fold). Inferred regional sinistral transtensional setting that affected the Muskoka domain and the upper part of the underlying Algonquin domain during post-peak orogenic collapse is shown by orthogonal orogen-perpendicular and orogen-parallel displacement vectors (blue arrows). Inset sketch shows the 2-D setup for extension-dominated sinistral transtension in which $20° < \alpha < 90°$. Base map modified from Davidson (1984). A – Allochthonous, AB – Allochthon Boundary, GF – Grenville Front, P – Parautochthonous.

Muskoka domain it is possible that other foliation megaboudins with relict granulite cores also exist.

The age ranges of cross-folding and megaboudinage in the Muskoka domain have not been precisely determined, but considering that both occurred at high temperature under suprasolidus upper amphibolite-facies conditions, they are assumed to have initiated shortly after the metamorphic peak in the early stages of exhumation and retrogression. In the specific case of the km-scale Bracebridge antiform, extension parallel to the fold hinge giving rise to megaboudinage must have begun after initiation of the transtensional folds. This leads us to tentatively deduce that both are responses to the constrictional part of the regional transtension regime.

Considering that the cross-folds in the Muskoka domain deform the attenuated amphibolite-facies fabric, and that the published age of amphibolite-facies metamorphism in the domain is ~1060 Ma (e.g. Bussy et al. 1995; Timmermann et al. 1997; 2002; Slagstad 2004a, b), cross-folds likely initiated at about this time there. However, cross-folds in the ORGC also transect the Allochthon Boundary and continue into the Parautochthonous Belt in its footwall (Fig. 9), where the age of the dominant Grenvillian metamorphism (Ottawan or Rigolet) is less well constrained (e.g. Rivers 1997, 2009; Carr et al. 2000; Rivers et al. 2012). An age range of ~1070–1040 Ma for peak metamorphism in the parautochthonous part of the ORGC is given by Carr et al. (2000), implying the cross-folds there may have formed at about the same time as those in the overlying Allochthonous Belt. This issue has implications for extensional reactivation of the Allochthon Boundary at ~1020 Ma (Ketchum et al. 1998), and for interactions between the parautochthon and the overlying allochthonous thrust stack during the later stages of the Grenvillian Orogeny that warrant further study.

Brittle-Ductile Post-peak Structural Evolution — FPFs and Granite Pegmatite Dykes

Extensional fault propagation folds (FPFs) are widespread late-stage structures in the ORGC that developed in mid-crustal rocks after they had undergone substantial exhumation and cooling and they are testament to the transition to brittle-ductile behaviour. The short limbs of these structures are mostly < 10–15 m in length, but our observations are constrained by the height of the outcrops and it is possible that larger examples occur. The preferred orientation of their subhorizontal axes is approximately NE-SW, with monoclinal limbs mostly dipping SE and axial surfaces dipping steeply NW. Individual FPFs thus record evidence for limited, late-stage, orogen-perpendicular extension, but they are common structures and the overall attenuation of the crust accommodated by the population as a whole is unknown.

Dilational granite pegmatite dykes intruded into the exhumed and cooled ORGC are widespread and ubiquitous, and available geochronological data indicate they crystallized at ≤ 1000 Ma. The temperature of the crust into which the pegmatite dykes were intruded is not constrained in the study area, but in the Key Harbour area in the Parautochthonous Belt (see Fig. 1), pegmatite dyke emplacement at 990 ±2 Ma overlapped within uncertainties with the closure of Pb diffusion in titanite in the surrounding country rocks (Corrigan et al. 1994), implying a temperature of 600–650°C there. In the Muskoka domain, the occurrence of set-1 dykes along the short limbs of FPFs suggests they were emplaced as the latter structures developed, whereas the set-2 dykes were emplaced subparallel to their axial surfaces after most ductile deformation in the ORGC had ceased. The presence of both dyke sets implies the underlying deeper crust in the orogenic hinterland beneath the exposed ORGC remained suprasolidus at ≤ 1000 Ma, periodically releasing small volumes of fluid-rich melt that was injected into its overlying extending brittle-ductile carapace.

CONCLUSIONS

Following formation at the top of a pile of mid-crustal granulite-facies thrust sheets, the Muskoka domain underwent pervasive post-convergent thinning, retrogression and exhumation. On the basis of evidence presented in this paper, we conclude that the dominant amphibolite-facies metamorphic assemblages, fabrics, and structures of the Muskoka domain, including its prominent regional NW-trending synformal lobes, developed to a large degree after the peak of Ottawan metamorphism, record prolonged extensional or transtensional strain over ≥ 60 m.y., and document profound orogenic collapse. The principal result of this collapse was the juxtaposition of the underlying exhumed, hot ductile mid crust (Algonquin domain) against the overlying cool, brittle-ductile upper crust (Composite Arc Belt), the two being separated by a weak high-strain detachment zone (the Muskoka domain), collectively leading to the development of a crustal-scale metamorphic core complex partly surrounded at the present level of erosion by its lower-grade cover. Conductive heating of the base of the Composite Arc Belt by juxtaposition against the exhumed hot ORGC is predicted in this setting, but has not yet been recorded. Rheological weakening of peak granulite-facies rocks in the Muskoka domain was caused by the presence of abundant leucosome and widespread post-peak retrogression, the latter implying ingress of voluminous quantities of hydrous fluid into the suprasolidus mid crust. This weakening led to important vertical thinning and subhorizontal extension, forming what is now a ~7 km thick detachment zone. Collectively, these features are compatible with the *Collapsed LHO paradigm*.

The scale of the metamorphic core complex preserved in the ORGC is substantially greater than that illustrated schematically in a recent review of core complexes by Whitney et al. (2013), and the estimated 7 km thickness of the detachment zone (Muskoka domain) is similarly much greater than that of other examples described in the literature (mostly ≤ 2 km). We attribute this 'super-sizing' to the deep level of erosion, and to the large area of double thickness crust at the Ottawan metamorphic peak, the abundance of leucosome, and the inferred voluminous influx of melt and hydrous fluid after the metamorphic peak. Similarly, the estimated duration of extensional collapse of the Grenville Orogen (≥ 60 m.y.) is substantially longer than that determined for Phanerozoic examples (mostly < 20 m.y.).

Additional work is necessary to assess the implications of the *Collapsed LHO paradigm* for the tectonic interpretation of the ORGC as a whole, especially with respect to the proposed correlation within structural level 3 of the Muskoka domain in the southeast ORGC with the Shawanaga and Ahmic domains farther northwest (Fig. 2; Jamieson et al. 2007; Jamieson and

Beaumont 2011), and also to investigate possible continuation of the Muskoka domain / structural level 3 eastward into eastern Quebec. Recent work in central Quebec has concluded that the granulite-facies Mékinak domain and its amphibolite-facies structural cover, known as the Shawinigan domain, also comprise a metamorphic core complex (Soucy La Roche et al. 2015), supporting the contention that these structures are widespread in the Grenville Province (Rivers 2012). However, in that case the detachment zone comprises a system of anastomosing shear zones in which deformation was subsolidus, and the collapse process lasted a maximum of 35 m.y. These differences suggest that Grenvillian metamorphic core complexes were initiated at different times, were operative under different *P–T* conditions, and probably record different amounts of extensional strain.

ACKNOWLEDGEMENTS

This paper is an outgrowth of the introduction to the field guide for the 2014 Friends of the Grenville (FOG) field trip, which focussed on the geology of the Muskoka domain around Gravenhurst, Ontario (Rivers and Schwerdtner 2014). Both papers are attempts to integrate field observations in the Ontario segment of the Ottawa River Gneiss Complex, perhaps the best exposed and most intensively studied high-grade gneiss terrane in the Grenville Province, with published geophysical, structural and petrologic data, recent theoretical models of folding and faulting in extensional and transtensional systems, and numerical models of the orogenic collapse process. Important insight was gained by working across a range of scales, made possible by decades of observations and compilations by others. As such, our results owe a debt to the many who came before. We are delighted to submit the paper to the series honouring the contributions of Andrew Hynes, whose rigorous approach and insight into tectonic processes and ability to synthesize information from a range of scales we greatly admire. We hope it meets his high standards and that the ideas and concepts are tested and refined in other high-grade gneiss terranes in the Grenville Province and elsewhere. We thank Félix Gervais and Chris Yakymchuk for critical and perceptive journal reviews that challenged us to sharpen our arguments about crustal melting and migmatites, and the journal staff for meticulous editorial work. The research was partly supported by NSERC Discovery Grants to the first author.

REFERENCES

Anovitz, L.M., and Essene, E.J., 1990, Thermobarometry and pressure-temperature paths in the Grenville Province of Ontario: Journal of Petrology, v. 31, p. 197–241, http://dx.doi.org/10.1093/petrology/31.1.197.

Aranovich, L.Y., Newton, R.C., and Manning, C.E., 2013, Brine-assisted anatexis: Experimental melting in the system haplogranite–H_2O–NaCl–KCl at deep-crustal conditions: Earth and Planetary Science Letters, v. 374, p. 111–120, http://dx.doi.org/10.1016/j.epsl.2013.05.027.

Beaumont, C., Jamieson, R.A., Nguyen, M.H., and Lee, B., 2001, Mid-crustal channel flow in large hot orogens: Results from coupled thermal-mechanical models, *in* Slave–Northern Cordillera Lithospheric Evolution (SNORCLE) and Cordilleran Tectonics Workshop: Lithoprobe Secretariat, UBC, Vancouver, BC, Lithoprobe Report 79, p. 112–170.

Beaumont, C., Nguyen, M.H., Jamieson, R.A., and Ellis, S., 2006, Crustal flow modes in large hot orogens, *in* Law, R.D., Searle, M.P., and Godin, L., *eds.*, Channel Flow, Ductile Extrusion and Exhumation in Continental Collision Zones. Geological Society, London, Special Publications, v. 268, p. 91–145, http://dx.doi.org/10.1144/gsl.sp.2006.268.01.05.

Berman, R.G., 1991, Thermobarometry using multi-equilibrium calculations: a new technique with petrological applications: Canadian Mineralogist, v. 29, p. 833–855.

Brown, M., 2013, Granite: From genesis to emplacement: Geological Society of America Bulletin, v. 125, p. 1079–1113, http://dx.doi.org/10.1130/B30877.1.

Busch, J.P., and van der Pluijm, B.A., 1996, Late orogenic, plastic to brittle extension along the Robertson Lake shear zone: implications for the style of deep-crustal extension in the Grenville orogen, Canada: Precambrian Research, v. 77, p. 41–57, http://dx.doi.org/10.1016/0301-9268(95)00044-5.

Busch, J.P., van der Pluijm, B.A., Hall, C.M., and Essene, E.J., 1996a, Listric normal faulting during postorogenic extension revealed by $^{40}Ar/^{39}Ar$ thermochronology near the Robertson Lake shear zone, Grenville orogen, Canada: Tectonics, v. 15, p. 387–402, http://dx.doi.org/10.1029/95TC03501.

Busch, J.P., Essene, E.J., and van der Pluijm, B.A., 1996b, Evolution of deep-crustal normal faults: Constraints from thermobarometry in the Grenville orogen, Ontario, Canada: Tectonophysics, v. 265, p. 83–100, http://dx.doi.org/10.1016/S0040-1951(96)00147-3.

Busch, J.P., Mezger, K., and van der Pluijm, B.A., 1997, Suturing and extensional reactivation in the Grenville orogen, Canada: Geology, v. 25, p. 507–510, http://dx.doi.org/10.1130/0091-7613(1997)025<0507:SAERIT>2.3.CO;2.

Bussy, F., Krogh, T.E., Klemens, W.P., and Schwerdtner, W.M., 1995, Tectonic and metamorphic events in the westernmost Grenville Province, central Ontario: new results from high-precision U–Pb zircon geochronology: Canadian Journal of Earth Sciences, v. 32, p. 660–671, http://dx.doi.org/10.1139/e95-055.

Carr, S.D., Parrish, R.R., and Brown, R.L., 1987, Eocene structural development of the Valhalla complex, southeastern British Columbia: Tectonics, v. 6, p. 175–196, http://dx.doi.org/10.1029/TC006i002p00175.

Carr, S.D., Easton, R.M., Jamieson, R.A., and Culshaw, N.G., 2000, Geologic transect across the Grenville orogen of Ontario and New York: Canadian Journal of Earth Sciences, v. 37, p. 193–216, http://dx.doi.org/10.1139/e99-074.

Clemens, J.D., and Droop, G.T.R., 1998, Fluids, *P–T* paths and the fates of anatectic melts in the Earth's crust: Lithos, v. 44, p. 21–36, http://dx.doi.org/10.1016/S0024-4937(98)00020-6.

Coney, P.J., 1974, Structural analysis of the Snake Range 'Décollement,' east-central Nevada: Geological Society of America Bulletin, v. 85, p. 973–978, http://dx.doi.org/10.1130/0016-7606(1974)85<973:saotsr>2.0.co;2.

Coney, P.J., 1980, Cordilleran metamorphic core complexes: An overview, *in* Crittenden, M.D., Jr., Coney, P.J., and Davis, G.H., *eds.,* Cordilleran Metamorphic Core Complexes: Geological Society of America Memoirs, v. 153, p. 7–31, http://dx.doi.org/10.1130/MEM153-p7.

Corrigan, D., and van Breemen, O., 1997, U–Pb constraints for the lithotectonic evolution of the Grenville Province along the Mauricie transect, Quebec: Canadian Journal of Earth Sciences, v. 34, p. 299–316, http://dx.doi.org/10.1139/e17-027.

Corrigan, D., Culshaw, N.G., and Mortensen, J.K., 1994, Pre-Grenvillian evolution and Grenvillian overprinting of the Parautochthonous Belt in Key Harbour, Ontario: U–Pb and field constraints: Canadian Journal of Earth Sciences, v. 31, p. 583–596, http://dx.doi.org/10.1139/e94-051.

Corriveau, L., and Gorton, M.P., 1993, Co-existing K-rich alkaline and shoshonitic magmatism of arc affinities in the Proterozoic: a reassessment of syenitic rocks in the southwestern Grenville Province: Contributions to Mineralogy and Petrology, v. 113, p. 262–279, http://dx.doi.org/10.1007/BF00283233.

Corriveau, L., Heaman, L.M., Marcantonio, F., and van Breemen, O., 1990, 1.1 Ga K-rich alkaline plutonism in the SW Grenville Province, U–Pb constraints for the timing of subduction-related magmatism: Contributions to Mineralogy and Petrology, v. 105, p. 473–485, http://dx.doi.org/10.1007/BF00286834.

Cosca, M.A., Sutter, J.F., and Essene, E.J., 1991, Cooling and inferred uplift/erosion history of the Grenville orogen, Ontario: Constraints from $^{40}Ar/^{39}Ar$ thermochronology: Tectonics, v. 10, p. 959–977, http://dx.doi.org/10.1029/91TC00859.

Cosca, M.A., Essene, E.J., Kunk, M.J., and Sutter, J.F., 1992, Differential unroofing within the Central Metasedimentary Belt of the Grenville Orogen: Constraints from $^{40}Ar/^{39}Ar$ thermochronology: Contributions to Mineralogy and Petrology, v. 110, p. 211–225, http://dx.doi.org/10.1007/BF00310739.

Cosca, M.A., Essene, E.J., Mezger, K., and van der Pluijm, B.A., 1995, Constraints on the duration of tectonic processes: Protracted extension and deep-crustal rotation in the Grenville orogeny: Geology, v. 23, p. 361–364, http://dx.doi.org/10.1130/0091-7613(1995)023<0361:COTDOT>2.3.CO;2.

Culshaw, N., 2005, Buckle folding and deep-crustal shearing of high-grade gneisses at the junction of two major high-strain zones, Central Gneiss Belt, Grenville Province, Ontario: Canadian Journal of Earth Sciences, v. 42, p. 1907–1925, http://dx.doi.org/10.1139/e05-078.

Culshaw, N.G., Davidson, A., and Nadeau, L., 1983, Structural subdivisions of the Grenville Province in the Parry Sound–Algonquin region, Ontario: Geological Survey of Canada, Current Research, Part B, Paper 83-1B, p. 243–252.

Culshaw, N.G., Ketchum, J.W.F., Wodicka, N., and Wallace, P., 1994, Deep crustal ductile extension following thrusting in the southwestern Grenville Province, Ontario: Canadian Journal of Earth Sciences, v. 31, p. 160–175, http://dx.doi.org/10.1139/e94-013.

Culshaw, N.G., Jamieson, R.A., Ketchum, J.W.F., Wodicka, N., Corrigan, D., and Reynolds, P.H., 1997, Transect across the northwestern Grenville orogen, Georgian Bay, Ontario: Polystage convergence and extension in the lower orogenic crust: Tectonics, v. 16, p. 966–982, http://dx.doi.org/10.1029/97TC02285.

Culshaw, N.G., Corrigan, D., Ketchum, J.W.F., Wallace, P., Wodicka, N., and Easton, R.M., 2004, Georgian Bay geological synthesis, Grenville Province: Explanatory notes for Preliminary Maps P.3548 to P.3552: Ontario Geological Survey, Open File Report 6143.

Davidson, A., 1984, Identification of ductile shear zones in the southwestern Grenville Province of the Canadian Shield, *in* Kröner, A., and Greiling, R., *eds.,* Precambrian Tectonics Illustrated: E. Schweizerbart'sche Verlagsbuchhandlung, Stuttgart, p. 263–280.

Davidson, A., 1990, Evidence for eclogite metamorphism in the southwestern Grenville Province: Geological Survey of Canada, Current Research Part C, Paper 90-1C, p. 113–118.

Davidson, A., and Morgan, W.C., 1981, Preliminary notes on the geology east of Georgian Bay, Grenville Structural Province, Ontario: Geological Survey of Canada, Paper 81-A, p. 175–190.

Davidson, A., Culshaw, N.G., and Nadeau, L., 1982, Preliminary notes on the geology east of Georgian Bay, Grenville Structural Province, Ontario: Geological Survey of Canada, Current Research Part A, Paper 81-1A, p. 291–298.

Dewey, J.F., Holdsworth, R.E., and Strachan, R.A., 1998, Transpression and transtension zones, *in* Holdsworth, R.E., Strachan, R.A., and Dewey, J.F., *eds.,* Continental Transpressional and Transtensional Tectonics: Geological Society, London, Special Publications, v. 135, p. 1–14, http://dx.doi.org/10.1144/gsl.sp.1998.135.01.01.

Dickin, A.P., and Guo, A., 2001, The location of the Allochthon Boundary Thrust and the Archean−Proterozoic suture in the Mattawa area of the Grenville Province: Nd isotopic evidence: Precambrian Research, v. 107, p. 31–43, http://dx.doi.org/10.1016/S0301-9268(00)00153-4.

Dickin, A.P., and McNutt, R.H., 1990, Nd model-age mapping of Grenville lithotectonic domains: mid-Proterozoic crustal evolution in Ontario, *in* Gower, C.F., Rivers, T., and Ryan, A.B., *eds.,* Mid-Proterozoic Laurentia-Baltica: Geological Association of Canada Special Paper 38, p. 79–94.

Dickin, A.P., Moretton, K., and North, R., 2008, Isotopic mapping of the Allochthon Boundary Thrust in the Grenville Province of Ontario, Canada: Precambrian Research, v. 167, p. 260–266, http://dx.doi.org/10.1016/j.precamres.2008.08.007.

Dickin, A.P., Herrell, M., Moore, E., Cooper, D., and Pearson, S., 2014, Nd isotope mapping of allochthonous Grenvillian klippen: Evidence for widespread 'ramp-flat' thrust geometry in the SW Grenville Province: Precambrian Research, v. 246, p. 268–280, http://dx.doi.org/10.1016/j.precamres.2014.03.012.

Docka, R.K., Ross, T.M., and Lu, G., 1998, The Trans Mojave–Sierran shear zone and its role in Early Miocene collapse of southwestern North America, *in* Holdsworth, R.E., Strachan, R.A., and Dewey, J.F., *eds.,* Continental Transpressional and Transtensional Tectonics: Geological Society, London, Special Publications, v. 135, p. 183–202, http://dx.doi.org/10.1144/gsl.sp.1998.135.01.12.

Easton, R.M., 1992, The Grenville Province and the Proterozoic history of central and southern Ontario, *in* Thurston, P.C., Williams, H.R., Sutcliffe, R.H., and Stott, G.M., *eds.*, Geology of Ontario: Ontario Geological Survey, Special volume 4, p. 715–904.

Ferrill, D.A., Morris, A.P., and McGinniss, R.N., 2012, Extensional fault-propagation folding in mechanically layered rocks: The case against the frictional drag mechanism: Tectonophysics, v. 576–577, p. 78–85, http://dx.doi.org/10.1016/j.tecto.2012.05.023.

Fossen, H., Teyssier, C., and Whitney, D.L., 2013, Transtensional folding: Journal of Structural Geology, v. 56, p. 89–102, http://dx.doi.org/10.1016/j.jsg.2013.09.004.

Gordon, S.M., Whitney, D.L., Teyssier, C., Grove, M., and Dunlap, W.J., 2008, Timescales of migmatization, melt crystallization, and cooling in a Cordilleran gneiss dome: Valhalla complex, southeastern British Columbia: Tectonics, v. 27, TC4010, http://dx.doi.org/10.1029/2007TC002103.

Gordon, S.M., Grove, M., Whitney, D.L., Schmitt, A.K., and Teyssier, C., 2009, Fluid-rock interaction in orogenic crust tracked by zircon depth profiling: Geology, v. 37, p. 735–738, http://dx.doi.org/10.1130/G25597A.1.

Gower, R.J.W., 1992, Nappe emplacement direction in the Central Gneiss Belt, Grenville Province, Ontario, Canada: Evidence for oblique collision: Precambrian Research, v. 59, p. 73–94, http://dx.doi.org/10.1016/0301-9268(92)90052-P.

Hinchey, A.M., Carr, S.D., McNeill, P.D., and Rayner, N., 2006, Paleocene–Eocene high-grade metamorphism, anatexis, and deformation in the Thor–Odin dome, Monashee complex, southeastern British Columbia: Canadian Journal of Earth Sciences, v. 43, p. 1341–1365, http://dx.doi.org/10.1139/e06-028.

Hobbs, B.E., Means, W.D., and Williams, P.F., 1976, An Outline of Structural Geology: John Wiley and Sons, Inc., 571 p.

Holk, G.J., and Taylor, H.P., Jr., 2007, $^{18}O/^{16}O$ Evidence for contrasting hydrothermal regimes involving magmatic and meteoric-hydrothermal waters at the Valhalla metamorphic core complex, British Columbia: Economic Geology, v. 102, p. 1063–1078, http://dx.doi.org/10.2113/gsecongeo.102.6.1063.

Jamieson, R.A., and Beaumont, C., 2011, Coeval thrusting and extension during lower crustal ductile flow—implications for exhumation of high-grade metamorphic rocks: Journal of Metamorphic Geology, v. 29, p. 33–51, http://dx.doi.org/10.1111/j.1525-1314.2010.00908.x.

Jamieson, R.A., Ketchum, J.W.F., Slagstad, T., Rivers, T., and Culshaw, N.G., 2003, Omphacite and zircon in high-pressure metabasite, Shawanaga domain, western Grenville Province: the truth about some beauties (Abstract): Geological Association of Canada–Mineralogical Association of Canada Annual Meeting, v. 28, A325.

Jamieson, R.A., Beaumont, C., Nguyen, M.H., and Culshaw, N.G., 2007, Synconvergent ductile flow in variable-strength continental crust: Numerical models with application to the western Grenville orogen: Tectonics, v. 26, TC5005, http://dx.doi.org/10.1029/2006TC002036.

Jamieson, R.A., Beaumont, C., Warren, C.J., and Nguyen, M.H., 2010, The Grenville orogen explained? Applications and limitations of integrating numerical models with geological and geophysical data: Canadian Journal of Earth Sciences, v. 47, p. 517–539, http://dx.doi.org/10.1139/E09-070.

Janák, M., Plašienka, D., Frey, M., Cosca, M., Schmidt, S.TH, Lupták, B., and Méres, Š., 2001, Cretaceous evolution of a metamorphic core complex, the Veporic unit, western Carpathians (Slovakia): *P–T* conditions and *in situ* $^{40}Ar/^{39}Ar$ UV laser probe dating of metapelites: Journal of Metamorphic Geology, v. 19, p. 197–216, http://dx.doi.org/10.1046/j.0263-4929.2000.00304.x.

Kargaranbafghi, F., and Neubauer, F., 2015, Lithospheric thinning associated with formation of a metamorphic core complex and subsequent formation of the Iranian plateau: GSA Today, v. 25, p. 4–8, http://dx.doi.org/10.1130/GSATG229A.1.

Ketchum, J.W.F., and Davidson, A., 2000, Crustal architecture and tectonic assembly of the Central Gneiss Belt, southwestern Grenville Province, Canada: a new interpretation: Canadian Journal of Earth Sciences, v. 37, p. 217–234, http://dx.doi.org/10.1139/e98-099.

Ketchum, J.W.F., and Krogh, T.E., 1997, U–Pb constraints on high-pressure metamorphism in the Central Gneiss Belt, southwestern Grenville orogeny (Abstract): Geological Association of Canada–Mineralogical Association of Canada Annual Meeting, v. 22, A78.

Ketchum, J.W.F., and Krogh, T.E., 1998, U–Pb constraints on high-pressure metamorphism in the southwestern Grenville orogeny (Abstract): Goldschmidt Conference 1998, Mineralogical Magazine, v. 62A, p. 775−776.

Ketchum, J.W.F., Heaman, L.M., Krogh, T.E., Culshaw, N.G., and Jamieson, R.A., 1998, Timing and thermal influence of late orogenic extension in the lower crust: a U–Pb geochronological study from the southwest Grenville orogen, Canada: Precambrian Research, v. 89, p. 25–45, http://dx.doi.org/10.1016/S0301-9268(97)00079-X.

Klemens, W.P., 1996, Structural analysis of the Ahmic domain and its border zones, southwestern Grenville orogen, Ontario, Canada: Unpublished PhD thesis, University of Toronto, Toronto, ON, 197 p.

Krabbendam, M., and Dewey, J.F., 1998, Exhumation of UHP rocks by transtension in the Western Gneiss Region, Scandinavian Caledonides, *in* Holdsworth, R.E., Strachan, R.A., and Dewey, J.F., *eds.,* Continental Transpressional and Transtensional Tectonics: Geological Society, London, Special Publications, v. 135, p. 159–181, http://dx.doi.org/10.1144/gsl.sp.1998.135.01.11.

Kruckenberg, S.C., Vanderhaeghe, O., Ferré, E.C, Teyssier, C., and Whitney, D.L., 2011, Flow of partially molten crust and the internal dynamics of a migmatite dome: Tectonics, v. 30, TC3001, http://dx.doi.org/10.1029/2010TC002751.

Lister, G.S., and Davis, G.A., 1989, The origin of metamorphic core complexes and detachment faults formed during Tertiary continental extension in the northern Colorado region, U.S.A.: Journal of Structural Geology, v. 11, p. 65–94, http://dx.doi.org/10.1016/0191-8141(89)90036-9.

Lumbers, S.B., and Vertolli, V.M., 2000a, Precambrian geology, Bracebridge area: Ontario Geological Survey, Preliminary Map P.3412, NTS: 31E/4, scale 1:50,000.

Lumbers, S.B., and Vertolli, V.M., 2000b, Precambrian geology, Lake Joseph area: Ontario Geological Survey, Preliminary Map P.3411, NTS: 31E/3, scale 1:50,000.

Lumbers, S.B., and Vertolli, V.M., 2000c, Precambrian geology, Orrville area: Ontario Geological Survey, Preliminary Map P.3414, NTS: 31E/5, scale 1:50,000.

Lumbers, S.B., Vertolli, V.M., and Schwerdtner, W.M., 2000, Precambrian geology, Gravenhurst area: Ontario Geological Survey, Preliminary Map P.3409, NTS: 31D/14, scale 1:50,000.

Malavieille, J., 1993, Late orogenic extension in mountain belts: Insights from the Basin and Range and the late Paleozoic Variscan Belt: Tectonics, v. 12, p. 1115–1130, http://dx.doi.org/10.1029/93TC01129.

Malavieille, J., Guihot, P., Costa, S., Lardeaux, J.M., and Gardien, V., 1990, Collapse of the thickened Variscan crust in the French Massif Central: Mont Pilat extensional shear zone and the St. Etienne late Carboniferous basin: Tectonophysics, v. 177, p. 139–149, http://dx.doi.org/10.1016/0040-1951(90)90278-G.

Martignole, J., and Calvert, A.J., 1996, Crustal-scale shortening and extension across the Grenville Province of western Québec: Tectonics, v. 15, p. 376–386, http://dx.doi.org/10.1029/95TC03748.

Martignole, J., Calvert, A.J., Friedman, R., and Reynolds, P., 2000, Crustal evolution along a seismic section across the Grenville Province (western Quebec): Canadian Journal of Earth Sciences, v. 37, p. 291–306, http://dx.doi.org/10.1139/e99-123.

McFadden, R.R., Teyssier, C., Siddoway, C.S., Whitney, D.L., and Fanning, C.M., 2010, Oblique dilation, melt transfer, and gneiss dome emplacement: Geology,

v. 38, p. 375–378, http://dx.doi.org/10.1130/G30493.1.
McGregor, V.R., and Friend, C.R.L., 1997, Field recognition of rocks totally retrogressed from granulite facies: an example from Archaean rocks in the Paamiut region, South-West Greenland: Precambrian Research, v. 86, p. 59–70, http://dx.doi.org/10.1016/S0301-9268(97)00041-7.
McLelland, J.M., Selleck, B.W., and Bickford, M.E., 2013, Tectonic evolution of the Adirondack Mountains and Grenville Orogen inliers within the USA: Geoscience Canada, v. 40, p. 318–352, http://dx.doi.org/10.12789/geocanj.2013.40.022.
McMullen, S.M., 1999, Tectonic evolution of the Bark Lake area, eastern Central Gneiss Belt, Ontario Grenville: Constraints from geology, geochemistry and U–Pb geochronology: Unpublished MSc thesis, Carleton University, Ottawa, ON, 175 p.
Mezger, K., van der Pluijm, B.A., Essene, E.J., and Halliday, A.N., 1991, Synorogenic collapse: A perspective from the middle crust, the Proterozoic Grenville orogeny: Science, v. 254, p. 695–698, http://dx.doi.org/10.1126/science.254.5032.695.
Mulch, A., Teyssier, C., Cosca, M.A., and Vennemann, T.W., 2006, Thermomechanical analysis of strain localization in a ductile detachment zone: Journal of Geophysical Research, v. 111, B12405, http://dx.doi.org/10.1029/2005JB004032.
Nadeau, L., and van Breemen, O., 1998, Plutonic ages and tectonic setting of the Algonquin and Muskoka allochthons, Central Gneiss Belt, Grenville Province, Ontario: Canadian Journal of Earth Sciences, v. 35, p. 1423–1438, http://dx.doi.org/10.1139/e98-077.
Pattison, D.R.M., 1991, Infiltration-driven dehydration and anatexis in granulite facies metagabbro, Grenville Province, Ontario, Canada: Journal of Metamorphic Geology, v. 9, p. 315–332.
Rey, P., Vanderhaegue, O., and Teyssier, C., 2001, Gravitational collapse of the continental crust: definition, regimes and modes: Tectonophysics, v. 342, p. 435–449, http://dx.doi.org/10.1016/S0040-1951(01)00174-3.
Rey, P.F., Teyssier, C., and Whitney, D.L., 2009, The role of partial melting and extensional strain rates in the development of metamorphic core complexes: Tectonophysics, v. 477, p. 135–144, http://dx.doi.org/10.1016/j.tecto.2009.03.010.
Rivers, T., 1997, Lithotectonic elements of the Grenville Province: review and tectonic implications: Precambrian Research, v. 86, p. 117–154, http://dx.doi.org/10.1016/S0301-9268(97)00038-7.
Rivers, T., 2008, Assembly and preservation of lower, mid, and upper orogenic crust in the Grenville Province – Implications for the evolution of large hot long-duration orogens: Precambrian Research, v. 167, p. 237–259, http://dx.doi.org/10.1016/j.precamres.2008.08.005.
Rivers, T., 2009, The Grenville Province as a large hot long-duration orogen – insights from the spatial and thermal evolution of its orogenic fronts, *in* Murphy, J.B., Keppie, J.D., and Hynes, A.J., *eds.,* Ancient Orogens and Modern Analogues: Geological Society, London, Special Publications, v. 327, p. 405–444, http://dx.doi.org/10.1144/SP327.17.
Rivers, T., 2012, Upper-crustal orogenic lid and mid-crustal core complexes: signature of a collapsed orogenic plateau in the hinterland of the Grenville Province: Canadian Journal of Earth Sciences, v. 49, p. 1–42, http://dx.doi.org/10.1139/e11-014.
Rivers, T., 2015, Tectonic setting and evolution of the Grenville Orogen: An assessment of progress over the last 40 years: Geoscience Canada, v. 42, p. 77–124, http://dx.doi.org/10.12789/geocanj.2014.41.057.
Rivers, T., and Corrigan, D., 2000, Convergent margin on southeastern Laurentia during the Mesoproterozoic: tectonic implications: Canadian Journal of Earth Sciences, v. 37, p. 359–383, http://dx.doi.org/10.1139/e99-067.
Rivers, T., and Schwerdtner, W.M., 2014, New ideas on the post-peak development of the Central Gneiss Belt in the Muskoka region: Friends of the Grenville / Amis du Grenville field guide, 44 p. Available at: www.friendsofthegrenville.org.
Rivers, T., Culshaw, N., Hynes, A., Indares, A., Jamieson, R., and Martignole, J., 2012, The Grenville Orogen–A post-LITHOPROBE perspective. Chapter 3, *in* Percival, J.A., Cook, F.A., and Clowes, R.M., *eds.,* Tectonic Styles in Canada: the LITHOPROBE Perspective: Geological Association of Canada Special Paper 49, p. 97–236.
Sanderson, D.J., and Marchini, W.R.D., 1984, Transpression: Journal of Structural Geology, v. 6, p. 449–458, http://dx.doi.org/10.1016/0191-8141(84)90058-0.
Schaubs, P.M., Carr, S.D., and Berman, R.G., 2002, Structural and metamorphic constraints on ca. 70 Ma deformation of the southern Valhalla complex, British Columbia: implications for the tectonic evolution of the southern Omineca belt: Journal of Structural Geology, v. 24, p. 1195–1214, http://dx.doi.org/10.1016/S0191-8141(01)00101-8.
Schlische, R.W., 1995, Geometry and origin of fault-related folds in extensional settings: American Association of Petroleum Geologists Bulletin, v. 37, p. 75–88.
Schwerdtner, W.M., 1970, Distribution of longitudinal finite strain in lenticular boudins and bending folds: Tectonophysics, v. 9, p. 537–545, http://dx.doi.org/10.1016/0040-1951(70)90004-1.
Schwerdtner, W.M., 1977, Distortion and dilatation in paleostrain analysis: Tectonophysics, v. 40, p. T9–T13, http://dx.doi.org/10.1016/0040-1951(77)90062-2.
Schwerdtner, W.M., 1987, Interplay between folding and ductile shearing in the Proterozoic crust of the Muskoka−Parry Sound region of central Ontario: Canadian Journal of Earth Sciences, v. 24, p. 1507–1525, http://dx.doi.org/10.1139/e87-148.
Schwerdtner, W.M., and Klemens, W., 2008, Structure of Ahmic domain and its vicinity, southwestern Central Gneiss Belt, Grenville Province of Ontario (Canada): Precambrian Research, v. 167, p. 16–34, http://dx.doi.org/10.1016/j.precamres.2008.07.002.
Schwerdtner, W.M., and Mawer, C.K., 1982, Geology of the Gravenhurst region, Grenville Structural Province, Ontario: Geological Survey of Canada, Current Research, Part B, Paper 82-1B, p. 197–207.
Schwerdtner, W.M., and van Berkel, J.T., 1991, The origin of fold abutments in the map pattern of the westernmost Grenville Province, central Ontario: Precambrian Research, v. 49, p. 35–59, http://dx.doi.org/10.1016/0301-9268(91)90055-F.
Schwerdtner, W.M., Waddington, D.H., and Stollery, G., 1974, Polycrystalline pseudomorphs as natural gauges of incremental paleostrain: Neues Jahrbuch fuer Mineralogie, Monatshefte, v. 314, p. 174–182.
Schwerdtner, W.M., Bennett, P.J., and Janes, T.W., 1977, Application of L–S fabric scheme to structural mapping and paleostrain analysis: Canadian Journal of Earth Sciences, v. 14, p. 1012–1032, http://dx.doi.org/10.1139/e77-094.
Schwerdtner, W.M., Klemens, W.P, Waddington, D.H., and Vertolli, V.M., 1998, Late-Grenvillian horizontal extension and vertical thinning of Proterozoic gneisses, central Ontario: Geological Society of America Annual Meeting, Toronto, Canada, Field Trip Guide Number 14.
Schwerdtner, W.M., Riller, U.P., and Borowik, A., 2005, Structural testing of tectonic hypotheses by field-based analysis of distributed tangential shear: examples from major high-strain zones in the Grenville Province and other parts of the southern Canadian Shield: Canadian Journal of Earth Sciences, v. 42, p. 1927–1947, http://dx.doi.org/10.1139/e05-047.
Schwerdtner, W.M., Lu, S.J., and Landa, D., 2010a, S and Z buckle folds as shear-sense indicators in the ductile realm: Field examples from the Grenville Province of Ontario and the Appalachians of South Carolina, *in* Tollo, R.P., Bartholomew, M.J., Hibbard, J.P., and Karabinos, P.M., *eds.,* From Rodinia to Pangea: The Lithotectonic Record of the Appalachian Region: Geological Society of America, Memoirs, v. 206, p. 773–794, http://dx.doi.org/10.1130/2010.1206(30).
Schwerdtner, W.M., Lu, S.J., and Yang, J.F., 2010b, Wall-rock structure at the present contact surfaces between repeatedly deformed thrust sheets, Grenville Orogen of central Ontario: Canadian Journal of Earth Sciences, v. 47, p. 875–899, http://dx.doi.org/10.1139/E10-007.
Schwerdtner, W.M., Rivers, T., Zeeman, B., Wang, C.C., Tsolas, J., Yang, J., and Ahmed, M., 2014, Post-convergent structures in lower parts of the 1090–1050 Ma (early-Ottawan) thrust-sheet stack, Grenville Province of Ontario, southern Canadian Shield: Canadian Journal of Earth Sciences, v. 51, p. 243–265, http://dx.doi.org/10.1139/cjes-2013-0108.
Schwerdtner, W.M., Rivers, T., Tsolas, J., Waddington, D.H., Page, S., and Yang, J., submitted, Transtensional origin of multi-order cross-folds in a high-grade gneiss complex, southwestern Grenville Province, Canada: formation during post-peak gravitational collapse: Canadian Journal of Earth Sciences.
Selleck, B.W., McLelland, J.M., and Bickford, M.E., 2005, Granite emplacement during tectonic exhumation: The Adirondack example: Geology, v. 33, p. 781–784, http://dx.doi.org/10.1130/G21631.1.
Slagstad, T., Culshaw, N.G., Jamieson, R.A., and Ketchum, J.W.F., 2004a, Early Mesoproterozoic tectonic history of the southwestern Grenville Province, Ontario: Constraints from geochemistry and geochronology of high-grade gneisses, *in* Tollo, R.P., Corriveau, L., McLelland, J., and Bartholomew, M.J., *eds.,* Proterozoic tectonic evolution of the Grenville orogen in North America: Geological Society of America Memoirs, v. 197, p. 209–241, http://dx.doi.org/10.1130/0-8137-1197-5.209.
Slagstad, T., Hamilton, M.A., Jamieson, R.A., and Culshaw, N.G., 2004b, Timing and duration of melting in the mid orogenic crust: Constraints from U–Pb (SHRIMP) data, Muskoka and Shawanaga domains, Grenville Province, Ontario: Canadian Journal of Earth Sciences, v. 41, p. 1339–1365, http://dx.doi.org/10.1139/e04-068.
Slagstad, T., Jamieson, R.A., and Culshaw, N.G., 2005, Formation, crystallization and migration of melt in the mid-orogenic crust: Muskoka domain migmatites, Grenville Province, Ontario: Journal of Petrology, v. 46, p. 893–919, http://dx.doi.org/10.1093/petrology/egi/004.
Slagstad, T., Culshaw, N.G., Daly, J.S., and Jamieson, R.A., 2009, Western Grenville Province holds key to midcontinental Granite-Rhyolite Province enigma: Terra Nova, v. 21, p. 181–187, http://dx.doi.org/10.1111/j.1365-3121.2009.00871.x.
Soucy La Roche, R., Gervais, F., Tremblay, A., Crowley, J.L., and Ruffet, G., 2015, Tectono-metamorphic history of the eastern Taureau shear zone, Mauricie area,

Québec: Implications for the exhumation of the mid-crust in the Grenville Province: Precambrian Research, v. 257, p. 22–46, http://dx.doi.org/10.1016/j.precamres.2014.11.012.

Streepey, M.M., Lithgow-Bertelloni, C., van der Pluijm, B.A., Essene, E.J., and Magloughlin, J.F., 2004, Exhumation of a collisional orogen: A perspective from the North American Grenville Province, *in* Tollo, R.P., Corriveau, L., McLelland, J., and Bartholomew, M.J., *eds.,* Proterozoic tectonic evolution of the Grenville orogen in North America: Geological Society of America Memoirs, v. 197, p. 391–410, http://dx.doi.org/10.1130/0-8137-1197-5.391.

Teyssier. C., and Tikoff, B., 1999, Fabric stability in oblique convergence and divergence: Journal of Structural Geology, v. 21, p. 969–974, http://dx.doi.org/10.1016/S0191-8141(99)00067-X.

Teyssier, C., and Whitney, D.L., 2002, Gneiss domes and orogeny: Geology, v. 30, p. 1139–1142, http://dx.doi.org/10.1130/0091-7613(2002)030<1139:GDAO>2.0.CO;2.

Thomson, S.N., Ring, U., Brichau, S., Glodny, J., and Will, T.M., 2009, Timing and nature of formation of the Ios metamorphic core complex, southern Cyclades, Greece, *in* Ring, U., and Wernicke, B., *eds.,* Extending a Continent: Architecture, Rheology and Heat Budget: Geological Society, London, Special Publications, v. 321, p. 139–167, http://dx.doi.org/10.1144/sp321.7.

Timmermann, H., Jamieson, R.A., Culshaw, N.G., and Parrish, R.R., 1997, Time of metamorphism beneath the Central Metasedimentary Belt boundary thrust zone, Grenville Orogen, Ontario: accretion at 1080 Ma?: Canadian Journal of Earth Sciences, v. 34, p. 1023–1029, http://dx.doi.org/10.1139/e17-084.

Timmermann, H., Jamieson, R.A., Parrish, R.R., and Culshaw, N.G., 2002, Coeval migmatites and granulites, Muskoka domain, southwestern Grenville Province, Ontario: Canadian Journal of Earth Sciences, v. 39, p. 239–258, http://dx.doi.org/10.1139/e01-076.

van der Pluijm, B.A., and Carlson, K.A., 1989, Extension in the Central Metasedimentary Belt of the Ontario Grenville: timing and tectonic significance: Geology, v. 17, p. 161–164, http://dx.doi.org/10.1130/0091-7613(1989)017<0161:EITCMB>2.3.CO;2.

Vanderhaeghe, O., 2009, Migmatites, granites and orogeny: Flow modes of partially molten rocks and magmas associated with melt/solid segregation in orogenic belts: Tectonophysics, v. 477, p. 119–134, http://dx.doi.org/10.1016/j.tecto.2009.06.021.

Vanderhaeghe, O., Burg, J-P., and Teyssier, C., 1999, Exhumation of migmatites in two collapsed orogens: Canadian Cordillera and French Variscides, *in* Ring, U., Brandon, M.T., Lister, G.S., and Willett, S.D., *eds.,* Exhumation Processes: Normal Faulting, Ductile Flow and Erosion: Geological Society, London, Special Publications, v. 154, p. 181–204, http://dx.doi.org/10.1144/gsl.sp.1999.154.01.08.

Vanderhaeghe, O., Teyssier, C., McDougall, I., and Dunlap, W.J., 2003, Cooling and exhumation of the Shuswap Metamorphic Core Complex constrained by $^{40}Ar/^{39}Ar$ thermochronology: Geological Society of America Bulletin, v. 115, p. 200–216, http://dx.doi.org/10.1130/0016-7606(2003)115<0200:CAEOTS>2.0.CO;2.

Venkat-Ramani, M., and Tikoff, B., 2002, Physical models of transtensional folding: Geology, v. 30, p. 523–526, http://dx.doi.org/10.1130/0091-7613(2002)030<0523:PMOTF>2.0.CO;2.

Waddington, D.H., 1973, Foliation and mineral lineation in the Moon River synform, Grenville structural province, Ontario: Unpublished MSc thesis, University of Toronto, Toronto, ON.

Ward, R., Stevens, G., and Kisters, A., 2008, Fluid and deformation induced partial melting and melt volumes in low-temperature granulite-facies metasediments, Damara Belt, Namibia: Lithos, v. 105, p. 253–271, http://dx.doi.org/10.1016/j.lithos.2008.04.001.

Weinberg, R.F., and Hasalová, P., 2015, Water-fluxed melting of the continental crust: A review: Lithos, v. 212–215, p. 158–188, http://dx.doi.org/10.1016/j.lithos.2014.08.021.

White, D.J., Forsyth, D.A., Asudeh, I., Carr, S.D., Wu, H., Easton, R.M., and Mereu, R.F., 2000, A seismic-based cross-section of the Grenville Orogen in southern Ontario and western Quebec: Canadian Journal of Earth Sciences, v. 37, p. 183–192, http://dx.doi.org/10.1139/e99-094.

White, I.R., and Crider, J.G., 2006, Extensional fault-propagation folds: mechanical models and observations from the Modoc Plateau, northeastern California: Journal of Structural Geology, v. 28, p. 1352–1370, http://dx.doi.org/10.1016/j.jsg.2006.03.028.

Whitney, D.L., and Evans, B.W., 2010, Abbreviations for names of rock-forming minerals: American Mineralogist, v. 95, p. 185–187, http://dx.doi.org/10.2138/am.2010.3371.

Whitney, D.L., Teyssier, C., and Heizler, M.T., 2007, Gneiss domes, metamorphic core complexes, and wrench zones: Thermal and structural evolution of the Niğde Massif, central Anatolia: Tectonics, v. 26, TC5002, http://dx.doi.org/10.1029/2006TC002040.

Whitney, D.L., Teyssier, C., Rey, P., and Buck, W.R., 2013, Continental and oceanic core complexes: Geological Society of America Bulletin, v. 125, p. 273–298, http://dx.doi.org/10.1130/B30754.1.

Wong, M.S., Williams, M.L., McLelland, J.M., Jercinovik, M.J., and Kowalkoski, J., 2012, Late Ottawan extension in the eastern Adirondack Highlands: Evidence from structural studies and zircon and monazite geochronology: Geological Society of America Bulletin, v. 124, p. 857–869, http://dx.doi.org/10.1130/B30481.1.

Wynne-Edwards, H.R., 1972, The Grenville Province, *in* Price, R.A., and Douglas, R.J.W., *eds.,* Variations in Tectonic Styles in Canada: Geological Association of Canada Special Paper No. 11, p. 263–334.

Yakymchuk, C., and Brown, M., 2014, Consequences of open-system melting in tectonics: Journal of the Geological Society, v. 171, p. 21–40, http://dx.doi.org/10.1144/jgs2013-039.

Received April 2015
Accepted as revised August 2015

SERIES

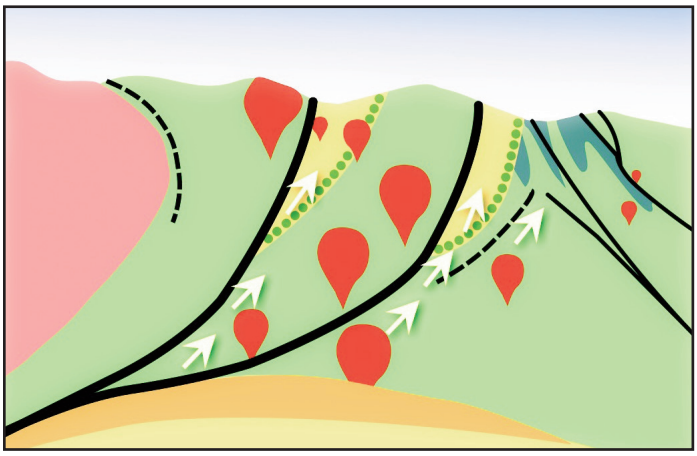

Igneous Rock Associations 19. Greenstone Belts and Granite–Greenstone Terranes: Constraints on the Nature of the Archean World

P.C. Thurston

Department of Earth Sciences
Laurentian University
935 Ramsay Lake Road, Sudbury
Ontario, P3E 2C6, Canada
E-mail: pthurston@Laurentian.ca

SUMMARY

Greenstone belts are long, curvilinear accumulations of mainly volcanic rocks within Archean granite–greenstone terranes, and are subdivided into two geochemical types: komatiite–tholeiite sequences and bimodal sequences. In rare instances where basement is preserved, the basement is unconformably overlain by platform to rift sequences consisting of quartzite, carbonate, komatiite and/or tholeiite. The komatiite–tholeiite sequences consist of km-scale thicknesses of tholeiites, minor intercalated komatiites, and smaller volumes of felsic volcanic rocks. The bimodal sequences consist of basal tholeiitic flows succeeded upward by lesser volumes of felsic volcanic rocks. The two geochemical types are unconformably overlain by successor basin sequences containing alluvial–fluvial clastic metasedimentary rocks and associated calc-alkaline to alkaline volcanic rocks.

Stratigraphically-controlled geochemical sampling in the bimodal sequences has shown the presence of Fe-enrichment cycles in the tholeiites, as well as monotonous thicknesses of tholeiitic flows having nearly constant MgO, which is explained by fractionation and replenishment of the magma chamber with fresh mantle-derived material. Geochemical studies reveal the presence of boninites associated with the komatiites, in part a result of alteration or contamination of the komatiites. Within the bimodal sequences there are rare occurrences of adakites, Nb-enriched basalts and magnesian andesites.

The greenstone belts are engulfed by granitoid batholiths ranging from soda-rich tonalite–trondhjemite–granodiorite to later, more potassic granitoid rocks. Archean greenstone belts exhibit a unique structural style not found in younger orogens, consisting of alternating granitoid-cored domes and volcanic-dominated keels. The synclinal keels are cut by major transcurrent shear zones.

Metamorphic patterns indicate that low-pressure metamorphism of the greenstones is centred on the granitoid batholiths, suggesting a central role for the granitoid rocks in metamorphosing the greenstones. Metamorphic patterns also show that the proportion of greenstones in granite–greenstone terranes diminishes with deeper levels of exposure.

Evidence is presented on both sides of the intense controversy as to whether greenstone belts are the product of modern plate tectonic processes complete with subduction, or else the product of other, lateral tectonic processes driven by the 'mantle wind.' Given that numerous indicators of plate tectonic processes – structural style, rock types, and geochemical features – are unique to the Archean, it is concluded that the evidence is marginally in favour of non-actualistic tectonic processes in Archean granite–greenstone terranes.

RÉSUMÉ

Les ceintures de roches vertes sont des accumulations longiformes et curvilinéaires, principalement composées de roches volcaniques au sein de terranes granitique archéennes, et étant subdivisées en deux types géochimiques: des séquences à komatiite–tholéite et des séquences bimodales. En de rares occasions, lorsque le socle est préservé, ce dernier est recouvert en discordance par des séquences de plateforme ou de rift, constituées de quartzite, carbonate, komatiite et/ou de tholéiite. Les séquences de komatiite-tholéiite forment des épais-

Geoscience Canada, v. 42, http://www.dx.doi.org/10.12789/geocanj.2015.42.081 pages 437–484

seurs kilométriques de tholéiite, des horizons mineurs de komatiites, et des volumes de moindre importance de roches volcaniques felsiques. Les séquences bimodales sont constituées à la base, de coulées tholéiitiques surmontées par des volumes mineurs de roches volcaniques felsiques. Ces deux types géochimiques sont recouverts en discordance par des séquences de bassins en succession contenant des roches métasédimentaires clastiques fluvio-alluvionnaires associées à des roches volcaniques calco-alcalines à alcalines.

Un échantillonnage à contrôle stratigraphique des séquences bimodales a révélé la présence de cycles d'enrichissement en Fe dans les tholéiites, ainsi que des épaisseurs continues d'épanchements tholéiitiques ayant des valeurs presque constante en MgO, qui s'explique par la cristallisation fractionnée et le réapprovisionnement de la chambre magmatique par du matériel mantélique. Les études géochimiques montrent la présence de boninites associées aux komatiites, résultant en partie de l'altération ou de la contamination des komatiites. Au sein des séquences bimodales, on retrouve en de rares occasions des adakites, des basaltes enrichis en Nb et des andésites magnésiennes.

Les ceintures de roches vertes sont englouties dans des batholites granitoïdes de composition passant des tonalites–trondhjémites–granodiorites enrichies en sodium, à des roches granitoïdes tardives plus potassiques. Les ceintures de roches vertes archéennes montrent un style structural unique que l'on ne retrouve pas dans des orogènes plus jeunes, et qui est constitué d'alternances de dômes à cœur granitoïdes et d`affaissements principalement composés de roches volcaniques. Les synclinaux formant les affaissements sont recoupés par de grandes zones de cisaillement.

Les profils métamorphiques indiquent que le métamorphisme de basse pression des roches vertes est centré sur les batholites, indiquant un rôle central des roches granitoïdes durant le métamorphisme des roches vertes. Les profils métamorphiques montrent également que la proportion de roches vertes dans les terranes granitiques diminue avec l'exposition des niveaux plus profonds.

On présente les arguments des deux côtés de l'intense controverse voulant que les ceintures de roches vertes soient le produit de processus moderne de la tectonique des plaques incluant la subduction, ou alors le produit d'autres processus tectoniques découlant du « flux mantélique ». Étant donné la présence des indicateurs des processus de tectonique des plaques – style structural, les types de roches, et les caractéristiques géochimiques – ne se retrouvent qu'à l'Archéen, nous concluons que les indices favorisent légèrement l'option de processus tectoniques non-actuels dans les terranes granitiques de roches vertes à l'Archéen.

Traduit par le Traducteur

INTRODUCTION

Greenstone belts are long, linear accumulations of predominantly volcanic rocks that typically feature relatively low metamorphic grade. The belts range from the ~3825 Ma volcanic rocks of the Porpoise Cove belt of northeastern Québec (O'Neil et al. 2008) and the 3710 Ma Isua greenstones of western Greenland (Baadsgaard et al. 1984), to Paleoproterozoic greenstones such as the Trans-Hudson orogen (Canada) and the Ashanti gold belt of west Africa. Archean greenstone belts are an important component of granite–greenstone subprovinces that form the major part of Archean cratons (Fig. 1; Percival and Stott 2010). Granite–greenstone subprovinces consist of the greenstone belts themselves and related granitoid rocks, which include granitoid basement and synvolcanic, syn-tectonic and post-tectonic plutons. Greenstone belts are sensitive recorders of their environment of formation, such as atmospheric composition (Farquhar and Wing 2003), oceanic chemistry and depth (Bolhar et al. 2005; Kamber 2010; Thurston et al. 2012) and mantle dynamics, such as the presence or absence of subduction (Wyman et al. 2002; Bédard et al. 2013). Greenstone belts are economically important as a repository for syngenetic mineralization, e.g. volcanogenic massive sulphides (VMS) deposits (Galley et al. 2007a), uranium, komatiite-associated nickel deposits (Lesher and Keays 2002), and epigenetic deposits, such as lode gold. The petrogenetically associated granitoid rocks are sources of rare metal mineralization in pegmatites and accessory phases. The orogenic lode gold deposits of Canada are almost exclusively in the volcanic rocks and successor basin units of Archean greenstone belts (Goldfarb et al. 2005), whereas their occurrence in granitoid plutons of the greenstone belts is minor (Robert et al. 1997).

The objectives of this paper are to describe all the major aspects of granite–greenstone terranes: rock types, volcanology, sedimentology, igneous petrology, structural geology, and metamorphism, and to assess the merits of tectonic models required to produce these terranes. This review will concentrate upon the Superior Province but will provide examples from other shields, principally to illustrate that the features and processes described are not unique to the Superior Province.

It is important to recognize that there are two points of view concerning the origin of greenstones: a) an actualistic point of view involving the operation of plate tectonics in the Archean, and b) various non-plate tectonic scenarios invoked only for Archean and some Proterozoic greenstones. There is at this time an intense debate as to which of these scenarios is correct (Stern 2005; Percival 2007; Percival and Stott 2010; Wyman et al. 2011; Hamilton 2011; Bédard et al. 2013). In this paper, a balance is sought between the largely geochemical arguments presented for Archean subduction (Hollings 1999, 2002; Kerrich et al. 1999; Polat and Kerrich 2001, 2002; Wyman et al. 2002) *vs.* the geodynamic and geochemical arguments opposing Archean subduction (Hamilton 2011; Bédard et al. 2013; Kamber 2015).This paper also seeks to highlight the importance of integration of geochemical arguments with stratigraphy and structure.

CRATON SUBDIVISIONS

The Superior Province is subdivided into Paleo- to Mesoarchean continental fragments, Neoarchean juvenile oceanic fragments, and orogenic flysch terranes (Percival and Stott 2010). The individual terranes are mainly fault-bounded. A less controversial subdivision of Archean cratons used herein recognizes 'granite–greenstone' terranes or subprovinces and 'orogenic flysch' terranes (Fig. 1). Orogenic flysch units are relatively rare; the other major non-Superior Province occurrence is the Limpopo orogen linking the Kaapvaal and Zimbabwe cratons (Eglington and Armstrong 2004; Schmitz et al. 2004). Review of other Archean cratons shows that they

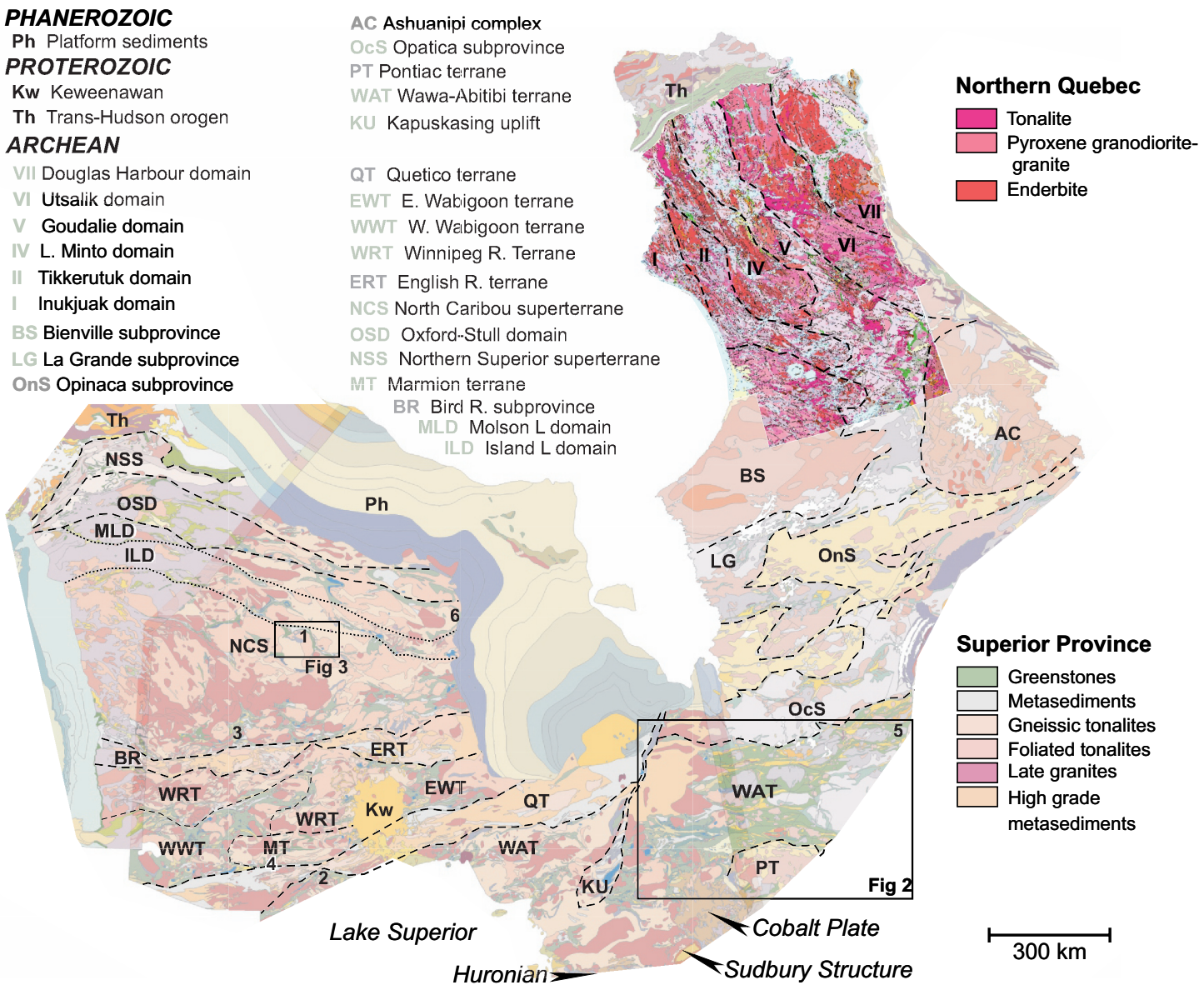

Figure 1. The Superior Province showing granite–greenstone terranes and orogenic flysch terranes (after Percival 2007). In the legend on the figure, abbreviations for Archean granite-greenstone terranes and domains are in green and abbreviations for Archean orogenic flysch terranes are shown in beige. Localities mentioned in the text: 1 – North Caribou greenstone belt, 2 – Shebandowan greenstone belt in the Wawa-Abitibi terrane, 3 – Confederation Lake greenstone belt, 4 – Steeprock greenstone belt in the Marmion terrane, 5 – Chibougamau area within the Abitibi greenstone belt, 6 – Ring of Fire area shown on Figure 26. Figure is after Percival (2007).

are dominated by granite–greenstone terranes; the greenstones are mostly at greenschist grade, but smaller areas achieve amphibolite–granulite grade.

BASEMENT – A RARE RELATIONSHIP

A small number of Archean greenstone belts lie unconformably upon basement in the Superior Province (Wilks and Nisbet 1988; Breaks et al. 2001) and in the Zimbabwe craton (Martin et al. 1993; Bickle et al. 1994). In places, the greenstone–granitoid contact is a regolith, reflecting subaerial exposure, for example at the base of the Keeyask assemblage in the North Caribou belt of the Superior Province (Fig. 2) and at the base of Zimbabwe greenstones (Thurston et al. 1991; Martin et al. 1993). However, at Steeprock in the Superior Province (Wilks and Nisbet 1988) the unconformity is a submarine contact consisting of quartzose clastic units overlying the granitoid substrate. These basal unconformities and inter-assemblage unconformities clearly indicate that some greenstones formed in place. Additional evidence for autochthonous origin of some greenstones is discussed in a subsequent section.

LITHOTECTONIC ASSEMBLAGES

Since the 1920s, geologists have been able to decipher the stratigraphy of greenstone belts with way-up indicators such as pillows and graded bedding in sedimentary and volcaniclastic units. With the knowledge of stratigraphic polarity, greenstones are observed to occupy synclinoria or keels that are interspersed with domes cored by granitoid batholiths (Fig. 3). Historically, greenstone belts were divided into Keewatin and Timiskaming units (Gunning and Ambrose 1939). Keewatin units are pre-deformation, largely volcanic units containing minor intercalated metasedimentary rocks, whereas Timiskaming units refer to unconformably overlying successor basins comprising post-early deformation, alluvial–fluvial to deep-

basin metasedimentary rocks that contain lesser fine clastic units and calc-alkaline to alkaline volcanic rocks.

The concept of lithotectonic assemblages developed for the Cordilleran orogen (Tipper et al. 1981) was applied to greenstone belts to distinguish units of differing age or geodynamic setting (Thurston 1991; Thurston and Ayres 2004). Within Archean greenstone belts, the following assemblage types are recognized: 1) shallow-water, quartz- and carbonate-rich platforms with minor volcanic rocks, unconformably overlying granitoid or volcanic basement; 2) shallow- to deep-water komatiites and tholeiitic basalts overlying platformal sequences or granitoid basement; 3) deep-water komatiite–tholeiite or tholeiite sequences; 4) bimodal deep-water sequences dominated by tholeiitic basalt and containing minor felsic volcaniclastic rocks, chert, and iron-formation; 5) shallow-water to emergent bimodal successions; and 6) subaerial sedimentary rocks intercalated with subordinate alkaline to calc-alkaline volcanic rocks (Thurston and Chivers 1990). Greenstone belts commonly contain multiple assemblages (Fig. 2). At the craton scale, a stratigraphic/temporal progression from assemblage types 1 to 6 is observed (Thurston and Chivers 1990; Thurston and Ayres 2004).

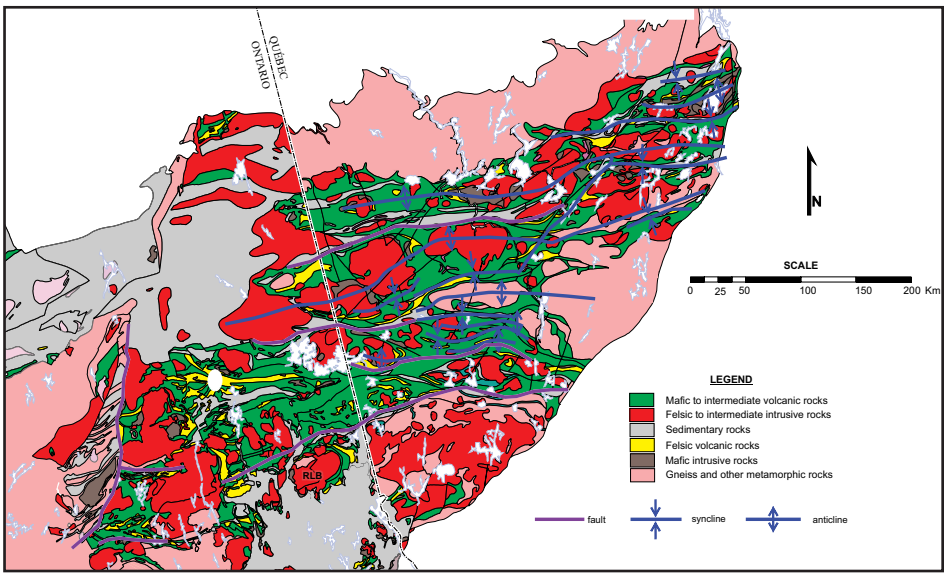

Figure 2. Structural map of the Abitibi greenstone belt showing alternation of domes cored by granitoid rocks and keels dominated by volcanic rocks (after Dubé et al. 2004). A selection of stratigraphy-parallel and cross-cutting faults is shown.

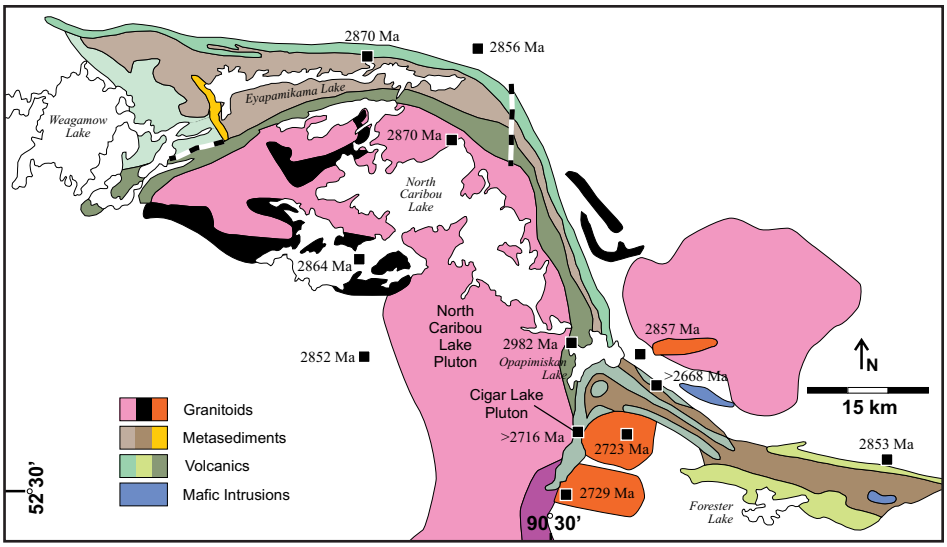

Figure 3. The North Caribou greenstone belt in the North Caribou terrane showing multiple ages and types of assemblages within a single greenstone belt. Geology after Breaks et al. (2001) with plutons based on Biczok et al. (2012).

Quartzite–Carbonate Platforms

Quartzite–carbonate platforms are relatively rare but have been described in the Superior, Churchill, and Slave Provinces of Laurentia (Donaldson and de Kemp 1998; Bleeker 2002), as well as in the Yilgarn (Gee et al. 1981), Pilbara (Van Kranendonk et al. 2007b) and Baltic (Thurston and Kozhevnikov 2000) cratons (Fig. 4A, B). These sequences contain shallow-water structures such as hummocky and herringbone cross-stratification and mudstone drapes, and progress upward through stromatolite-bearing carbonates (Arias et al. 1986; Wilks and Nisbet 1988; Bleeker 2002) and shales to deeper water komatiite–tholeiite sequences (described below). These shallow-water sedimentary units are overlain by shale and banded iron-formation (BIF) that are finely laminated and, based on the lack of structures other than loading structures, represent deposition below storm wave base. Quartzite-bearing sequences in the Slave craton are related to craton rifting (Mueller and Pickett 2005), a model which also fits the Superior Province (Thurston 2003).

Shallow- to Deep-Water Komatiite– Tholeiite Sequences

The platformal sequences are overlain by relatively thin (metres to hundreds of metres), areally restricted sequences of komatiitic and tholeiitic flows. Primary structures range from spinifex-textured komatiitic flows to pillowed mafic flows, all representative of uncertain water depth. These sequences are in tectonic or stratigraphic contact with overlying kilometre-scale thicknesses of intercalated komatiite and tholeiite flows (Thurston et al. 1991).

Deep-Water Komatiite–Tholeiite Sequences

Individual tholeiitic basalt flows displaying distinctive textures (e.g. glomeroporphyritic or variolitic) are traceable for tens of km and grade from thick, proximal, massive gabbroic-textured flows, to master tubes with branching megapillows that grade distally into normal-sized pillows with a cross-sectional area averaging 2600 cm^2 (Sanschagrin 1982). Glomeroporphyritic basalts are commonly high in the stratigraphy and serve as marker horizons (Phinney et al. 1988; Blackburn et al. 1991).

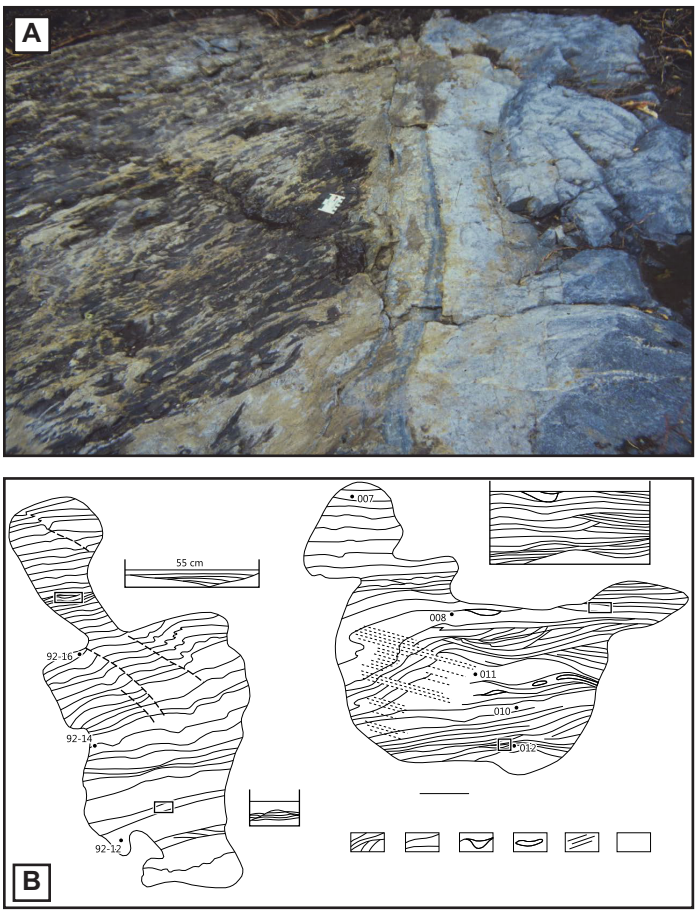

Figure 4. Basal unconformity in a greenstone belt and primary structures in basal quartz arenites. A. Unconformity at the base of the Keeyask metasedimentary assemblage in the North Caribou greenstone belt, North Caribou terrane, Superior Province. (Photo by F. Breaks). To the left is a weathered basalt flow with increasing intensity of alteration to the right, approaching the contact with the quartz arenite. B. Hummocky cross-stratification in quartz arenites of the Hisovaara greenstone belt in the Baltic Shield (Thurston and Kozhevnikov 2000).

The komatiites constitute a maximum of 5% of the stratigraphy in the Abitibi[1] greenstone belt (Sproule et al. 2002) and their position in the stratigraphic column is not consistent, occurring as basal units such as the Tisdale assemblage, or higher in the stratigraphy such as the Kidd–Munro assemblage (Houlé et al. 2008b).

Komatiitic magmas differ from basalts in being hotter (~1600° *vs.* ~1200°C) and less viscous. These two parameters profoundly affect the physical volcanology of these magmas. In the classic exposures in the Pyke Hill area (Pyke et al. 1973) of the Abitibi greenstone belt, flows have rubbly flow tops, followed downward by spinifex-textured olivine, a cumulate olivine zone and a chilled base. Komatiitic magmas display: 1) a flood-flow facies of substantial extent consisting of intrusive and extrusive units; 2) a laterally extensive compound-flow facies with linear troughs up to 150 m thick flanked by metre-scale flows; and 3) a ponded-flow facies. Initial flows have a low aspect ratio and propagate laterally beneath a solidified crust (Hill 2001). As the upper crust thickens, it begins to slow the advance of the flow and additional magma is accommodated by flow inflation (Dann 2001; Hill 2001) in an ordered process of flow advance, inflation and endogenous growth. The relationship between komatiite volcanology and komatiite-associated mineralization is discussed in a subsequent section.

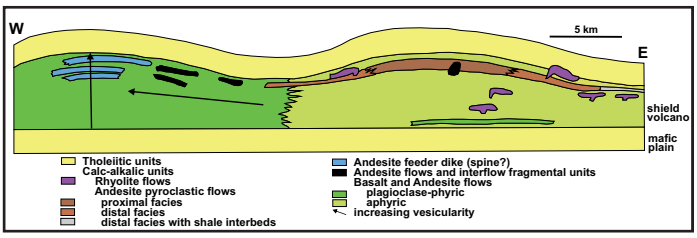

Figure 5. Mafic plain stratigraphy (after Thurston and Ayres 2004).

Komatiitic and/or basaltic flows, particularly at magma clan transitions, are commonly capped by thin, cm-scale argillite units. A deep water environment is suggested by the rarity of oxide-facies iron-formation, vesicular flows, hyaloclastite units (Dimroth et al. 1985) and mafic pyroclastic units. Lava plains and shield volcanoes dominated by mafic volcanism represent the normal base of greenstone belt stratigraphic sequences. They form 5–7 km-thick subaqueous plains 100–150 km in length consisting of overlapping shield volcanoes >25 km in diameter (Dimroth and Rocheleau 1979; Thurston and Chivers 1990; Fig. 5). Shield volcanoes of the Abitibi greenstone belt are up to 7 km thick and >30 km in diameter (Leclerc et al. 2011). Similar features are seen in mafic sequences in the Pilbara (Kiyokawa and Taira 1998; Krapez and Eisenlohr 1998), the Yilgarn (Brown et al. 2002), and the Baltic (Kozhevnikov 1992) cratons.

The shield volcanoes typifying mafic plain volcanism are succeeded by subaqueous composite volcanoes with steeper dips and higher proportions of pillowed flows, hyaloclastites, and vesicularity, perhaps related to a shallowing-upward depositional environment, e.g. the Monsabrais area in the Blake River Group of the Abitibi greenstone belt (Dimroth et al. 1974; Ross et al. 2008). Flow-foot breccias form prograding deltas typical of a littoral environment (Dimroth et al. 1985) and are consistent with a shallowing-upward hypothesis. Sheets of massive lava-forming topsets and foresets, which grade both upward and downward into pillow lava and pillow breccia, also suggest a littoral environment.

These sequences are linked to 'deep' water solely on the basis of the presence of textures such as pillows that are diagnostic of submarine deposition, and the fact that the geometry and thickness of the volcanic edifices require at least a few hundred metres of water depth. Pyroclastic and volcaniclastic units can likewise represent a broad range of depths. This caveat is applicable to the discussion in the following sections.

Deep-Water Bimodal Volcanic Sequences

The bimodal sequences consist of up to 90% basalt or basaltic andesite, and subordinate felsic volcanic rocks. Volcanologically, the mafic component is marked by the transition from shield volcanoes that erupted mafic lavas, to composite volcanoes having multiple vents (Lafrance et al. 2000), volcanic

[1] The Abitibi greenstone belt is the major greenstone belt within the Abitibi–Wawa terrane (Figs. 1, 2).

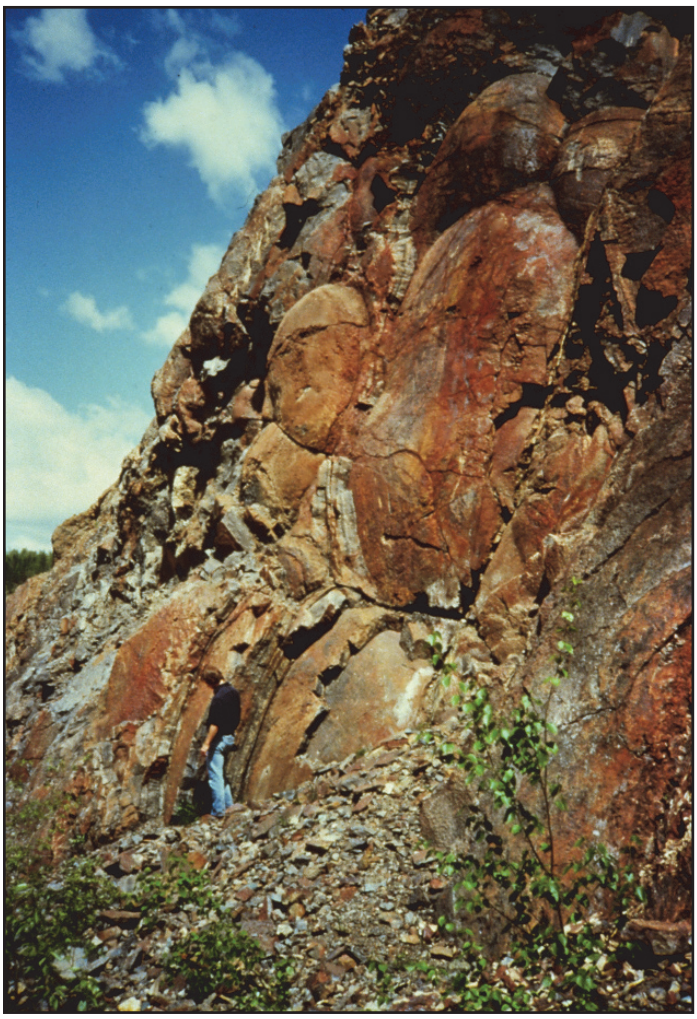

Figure 6. Domical stromatolites at the Steeprock mine, Marmion Terrane. Photo from stromatolites.blogspot.ca.

complexes (Legault et al. 2002), calderas and/or cauldrons (Gibson and Watkinson 1990) and small felsic centres formed along major structures (Scott et al. 2002). In this style of volcanism, the edifices were predominantly submerged, but short-term emergence is recorded in the upper parts of these sequences (Thurston 1980; Lambert et al. 1990), as well as shallow-water features such as stromatolite-bearing carbonate rocks in the Abitibi greenstone belt (Hofmann and Masson 1994), the North Caribou terrane, at Steeprock in the Marmion terrane of the Superior Province (Hofmann et al. 1985; Stone et al. 1992; Fig. 6), and the Back River volcanic complex in the Slave Province (Lambert et al. 1990, 1992). Further constraints on water depth are absent.

Two main types of felsic rocks occur in deep-water bimodal sequences: 1) lava flows, domes, and related autoclastic units (de Rosen-Spence 1976; de Rosen-Spence et al. 1980); and 2) volcaniclastic units, including pyroclastic rocks possibly associated with calderas (Ross and Mercier-Langevin 2014). Some volcaniclastic units are interpreted as welded to non-welded pyroclastic flows (Thurston et al. 1985), mass flows (lahars), and air fall eruptives (Hallberg 1986; Barley 1992; Krapez and Eisenlohr 1998). Subaqueous pyroclastic flows have been proposed for calderas at Sturgeon Lake in the western Wabigoon subprovince (Morton et al. 1991), for the Selbaie and Noranda calderas in the Abitibi greenstone belt (Larson and Hutchinson 1993), in the Pilbara greenstones (Van Kranendonk 2000), and for subaerial welded ignimbrites in the North Caribou terrane (Thurston 1980).

Stratigraphically, the bimodal sequences are characterized by a mafic base and minor felsic volcanic rocks at the top (Fig. 7). The transition to the next volcanic cycle is marked by numerous mafic dikes cutting the felsic rocks, followed by mafic flows; alternatively, the felsic volcanic rocks are overlain by a 'sedimentary interface zone' (Thurston et al. 2008) characterized by clastic and chemical sedimentary rocks from a few cm to ~500 m thick.

Subaerial to Emergent Successor Basins

The deep-water bimodal successions are succeeded by unconformably overlying successor basins deposited synorogenically and characterized by the first appearance of plutonic detritus and calc-alkaline to alkaline volcanic rocks. These units are classically termed 'Timiskaming'-type sequences in Canada (Gunning and Ambrose 1939; Fig. 8). Examples are found in all Archean cratons. In the Superior Province, examples include the Wabigoon (Ayer and Davis 1997), the Abitibi (Mueller and Dimroth 1987; Dostal and Mueller 1992) and the North Caribou (Parks et al. 2006) terranes. They also occur in the Slave (Mueller and Corcoran 2001), the Pilbara (Krapez and Barley 1987) and the Yilgarn (Swager et al. 1990) cratons. The successor basins contain up to 40% volcanic units (Swager et al. 1990; Mueller and Corcoran 1998), ranging in composition from calc-alkaline to shoshonitic. Shoshonites[2] are found at Oxford Lake in the Oxford–Stull terrane (Brooks et al. 1982), in the Wawa–Abitibi terrane (Capdevila et al. 1982) and at Lake of the Woods in the western Wabigoon terrane (Ayer and Davis 1997). These successor basin volcanic rocks include 2–30 m-thick pillowed tholeiitic basalts and subaerial, calc-alkaline, felsic lobate and brecciated flows at Stormy Lake (Mueller and Corcoran 1998), and, at Kirkland Lake in the Abitibi greenstone belt, ultrapotassic lava flows with blocky or aa flow texture accompanied by pyroclastic surge and air fall deposits containing accretionary lapilli (Cooke 1966).

VOLCANIC GEOCHEMISTRY AND PETROGENESIS

Introduction

Volcanic rocks in Archean greenstone belts consist of two major geochemical associations, each typically making up one assemblage: 1) komatiite–tholeiite sequences (Sun and Nesbitt 1978; Arndt and Nesbitt 1982; Polat et al. 1998; Kerrich et al. 1998); and 2) bimodal basalt to dacite/rhyolite sequences (Condie 1981; Thurston et al. 1985; Laflèche et al. 1992). Basalts of the latter association vary from tholeiitic to calc-alkaline, and more recent work (Wyman et al. 2000; Polat and Kerrich 2001; Hollings 2002) has shown that magnesian andesites, Nb-enriched basalt/andesite, and adakites common-

[2] Shoshonites are basaltic alkalic volcanic rocks that have high total alkalies ($Na_2O + K_2O$ >5%), K_2O >Na_2O, and are nearly saturated in silica.

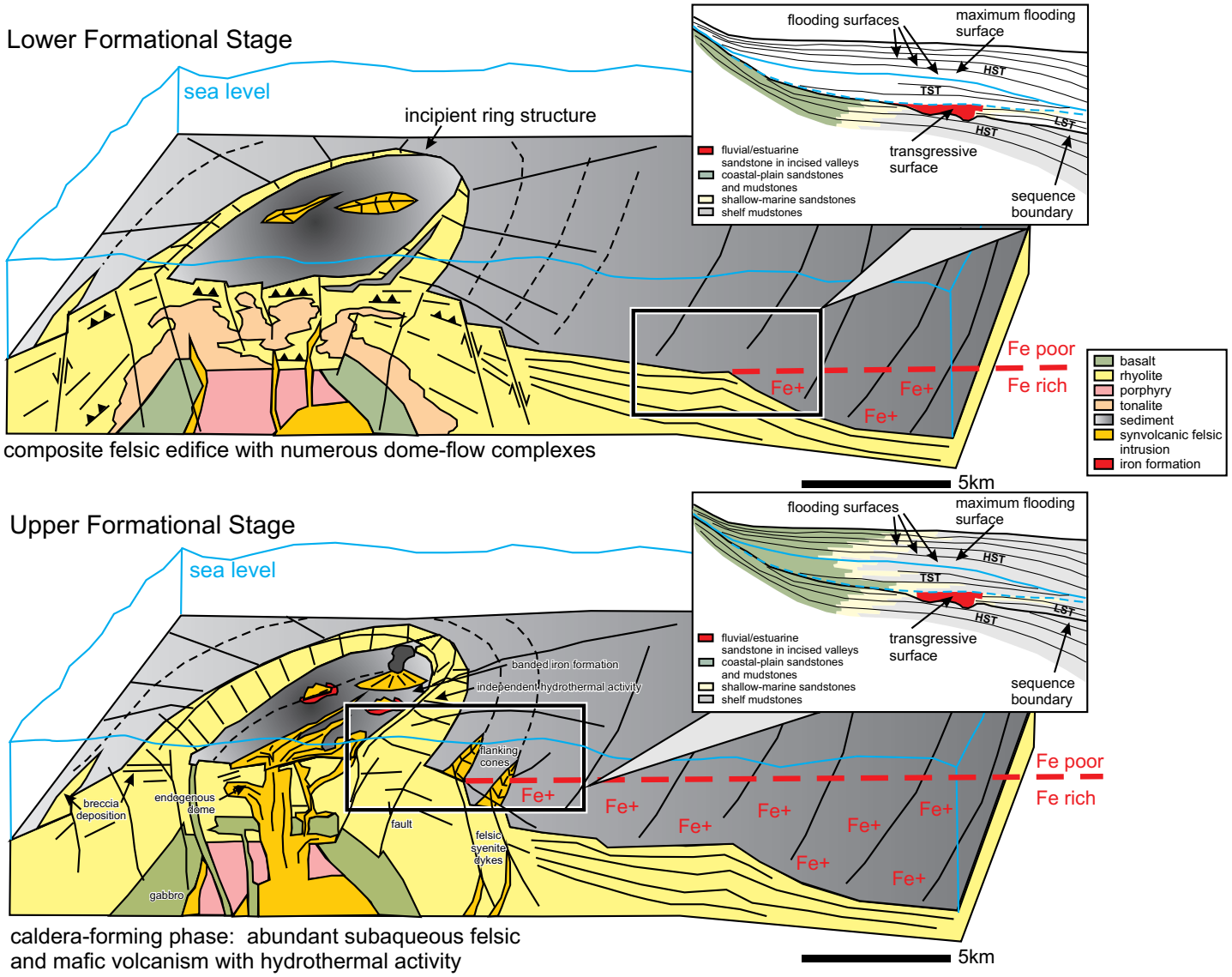

Figure 7. Stylized view of subaqueous calderas in bimodal associations of the Abitibi greenstone belt (after Mueller and Mortensen 2002; Thurston et al. 2008).

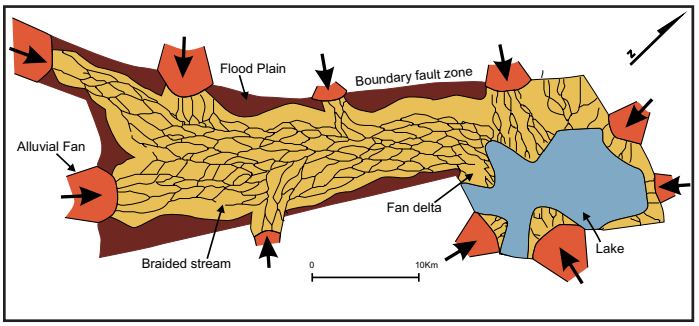

Figure 8. Diagrammatic view of an Archean successor basin prior to deformation (after Krapez and Barley 1987).

ly occur in the upper units of this association. Archean volcanic rocks have been subject to hydrothermal as well as metamorphic alteration. Conventionally, alteration is identified by volatile contents over 3.8% and presence of normative corundum (Gélinas et al. 1977), and various alteration indices such as the Ishikawa index (Ishikawa et al. 1976) or the alteration box plot of Large et al. (2001). Within individual lava flows, a uniformity of inter-element ratios such as Al_2O_3/TiO_2, Ti/Zr, and Ti/Sc indicate a lack of large-scale mobility of some elements during alteration (Kerrich and Wyman 1996). General experience with trace element geochemistry has shown that on the extended trace element diagram ('spidergram') the large ion lithophile elements (LILE), Cs, Rb, Ba, and U can show erratic behaviour because of alteration, and therefore they are commonly omitted on plots of Archean volcanic rocks. In the following paragraphs, the geochemistry of the two sequence types is discussed. This is followed by a discussion of the implications of stratigraphic geochemical variations in selected Archean greenstone belts.

Komatiite–Tholeiite Sequences

Komatiite–tholeiite sequences consist of intercalated komatiitic and tholeiitic flows, and rare volcaniclastic units. Komatiites include ultramafic volcanic and coeval intrusive rocks, and are classified on the basis of Al_2O_3/TiO_2 and Gd/Yb_{CN} ($_{CN}$ = chondrite-normalized) (Table 1). By definition, they have >18% MgO, high concentrations of Ni and Cr, and FeOt about 11%. The geochemistry of komatiites is a function of:

Table 1. Petrogenetic classification of komatiites (after Sproule et al. 2002).

Geochemical Type	Al undepleted (AUK)	Al depleted (ADK)	Ti enriched	Ti depleted
Type area	Munro	Barberton	Finland	Shining Tree
Al_2O_3/TiO_2	15–25	<15	<15	15–25
Gd/Yb	~1	1.2–2.8	>1.2	0.6–0.8
Degree of partial melting	30–50%	20–40%	>20%	20–50%
Depth of melt separation	Plume head: 2–8 Gpa	Plume tail: 6–9 Gpa	Plume head: 2–8 Gpa	Plume tail: 6–9 Gpa

1) source composition; 2) conditions of melting; 3) melting mechanisms; 4) extent and type of contamination; 5) degree of fractionation or accumulation; and 6) post-crystallization modification (Ludden et al. 1986; Xie et al. 1993). Komatiites are considered to be the product of mantle plumes, based upon thermodynamic models, experimental petrology, melt inclusions, trace element systematics, and the presence of comparable rocks on oceanic plateaux and oceanic hotspots (Storey et al. 1991; Herzberg 1992; McDonough and Ireland 1993; Kerr 1996). Most Archean plumes were derived from depleted mantle (Campbell et al. 1989; Storey et al. 1991) that was tapped at various depths, as summarized in Table 1. It is interesting to note that Al-depleted and Al-undepleted komatiites are intercalated in the south-central part of the Abitibi greenstone belt, suggesting a rising plume source (Dostal and Mueller 1997). The major modern analogue to Archean komatiites is the Gorgona komatiite at the base of the Columbia–Caribbean Large Igneous Province (Kerr 1996). A contrasting view suggests that komatiites originated as hydrous magmas (Grove and Parman 2004), possibly in a subduction zone setting (Parman et al. 2001); however, as indicated by Arndt et al. (2008, p. 349), this hypothesis is not widely supported.

Komatiitic basalts have MgO contents of 18–26% and relatively low abundances of TiO_2 (<1%) and incompatible trace elements (Arndt et al. 2008). They have lower contents of Fe, high-field-strength elements (HFSE) and light rare-earth elements (LREE) than tholeiites (Arndt et al. 2008). Trace elements indicate that Archean basalts associated with komatiites are predominantly Mg- to Fe-tholeiites displaying flat REE patterns (Fig. 9). On the basis of their consistent stratigraphic association with komatiites and picrites, the tholeiites are interpreted as products of a rising plume head that entrained some of the surrounding mantle (Campbell et al. 1989; Arndt 1991). These tholeiites therefore represent a mixture of plume head material and upper mantle melts (Campbell et al. 1989; Arndt 1991). Archean basalts display a continuous trend from high to low Mg# accompanied by a rise in FeOt, Nb, Th, Zr, Hf, REE and Y, accompanied by decreasing Cr and Ni contents (Kerrich et al. 1999). In general terms, Archean basalts have higher Fe contents than younger counterparts, clearly seen on an Fe/Ti *vs.* Al/Ti cation diagram (Francis et al. 1999; Fig. 10). The tholeiites within komatiite–tholeiite sequences are commonly divided into Mg- and Fe-tholeiites and LREE-enriched units (Maurice et al. 2009). A recently developed subdivision applied on a regional scale consists of Mg-tholeiites with 4–10% MgO, 9–15% Fe_2O_3t, and 0.4–1.2% TiO_2, and Fe-tholeiites

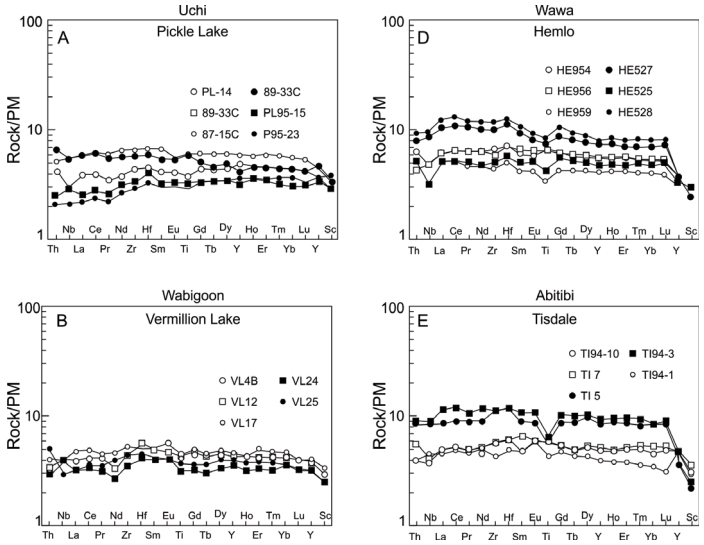

Figure 9. Representative primitive mantle-normalized extended trace element diagrams of Archean tholeiites from the Superior Province (after Kerrich et al. 1999). Normalization to primitive mantle values of Sun and McDonough (1989).

having a similar range of MgO content, but higher Fe_2O_3t (11–20%), and TiO_2 (1.0–2.6%). The Fe-tholeiites contain greater abundances of incompatible trace elements (e.g. 50–155 ppm Zr), lower Al_2O_3/TiO_2 (<15), and higher Gd/Yb_{CN} (1.2–2.0) (Maurice et al. 2009).

Kerrich et al. (1999), in discussing the origin of Archean tholeiites and komatiites from the Abitibi and the Lumby Lake greenstone belts, dismiss the possibility of contamination affecting trace element geochemistry on the basis of: 1) the lack of geochemical signatures of contamination; 2) the lack of xenocrystic zircons; and 3) the lack of isotopic evidence for contamination. All of these criteria have subsequently been disproven in at least part of the Wawa–Abitibi terrane and the Marmion terrane of the Superior Province (Thurston 2002; Ayer et al. 2005; Buse et al. 2010). The probability of contamination is inherent in the autochthonous development of many other Superior Province greenstones (Thurston 2002). The notion that magmas in granite–greenstone terranes transect older units is supported by the presence of dikes of younger greenstones cutting older greenstones in the North Caribou terrane (Rogers et al. 2000) and the Wawa–Abitibi terrane (Ayer et al. 2005). Xenocrystic zircons in Archean greenstones have been found in about 20% of post-millennial geochronological studies, which have been carried out mainly in the Wawa–Abitibi terrane and in the Marmion terrane of the Superior Province (Buse et al. 2010).

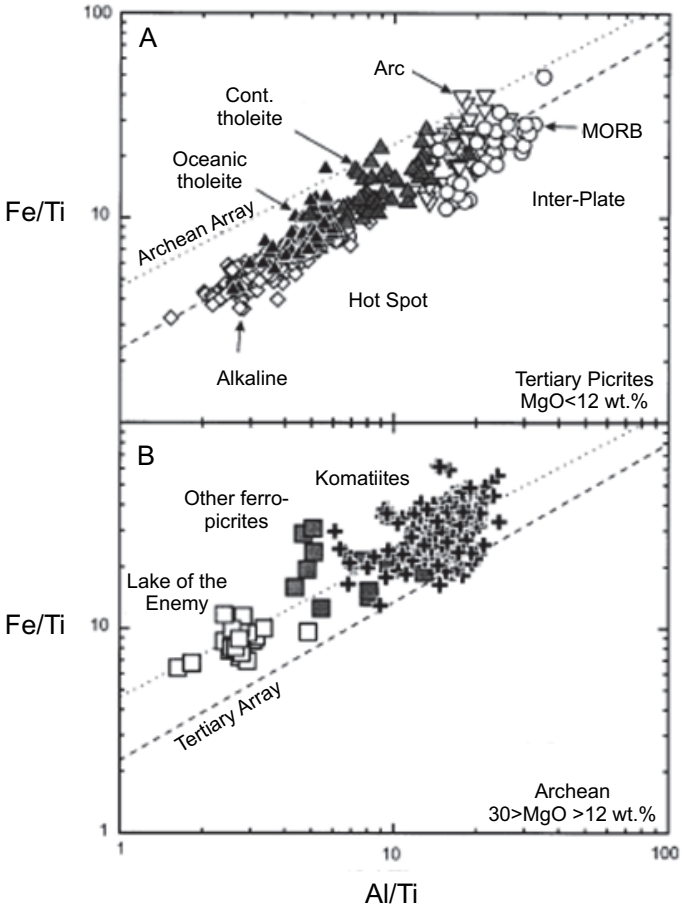

Figure 10. Plot of Fe/Ti *vs.* Al/Ti (each in wt. percent) demonstrating the high Fe nature of Archean mantle, as shown in the chemistry of Archean picritic lavas (Francis et al. 1999).

The advent of ICP–MS analysis has brought about many studies of the trace element geochemistry of Archean volcanic rocks and possible relationships with geodynamic settings (Hollings and Kerrich 1999, 2002; Hollings et al. 1999a, b; Kerrich et al. 1999; Wyman and Kerrich 2009). For example, in northwestern Ontario, Hollings et al. (1999b) have documented basalt geochemistry in 2.9−3.0 Ga komatiite−tholeiite sequences (Fig. 11). They observed that the majority of basalts are Mg-tholeiites with flat REE patterns. However, some samples display negative Nb anomalies, La/Sm_{CN} 1.8−3.4, and Gd/Yb_{CN} 1.0−1.6; some samples display LREE depletion. Many of the northwestern Ontario greenstone belts examined in this study are underlain by older greenstone and granitoid rocks. In support of this, it was noted that Nb anomalies increase with increasing SiO_2, La/Sm_{CN}, and Th/Ce_{CN}, all suggestive of contamination by a felsic component, given the high La/Sm_{CN} and Th/Ce_{CN} of granitoid magmas. The so-called Siliceous High Magnesium Basalts (SHMB) documented in the Archean of Australia and elsewhere (Sun et al. 1989) have similar high SiO_2 (51−55%) and MgO (10−16%), and are shown to be produced by contamination, as validated by Pb and Sm−Nd isotopic and trace element studies.

Boninites

Boninites are primitive andesites occurring within komatiite−tholeiite sequences. They contain >53% SiO_2, 8−15%

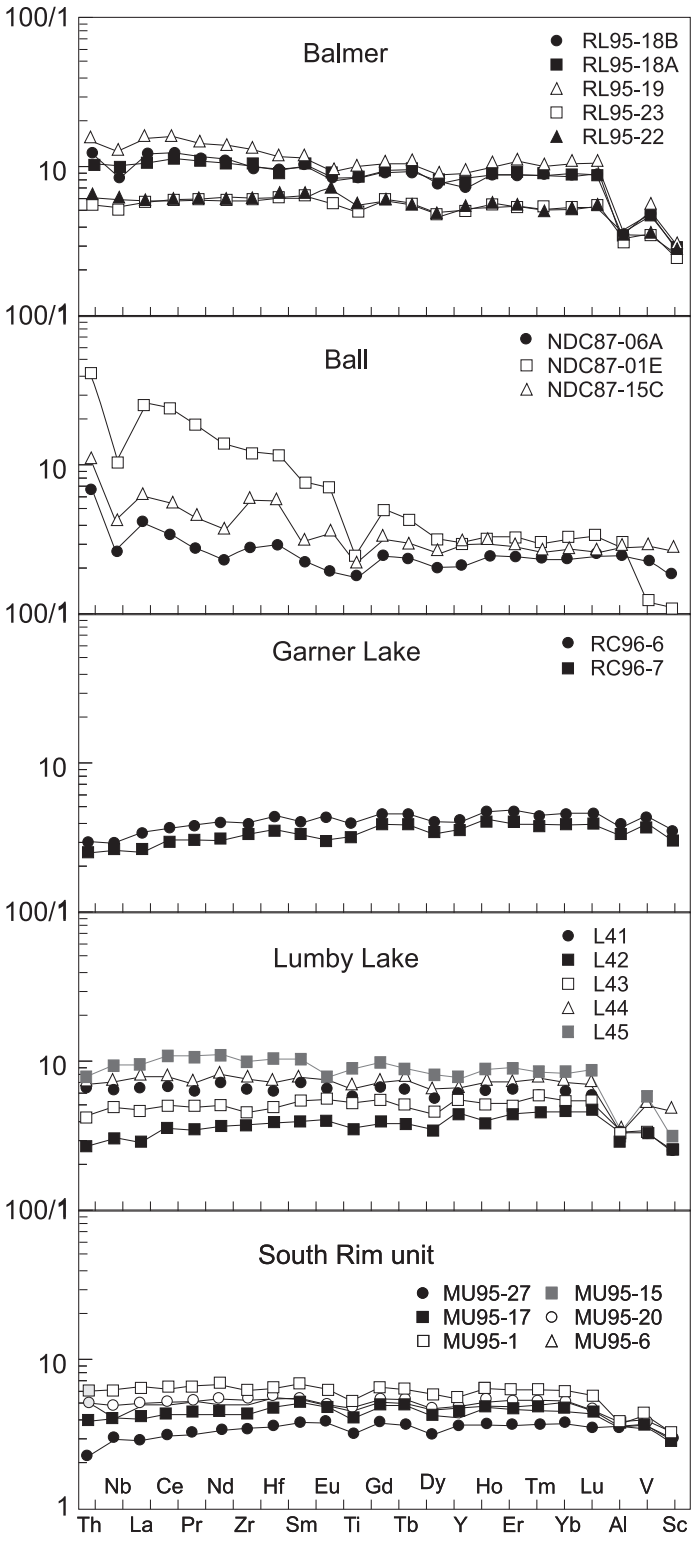

Figure 11. Tholeiitic and komatiitic volcanic rocks from greenstone belts of the northern Superior Province (Hollings et al. 1999). A. Tholeiitic flows from the ~3 Ga Balmer assemblage, Red Lake greenstone belt; B. Tholeiitic flows from the ~3 Ga Ball assemblage, Red Lake greenstone belt; C. Tholeiitic flows from Garner Lake in the Rice Lake greenstone belt of the Bird River terrane; D. Tholeiites from the Lumby Lake greenstone belt of the Marmion terrane; and E. Tholeiites from the ~3 Ga South Rim assemblage of the North Caribou greenstone belt (shown in Figure 3). Data are normalized to the primitive mantle values of Sun and McDonough (1989).

MgO, Mg# >60, low (<0.5%) TiO_2, enrichment in LREE compared to tholeiites, and fractionated HREE (Crawford et al. 1989; Fig. 12). Representative Archean boninites (Kerrich et al. 1998) are characterized by Gd/Yb_{CN} 0.3−0.7, Zr/Y 1.2−1.7, positive Zr and Hf anomalies, Zr/Hf >36, LREE depletion to enrichment (La/Sm_{CN} 0.72−1.40), and negative Nb anomalies (Nb/La_{PM} 0.76−0.93; PM = primitive mantle-normalized; Fig. 12). Boninite petrogenesis is a two-stage process, beginning with extraction of a melt from the mantle and leaving a refractory residue that is fluxed by fluids enriched in Si, Na, LILE, ± LREE, and in some instances Zr and Hf. This two-stage process generates the variably enriched or depleted LREE pattern, and the negatively fractionated HREE of boninites and low-Ti tholeiites (Crawford et al. 1989). In the Phanerozoic, boninites have been reported from ophiolites, intraoceanic arcs, back arcs, forearcs, continental margin settings, and intra-continental rifts (Kerrich et al. 1998, and references therein). Boninites in the Abitibi greenstone belt are associated with komatiites and tholeiites. Boninites are noted also in the Yilgarn (Angerer et al. 2013), Pilbara (Smithies 2002), and Baltic (Shchipansky et al. 2004) cratons. Kerrich et al. (1998) favour a petrogenesis for the Abitibi boninites involving derivation from a depleted mantle source rather than the second-stage petrogenesis involving fluid fluxing of a depleted source. In more detail, the association with komatiites and a progression from primitive tholeiites to more evolved tholeiites is considered by Kerrich et al. (1998) to represent interaction of plume-derived komatiites and basalts with subduction zone-derived tholeiites.

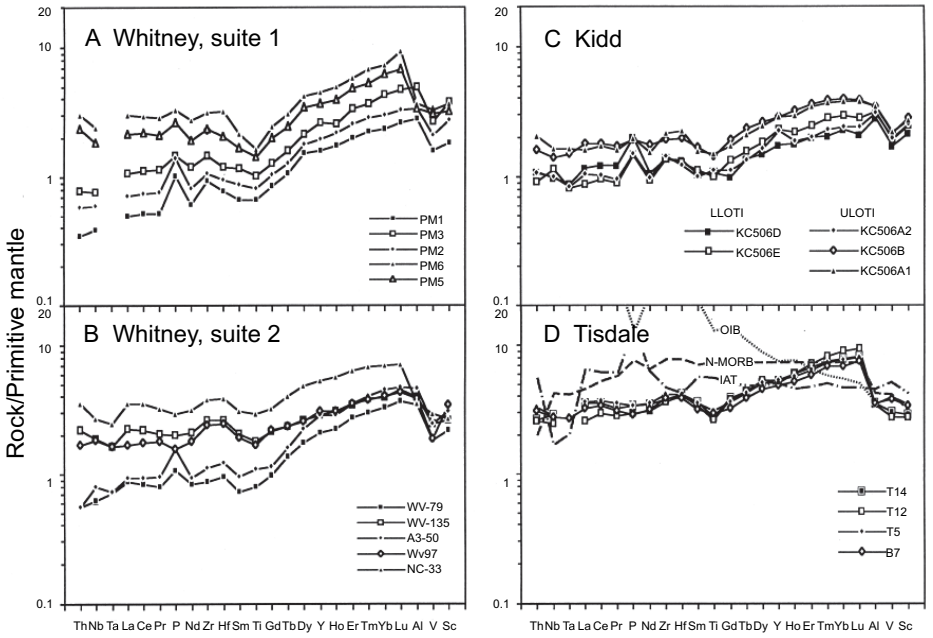

Figure 12. Boninites from the Abitibi greenstone belt of the Superior Province (Kerrich et al. 1998). Note the positive Zr and Hf anomalies and the fractionated HREE. Normalizing values, the normal mid-ocean ridge basalt (N-MORB) and the average ocean island basalt (OIB) are from Sun and MacDonough (1989) and the island arc basalt from Pearce and Peate (1995).

Archean boninites are more aluminous, slightly less depleted in the heavy REEs, and have higher TiO_2 contents than Phanerozoic analogues (Bédard et al. 2013). Given the variety of geodynamic settings of boninites, the only common thread is derivation from a depleted source, with or without fluid fluxing. However, it must be kept in mind that Archean boninites are exceedingly rare, and only a few tens of analyses exist, a function of rarity or perhaps a lack of recognition by investigators other than specialized petrologists. The above-cited studies provide some data on location, but stratigraphic position and primary structures are not described in all the cited studies. Excellent petrographic detail is presented by Wyman and Kerrich (2012) for boninites in the Youanmi terrane of the Yilgarn craton. The consistent features of their petrogenesis are high-temperature melting and derivation from depleted mantle. These komatiite−tholeiite sequences are distinct from more evolved basalt – andesite sequences such as the Blake River Group of the Abitibi greenstone belt, which are characterized by LREE enrichment and negative Ti, Nb and Eu anomalies (Ayer et al. 2005). Geochemically similar rocks have been considered to originate by crustal contamination of komatiitic material (e.g. Sylvester et al. 1997).

Ferropicrites

Ferropicrites are ultramafic rocks having MgO contents similar to komatiites (>18% MgO) but lower Al_2O_3 (<10% to <5%); they are defined as ferropicrites based on FeOt >14% (Hanski and Smolkin 1989). The Al_2O_3 content remains relatively constant with increasing MgO, and Al_2O_3/TiO_2 values are ~4; these characteristics are similar to moderately alkaline olivine basalts associated with hotspots. On the classification diagram for ultramafic rocks (Hanski et al. 2001), the Superior Province ferropicrites fall between the picrite and the Al-depleted picrite fields. They are enriched in TiO_2 (1−2%) and HFSE (e.g. Nb = 10−17 ppm, Nb/La_{CN} = 0.8−1.3) relative to komatiites, and display fractionated REE profiles (La/Yb_{CN} = 8−18; Goldstein and Francis 2008) and HREE depletion (Gd/Yb_{CN} ~3; Fig. 13A). Furthermore, they have higher ratios of some incompatible elements (e.g. Zr/Y ~6). Given these differences from komatiites, ferropicrites require a distinct petrogenesis (Goldstein and Francis 2008). In support of this, a Mg# *vs.* Ni diagram (Fig. 13B) illustrates that Ni values in ferropicrites rise asymptotically at Mg# 83, whereas for komatiites the rapid rise is at Mg# 90 (Goldstein and Francis 2008). Thus, sources for ferropicrite magmas have lower Mg# values than komatiite source mantle, indicating that they are distinct. Ferropicrites contain higher Ni but lower Cr than komatiites, indicating higher normative olivine in ferropicrites in contrast to the importance of normative pyroxene in komatiites.

Ferropicrites have liquidus temperatures similar to komatiites, but their source was olivine-rich mantle that, compared to komatiites, was enriched in incompatible trace elements (Goldstein and Francis 2008). Postulated petrogenetic mechanisms for this suite include liquid immiscibility, mixing of an Fe-rich immiscible liquid with a komatiitic liquid, melting of isolated enriched mantle domains, melting of a peridotite−basalt mixture, or melting of an Fe-rich mantle source that was depleted

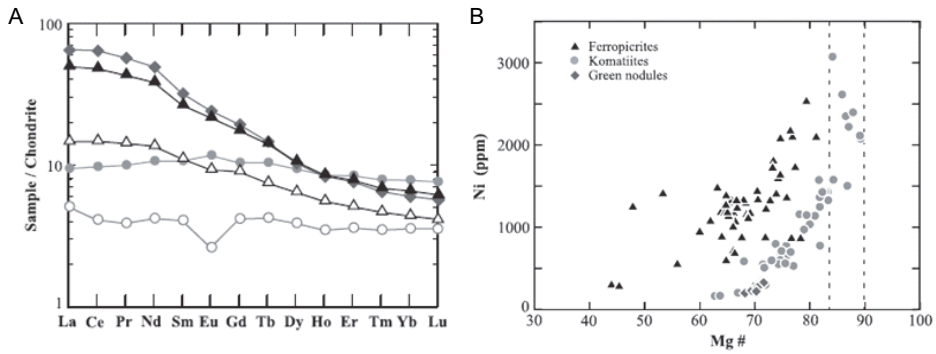

Figure 13. Ferropicrites in greenstone belts. A. REE profiles for an average pyroclastic ferropicrite , ferropicritic intrusive rocks, fine-grained spinifex and chilled margins of komatiitic flows, samples of cumulate zones of komatiitic flows, and green nodules normalized to CI chondrites. Solid triangles: pyroclastic ferropicrites, open triangles: intrusive ferropicrites, solid circle: fine-grained spinifex and chilled margins, open circles: cumulate zones of komatiites, and diamond symbol: green nodules. (after Goldstein and Francis 2008, their figure 5). B. Illustrating the varying Ni *vs.* Mg# systematics of komatiites and ferropicrites (after Goldstein and Francis 2008, their figure 12).

relative to CHUR (chondritic uniform reservoir) (Goldstein and Francis 2008). Such a melt would have the fractionated REE patterns seen in Archean ferropicrites. In the end, the favoured model is one in which an olivine-rich mantle source is melted at ~5 Gpa (Goldstein and Francis 2008).

Ferropicrites are spatially associated with komatiite–tholeiite sequences within greenstone belts of the Wawa–Abitibi terrane (Green and Schulz 1977; Stone et al. 1995; Goldstein and Francis 2008), the Kolar schist belt of India (Rajamani et al. 1985), and the Lake of the Enemy terrane in the Slave Province (Francis et al. 1999). More recently, they have been reported in the Marmion terrane at Steeprock Lake, at Lumby Lake, and Grassy Portage Bay in the western Wabigoon terrane (Goldstein and Francis 2008). The Marmion terrane occurrences were also described as Al-depleted komatiites (Hollings and Wyman 2000). Ferropicrites may occur either as typical subaqueous pillowed flows (Francis et al. 1999), pyroclastic rocks (Steeprock Lake, Lumby Lake and Grassy Portage Bay) or as intrusive plugs (Dayohessarah Lake; Goldstein and Francis 2008). The western Superior Province ferropicrites of Goldstein and Francis (2008) are somewhat higher in MgO (~19%) compared to those referred to above from Minnesota, Boston Township (in the Abitibi greenstone belt) and India. However, the western Superior Province ferropicrites have similar trace element patterns.

Bimodal Tholeiitic to Calc-Alkaline Basalt–Dacite/Rhyolite

The bimodal basalt–dacite association occurs in many of the greenstone belts of the Superior Province and most other Archean cratons. Basalts and basaltic andesites of the bimodal association generally display flat REE patterns and typically contain ca. 5% MgO, whereas FeOt increases ~ 5% up to a maximum of 18–20% (Thurston and Fryer 1983; Jensen 1985; Thurston et al. 1985). There is a continuous transition from tholeiites with flat REE patterns to calc-alkaline basalts with fractionated REE patterns (Leclerc et al. 2011; Bédard et al. 2013). A typical suite from the Schreiber–Hemlo and White River–Dayohessarah greenstone belts of the Wawa–Abitibi terrane is characterized by Mg- to Fe-tholeiites having La/Yb_{CN} = 2.7–24.5 (Polat et al. 1998). In the bimodal association, andesites in general are not prominent (Taylor and McLennan 1985; Condie 1986), where present, they vary from primary andesitic liquids to fractionated basalts (Thurston and Fryer 1983). In the Yilgarn craton, a fractionation sequence from basalt through andesite to rhyolite is reported for the Welcome Well and Marda complexes (Taylor and Hallberg 1977). In the Abitibi greenstone belt, primary andesites range from low- to high-K andesites (Ayer et al. 2005) using the classification of Gill (1981). The felsic end-members of this association range from dacite to rhyolite. In terms of trace element geochemistry, these units display flat, 'tholeiitic' patterns through to extremely fractionated patterns (Thurston 1981; Lesher et al. 1986; Hart et al. 2004). This bimodal association is more fractionated than the komatiite–tholeiite association and has the negative Ti and Nb anomalies considered by some to represent arc petrogenesis (Hart et al. 2004). Similar features are seen in the Blake River Group of the Abitibi greenstone belt and throughout the Superior craton (Thurston et al. 1985; Scott et al. 2002).

Associated with the bimodal suite are a number of relatively unusual rock types for Archean greenstone belts: the so-called adakite suite, consisting of magnesian andesites, Nb-enriched basalts and andesites, and adakites. Their geochemistry is discussed below. In modern arc systems, adakites, Nb-enriched basalts and magnesian andesites are spatially and temporally associated (Kepezhinskas et al. 1995). For example, in Panama and Costa Rica, normal arc volcanic rocks are succeeded by an adakite–Nb enriched basalt association (Defant et al. 1992). The adakite suite is interrelated in the sense that their geochemical variation is a function of garnet fractionation (Richards and Kerrich 2007).

Adakites

Adakites, formerly termed tonalite–trondhjemite–granodiorite (TTG) series volcanic rocks (including low-K dacites) (Richards and Kerrich 2007), were defined by Defant and Drummond (1990, 1993) as a term for magnesian andesites and more felsic derivatives in the Aleutian arc, where they were interpreted to have formed by the melting of subducted oceanic crust. They are characterized by high La/Yb, high Sr (~1800 ppm), 'relatively high' Mg#, Cr, and Ni (Richards and Kerrich 2007) compared to normal andesites, and non-radiogenic Pb and Sr isotopic compositions. Further details of the geochemistry of adakite-like rocks are listed in Table 2. Archean volcanic rocks of this association are enriched in elements mobilized by aqueous fluids (e.g. W, Pb, Be, Li), whereas HFSE such as Ti, Nb and Ta are depleted. The central question is whether this geochemical signature is unique to the subduction environment or whether other geodynamic settings can produce the same features. Defant and Drummond (1990) used Sr/Y *vs.* Y and La/Yb *vs.* Yb binary plots to demonstrate the role of garnet fractionation in adakites *vs.* plagioclase fractionation typical of normal modern arc suites. The general term 'adakite' or adakitic has been used to describe Mg-rich

Table 2. Adakite suite details.

Rock type	Defining Characteristics	Examples	Petrogenesis
Adakite	SiO_2> 56%, Al_2O_3>15%, MgO <3%, Mg#~5 Y<18 ppm, Yb<1.9 ppm, Ni>18 ppm, Cr>30 ppm High La/Yb High Sr/Y High Mg#, Cr, Ni compared to normal andesites[1]	Superior Province: Schreiber-Hemlo, White River-Dayohessarah, Winston L. – Big Duck L., Manitouwadge[2], NE Quebec[3]. Baltic Shield[4], Dharwar craton[5], N. China craton[6]	Evolution by garnet fractionation. Generated by slab melting OR by MASH or AFC.[1]
Nb-enriched basalts	Nb >20 ppm, Nb/La_{MN}, 0.5-1.4;[7]	Superior Province: Wabigoon; North Caribou[8-9]; Pilbara[10]; Dharwar[11], Baltic shield[4]	Lithospheric or asthenospheric OIB in source; small degree of melting of a MORB source in slab window; adakitic metasomatism above mantle wedge
Andesites and Magnesian andesites	High MgO relative to SiO_2 Sr/Y > 20[1]	Northern part of Wawa-Abitibi terrane[12]	Evolution by garnet fractionation. Generated by slab melting OR by MASH or AFC[1]

[1]Richards and Kerrich (2007); [2]Polat and Kerrich (2001); [3]Boily and Dion (2002); [4]Svetov et al. (2004); [5]Manikyamba et al. (2009); [6]Wang et al. (2004); [7]Wyman et al. (2000); [8]Hollings and Kerrich (2000); [9]Hollings (2002); [10]Smithies et al. (2005); [11]Kerrich and Manikyamba (2012); [12]Ayer et al. (2010).

andesites, Nb-enriched basalts and andesites, and adakites (Polat and Kerrich 2001; Svetov 2001; Slabunov et al. 2006). Several other rock types in the basalt–rhyolite fractionation series share the high La/Yb, and high MgO, Cr and Ni of adakites, such as high-Mg andesites and Nb-enriched basalts in modern arcs (Sajona et al. 1996). However, Richards and Kerrich (2007) show that Melting–Assimilation–Storage–Homogenization (MASH) (Hildreth and Moorbath 1988) or Assimilation–Fractional Crystallization (AFC; Depaolo 1981) processes that control tholeiitic and calc-alkaline magmas can also produce adakitic compositions. Therefore, although some authors appeal to subduction processes for the origin of the adakite suite, the MASH and AFC processes simply require a subjacent magma chamber; in this way, the high La/Yb and Sr are hallmarks of petrogenesis involving mafic sources within the garnet stability field (Richards and Kerrich 2007). Alternatively, Johnson et al. (2014) modelled trace element distribution in a hotter Archean Earth and found that convergent plate margins are not necessary.

Adakite-like rocks occur in three magmatic associations in greenstone belts: 1) volcanic rocks and related minor intrusive bodies forming part of the bimodal association (Kerrich and Fryer 1979; Hollings and Kerrich 2000; Wyman et al. 2000; Polat and Kerrich 2001; Naqvi et al. 2006); 2) syn- to late-tectonic batholiths of the high-Al-TTG association, such as the Lake Abitibi and Round Lake batholiths of the Abitibi greenstone belt (Feng and Kerrich 1992); and 3) post-tectonic high-Mg diorites/sanukitoids (Smithies and Champion 2000).

Adakites and related magnesian andesites and Nb-enriched basalt–andesite are not common rock types within the bimodal association in Superior Province greenstone belts (Boily and Dion 2002; Percival et al. 2003; Ujike et al. 2007). Given the lack of stratigraphic detail in the papers describing these rocks in the Superior Province, it is not currently possible to understand how the adakitic rocks relate to greenstone chemostratigraphy. However, adakitic rocks occur as lava flows in the Superior Province, and as volcaniclastic rocks in the Baltic shield (upper part of the Hautavaara greenstone belt; Svetov et al. 2004).

Magnesian Andesites

Magnesian andesites in Archean greenstone belts have high MgO contents (e.g. 4.8%) relative to SiO_2 (Polat and Kerrich 2001), and high Cr and Ni. Thus, by definition, they plot above the divide between arc andesites and magnesian andesites on a MgO *vs.* SiO_2 diagram (McCarron and Smellie 1998). Compared to normal andesites in the Abitibi–Wawa terrane, magnesian andesites contain lower TiO_2 at a given MgO content, and tend to have higher Th and Ce, lower Nb, and nearly flat patterns for Zr, Y and Yb with respect to MgO. Magnesian andesites form a minor constituent of the ca. 2720 Ma greenstones on the northern fringe of the Wawa–Abitibi terrane west of the Kapuskasing structural zone (Ayer et al. 2010).

Magnesian andesites are interpreted to form through hybridization of adakitic liquids with peridotitic mantle wedge material, which explains their high Mg, Cr, Ni, Th and Ce, fractionated REE, low Yb content and negative Nb and Ti anomalies (Keleman 1995; Yogodzinski et al. 1995). Details on volcanology or stratigraphic association are not available. Examples of their trace element geochemistry in the Wawa–Abitibi terrane are shown in Figure 14.

Nb-Enriched Basalts

Nb-enriched basalts are LREE-enriched basalts containing >20 ppm Nb and Nb/La_{CN} >1. In modern orogens, Nb-enriched basalt occurs in arcs, rifted arcs, and back arc settings.

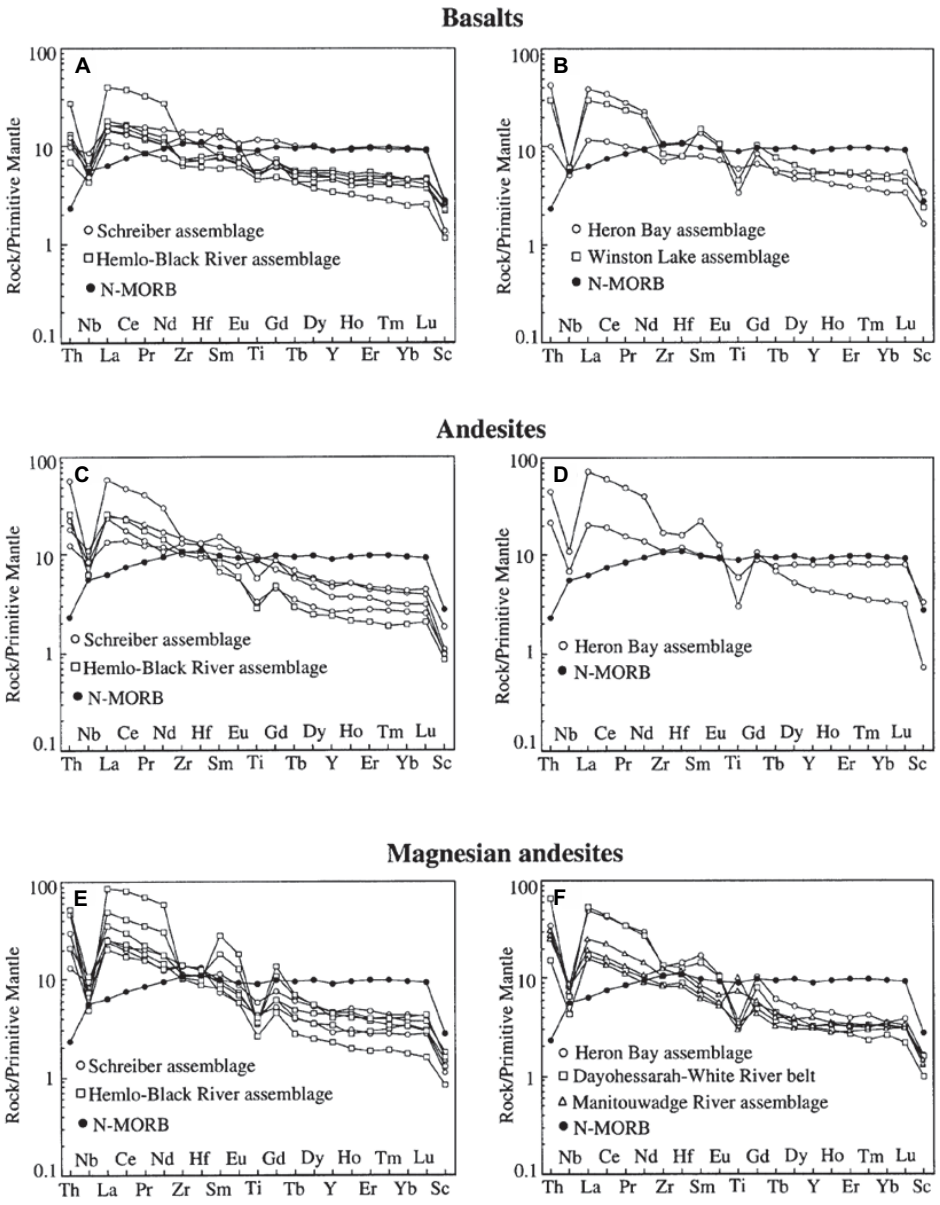

Figure 14. Extended trace element plots of basalts, andesites and magnesian andesites from greenstone belts of the Wawa–Abitibi terrane west of the Kapuskasing structural zone (Polat and Kerrich 2001). Normalizing factors from Hofmann (1988).

The trace element characteristics are similar to those of ocean island basalts (OIB) and have been attributed either to an asthenospheric or lithospheric component in their sources, or to small degrees of melting of a mid-ocean-ridge basalt (MORB) source in a slab window (D'Orazio et al. 2000). Nb-enriched basalts have also been attributed to adakitic metasomatism above a mantle wedge (Sajona et al. 1996). Nb-enriched basalts occur in the western Wabigoon subprovince of the Superior craton (Wyman et al. 2000), the south margin and elsewhere in the North Caribou terrane (Hollings and Kerrich 2000, 2002; Fig. 15), and the Pilbara (Smithies et al. 2005), Dharwar (Kerrich and Manikyamba 2012) and Karelian (Svetov et al. 2004) cratons. No stratigraphic or volcanological context is provided in the above studies except for the work of Svetov et al. (2004).

Felsic Volcanic Units

Felsic rocks of the bimodal association in Archean greenstone belts range from dacite to rhyolite and so-called high-silica rhyolite. Thurston (1981) noted that these rocks vary enormously in their trace element character. Subsequent work by Lesher et al. (1986) resulted in a classification based on their trace element chemistry, later modified by Hart et al. (2004). The felsic volcanic rocks are classified by Zr/Y, as shown in Table 3. The common feature of the petrogenetic schemes in Table 3 is that they involve fractional crystallization or melting of a tholeiitic basaltic precursor. Felsic volcanic units also occur in the komatiite–tholeiite association, the rhyolites associated with the Kidd Creek VMS deposit being the most prominent example (Bleeker 1999).

Successor Basins

After early deformation of greenstone belts, successor basins developed unconformably above the volcanic rocks. The basal unconformities are generally paleosols (Ayer et al. 1999), indicating that the greenstone belts were at least briefly subaerial. The basins occur in proximity to major transcurrent faults in the greenstone belts and, although relatively late, the basins preserve the same metamorphic grade as the surrounding greenstones. The successor basins are only a few km in width but extend several tens of km along strike. They are the remnants of originally much more extensive basins, as outliers are found tens of km away from the main preserved basins (Thomson 1946).

Successor Basin Sedimentary Units

Two periods of deposition of Archean successor basin metasedimentary rocks are recorded in the Abitibi greenstone belt: early sand-grade clastic units in the western Wawa–Abitibi terrane (the so-called Porcupine metasediments), followed by later conglomerates displaying gravel lags and intercalated cross-bedded sands (the so-called Timiskaming metasediments). Together, these rocks are diagnostic of alluvial–fluvial environments (Dimroth et al. 1982; Thurston and Chivers 1990; Mueller and Corcoran 1998) that grade laterally to deep marine sands (Dimroth et al. 1982). These units unconformably overlie the older volcanic rocks and occur along major transcurrent shear zones within greenstone belts, suggesting that the basins are, at least in part, fault-controlled. The early sand-grade units (Porcupine type) are more laterally extensive than the later, coarser Timiskaming type units. The presence of foliated and massive granitoid clasts in the conglomerates (e.g. Mueller and Corcoran 1998) indicates that early deformation preceding the development of the successor basins included emplacement and unroofing of

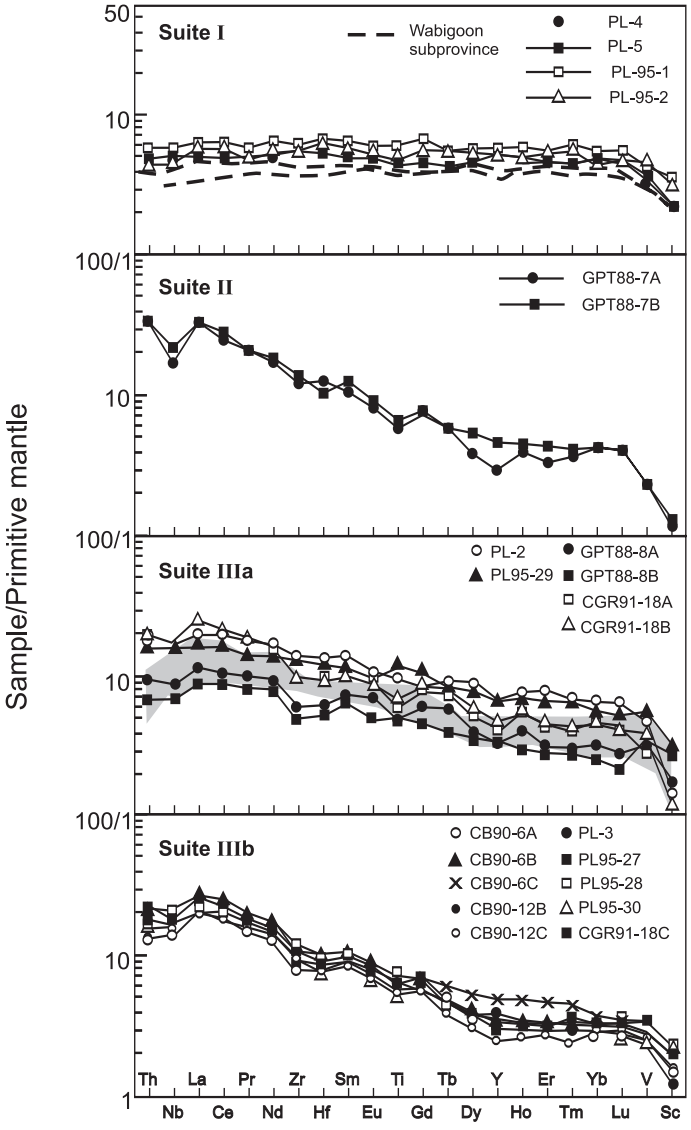

Figure 15. Primitive mantle normalized extended trace element plots for Nb-enriched basalts of the Northern Pickle Assemblage rocks (after Hollings 2002). Wabigoon subprovince data are unpublished data from D. Wyman. The grey field is Niobium-enriched basalts from the Sturgeon Lake greenstone belt in the western Wabigoon terrane (Wyman et al. 2000). Normalizing values from Sun and McDonough (1989). Suite I is unfractionated tholeiites, Suite II is fractionated tholeiites, Suite IIIa is high Fe tholeiites which are more fractionated than Suite IIIb.

granitoid batholiths. Iron-formation clasts in the type Timiskaming of the Kirkland Lake area in the Abitibi greenstone belt suggest a widespread pelagic sedimentation event that terminated Keewatin deposition in that region and elsewhere. Similar units are found in the Slave (Bleeker and Hall 2007), Zimbabwe (Martin et al. 1993), Pilbara (Van Kranendonk et al. 2002), Yilgarn (Krapez and Barley 1987); and Baltic (Slabunov et al. 2006) cratons. Development of the basins is discussed in a subsequent section.

Successor Basin Volcanic Units

Magma emplaced during successor basin development generally range from calc-alkaline to alkaline in composition; one instance of komatiitic volcanism is associated with the Porcupine unit in the Abitibi greenstone belt (Wray 2014). The alkaline volcanic rocks are generally shoshonitic (K_2O/Na_2O >1), hornblende-phyric andesite and more siliceous derivatives (Shegelski 1980; Brown 1995). An example of the calc-alkaline type is the Shebandowan assemblage in the Wawa–Abitibi terrane just west of Thunder Bay (No. 1 in Fig. 1). Rocks of this assemblage are characterized by LREE abundances about 100 times that of chondrites (Brown 1995), and are spatially associated with more fractionated types (Carter 1993). In the Wawa–Abitibi terrane, the proximal successor basin volcanic rocks of the type Timiskaming have shoshonitic geochemistry, and alkalic dikes and plutons are proximal to major strike-slip structures (Wyman and Kerrich 1989; Othman et al. 1990; Dostal and Mueller 1992). In the northern reaches of the Superior Province, shoshonitic volcanic rocks occur in the North Caribou terrane at Oxford Lake (Brooks et al. 1982) and at North Spirit Lake (Smith and Longstaffe 1974). In the Wabigoon subprovince, alkalic volcanic rocks occur in the Lake of the Woods area (Dostal et al. 2004). Late stage alkalic magmatism also occurs in the western Dharwar (Manikyamba et al. 2012), the Yilgarn (Taylor et al. 1990), and Pilbara (Krapez and Barley 1987) cratons, the Shamvaian sequence in the Zimbabwe craton (Blenkinsop et al. 1997) and in the Baltic shield (Slabunov et al. 2006). In general, the successor basins occur at the margins of terranes or proximal to major structures such as the Porcupine–Destor shear zone in the Abitibi greenstone belt. The extremely fractionated REE patterns of the shoshonitic units suggests that they represent direct mantle melts involving low percentages of partial melting (Othman et al. 1990).

Sedimentary Subprovince Volcanic Units

The volcanic rocks of greenstone belts are overlain by wacke–pelite turbidites of adjacent metasedimentary subprovinces. For example, North Caribou terrane greenstones are overlain by wacke–pelite units of the English River subprovince (Breaks 1991; Stott and Corfu 1991). Volcanic rocks form a minor component of the sedimentary subprovinces; the Piché Group within the Pontiac metasedimentary subprovince (Simard et al. 2013) immediately south of the Abitibi greenstone belt is the best known example. These volcanic units are thin, but have a lateral extent of tens to hundreds of kilometres. They vary from komatiite through tholeiitic basalt and calc-alkaline basalt to rhyolite (Stone 1990; Simard et al. 2013). Similar minor metavolcanic rocks form unnamed metavolcanic units in the English River subprovince (Breaks 1991) and the Quetico subprovince (Williams 1991); however, there are limited geochemical data.

SEDIMENTARY UNITS IN GREENSTONE BELTS

Introduction

Archean greenstone belts typically have <10% sedimentary rocks in the pre-deformation mafic-to-felsic volcanic cycles. Four types of sedimentary sequences are recognized, as summarized by Bédard et al. (2013): 1) subaerial to shallow-water clastic sequences rich in continental detritus; 2) continental rupture sequences containing shallow-water quartz-rich sedimentary and carbonate rocks, succeeded by BIF and deeper-water komatiite–tholeiite units; 3) deep-water chemical sedimentary units (the 'sedimentary interface zones' of Thurston et al. 2008); and 4) clastic and chemical sequences fringing or

Table 3. Geochemistry of Archean felsic metavolcanic rocks (after Hart et al. 2004).

	FI1	FII	FIIIa	FIIIb	F IV
Lithology	Dacite-rhyolite	Dacite-rhyolite	Rhyodacite-high Si rhyolite	Rhyodacite-high Si rhyolite	Rhyolite-high Si Rhyolite
SiO_2	64–72	64–81	67–78	67–84	69–81
TiO_2	0.16–0.65	0.16–0.89	0.21–0.99	0.09–0.73	0.09–0.57
Zr/Y	8.8–31	3.2–12.12	3.9–7.7	1.7–6.2	18–63
Yb	0.43–3.8	1.3–7	3.4–9.3	5–32	1.5–8.4
La/Yb	5.8–34	1.7–8.8	1.5–3.5	1.1–4.9	0.22–2.1
Eu/Eu*	0.87–1.5	0.35–0.91	0.37–0.94	0.20–0.61	
Petrogenesis	Low degree partial melting of mafic precursor at high pressure (Lesher et al. 1986).	Fractionation of intermediate magma (Campbell et al. 1981, 1982); high degree partial melting of feslic granulite at intermediate depths (Lesher et al. 1986); partial melting of hydrated, subducted oceanic slab (Barrie et al. 1993); partial melting of metsomatized mantle wedge above subducted slab, with fractional crystallization of resultant mafic magma (Barrett and MacLean 1999); high temperature partial melting of crustal material.	Low pressure partial melting of tholeiite without residual amphibole (Hart 1984) or garnet (Campbell et al. 1981; Lesher et al. 1986; Barrie et al. 1993) in a subvolcanic chamber, plagioclase-dominated fractionation of intermediate magma (Lesher et al. 1986); partial melting of crustal material yielding various felsic magmas (Lentz 1998); partial melting of continental crust with minor AFC yielding alkaline to subalkaline rhyolites (Barrett and MacLean 1999).		Low pressure moderate partial melting of depleted tholeiitic basalt (Hart et al. 2004).
Source depth	Deep >30 km	Intermediate 10–15 km	Shallow <10 km	Shallow <10 km	

capping older cratonic blocks. The syn-orogenic flysch deposits and Timiskaming metasedimentary units are described elsewhere in this contribution.

Continentally-Derived Clastic Rocks

Some of the greenstones deposited on or above the margins of older cratonic blocks (Kamber et al. 2004; Fralick et al. 2008) represent fluvial−deltaic environments dominated by coarse clastic rocks of TTG provenance. Subsequent basin subsidence and transgression led to basin starvation and deposition of carbonates, chert and BIF. This style of deposition is present in the 3.0−2.8 Ga Marmion Terrane of northwestern Ontario (Buse et al. 2010) and in the Zimbabwe craton, where shallow-water, quartz-rich metasedimentary rocks are succeeded by argillite and sulphide-facies iron-formation (Prendergast 2004).

Continental Rupture Sequences

These sequences of quartz-rich metasedimentary rocks are deposited unconformably above older greenstone and granitoid rocks in most cratons, including the Superior (Donaldson and de Kemp 1998), Slave (Mueller and Pickett 2005; Bleeker and Hall 2007), Zimbabwe (Prendergast 2004), and Yilgarn (Myers and Swager 1997) cratons. In some cases, these sequences mark the base of greenstone belts, whereas elsewhere (e.g. Ponask Lake in the North Caribou terrane; Thurston et al. 1991) they mark the edges of cratonic blocks. The quartz-rich metasedimentary units are underlain by paleosols (Breaks 1991) and contain shallow-water structures such as hummocky cross-stratification and mud drapes, followed in turn by stromatolitic carbonates and siliciclastic rocks (Arias et al. 1986), a deepening basin sequence of shale and BIF, and upon basin rifting, emplacement

of komatiite–tholeiite sequences. Although similar to sequences within Atlantic-style passive margins, the lateral distance from the tidal environment to submarine fan structures is commonly only 5–8 km (Goutier et al. 1999), much less than an Atlantic-style margin.

Sedimentary Interface Zones

'Sedimentary Interface Zones' (Thurston et al. 2008) are zones of chemical and lesser clastic sedimentary rocks capping mafic to felsic volcanic cycles in greenstone belts worldwide. These zones are accumulations of chemical metasedimentary rocks and minor clastic material from a few cm to ~500 m thick. Their stratigraphic association with volcanic rocks, petrography, geochemistry and isotopic composition indicates that these units are dominated by Algoma-type BIF (Thurston et al. 2008; Baldwin 2009) deposited below storm wave base by one or more of the following processes: 1) direct precipitation from seawater; 2) deposition from hydrothermal fluids; or 3) replacement of precursor rock types.

U–Pb zircon geochronology of rhyolites at the top of the ca. 2734 Ma Deloro assemblage in the Abitibi greenstone belt and in the immediately overlying 2710 Ma sequence show a locally developed ca. 25 m.y. age gap. The fundamental question stemming from these apparent age gaps between dated rhyolites in neighbouring assemblages is whether they represent slow, continued volcanic evolution, or lengthy deposition of the chemical sedimentary rocks separating mafic to felsic cycles. Thurston et al. (2008) modelled accumulation of the 750,000 km^3 of volcanic rocks in the Deloro assemblage south of Timmins (Abitibi greenstone belt) over periods ranging from 7.5 k.y. to 5 m.y., using rates of magma accumulation for chemically-zoned ash flow magma chambers, plume systems, and modern arc systems, all representing minimal accumulation rates given a hotter Archean Earth. These rapid rates of volcanism compared to the time gaps between assemblages in the western part of the Abitibi greenstone belt suggest that chemical sedimentary units marking magma clan transitions represent periods of slow deposition. These estimates of depositional rates were corroborated by U–Pb dating of bounding rhyolite units (Baldwin 2009), which indicate that the rate of deposition was fairly slow, i.e. 0.060–0.008 mm/y (Baldwin 2009) for a 40 m-thick BIF, perhaps comparable to sedimentation rates in the mid-Pacific Ocean (Gleason et al. 2004). Thus, apparently minor chemical and associated clastic sedimentary units, including minor cm-scale graphitic argillites marking magma clan transitions, are important in assessing the rate of accumulation and volcanic evolution in greenstone belts. However, it should be noted that the 'key tuffite,' a chert and/or fine-grained felsic ash marker horizon 2734–2724 Ma at Matagami, is bounded above and below by rhyolite having ages that overlap within error (Ross et al. 2014).

Continental Margin Sedimentation

The margins of Archean microcontinental fragments in the Superior and Yilgarn cratons are the sites of off-lapping, mixed clastic and chemical metasedimentary units. The Superior Province example is composed of a 2.85–2.75 Ga, southwest-younging sequence of wackes, siltstones and iron-formation along the south margin of the 3.4–2.8 Ga Winnipeg River subprovince, where it is juxtaposed against 2.75–2.72 Ga juvenile volcanic rocks of the western Wabigoon subprovince (Sanborn-Barrie and Skulski 2006). Some microcontinental terranes in the Superior Province (Fralick and Pufahl 2006) and the Yilgarn craton (Angerer et al. 2010) have unconformably overlying shallow-water iron-formation.

Archean Sedimentary Patterns

Basement–cover relationships of older *vs.* younger greenstones (Blenkinsop et al. 1993; Buick et al. 1995; Bleeker 2003), abundant compositionally mature sedimentary units (Krapez and Barley 1987; Hessler and Lowe 2006), isotopic and trace element evidence (Kamber 2010), and generally coarse-grained epiclastic units associated with greenstone mafic to felsic cycles (Mueller and Corcoran 1998; Corcoran and Mueller 2007), all point to the presence of exposed continents and subaerial weathering. This evidence is also supported by isotopic considerations (Dhuime et al. 2012). The sand-rich nature of Archean sedimentary rocks points to a depositional system in which the sediment source is proximal and characterized by high relief and a narrow shelf, whereas mud-rich systems (seen mainly in sedimentary subprovinces of the Superior Province), reflect a sediment source distant from the shoreline in a low relief environment (Bouma 2000).

The quartz-rich nature of Meso- and Neoarchean metasedimentary rocks is a function of a largely granitoid source and intense chemical weathering under reducing conditions. The paucity of clays and feldspars, and enrichment of Archean mudstones in Al relative to younger mudstones (Eriksson and Soegaard 1985; Hessler and Lowe 2006) reflect this style of weathering. The erosion of Archean volcanic rocks brought about similar Al enrichment in Archean metasedimentary rocks relative to younger equivalents, whereas sedimentary units display a steady decrease in Mg content over time (Migdisov et al. 2003). Enrichment in Al is a function of a largely granodioritic source and extensive weathering, and the decrease in Mg is a function of the overall decrease in komatiite eruptions over time (Arndt et al. 2008; Van Kranendonk 2012).

Archean sedimentary carbonate units are scarce (Ojakangas 1985), and where present, commonly occur at the top of mafic to felsic volcanic cycles in sedimentary interface zones (Thurston et al. 2008). These carbonate rocks are shallow-water rocks featuring multiple forms of stromatolites (Hofmann et al. 1985; Arias et al. 1986; Wilks and Nisbet 1988; Hofmann et al. 1991; Hofmann and Masson 1994).

There is little evidence constraining the depth of water in greenstone belt metasedimentary units, except, for example, quartzose sedimentary rocks of the continental rupture sequences that display hummocky cross-stratification and mud drapes typical of the tidal environment (Donaldson and de Kemp 1998). Estimates of mean ocean depth in the Archean are ~2.6 km (Bickle et al. 1994). With this mean depth in mind, one might conclude that greenstone belts represent deep-water deposits; however, the near total absence of mudstones, which typically form 70% of Phanerozoic abyssal sedimentary sequences (Aplin and Macquaker 2011) suggests that greenstone belts either do not represent a deep-water environment, or that Archean oceans were remarkably free of fine-grained detritus.

CONTROLS ON VOLCANIC CYCLICITY

Introduction

Many of the geochemical studies referred to in the preceding sections provide limited stratigraphic detail beyond the level of major geochemical groupings and the relationship of the geochemistry to broad stratigraphic groups. However, in the minority of studies that utilized detailed stratigraphy as a control on geochemical variation, insight into magma chamber dynamics can be obtained.

Fe-Enrichment Cycles: Evidence for Fractionation

Tholeiitic basaltic sequences within the komatiite–tholeiite association (e.g. the western Abitibi greenstone belt; Jensen 1985) and the bimodal basalt–dacite association (e.g. the Confederation assemblage on the south margin of the North Caribou terrane; Thurston and Fryer 1983) show Fe-enrichment cycles ranging from 6–8% to 18–20% FeO*. Similar Fe-enrichment cycles are observed in the Fe-rich tholeiites of northern Québec (Maurice et al. 2009) and in many tholeiitic sequences throughout the Superior Province (Ludden et al. 1986), the Pilbara craton (Van Kranendonk et al. 2002), the Yilgarn craton (Barley 1997) and the Slave Province (Bleeker and Hall 2007). The high-Fe tholeiites are occasionally capped by variolitic flows (Gélinas et al. 1976; Thurston and Fryer 1983), with or without minor sedimentary rocks. Fe-enrichment cycles in tholeiitic basalts are interpreted to represent an initial mantle-derived tholeiitic liquid evolving by fractionation of olivine and plagioclase in a low pressure magma chamber, in rare cases to the point of developing liquid immiscibility (Gélinas et al. 1976; Thurston and Fryer 1983).

Fractionation *vs.* Mantle Input

In the Chibougamau area of the Abitibi greenstone belt, Leclerc et al. (2011) divided the ca. 2730 Ma Roy Group into multiple units (Fig. 16) of largely tholeiitic and minor calc-alkaline units. Insight comes from examination of the stratigraphically controlled geochemistry of the David Member of the Obatogamau Formation. The authors report that the basalts and basaltic andesites of this member show no chemical variability with stratigraphic position in spite of their relatively evolved compositions (about 5% MgO). This lack of variation is explained in terms of fractionation being balanced by input of fresh mantle-derived magma. An upward decrease in Zr/Y, P_2O_5 and TiO_2 at near constant MgO are explained as sampling of increasingly depleted starting material by successive magma batches. The authors further speculate as to whether this represents exhaustion of fertile components in the mantle, changes in the mantle source, or a progressive increase in the degree of partial melting.

Overlying the David Member, felsic units of the Allard and the Queylus members are calc-alkaline. Their fractionated REE patterns reflect a garnet-bearing residue, suggesting that a metabasite source was melting at high pressure. Transitional to calc-alkaline mafic rocks are interpreted as mixtures of minor volumes of these melts with variable proportions of background tholeiites, which are interfingered with the felsic units. However, in the upper part of the Allard Member, tholeiites are absent, implying that the crust acted as a density filter (Hildreth 1981; Thurston and Sutcliffe 1986), preventing eruption of the tholeiites.

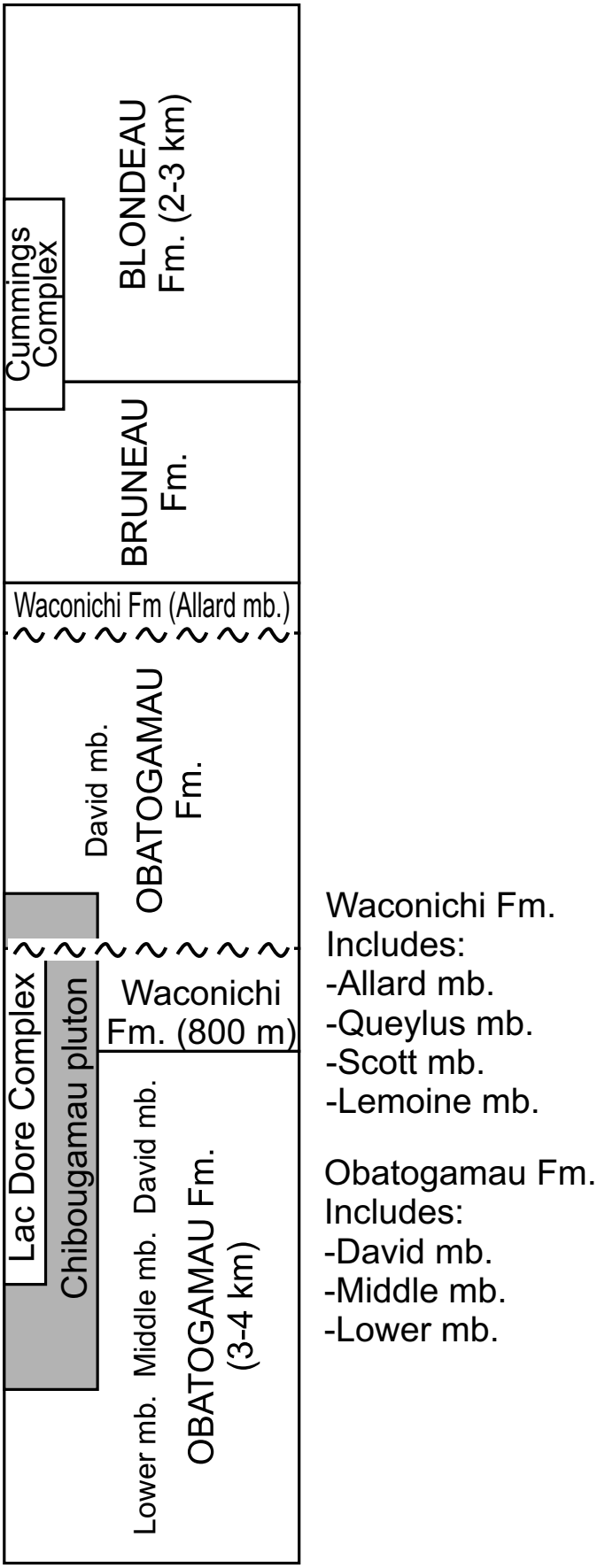

Figure 16. Stratigraphic nomenclature for the Chibougamau greenstone belt (after Leclerc et al. 2011).

Origin of Felsic Volcanic Rocks by Contamination – or Two Separate Sources?

Felsic metavolcanic rocks are a minor constituent of greenstone belts and their petrogenesis is largely independent of basalt petrogenesis. A full fractionation sequence from basalt to andesite and rhyolite is reported in the Marda complex of the Yilgarn craton (Taylor and Hallberg 1977); however, Thurston and Fryer (1983) demonstrated that fractionation of a basaltic sequence in the North Caribou terrane could not produce the volume of rhyolite capping the 2.74 Ga Confederation assemblage east of Red Lake (No. 2 on Fig. 1). In fact, many basaltic sequences are capped by sedimentary interface zones (Thurston et al. 2008), indicating the cessation of volcanism. In the Abitibi greenstone belt (Leclerc et al. 2011), the calc-alkaline Allard Member is a 500 m-thick package of andesite to dacite/rhyodacite within a thick sequence of tholeiites. Several authors (Barrie et al. 1993; Hart et al. 2004; Leclerc et al. 2011) envision that basalts represent one end member and rhyodacites produced by anatexis (crustal melting) form the other end member. Modelling indicates that intermediate units represent mixing of varying proportions of basalt and anatectic rhyodacite in the magma conduit (Leclerc et al. 2011; J. Bédard personal communication; Fig. 17).

Archean Andesites

Phanerozoic andesites are plagioclase- and pyroxene-phyric intermediate volcanic rocks found in continental and island arcs, and more rarely in oceanic islands, oceanic plateaus, Large Igneous Provinces and back-arc settings (Hooper et al. 2002; Scarrow et al. 2009; Willbold et al. 2009). The origin of these andesites is mainly by mixing of mafic and felsic magmas regardless of geodynamic setting (Reubi and Blundy 2009). However, icelandites (low-Al, high-Fe andesites, a relatively rare rock type; Carmichael 1964) form by fractionation (Sensarma and Palme 2013). Andesites in Phanerozoic continental arcs are mainly produced by mixing of mantle-derived basalt with melted continental crust (Gill 1981; Tatsumi 2005). As andesites can constitute up to 35−40% of continental arcs and represent about 30% of rock types in island arcs, based on a compilation by Winter (2001; p. 326) of 397 Andean and 1484 southwest Pacific analyses from Ewart (1982), they can be considered a hallmark of plate tectonics. Modern andesites possess negative Ti, Nb and Ta anomalies, which have been related to the presence of residual Nb- and Ta-bearing minerals such as rutile, ilmenite, titanite, and perhaps hornblende (Morris and Hart 1983; Saunders et al. 1991). Others argue for enrichment of the adjacent elements on extended trace element diagrams, and suggest that the HFSE are similar in abundance to MORB and reflect source characteristics (McCulloch and Gamble 1991). However, Jahn (1994) calculated that contamination of primitive mantle by ~2% upper crustal material would produce negative Nb and Ta anomalies. Bédard (2006), using partition coefficient data, states that 2% rutile in the source would have a similar effect.

Archean andesites are rare (Condie 1981; Ayres and Thurston 1985) and generally lack the plagioclase and pyroxene phenocrysts typical of Phanerozoic andesites. Proposed origins for Archean andesites include extensive fractionation of large basaltic magma chambers accompanied by some admixing of felsic melts (Smithies et al. 2007), as well as simpler mixing scenarios (Bédard et al. 2013). In the Yilgarn craton, Barnes and Van Kranendonk (2014) provided convincing field evidence and modelling to conclude that Archean andesites in the Yilgarn are a product of plume-related tholeiites mixed with rocks having TTG compositions. Thurston and Fryer (1983) postulated two possible additional origins for Archean andesites: 1) primary andesitic melts; and 2) fractionation of basaltic precursors.

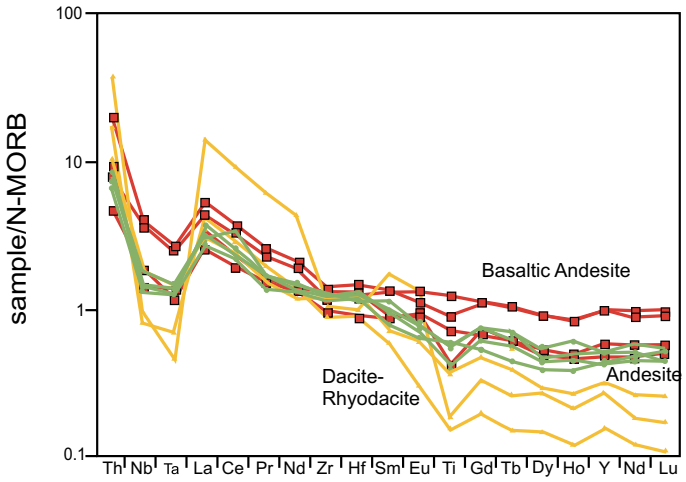

Figure 17. MORB-normalized analyses of basaltic andesite to rhyodacite in the Chibougamau greenstone belt of the Abitibi–Wawa terrane (after Bédard et al. 2013). MORB normalizing factors after Sun and McDonough (1989).

STRUCTURAL GEOLOGY OF GRANITE–GREENSTONE TERRANES

Introduction

The structural style of greenstones plays a pivotal role in constraining geodynamic models for greenstone belt development (Anhaeusser 2014). The two major points of view are that tectonic processes were dominated by either gravitational tectonics or compressional forces. The so-called 'granite−greenstone pattern' (Macgregor 1951) consists of upward-younging and upward-facing volcanic stratigraphy, surrounded by granitoid rocks.

Structural Style

The predominant structural style of Archean granite−greenstone terranes is a series of alternating high-amplitude (minimum 15 km), long-wavelength (ca. 20 km) domes of TTG and keels of volcanic rocks – a style unique in Earth history (Fig. 2). This structural style is broadly similar world-wide, whether an older granitoid basement is identified, such as in the Pilbara craton (Van Kranendonk et al. 2002, 2004) or if identification of basement is elusive, such as in most Superior Province greenstone belts (Williams et al. 1992; Thurston et al. 2008). The best understood example, by virtue of extensive mapping and geochronology of both granitoid rocks and supracrustal rocks, is the eastern Pilbara terrane (Fig. 18), where tightly folded synclines of volcanic rocks alternate with broad domes of TTG batholiths (Van Kranendonk et al. 2004). Wrapping of supracrustal rocks around the granitoid domes is a function of upward movement of the domes, i.e. diapiric emplacement of the granitoid rocks − a pattern also seen in the Abitibi green-

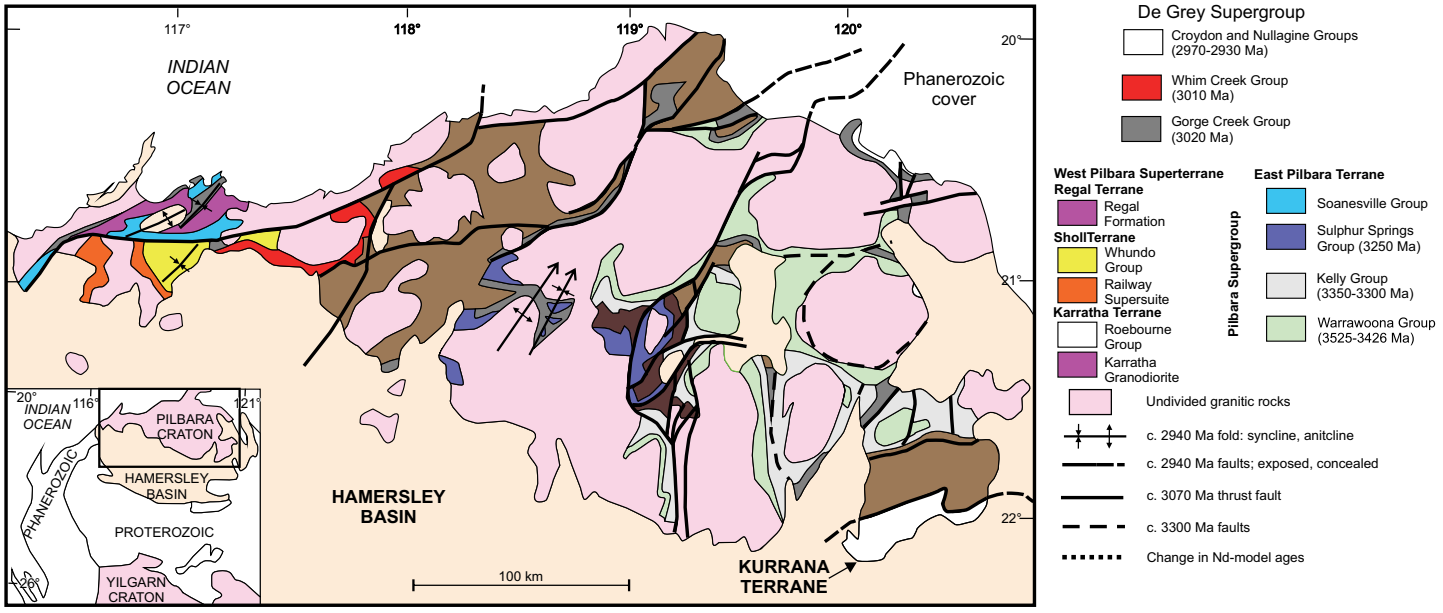

Figure 18. The dome and basin structural style of Archean greenstone belts exemplified by the East Pilbara greenstone belt (after Van Kranendonk et al. 2004). The oldest volcanic units are close to the granitic batholiths, whereas the younger volcanic units are further away. Note the difference in structural style north and west of the Sholl fault (SSZ). Successor basins (Mallina Basin MB; Mosquito Creek MCB and Lalla Rookh LLR) lie unconformably above the Pilbara Supergroup strata. The Sholl Shear Zone (SSZ) separates the East Pilbara terrane with typical granite-greenstone architecture from the West Pilbara Terrane which has a structural style dominated by thrusting. LWSC =Lalla Rookh-Western Shaw structural corridor.

stones (Heather 2001). The granitoid units of the domes display an inward-younging pattern (Van Kranendonk et al. 2002, 2004), unlike classical diapirs. The ubiquity of isotopic inheritance in Archean batholiths implies ensialic magmatism, i.e. magmatism within a granitic, continental environment (Larbi et al. 1999; Davis et al. 2000; Smithies et al. 2007).

The emplacement of granitoid bodies by diapirism is a key piece of evidence for vertical tectonics in granite–greenstone terranes. Examples of diapiric granitoid rocks occur in the East Pilbara terrane (Van Kranendonk et al. 2004), the Barberton greenstone belt in the Kaapvaal craton (Anhaeusser 1984), the Zimbabwe craton (Jelsma et al. 1993), the Yilgarn craton (Bloem et al. 1997), the Yellowknife greenstone belt in the Slave craton (Drury 1977), and the Wabigoon subprovince of the Superior Province (Schwerdtner 1984). Granitoid domes surrounded by greenstones occur throughout the Superior Province (Williams et al. 1992), but most examples lack the detailed structural studies necessary to postulate diapiric emplacement.

Worldwide, the stratigraphy of Archean greenstone belts is characterized by upward structural facing and upward younging, except where dismembered by subsequent deformation. Examples having good stratigraphic and geochronologic control include the Superior craton (Stott and Corfu 1991; Thurston et al. 2008) and the Pilbara craton (Van Kranendonk et al. 2002). Stratigraphic units decrease in age with increasing distance from the batholiths, suggesting that these batholith-centered zones are mid- to upper-crustal sections (Thurston et al. 2008).

An elegant explanation of this dome-and-keel structural style is provided by the 'punctuated partial convective overturn' model of Van Kranendonk et al. (2004). This model consists of granitoid basement overlain by higher density greenstone belt basalt. TTG sills were emplaced into the base of the greenstone succession and also fed felsic eruptive centres in the overlying basalts, creating an uneven distribution of denser basalts *vs.* less dense TTGs and coeval volcanic units. In the second stage, a younger, extensive and thick basaltic sequence was deposited on the older units. Meanwhile, the elevated content of radiogenic heat-producing elements (U, Th, and K) in the underlying granitoid rocks rendered the latter somewhat plastic. The overall gravitational instability of dense basaltic material overlying softened granitic material led to sagging of the basaltic domain, forming keels between up-rising, less dense, dome-forming granitoid rocks.

Some greenstone belts display a long, linear form, such as the Yilgarn craton (Gee et al. 1981; Swager et al. 1990). At the scale of terranes, the Superior Province consists of long, linear granite–greenstone terranes, but the greenstone belts within these terranes in the northern part of the Superior Province commonly display dome-and-keel structural style (Stott and Corfu 1991; Thurston et al. 1991). The dome-and-keel structural style in the eastern Pilbara is bordered to the north and west by the West Pilbara granite–greenstone terrane. The latter greenstones are somewhat younger than those in the classic East Pilbara stratigraphic section, but the important distinction between the two is the northeasterly structural grain of the West Pilbara and the fact that granitoid rocks are structurally simpler than in the East Pilbara, and discordant to the supracrustal units. Thus, Van Kranendonk et al. (2002) invoke an early episode of vertical tectonics followed by later horizontal tectonics, including major, terrane-bounding shear zones and thrust-based stratigraphic transport and duplication.

Successor Basin Structural Style and Genesis

The dome-and-keel structural style described above must be modified to accommodate the presence of scattered successor basins having the following characteristics: 1) metamorphic

grades similar to the surrounding greenstones; 2) rapid transition from fluvial to deep-water facies; and 3) the presence of mantle-derived alkaline magmatism. Bleeker (2012) has synthesized a model for the late structural evolution of greenstone belts (concentrating on the western part of the Abitibi greenstone belt) and the place of orogenic gold deposits in that process, as follows (Fig. 19): 1) early folding, thrusting and terrane imbrication (Bleeker and Van Breemen 2011); 2) synorogenic extension; 3) later thick-skinned extension that inverted earlier extensional structures; 4) further shortening and steepening of structures; and 5) transpression and associated sinistral and later dextral strike-slip movement.

Early folding was involved in the development of the above-noted dome-and-keel structures, and was followed by local-scale thrusting (e.g. the out-of-sequence position of the Kidd–Munro assemblage north of the Porcupine–Destor structure). In the Timmins area, a second phase of folding has produced the so-called 'Porcupine syncline,' which is cut by the unconformity at the base of the Timiskaming rocks. Subsequent synorogenic extension is marked by uplift and erosion, filling the successor basins. Extension is required to explain the alkaline to calc-alkaline magmatism and the presence in the conglomerates of foliated granitoid clasts, indicative of uplift and exhumation of mid-crust. The rapid lateral transition within these basins from alluvial–fluvial facies to deep-water wackes is explicable by extension and strike-slip processes. The 'major breaks' or transcurrent faults in greenstone belts are not numerous and have a spacing perpendicular to strike of several tens of km. These 'major breaks' are late, and transect early thrusts, but are spatially associated with the successor basins. Given the close spatial relationship of the 'breaks' and the basins, Bleeker (2012) proposed that the 'breaks' are first-order extensional structures. The common development of extensional shear bands in granitoid plutons at greenstone belt margins (Beakhouse 2013) is consistent with extensional processes. The extent of these extensional detachments is shown in Figure 20 for an area in the western Superior Province. It should be noted that some of the faults near the interface between the Wabigoon subprovince and the older Winnipeg River subprovince represent originally shallow-dipping thrust faults that were steepened by collision of the two terranes (Beakhouse 2013).

Given the necessity of 10–15 km of uplift required by the exposed metamorphic facies in the successor basins, their preservation would indicate that they were tectonically buried. The basins are asymmetric: the contact with older greenstones is an unconformity, whereas the 'major break' lies on the other flank of the basin. Using the Abitibi greenstone belt as an example, successor basin stratigraphy youngs south but appears on the north side of these major structures. These patterns are best explained by late-stage thrust burial in which the major extensional 'breaks' became inverted, forming thick-skinned thrusts. The association of successor basins with gold mineralization is discussed in a subsequent section. It should be noted that the Bleeker (2012) model does not explain along-strike variations in the Porcupine–Destor structure east of Timmins (J. Goutier personal communication 2014).

Although the model for successor basin development is based on the Abitibi greenstone belt (Bleeker 2012), similar basins, complete with evidence of extension (alkaline to calc-alkaline magmatism) exist in the western part of the Wawa–Abitibi terrane (Lodge et al. 2013), in the Wabigoon subprovince (Mueller and Corcoran 1998), and the North Caribou terrane (Brooks et al. 1982; Parks et al. 2006). Similar successor basins exist in the Slave (Bleeker and Hall 2007), Yilgarn (Kositcin et al. 2008), Pilbara (Krapez and Barley 1987),

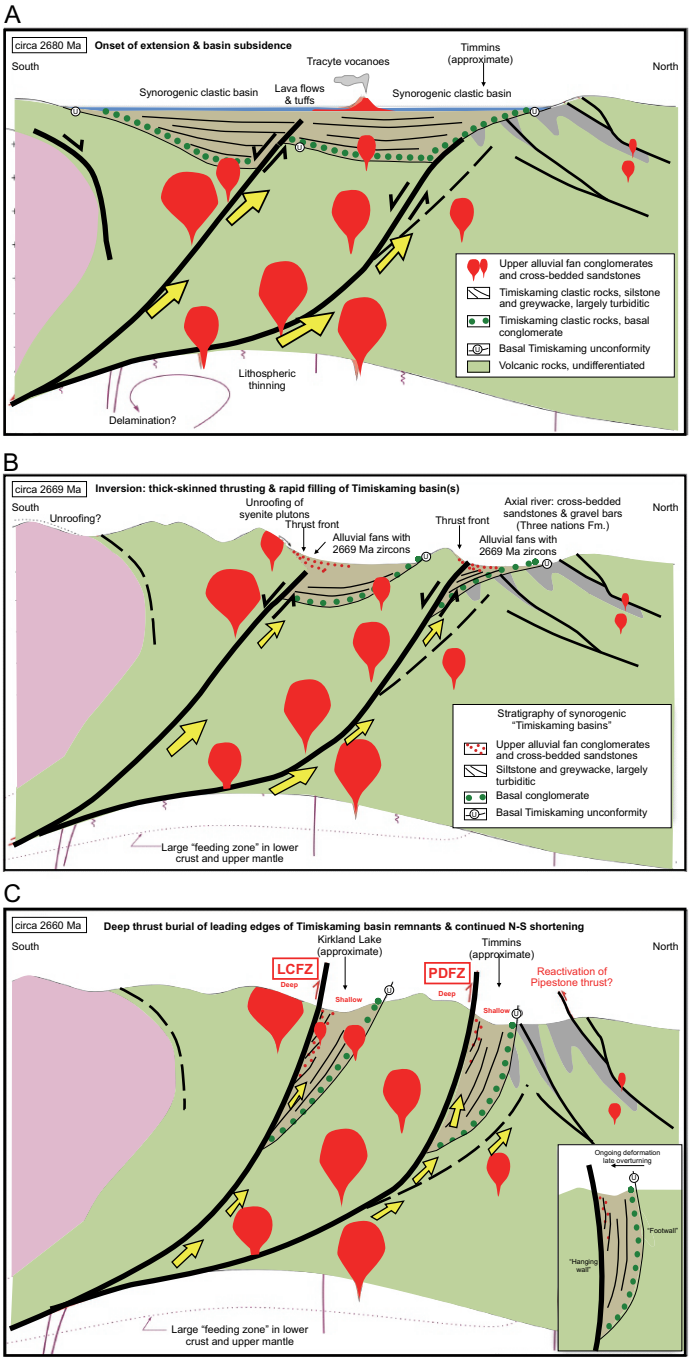

Figure 19. Late structural history of greenstone belts and the place of orogenic gold deposits based on the model of Bleeker (2012). A. Onset of regional extension at ~2680 Ma resulting in development of synorogenic late phases of successor basins. Extension provides access for alkalic magmatism. B. Transition from extension to renewed north-south shortening at ca. 2669 Ma with the major breaks becoming thick-skinned thrusts resulting in burial in the footwall of the clastic basins. C. Deep burial and steepening of thrusts at ca. 2660 Ma. Note that the region south of the basin represents deeper crustal levels exhumed during continued shortening.

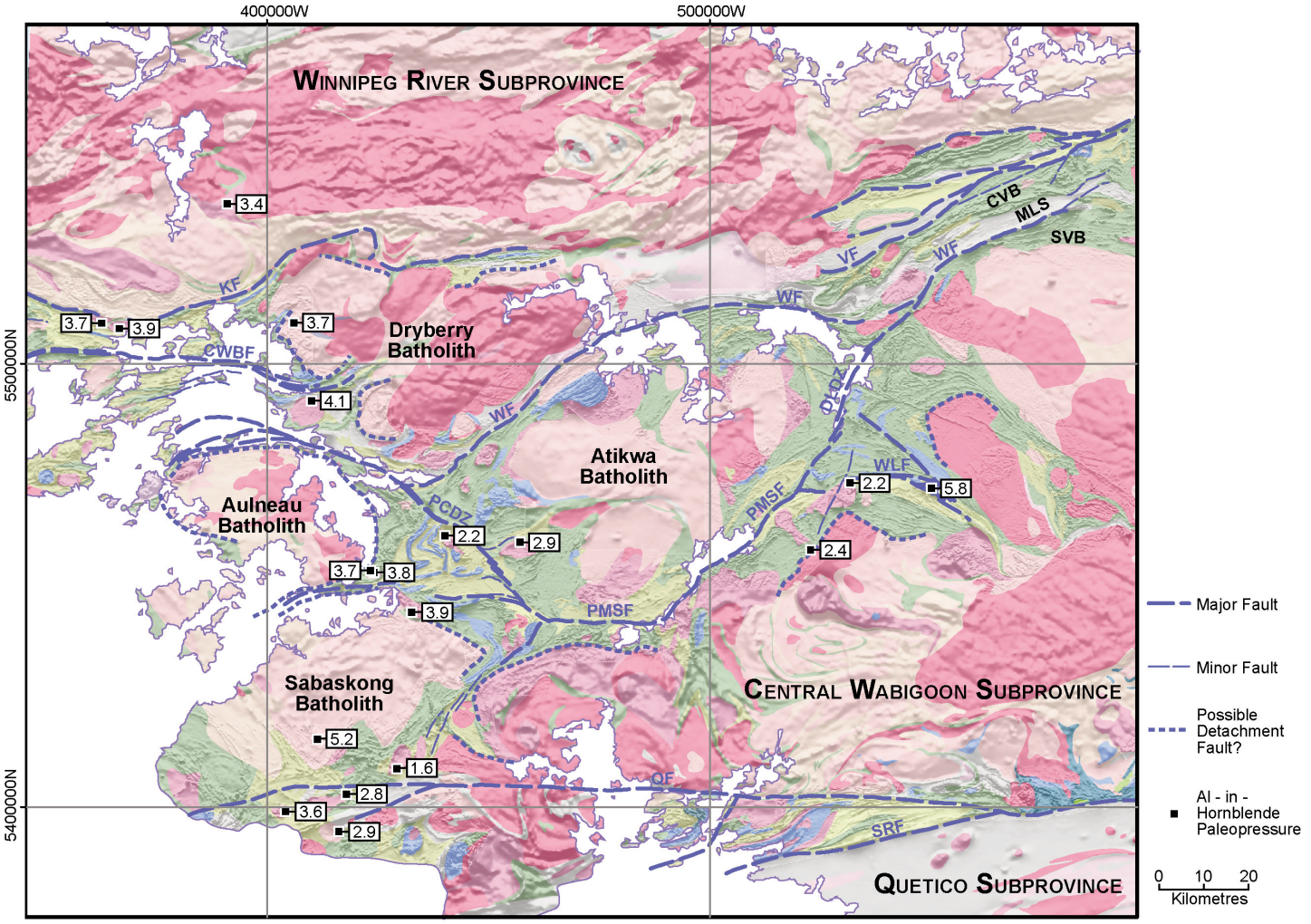

Figure 20. The western Wabigoon subprovince in the southwestern part of the Superior Province. The geology is generalized and draped over a shaded image of the first vertical derivative of the total magnetic field. Dashed lines denote potential detachment faults at the granite–greenstone contacts. Squares show location of aluminum-in-hornblende paleopressure determinations with pressure in kilobars in adjacent boxes. North of the Dryberry batholith, extensional structures are associated with the collision of the Wabigoon subprovince with the older Winnipeg River subprovince to the north (after Beakhouse 2013). The labeled features are: CVB–central volcanic belt; MLS–Minnitaki Lake sediments; SVB–southern volcanic belt; CWBF–Crowduck Lake-Witch Bay fault; DLDZ–Dinorwic Lake deformation zone; KF–Kenora Fault; PCDZ–Pipestone-Cameron deformation zone; PMSF–Pipestone-Manitou Straits fault; QF–Quetico Fault; SRF–Seine River fault; WF–Wabigoon fault; WLF–Washeibemaga Lake fault; VF–Vermilion fault.

Baltic (Slabunov et al. 2006), and Zimbabwe (Blenkinsop et al. 1997) cratons, among others.

METAMORPHISM

Metamorphic patterns reveal the thermal and structural history of Archean granite−greenstone terranes. Metamorphism of these terranes is of the low pressure, high temperature type, and isograds are broadly concentric with respect to the major batholiths (Thurston and Breaks 1978; Easton 2000; Fig. 21). The most intensely studied region in terms of metamorphism in the Superior Province is the Abitibi greenstone belt, where P_1, a seafloor metamorphism, produced prehnite−pumpellyite assemblages (Jolly 1978; Dimroth and Lichtblau 1979). In places, the early metamorphism includes development of contact aureoles around synvolcanic plutons such as the Flavrian and Powell plutons. These events predate cleavage development (Dimroth et al. 1983). The second metamorphic event in most greenstone belts, P_2, consists of up to 5 km-wide contact aureoles imposed on the greenstone belt and early plutonic rocks by intrusion of large TTG plutons and late alkaline plutons (Mortensen 1993). The P_2 assemblages overprint the earlier event, though the textural features could be explained by outward progression of the thermal anomalies surrounding granitoid intrusions. Thus, in the most intensely studied region, both burial and contact metamorphic processes are evident (Easton 2000). The metamorphic grade in greenstone belts elsewhere in the Superior Province and on other Archean cratons is in the greenschist to amphibolite facies (Thurston and Breaks 1978; Easton 2000; Goscombe et al. 2012; Bédard et al. 2013). The Abitibi greenstone belt is unusual in having sub-greenschist facies assemblages in the interior of the belt (Powell et al. 1995).

Regional mapping coupled with metamorphic studies demonstrate a systematic variation in structural style and metamorphic pressure (Bédard et al. 2013). At upper crustal levels having low metamorphic pressures, the dome-and-keel structural style predominates. At middle- to deep-crustal levels, greenstones form <10% of the crust and TTGs predominate

among steeply dipping, minor supracrustal enclaves. In deep crust such as the North Atlantic craton, gneissic units and supracrustal enclaves display subhorizontal structures and metamorphic pressures equivalent to 25–30 km depth (Windley and Garde 2009).

The early metamorphism (P_1) is the main metamorphic event in the granite–greenstone terranes north and west of the Abitibi–Wawa terrane (Easton 2000; Table 4). The higher-grade granite–greenstone terranes have somewhat later metamorphic events (e.g. P_2), whereas P_3 is the dominant metamorphic event in the southern Superior Province. P_4 is present mainly in amphibolite- to granulite-facies areas of the southern Wawa–Abitibi, Quetico and English River subprovinces (Easton 2000).

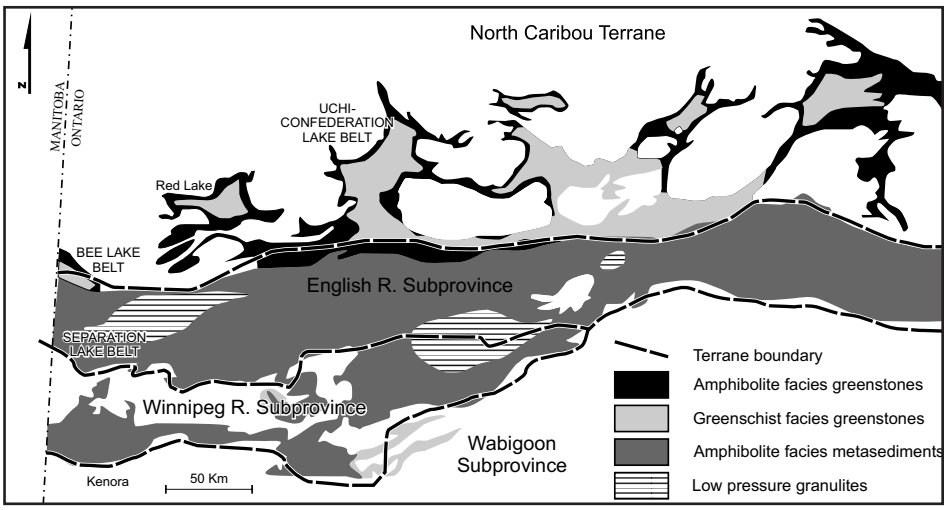

Figure 21. Metamorphic patterns in the southern part of the North Caribou terrane and the English River subprovince (after Thurston and Breaks 1978).

Metamorphic discontinuities at major tectonic boundaries, e.g. the North Caribou terrane–English River subprovince boundary (Thurston and Breaks 1978) are abrupt, commonly representing a difference of hundreds of degrees over a horizontal distance of a few metres. Metamorphic variations in the Superior Province indicate that the individual terranes were not tilted; for example, northeastern Québec displays broad areas of uniform metamorphic rank, whereas the metamorphic variation in the Baltic shield (Nehring et al. 2009) suggests that granite–greenstone terranes are large-scale tilted blocks.

GRANITOID ROCKS AND MAFIC/ULTRAMAFIC INTRUSIONS IN GRANITE–GREENSTONE TERRANES

Introduction

Granitoid rocks in granite–greenstone terranes are classified based on the system of Le Maitre (1989; Fig. 22), with modifications by Stone (2005). At a regional scale, the granitoid rocks surrounding greenstone belts in the Superior Province are subdivided into: 1) gneissic tonalite, 2) foliated tonalite, 3) granite, 4) peraluminous granite, and 5) sanukitoid suite plutons (Stone 2005; Table 5).

With minor variations in nomenclature, these subdivisions are present in all Archean cratons (Pawley et al. 2004; Martin et al. 2005). The gneissic tonalite suite commonly connects greenstone remnants in high-grade metamorphic zones in the northwestern and northeastern Superior Province (Percival et al. 1994; Stone 2005). The foliated tonalite suite, made up of biotite tonalite and hornblende tonalite, constitutes about 50% of the crust in northwestern Ontario (Stone 2005, 2010). It makes up greater proportions of the crust in areas of higher metamorphic grade, e.g. in northern Québec (Bédard et al. 2013). The dominant geochemical type of tonalite is the high-Al type of Martin (1993), which is produced in the garnet stability field, whereas in the East Pilbara terrane (Champion and Smithies 2007) and in the Baltic shield (P. Holtta personal communication 2009), both high- and low-Al types occur. Peraluminous granites form elongate to irregular bodies commonly found along major structures, e.g. along the Bearhead fault zone (Thurston et al. 1991). The sanukitoid suite intrusions occur in quasi-linear arrays along major strike-slip structures and along terrane boundaries (Thurston et al. 1991). The proportions of the various suites are a function of exposure level; the northern Superior Province represents mid-crustal depth (Stone 2005) and the northeastern Superior Province a somewhat deeper level wherein the proportion of tonalites increases slightly (Bédard et al. 2003, 2013). At higher crustal levels, such as in the Wawa–Abitibi terrane (Sutcliffe et al. 1993), the proportion of granite suite plutons increases slightly.

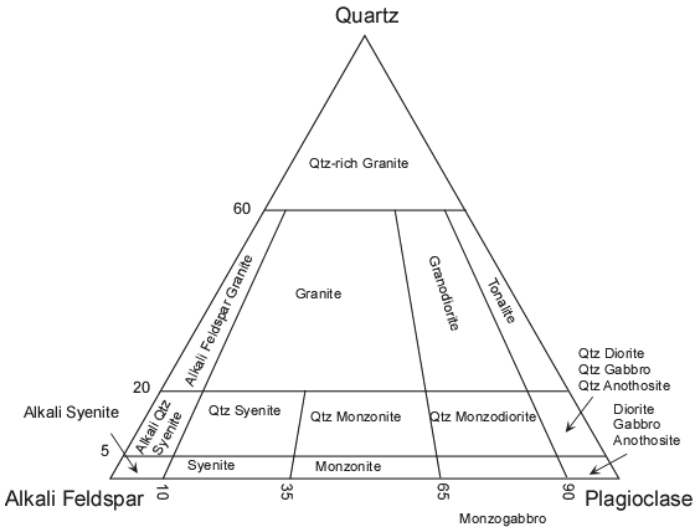

Figure 22. Classification of granitic rocks (after Le Maitre 1989).

Age Relationships of Archean Granitoid Rocks *vs.* Greenstones

Granitoid units in Archean granite–greenstone terranes range in timing of emplacement from synvolcanic to syn-tectonic to post-tectonic. In rare instances, where not overprinted by later structures or intrusions, granitoid rocks form basement to greenstones (Wilks and Nisbet 1988; Bickle et al. 1993). In a mechanical sense, kinematic indicators show that, at the granitoid–greenstone interface, the sense of motion is batholith-up and greenstones-down (Stott and Corfu 1991; Pawley et al.

Table 4. Bathozones in the Superior Province (after Easton 2000).

Event	Bathozone (depth in crust)		
	1-2 (3–8 km)	3-4 (9–14 km)	5-6 (15–24 km)
P1			
2710–2695 Ma	NW Superior (N. Caribou terrane) Wabigoon, Eastern Wawa-Abitibi (Abitibi greenstone belt)	Southern Winnipeg River	Quetico
P2			
2693–2680 Ma	Central Wawa-Abitibi	English River, northern Winnipeg River	Kapuskasing, Pikwetonei
P3			
2678–2665 Ma	Western Quetico, Eastern Wawa-Abitibi	SW Abitibi, English river, northern Winnipeg River, Wawa, central and eastern Quetico	South-central Quetico
P4			
2660–2648 Ma		North-central Wawa-Abitibi, Central Wawa-Abitibi gneisses	South central Quetico granulites, Kapuskasing, eastern Wawa-Abitibi gneisses, Levack granulites
P5			
<2640 Ma			Eastern Kapuskasing, western Pikwetonei

Table 5. Regionally important Granitoid types in the Superior Province (after Stone 2005).

Suite	Rock types	Fabric	Form/Occurrence and % of area	Inclusion types
Gneissic Tonalite	Biotite + hornblende tonalite to granodiorite	Foliated, layered, folded	Belts, masses; scattered near greenstone remnants 3%	Supracrustal xenoliths
Foliated Biotite Tonalite	Biotite tonalite to granodiorite	Foliated to gneissic; quartz and feldspar megacrystic	Irregular to crescentic and lobate bodies; scattered 34%	Amphibolite, supracrustal xenoliths
Foliated Hornblende Tonalite	Hornblende + biotite tonalite to granite	Foliated; granular; feldspar megacrystic	Irregular to elongate bodies of variable size; scattered; 14%	Lensoid dioritic inclusions
Biotite Granite	Biotite granodiorite to granite	Massive to weak magmatic layering	Dikes, irregular masses, oval batholiths; scattered 30%	Biotite tonalite, amphibolite
Peraluminous (S-type)	Biotite + muscovite granodiorite to granite	Massive; mylonitic	Elongate to irregular bodies <1%	Sediment
Sanukitoid	Biotite+hornblende+ pyroxene quartz diorite, tonalite, quartz monzodiorite, granodiorite, quartz monzonite, quartz syenite, granite	Massive to weak magmatic layering	Oval plutons 4.5%	Hornblendite, amphibolite

2004; Van Kranendonk et al. 2004; Robin and Bailey 2009). In granite–greenstone terranes worldwide, there is a regular progression from TTG units to true granites followed by sanukitoid plutons, as shown by relationships in the North Caribou terrane (Corfu and Stone 1998; Fig. 23), the Superior craton in northeastern Québec (Bédard et al. 2003), and the Pilbara craton (Van Kranendonk et al. 2004). Geochronology linked with phase-by-phase mapping of granitoid plutons and structural geology is not commonly done in granite–greenstone terranes, with some notable exceptions (Corfu and Stone 1998; Van Kranendonk et al. 2004; Stone 2005). Early units occur at the margins of batholiths and younger phases in the central zones in the East Pilbara craton (Van Kranendonk et al. 2004), the Wabigoon subprovince (Stone 2010), and the northern Superior Province (Stone 2005). A limited number of so-called 'late crescentic plutons' intruded along the interface between greenstones and granitoid rocks in the Wabigoon subprovince (Stott 1986). A more robust dataset indicates that the granite batholiths post-dated the tonalitic rocks and feature Al-in-hornblende barometry demonstrating that they crystallized at lower pressures than the surrounding, more abundant tonalites (Stone 2005, 2010).

Using integrated geochronology and Al-in-hornblende data on pressure at the time of emplacement, Beakhouse et al. (2011) demonstrated that after emplacement of the syntectonic phases of the Pukaskwa batholith, the batholith was uplifted as a structural dome. Similar features are seen in the Shaw batholith in the Pilbara craton (Pawley et al. 2004; Van Kranendonk et al. 2004). In a general sense, integrated studies of petrogenesis, structural geology and geochronology (Corfu and Stone 1998; Whalen et al. 2004) show that low-K granitoid rocks precede tectonism and that high-K granitoid rocks followed the major deformation events.

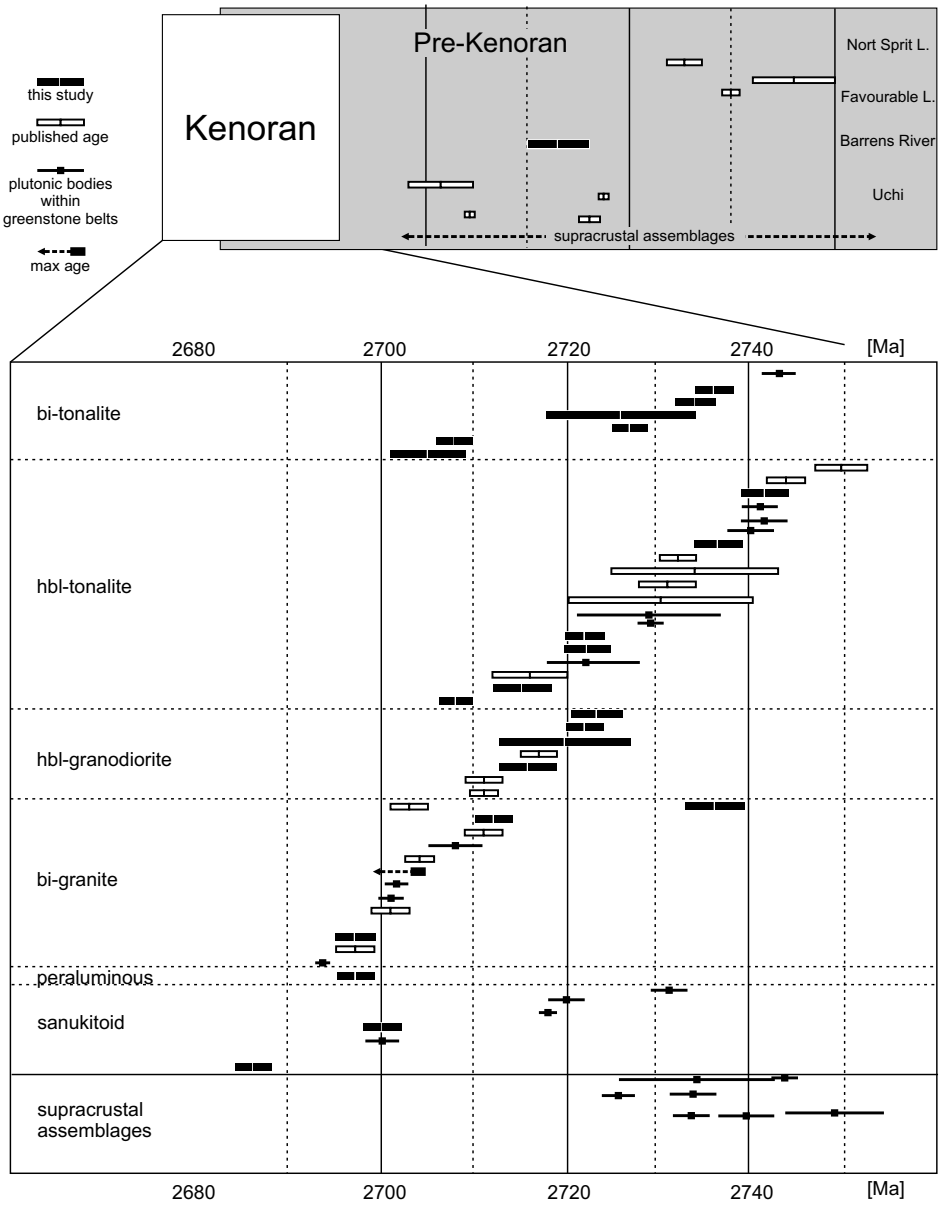

Figure 23. Geochronology of granitoid rocks in the North Caribou terrane in northwestern Superior Province (after Corfu and Stone 1998).

Mafic/Ultramafic Intrusions

Mafic to ultramafic intrusions occur across the Superior craton as synvolcanic to post-tectonic intrusions generally a few hundred metres to a few kilometres in diameter. The synvolcanic intrusions represent komatiitic to tholeiitic magmatism as synvolcanic sills, dikes and plutons (e.g. Kuiper 2010). Larger, and somewhat later, layered to massive mafic to ultramafic plutons are found cutting the volcanic units of greenstone belts across the Superior craton (Barrie et al. 1990; Jackson and Fyon 1991; Sappin et al. 2013). These intrusions vary from basaltic to ultramafic and range from synvolcanic to post-tectonic. An excellent example of large intrusions of synvolcanic age in the Abitibi greenstone belt is the Bell River Complex, a subvolcanic intrusion in the Matagami district (Maier et al. 1996). These intrusions bear no particular relationship to stratigraphy or structure at a large scale. Post-tectonic, kilometre-scale mafic/ultramafic intrusions are broadly associated with major tectonic boundaries in granite–greenstone terranes. These intrusions vary from concentrically zoned bodies to rather conventional layered complexes. The primary magma for the concentrically zoned Lac des Iles intrusion in the Marmion terrane is basaltic (Sutcliffe et al. 1989). A string of post-tectonic, concentrically zoned, ultramafic to mafic small intrusions are scattered along the interface between the Quetico subprovince and the western Wabigoon subprovince to the north (Pettigrew and Hattori 2006); their emplacement may well be tectonic (Devaney and Williams 1989a; Pettigrew and Hattori 2006).

Petrogenesis

Tonalite–Trondhjemite–Granodiorite Suite (TTGs)

Archean batholiths of the TTG suite vary from the dominant high-Al type (Martin 1987; Martin et al. 2005) displaying fractionated REE patterns, to less common low-Al type TTGs with less fractionated REE patterns. The lack of significant Eu anomalies and a lack of correlation between Eu* and MgO or SiO_2, particularly in the high-Al type, suggests that fractional crystallization within the plagioclase stability field was not a major process (Stone 2005, 2010; Champion and Smithies 2007). The Si-rich, low-Al TTGs do show evidence consistent with at least some fractional crystallization (Bagas et al. 2003). However, the consensus is that TTGs in general represent the partial melting of a mafic precursor (Barker and Arth 1976; Drummond and Defant 1990), and that variations in the LREE/HREE values reflect melt production in the garnet stability field (high values) or the plagioclase stability field (lower values). Champion and Smithies (2007) modelled the derivation of high-Al TTGs in the East Pilbara terrane by relatively modest degrees (~ 20%) of melting of low-K tholeiitic basalt from the neighbouring greenstone belts. They note that more enriched starting materials are required to produce the more LILE-rich granitoid rocks. Their modelling requires a residual phase retaining Nb, Ti and Ta (perhaps amphibole), or a source that has been depleted in Nb and Ti. The high-Al TTGs can be produced in a similar way from a garnet-free residue containing 20–40% residual plagioclase.

Using actualistic models, Martin (1993, 1999) promoted the generation of TTGs by melting of subducted slabs in what is known as the 'adakite' model, based on geochemical similarities to adakites. Alternatively, trace element modelling has shown that the elevated La/Yb and Sr/Y signature of TTGs can be explained by hornblende fractionation of a tonalitic parent melt (Bédard 2006). Further consideration of major element modelling (Bédard et al. 2013) suggests that a maximum of 25% fractionation is possible given the low abundances of FeO and MgO in TTGs. However, when these approaches are combined with εNd data, Champion and Smithies (2007) conclude that some form of intermediate to felsic crustal component is also required along with a basaltic protolith. The isotopic data in this instance also show that contributions to TTG melts had a crustal residence time of as much as 200 m.y. Similar results are seen in Sm−Nd studies of Superior craton granitoid rocks (Henry et al. 1998).

In summary, partial melting of a basaltic protolith at varying pressures controls the residual mineralogy and thus the geochemistry of the TTG suite. The existence of TTGs with high LILE, Th and U requires a source richer in LILE than typical Archean basalts. Therefore, the two types of TTGs may well reflect crustal thickness, the high-Al type indicating thicker Archean crust (Champion and Smithies 2007). The lack of high Mg#, Cr and Ni in high-Al TTGs probably precludes interaction with the mantle wedge (Champion and Smithies 2007) and instead suggests partial melting of thickened mafic crust, which is also seen in younger terranes (Gromet and Silver 1987). There are contrasting opinions that call upon subduction processes (Moyen and Stevens 2006; Laurent et al. 2014); however, representative crustal thickness beneath the Superior (White et al. 2003) and Pilbara (Drummond 1988) cratons (~40 km) and the dominantly felsic nature of that crust preclude the presence of mafic−ultramafic residua in the production of tonalite. Therefore, some form of recycling such as delamination (Smithies and Champion 1999) is required.

The high-alumina TTGs are explained (Wyman et al. 2011) by hornblende and titanite fractionation. If TTGs with high Sr/Y or La/Yb are not residua from fractionation of tonalites, then they must represent very small degrees of partial melting. But if adakites and tonalites are produced by slab melting, these small degree melts do not explain the large proportions of TTGs that characterize granite−greenstone subprovinces (Bédard et al. 2013). Fundamentally, the total variability of high- and low-Al tonalites is best explained by genesis at various temperatures and pressures. For example, Nehring et al. (2009) explain the variety of TTGs in the Baltic shield in terms of the melting of granulites and amphibolites.

Granodiorite to Granite

The last phase of granitoid magmatism is the broadly post-tectonic intrusion of granodiorite to granite. Conventional petrogenetic arguments indicate that granites are produced by melting of pre-existing granitic units, based on trace elements and Nd isotope systematics (Whalen et al. 2004). The granites consistently display negative Nb and Ti anomalies (Stone 2005, 2010), which can be explained by retention of trace minerals in residua, enrichment in adjacent trace elements, or a contamination, as discussed previously. The granite suite in northwestern Ontario is marginally peraluminous, indicating a petrogenetic link to the peraluminous granite suite and implying that these characteristics are present in the source, in turn suggesting that the source for this suite is perhaps the biotite tonalite suite (Stone 2005). The presence of depletions in Sr, Ba and Eu, and general REE enrichment is consistent with feldspar fractionation. Isotopic studies (Whalen et al. 2004) indicate that the late, high-K granitoid rocks have εNd values of −3.1 to +3.3, demonstrating that the K-rich granitoid rocks are produced with input from LREE-enriched older crustal materials and juvenile material. This suggests melting of older crust and young infracrustal material. Lastly, the biotite granite suite includes REE-enriched and REE-depleted units similar to those elsewhere in the Superior Province, implying a broadly similar petrogenesis across the Superior Province.

Peraluminous Granites

Peraluminous leucogranites are commonly found along major tectonic boundaries, e.g. within the North Caribou terrane (Stone 2005) and along the boundaries of the Wabigoon, Winnipeg River and English River terranes (Breaks and Moore 1992). The values of εNd vary from −2 to +2 for the leucogranite suite in the Wabigoon terrane, overlapping values for nearby metavolcanic and metasedimentary units. Thus, Larbi et al. (1999) concluded that the leucogranite suite was developed from both mantle and crustal sources. The leucogranite suite from across the Superior Province is ca. 2650 Ma in age (Larbi et al. 1999; Percival and Stott 2010), suggesting that this suite may be related to a large-scale process such as crustal delamination (Percival et al. 2004).

Sanukitoid Suite

The sanukitoid suite of plutonic rocks was defined by Shirey and Hanson (1986) as follows: SiO_2 <60%, MgO >6%, Mg# >0.6, Cr >100 ppm, Sr and Ba >500 ppm, and high Na_2O, K_2O, LREE, and La/Yb. This suite ranges in composition from dioritic to granodioritic. The high Cr, Ni and K_2O distinguish this suite from TTGs and mandate a mantle origin, yet high contents of LILE suggest a more complex origin. Modelling summarized in Martin et al. (2005) demonstrates that sanukitoids cannot be produced by contamination of komatiitic or basaltic magmas by LILE-rich felsic crust, as that scenario does not explain coincident high Cr, Ni and LILE. Therefore, the less-evolved sanukitoids must represent a peridotitic source, but any mantle source must also account for the high SiO_2 and LILE. Given the similarities with TTGs and adakites (high LILE, fractionated REE patterns, low Yb and Y concentrations), these characteristics are interpreted to represent slab melting (Martin et al. 2005); however, the possibility of melting of fertilized mantle has also been postulated (Shirey and Hanson 1986). Sanukitoid intrusions in Archean cratons are post-tectonic and, for example, in the Superior craton, they are spatially associated with major terrane-bounding, strike-slip shear zones.

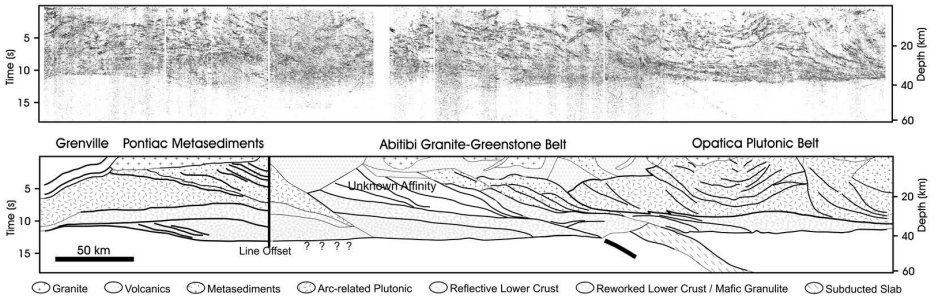

Figure 24. A reflection seismic profile of the Abitibi greenstone belt and the Opatica gneisses to the north, showing north-dipping reflections in the Opatica gneisses interpreted by Calvert and Ludden (1999) as subduction scars.

GEOPHYSICS OF GRANITE–GREENSTONE TERRANES

Introduction

Granite−greenstone terranes have been investigated using a variety of geophysical techniques. Early magnetic surveys optimized for regional mapping clearly distinguished greenstone belts from the surrounding granitoid rocks (Gupta 1991). Gravity maps and gravity modelling of granite−greenstone terranes have shown that the depth to tonalitic basement varies from 10−12 km in the low metamorphic grade Abitibi greenstone belt (Peschler et al. 2004; Benn and Peschler 2005) to about 5 km in the case of the Birch−Uchi greenstone belt in the North Caribou terrane (Gupta et al. 1982). Studies of seismic anisotropy (Silver and Chan 1991; Ferguson et al. 2005) have shown that the structural trends of greenstone belts persist into the upper mantle.

Reflection Seismic Studies

Reflection seismic studies of the Superior craton carried out as part of the LITHOPROBE project (summarized by Percival et al. 2004, 2006) indicate that Superior craton crust is about 40 km thick. Dipping structures interpreted as 'subduction scars' occur along the Abitibi−Grenville seismic line, the western Superior Province line, and the Slave Province line (van der Velden and Cook 2005; Fig. 24). Calvert et al. (2004) have developed a model in which the southern part of the North Caribou terrane (the former Uchi subprovince) is preserved at relatively low metamorphic grade along a south-dipping extensional shear zone truncating sub-horizontal reflectors in the interior of the North Caribou terrane gneisses. These authors note that early vertical tectonics is still possible and also note that the extensional event they portray is related to orogenic gold mineralization in the Uchi subprovince. However, numerical models of crustal processes (Gray and Pysklywec 2010) suggest that the features imaged can develop by shortening without subduction or accretion, although these authors invoke the production of "plate-like mantle lithosphere at depths of ~200–400 km," which may be interpreted as a possible early version of plate tectonics. The LITHOPROBE seismic profiles display few details of greenstone belt structure, although more recent detailed reflection seismic profiles specifically designed to image greenstone belt structure are revealing (Snyder et al. 2008). These studies do not image the prevailing vertical foliations of greenstone belts, but do show structures with dips of <~60°. Therefore, the shallowly dipping strata found in anticlinal domes are clearly revealed and it can be seen that seismically transparent units coring these domes are likely granitoid rocks (Fig. 25). Steeply dipping features such as the gold-associated Porcupine−Destor fault zone are imaged by virtue of the offset of greenstone belt stratigraphy and are seen to have a listric geometry at depth, passing at a depth of a few km into locally-developed antiformal thrust stacks (Snyder et al. 2008).

Similar seismic surveys designed to optimize the detail near greenstone-hosted gold deposits in the Yilgarn craton have been able to trace detachment faults at 4−7 km depth (i.e. at the base of the supracrustal rocks) that pass into a network of faults trending upward through the greenstones to sites of lode gold deposits (Goleby et al. 2004, 2006). Seismic profiles in the Superior Province lack the combination of detail and depth extent to enable similar interpretations.

RELATIONSHIP OF GRANITE–GREENSTONE TERRANES TO SEDIMENTARY SUBPROVINCES

Sedimentary subprovinces (Card 1990) are linear belts of largely amphibolite- to low-pressure granulite-facies clastic metasedimentary rocks that were termed orogenic flysch by Percival and Stott (2010). Typical examples are the English River, Quetico, Opinaca and Ashuanipi subprovinces in the Superior craton, and the Limpopo sedimentary rocks at the junction between the Kaapvaal and Zimbabwe cratons (Eglington and Armstrong 2004). Geochronological work indicates that the metasedimentary units are coeval with successor basin sedimentary rocks (Davis 1990; Davis et al. 1990). In numerous places in the Superior Province, sedimentary subprovince clastic units overlie greenstones (Breaks 1991; Williams 1991).

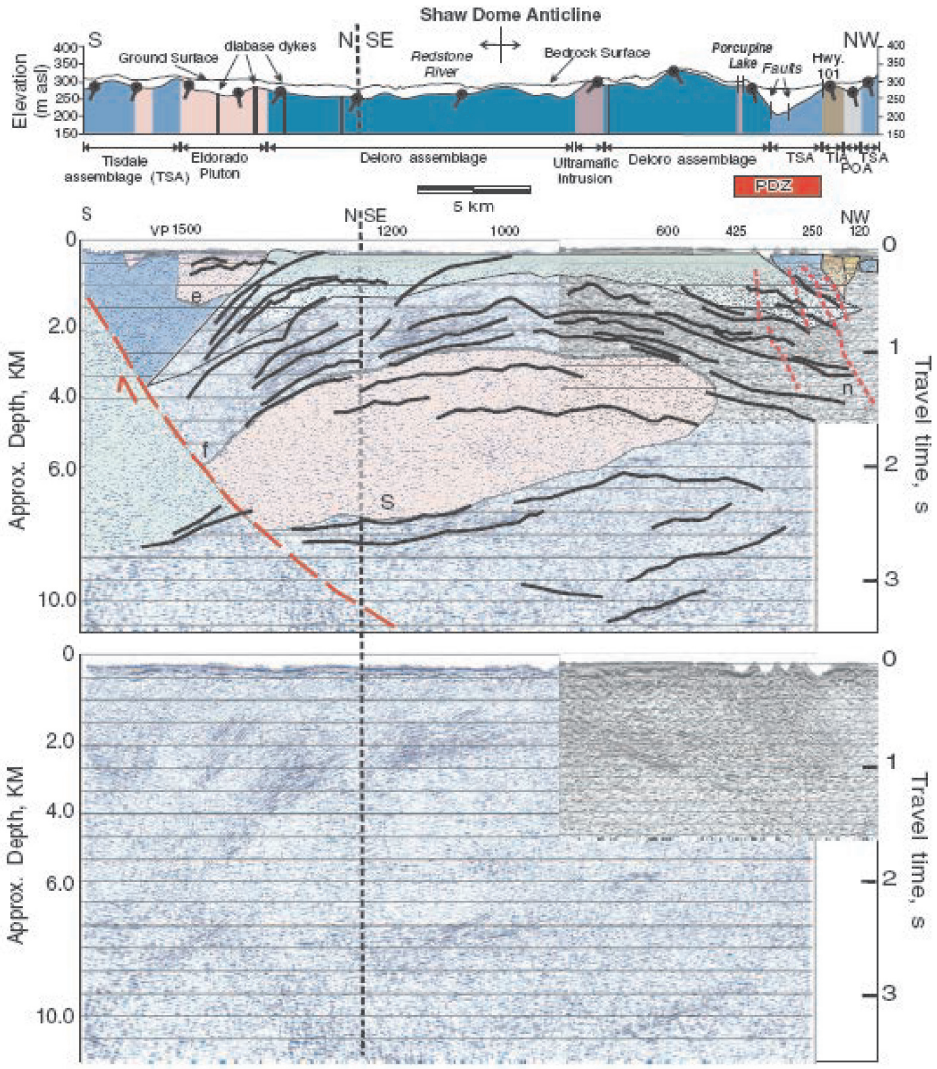

Figure 25. Shaw Dome reflection seismic line in the Abitibi greenstone belt (after Snyder et al. (2008) The data shows reflections from quasi-horizontal greenstone units over the Shaw Dome, a regional anticline south of Timmins, and a seismically transparent, nearly horizontal granitoid intrusion which bowed up the greenstones of the Deloro assemblage.

The sedimentary detritus is derived both from the adjacent granite–greenstone terranes and also from more distal and older plutonic terranes (Sanborn-Barrie and Skulski 2006; Percival 2007; Percival and Stott 2010). Structural and metamorphic studies indicate that the sedimentary subprovinces transition southward from lower-grade northern margins to higher-grade zones via extensive thrust telescoping (Devaney and Williams 1989; Hrabi and Cruden 2006). Structural mapping has also demonstrated that the strike-slip faults now bounding the sedimentary subprovinces are relatively late structures (Hrabi and Cruden 2006). Similar relationships are seen for the Limpopo sedimentary rocks and their relationship to the Kaapvaal and Zimbabwe cratons (Eglington and Armstrong 2004).

ORE DEPOSITS

Archean cratons are a major repository for mineral deposits. The major syngenetic deposit types are VMS deposits and komatiite-associated Cu–Ni–platinum group element (PGE) deposits. Other important types of mineralization in Archean granite–greenstone terranes are orogenic gold deposits, intrusion-hosted Cu–Ni–PGE and Cr deposits, and pegmatite-hosted rare metal deposits.

Volcanogenic Massive Sulphide (VMS) Deposits

Knowledge of stratigraphy is critical to evaluation of likely locales for VMS deposits. VMS deposits require subvolcanic pluton-centred hydrothermal circulation, largely during periods of volcanic quiescence (Franklin et al. 2005; Galley et al. 2007a). They are commonly associated with development of calderas in later stages of the evolution of major Archean volcanic systems at Noranda (Gibson and Watkinson 1990) and Sturgeon Lake (Hudak et al. 2003) in the Superior Province, although many VMS deposits are not associated with calderas (Allen et al. 2002; Ross and Mercier-Langevin 2014). The deposits consist of massive to disseminated chalcopyrite, sphalerite and pyrite forming massive lenses deposited on the seafloor, and subjacent stockwork vein systems representing zones of hydrothermal upwelling responsible for the seafloor deposits (Galley 2007a). The hydrothermal processes produced zones of metal leaching in sub-deposit semiconformable alteration zones. The metal content of the deposits is a function of the temperature and pH of the hydrothermal system; hotter systems are more Cu-rich and shallow water systems are possibly more gold-rich (Galley et al. 2007a).

Ore deposits can provide some insight into the geodynamic setting of greenstone belts in that modern VMS deposits, for example, are currently forming in a restricted range of settings (Franklin et al. 2005), e.g. oceanic arcs, back arcs, rifted supra-subduction zone epicontinental arcs, and mature epicontinental back arcs. On the modern seafloor, over 50% of VMS deposits are on ocean ridges (Hannington et al. 2005; Shanks and Thurston 2012). However, there is much debate as to the possible existence of preserved Archean oceanic floor; on one hand, many authors describe possible examples (Manikyamba and Naqvi 1998; Terabayashi et al. 2003; Shibuya et al. 2012), whereas a minority state that no unequivocal ocean floor of Archean age has been identified (Bickle et al. 1994; Bédard et al. 2013; Kamber 2015). Most interpretations of Archean VMS deposits relate them to oceanic arcs and back arcs (Franklin et al. 2005). Of the VMS deposits in the Superior Province, epicontinental arc and back arc settings are favoured by some, largely based on geochemical studies (Polat et al. 1998).

Komatiite-Associated Cu–Ni–PGE Mineralization

Komatiite-associated Cu–Ni–PGE mineralization occurs in two styles: 1) basal massive to disseminated (type I of Lesher

and Keays 2002); and 2) stratabound, internally disseminated (type II of Lesher and Keays 2002). Controlling the presence of mineralization are parameters such as magma composition, the presence of a suitable substrate in which to develop erosional channels later filled with mineralization, and the physical volcanology (Lesher 1989; Sproule et al. 2002, 2005). In the komatiite–tholeiite sequences, sulphur-undersaturated melts achieve sulphur saturation near surface, commonly by processes such as assimilation of iron-formation or graphitic argillites. Particularly well known examples of this style of mineralization are the nickel deposits of the Kambalda area of the Yilgarn craton (Lesher 1989; Hill 2001) and the deposits of the Abitibi greenstone belt of the Superior craton (Houlé et al. 2001, 2008a, 2009; Sproule et al. 2002). Similar mineralization is known in Zimbabwe (Prendergast and Wingate 2013).

Orogenic Gold Deposits

Epigenetic gold deposits are variously known as lode gold deposits (Poulsen et al. 2000), mesothermal gold deposits, and orogenic gold deposits (Goldfarb et al. 2005). Mineralization is syn- to late-deformational, post metamorphic peak, and associated with regional-scale alteration, hence the term 'orogenic gold' is preferred. They occur mainly in tholeiitic and variolitic basalts and iron-formation units, proximal to the major transcurrent structures forming the faulted margins of successor basins within Archean greenstone belts (Robert and Poulsen 1997; Poulsen et al. 2000; Dubé et al. 2004; Goldfarb et al. 2005; Dubé and Gosselin 2007). There are rare examples almost wholly within metasedimentary units (e.g. Gaillard et al. 2014). The deposits are associated with regional-scale Fe-carbonate and silica alteration of greenstone belt units (Dubé and Gosselin 2007). The mineralization occurs in quartz or quartz-carbonate fault-fill vein arrays, hydrothermal breccias, and shallowly dipping extensional veins cutting the greenstones. The deposits are hosted in greenschist- to amphibolite-facies metamorphic rocks, reflecting development at an intermediate depth of 5–10 km, and thus represent temperatures of 325–400°C (Goldfarb et al. 2005). Gold is confined to the vein and breccia systems, but given recent increases in the price of gold, not only are the vein arrays economic, but extensive hydrothermal aureoles around the vein systems are also exploited (e.g. Gaillard et al. 2014). The timing of this style of mineralization varies systematically across complex cratons such as the Superior Province, in which the age of deposits becomes younger from north to south (Fyon et al. 1992). The timing is also synchronous with magmatism spatially associated with major transcurrent faults cutting the greenstone belts and successor basins, representing the later stages of greenstone belt tectonism. Berger (2001) has shown that post-Archean vertical movements along the Porcupine–Destor fault have exposed along-strike variability in the style of gold mineralization. The deposit style along this structure varies from brittle in the west to ductile to the east, and deposit style varies within fault segments that are bounded by Proterozoic crosscutting structures.

Syngenetic models for orogenic gold deposits are no longer viable (Goldfarb et al. 2005), although gold may have been added to the greenstone belt system through seafloor hydrothermal processes producing Au-rich pyrite (Large et al. 2011). Gold transport and deposition are probably related to metamorphic processes, given the CO_2- and S-rich nature of the fluids, the decrease in abundance of gold-associated elements (As, Sb, W, Ba, etc.) as metamorphic grade increases, and the association of these deposits with greenschist- to amphibolite-grade metamorphism (Goldfarb et al. 2005). Bleeker (2012) relates the gold-mineralizing event to regional-scale extension of the greenstone belts, given the association with alkaline to calc-alkaline volcanic rocks in the successor basins, as discussed previously.

A new age of gold mineralization in the Wawa–Abitibi terrane is represented by the Coté deposit south of Timmins, wherein gold mineralization occurs in a brecciated phase of a granitoid intrusion adjacent to a strike-slip fault just east of the Swayze greenstone belt (Katz et al. 2015). The mineralization is in the Chester granitoid complex, which lies along the interface between the Ramsey–Algoma batholith to the south and the Kenogamissi Batholith to the north. The mineralization consists of orogenic-style mineralization hosted by an intrusion-related magmatic hydrothermal breccia. Significantly, the mineralization is dated at 2737 ± 8 Ma by Re–Os isotopic dating, in contrast with the ca. 2680–2670 Ma age for most Abitibi gold mineralization (Ayer et al. 1999).

Structural overprinting relationships and the spatial association of lode gold deposits with successor basins and their major strike-slip structures indicate that the lode gold style of mineralization occurs late in greenstone belt evolution. The association of gold mineralization with silicification, Fe-carbonate alteration and elevated LILE provides evidence that the hydrothermal system associated with the deposits circulated through the mid-to-deep crust (Goldfarb et al. 2005). Goleby et al. (2004) have shown that a relationship exists between gold mineralization in the Yilgarn craton and anticlinoria associated with subjacent granitoid rocks, and more importantly, with fault systems extending from the base of the crust through to the mineralized units of the greenstone belt.

Cu–Ni–PGE and Cr Mineralization

Copper–Ni–PGE mineralization within granite–greenstone terranes occurs in: 1) concordant sills; 2) layered gabbro–anorthosite complexes; and 3) komatiitic volcanic units and coeval plutons. In the Superior Province, concordant sills include the Katimiagamak sills in the Wabigoon Subprovince (Davis and Edwards 1986), and layered gabbro–anorthosite bodies include Big Trout Lake in the North Caribou terrane (Whittaker 1986), the Bad Vermilion anorthosite in the Wabigoon subprovince (Ashwal et al. 1983), and the Weese Lake gabbro–anorthosite (Thurston and Carter 1970). PGE mineralization at Lac des Iles in the Marmion terrane is associated with late hydrothermal alteration in the so-called Roby zone (Sutcliffe et al. 1989). Fe–Ti–V mineralization is present in some layered mafic intrusions of the Abitibi greenstone belt, such as the Dore Lake complex in Chibougamau and the Bell River complex in Matagami (Allard 1976; Daigneault and Allard 1990; Taner et al. 2000).

Because of their economic importance, synvolcanic komatiite–tholeiite sequences and their related intrusions are better known. They account for about 25% of the world nickel resource for deposits grading >0.8% Ni (Lesher 1989). These deposits are located close to the basal contact of individual komatiitic flows and consist of massive and brecciated sulphides toward the base of flows, and matrix-textured and

disseminated sulphides throughout the flows. In general, this type of mineralization requires a sulphur-undersaturated magma, which becomes sulphur-saturated by assimilation of sulphur-rich rock types enroute to eruption. The massive style of mineralization reflects late assimilation, whereas the more disseminated mineralization reflects slightly earlier assimilation of sulphur. This style of mineralization is found in the Yilgarn craton at Kambalda, where the komatiites consist of thin, extensive sheet flows and thicker, channelized flows (Perring et al. 1994; Hill et al. 1994). The channelized flows may be up to 15 km long and 100 m thick; mineralization is concentrated at the base of flows in masses up to 3 km long and 5 m thick. Similar mineralization is found in komatiites of the Tisdale and Kidd–Munro assemblages of the Abitibi greenstone belt (Fyon et al. 1992; Ayer et al. 2002a) and in the Zimbabwe craton (Prendergast and Wingate 2013).

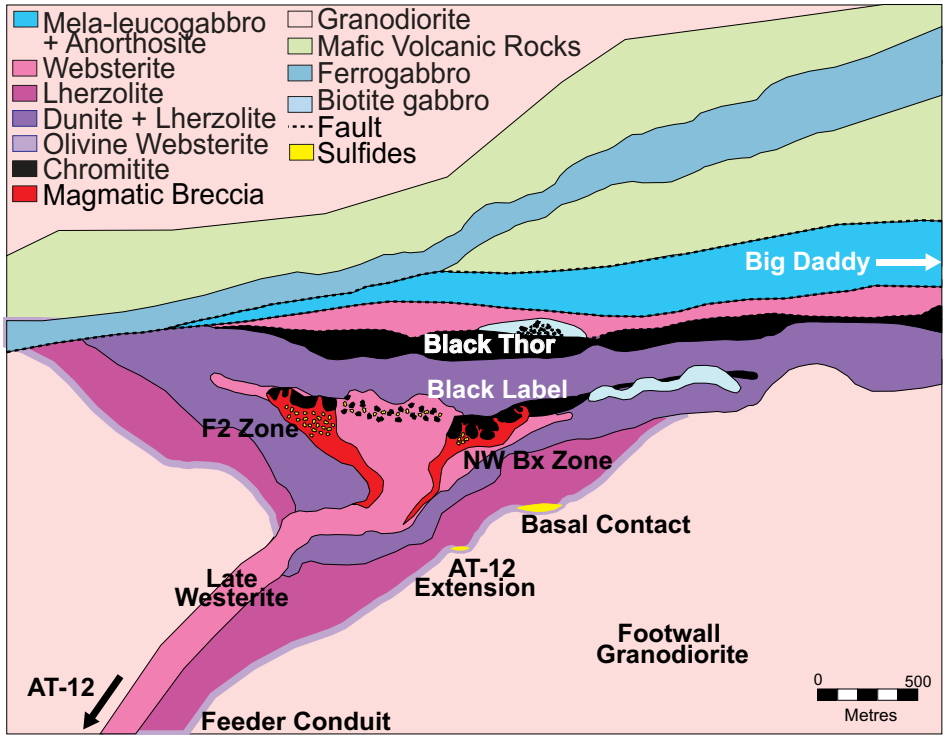

Figure 26. Schematic section of the Black Thor intrusion and associated chromite mineralization in the Ring of Fire area of the North Caribou terrane (after Carson et al. 2013).

Synvolcanic sills and intrusions of broadly komatiitic affinity also host Cu–Ni–PGE and Cr mineralization, e.g. the Bird River Sill in the Winnipeg River subprovince (formerly the Bird River subprovince; Scoates and Scoates 2013), the Shebandowan intrusion in the Wabigoon subprovince (Morin 1973), the Big Trout Lake intrusion in the North Caribou terrane (Whittaker 1986), the Kemi intrusion in the Baltic shield (Tormanen and Karinen 2011), and sills related to the Bulawayan Group komatiites (Prendergast and Wingate 2013). Largely post-tectonic intrusions also host Cu–Ni–PGE mineralization in the Superior Province, e.g. Lac des Iles (Sutcliffe et al. 1989).

High Cr, low-MgO (18–24%) komatiitic magmas may contain a distinct type of chromite mineralization that differs from the classic stratiform and podiform styles. This type occurs in the Baltic shield, Zimbabwe, Brazil and India as well as in the so-called 'Ring of Fire' intrusions in the eastern part of the North Caribou Terrane (Mungall et al. 2010; Carson et al. 2013). The Black Thor intrusive complex in the North Caribou terrane consists of lower and middle ultramafic zones and an upper ultramafic to mafic zone. The mineralization occurs mainly in the middle ultramafic zone as chromite-rich layers interstratified with dunite and peridotite. The deposit contains about 102 M tonnes, has an aggregate thickness of up to 100 m, and a strike length of 3 km within a relatively small intrusion (Carson et al. 2013; Fig. 26). The thickness and lateral extent of the chromite mineralization mitigates against *in situ* fractionation such as is observed in a layered intrusion. Instead, Carson et al. (2013) appeal to deposition of the large volumes of chromite in a conduit feeding superjacent komatiite-associated magmatism. Similar ages of mafic and ultramafic intrusions across the Superior Province (from the Bird River area, through the North Caribou terrane to the La Grande and Eastmain domains in Québec) suggest that mafic–ultramafic intrusions in these areas may constitute a distinct Cr–Ni–Cu–PGE–V metallotect 'fundamentally different' from the rest of the Superior Province (Houlé et al. 2012). Such a metallotect crossing many terrane boundaries late in Superior Province history implies a distinct, late event such as plume magmatism or crustal delamination.

Of tectonic importance is the observation of shear-bounded ultramafic intrusions along the interface between the Wabigoon subprovince and the Quetico metasedimentary subprovince to the south, which may indicate tectonic emplacement (Pettigrew and Hattori 2006). In areas removed from greenstone belts, mineralized, relatively small mafic to ultramafic intrusions occur among granitoid units. Given their limited importance, they are not discussed further.

Pegmatite-Hosted Rare Metal Deposits

Pegmatites and associated rare metal deposits occur within granitoid batholiths or as dikes in the country rock. The pegmatites originate by initial undercooling of granitoid magma to produce the outer zones of the pegmatites, followed by crystallization of very coarse-grained interiors rich in unusual minerals produced by 'constitutional zone refining.' This leads to build-up of fluxing components in a boundary layer, which advances within the pegmatite (London and Morgan 2012). Most Archean pegmatites occur within or proximal to peraluminous or S-type granites (Breaks and Moore 1992; Fyon et al. 1992; Stone 2005), which develop relatively late in the evolution of granitoid rocks in granite–greenstone terranes; they occur as linear plutons proximal to major transcurrent structures, and as batholiths within granite–greenstone terranes and sedimentary subprovinces. Examples of pegmatite-associated mineralization within the Superior Province include: 1) Li and Be occurrences in pegmatites located along a late structure crosscutting the central part of the North Caribou terrane

(Stone 1998); 2) pegmatites associated with peraluminous granites in the Abitibi greenstone belt; and 3) pegmatites along the Winnipeg River–Wabigoon subprovince boundary (Fyon et al. 1992). Similar peraluminous granite-associated deposits are known in the Yilgarn craton (Flint 2010) and on other Archean cratons.

ARCHEAN *VS.* PROTEROZOIC GREENSTONE BELTS

Introduction

This article has emphasized Archean greenstone belts, but when we consider a broad definition of greenstone belts as Precambrian belts of low grade, largely volcanic rocks surrounded by granitoid batholiths (e.g. Hunter and Stowe 1997), many Proterozoic orogens have regions that fulfill the definition. Examples include the Trans-Hudson orogen (Gibson et al. 2011) and the multitude of Proterozoic orogens of Africa (Allibone et al. 2002). The major differences between Archean and Proterozoic greenstone belts are summarized below.

Rock Types

Conventional wisdom has it that Proterozoic greenstone belts lack komatiites. However, the greenstone belts of West Africa (Abouchami et al. 1990) do contain komatiites. The inference is that, although there was a global mantle overturn event at approximately 2.5 Ga (Van Kranendonk 2012), komatiite generation continued for some time after. Comparisons of basalt compositions show that Proterozoic basalts do not display the high Fe content of Archean basalts (Francis et al. 1999).

Mapping in Paleoproterozoic orogens such as the Trans-Hudson orogen (Lucas et al. 1996), the Cape Smith belt (Lesher 2007), and the Fennoscandian shield (Gaál and Gorbatschev 1987) reveals the presence of oceanic floor and oceanic plateau basalts and ophiolites (Galley et al. 2007b). In contrast, there have been contrasting claims about whether or not Archean ocean floor rocks are preserved (Martin et al. 1993; Bickle et al. 1994; Kusky 1998; Kusky et al. 2001). This issue will be discussed more extensively in a subsequent section.

The abundance of TTGs decreased with time and they become lower in Al (Martin 1987); granitoid magmatism in general becomes more potassic in the Proterozoic (Fumerton et al. 1984). Successor basins developed in Proterozoic greenstone belts are similar to those in Archean greenstone belts; for example, they contain clast populations demonstrating granite unroofing (Ansdell et al. 1999).

Structural Style

In contrast to the dome-and-keel structural style of Archean greenstone belts, individual lithotectonic assemblages in Proterozoic greenstone belts are thrust-bounded packages (Lucas et al. 1996). When Proterozoic orogens as a whole are considered, they vary from clearly accretionary systems to abnormally thick crustal sections related to accretion (Korja et al. 2006).

ARCHEAN TECTONIC MODELS

General Considerations

The tectonic processes that produced the unusual rock types and structural style of Archean greenstone belts are important in developing a full understanding of the genesis of Archean granite–greenstone terranes. Identification of the processes involved centres upon the presence or absence of horizontal processes, i.e. Archean plate tectonics *vs.* vertical processes such as granitoid diapirism and convective overturn. If greenstone belts originate by completely autochthonous processes, this would tend to minimize the importance of horizontal tectonics. If, on the other hand, greenstone belts are allochthonous, complete with fold and thrust belts, metamorphic core complexes, ophiolites, blueschists, etc., then Archean tectonic processes should be little different from those observed in younger orogens. Like most geological problems, there are advocates on both sides of the issue; for example, Hamilton (1998), Stern (2005), and Bédard et al. (2013) favour the autochthonous model, whereas Langford and Morin (1976), Polat et al. (1998), Hollings and Kerrich (1999), and Percival et al. (2004) argue for the allochthonous model. This discussion will review the evidence for both hypotheses.

Plate Tectonic Origin for Granite–Greenstone Terranes

The plate tectonic model for the modern Earth is characterized by the presence of seafloor spreading, subduction (including its related distinctive magmatism), and continental drift. The operation of the model in the Archean should result in the preservation of rocks and primary structures representing distinct geodynamic settings: ocean floor, island arcs, continental arcs, passive margins, subduction-related mélanges, and metamorphic belts. Langford and Morin (1976) proposed a plate tectonic origin for the Superior Province. They noted the fundamentally different character of granite–greenstone terranes *vs.* sedimentary subprovinces in the northwestern part of the Superior Province in terms of rock types, metallogeny, stratigraphy and radiometric ages. The hypothesis was supported by a limited number of U–Pb zircon ages showing that the northern part of the Superior Province is older than the greenstone belts to the south (Krogh and Davis 1971). More recent syntheses of Superior Province geology (Card 1990; Williams et al. 1992) have fleshed out the concepts. Percival and coworkers (Percival et al. 2004, 2006; Percival and Helmstaedt 2006) established over 20 domains, terranes, subprovinces and superterranes in the Superior Province. These authors classify the various tectonic blocks as continental fragments (e.g. North Caribou, Marmion, and Winnipeg River terranes) separated by volcanic-rich oceanic domains (e.g. the Wawa–Abitibi and Wabigoon terranes, and Oxford–Stull domain) and orogenic flysch belts (e.g. the English River, Quetico, and Ashuanipi belts).

Evidence favouring the plate tectonic hypothesis in the Superior Province includes: 1) the long, linear nature of the various tectonic blocks; 2) an orderly southward-younging of the ages of volcanism, plutonism, and shear zones (Fig. 27) bounding major tectonic blocks; and 3) a crustal structure observed in reflection seismic images that is consistent with accretionary tectonics (Calvert et al. 1995; Calvert and Ludden 1999; White et al. 2003; Percival et al. 2004a; Percival and Helmstaedt 2006). The plate tectonic hypothesis calls for a ca. 2720 Ma amalgamation of the Hudson Bay terrane (or Northern Superior superterrane) with the North Caribou terrane, followed by the Uchian orogeny in which the North Caribou, English River, and Winnipeg River terranes are accreted at about 2700 Ma, and finally the Shebandowanian orogeny in

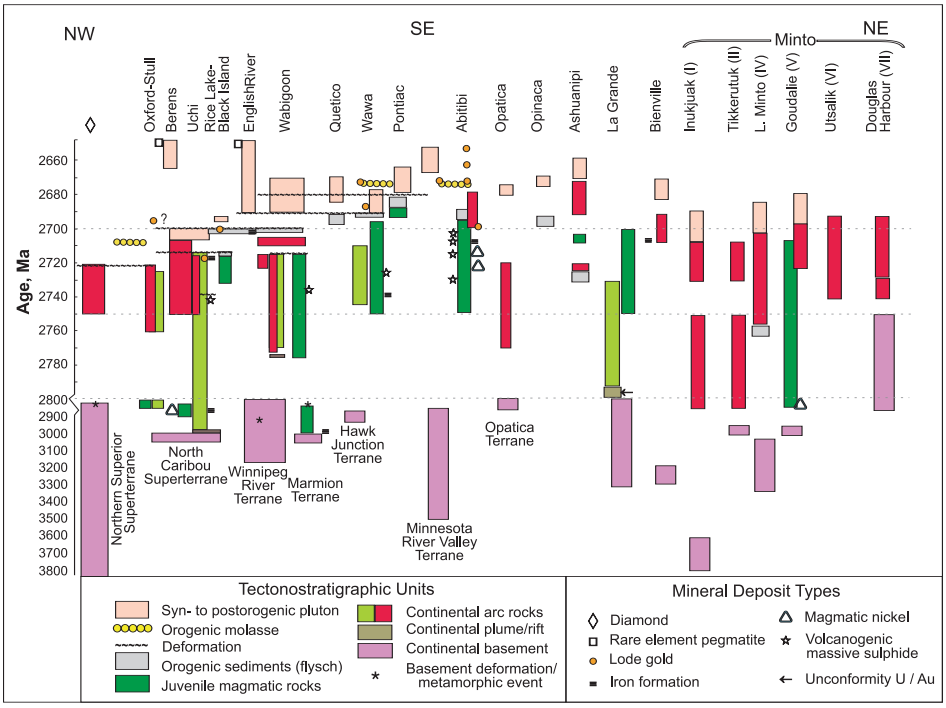

Figure 27. Time-space chart for the Superior Province by Percival (2007).

which the composite Superior superterrane collides with the Wawa–Abitibi terrane at about 2690 Ma (Fig. 1).

Another major line of evidence for the plate tectonic hypothesis is the presence in greenstone belts of relatively unusual, geochemically-defined rock types having linkages to plate tectonic processes in younger orogens, as discussed previously. The most extensive research on these unusual rocks has been done in the Superior Province. They include boninites (Kerrich et al. 1998) in the komatiite–tholeiite geochemical association, and adakites, high-Mg andesites, and Nb-enriched basalts in the bimodal geochemical association. The adakites and related rocks are found in volcanic units (e.g. Hollings and Kerrich 2000; Wyman et al. 2000; Polat and Kerrich 2001; Boily and Dion 2002), syn- to late-tectonic batholiths (Feng and Kerrich 1992), and in post-tectonic diorites/sanukitoids (Smithies and Champion 2000). These unusual rock types are also documented in the Yilgarn (Angerer et al. 2013), Pilbara (Smithies 2002), Baltic (Shchipansky et al. 2004), Dharwar (Manikyamba et al. 2005; Naqvi et al. 2006; Naqvi 2008), and Kaapvaal (Wilson 2002) cratons.

Many authors point to reflection seismic images as evidence for the operation of plate tectonics in the development of the Superior Province (Percival et al. 2004, and references therein). The presence of fossil subduction zones in reflection seismic profiles has been discussed in a previous section. However, similar structures beneath the Yilgarn craton are interpreted to indicate delamination at the base of the crust (Goleby et al. 2006).

The 'Metamorphic Core Complex' Model

Alpine-style thrusting allied with extension can produce so-called 'metamorphic core complexes.' Such a model has been proposed for the Superior (Sawyer and Barnes 1994) and Pilbara (Bickle et al. 1980; Zegers et al. 1996; Blewett 2002) cratons. This style of tectonics requires extensive normal faulting and extension such that domical zones of high metamorphic grade rocks (centred on granitic batholiths) form the structures known as metamorphic core complexes. The advent of widespread geochronology in granite–greenstone terranes has ruled out the extensive duplication of strata expected with such a model in either of these cratons, as seen in more recent descriptions (Van Kranendonk et al. 2007a; Thurston et al. 2008).

The 'Mantle Wind' Model

The continued northward motion of the Indian microcontinent leading to collision with Eurasia has taken place over ca. 50 m.y. without the presence of a plate boundary driving force. Alvarez (2010) advanced the concept of 'basal traction,' or more colloquially the 'mantle wind,' as the driving force for this movement. This mechanism is the basis for an alternative tectonic model for the Archean (Bédard et al. 2013), as summarized in the following paragraphs.

The model requires the development of cratonic 'roots' or 'keels' that extend to or beyond the lithosphere–asthenosphere boundary. These keels obstruct upper mantle flow, which deflects around the keels and also has the effect of moving them. This process provides the force to move continental blocks, resulting in the accretion of microcontinental fragments to make cratons. The individual microcontinental blocks represent oceanic plateaux in which komatiitic to tholeiitic greenstones develop, and the increasing thickness of these plateaux would bring basaltic material down to depths required to produce TTGs and TTG-related felsic volcanic rocks.

However, the oceanic plateaux suggested in the Bédard et al. (2013) model (Fig. 28) probably differ from modern equivalents. As noted by Kamber (2015), the consistent upward younging of greenstone stratigraphy described above for most greenstone belts is the essence of a volcanic plateau. Kamber (2010) also noted the existence in the Archean of a second type of landmass, based on the REE chemistry of marine chemical sediments and their Sr- and Nd-isotopic systematics. Any postulated Archean volcanic plateau would differ from modern oceanic plateaux in terms of: 1) the presence of syn-volcanic granitoid rocks; 2) the prevailing extensive hydration of Archean basalts in greenstone belts; and 3) the presence of thick cratonic mantle keels (Kamber 2015). The thickness and higher temperature of Archean plumes would have permitted the vertical growth of thick volcanic plateaux.

In the absence of plate tectonics, how are the overprinting structural fabrics and shortening in Archean orogens explained? If the Archean lacked subduction zones, then a global oceanic spreading ridge system cannot have existed, leaving only oceanic plateau crust – broadly comparable to the mafic units of greenstone belts. In this model, contractional structures and accreted terranes would develop at the leading edge of the craton and strike-slip structures at the sides.

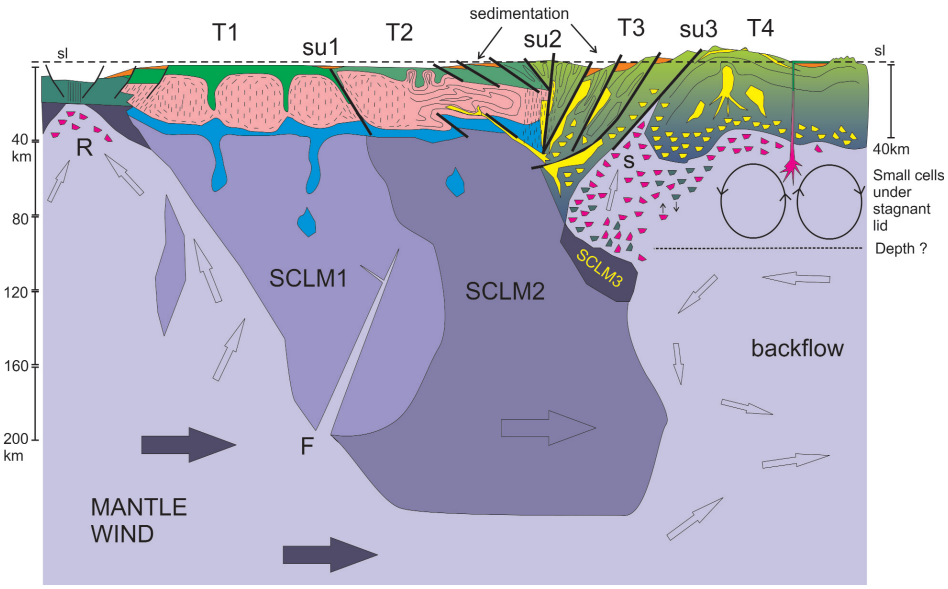

Figure 28. Bédard et al. (2013) mantle wind model. In this model, a composite older terrane consists of two terranes (T1 and T2) each with subjacent sub-continental lithospheric mantle keels (SCLM 1 and 2) separated by a soft-docking suture. Terrane 1 is characterized by vertical fabrics in the TTG dominated mid-crust, whereas T2, originally similar, has been overprinted during accretion to T1 and T3. Terranes T3 and T4 are simatic oceanic plateau crust. Mature sedimentary rocks develop in localized ensialic basins or at craton margins. Terrane 4 is building up a thick plateau through underplating and eruption of basalt (red) and is underlain by small convection cells. Anatexis generated juvenile TTGs (yellow) are produced and at this stage, dome and keel structures also develop. SU1 is a soft-docking suture between T1 and T2. SU2 is a suture separating T2 and T3 with much flattening in the proximal lower crust. SU3 separates T3 and T4 and has thinner crust underlain by hot mantle.

DISCUSSION

Introduction

Having described the essential elements of the plate tectonic model for Archean granite–greenstone terranes and the major competing 'mantle wind' model, a critical examination of the relationship of features of granite–greenstone terranes to one or the other tectonic model is useful. In contemplating whether plate tectonics operated in the Archean, it must be remembered that the dominant force in the plate tectonic paradigm is the sinking of cold, dense lithosphere. Therefore, plate tectonics requires a lithosphere that is sufficiently cool to allow it to sink into the asthenosphere (Stern 2008).

Missing Plate Tectonic Indicators

Numerous authors have noted the nearly complete absence of ophiolites, Atlantic-style passive margins, overprinting fold-and-thrust belts, paired metamorphic belts, ultra-high-pressure (UHP) and ultra-high-temperature (UHT) metamorphic assemblages, and subduction zone mélanges in Archean granite–greenstone terranes (Kröner 1991; Chardon et al. 1996; Hamilton 1998, 2007; Bleeker 2002; McCall 2003; Stern 2005, 2008; Brown 2006, 2007). Subsequent investigations (Bédard et al. 2013) have noted the absence in greenstone belts of both the extensive talus and lahar aprons surrounding 'arc' sequences (perhaps a preservation problem?), and the orogenic andesites typical of continental and island arc systems. Archean granite–greenstone terranes also lack the high proportion of mudstone found in modern orogens (Thurston 2012).

Ophiolites

Ophiolites consist of two types: 1) Cordilleran ophiolites that are scraped off downgoing oceanic crust; and 2) Tethyan ophiolites obducted onto continents by failed continental subduction (Sylvester et al. 1997). The presence of distinctive sheeted dike arrays within ophiolites is a function of the balance between spreading rate and magmatism (Robinson et al. 2009). Although Archean ophiolites have been proposed (Helmstaedt et al. 1986; de Wit et al. 1987; Kusky 1998; Kusky et al. 2001; Dilek and Polat 2008), nowhere is a full ophiolite section of Archean age preserved. In a putative example of Archean oceanic crust reported by Kusky and Kidd (1992), Bickle et al. (1994) found basal unconformities rather than tectonic contacts, xenocrystic zircons indicating interaction with older crust, isotopic and geochemical evidence of crustal contamination, and intrusive relationships between older basement and the internal stratigraphy of the purported ophiolite. If Archean oceanic crust were thicker than modern oceanic crust (Sleep and Windley 1982; Hoffman and Ranalli 1988), deeper crust characterized by distinctive ophiolite features such as sheeted dikes may well have been subducted (Condie and Benn 2006). The proposed ophiolite in the Kam Group of the Yellowstone greenstone belt in the Slave Province (Helmstaedt et al. 1986) has been disproved using trace element geochemistry and Nd isotopic data (Cousens 2000). Similarly, the proposed 2.5 Ga Dongwanzi ophiolite (Kusky et al. 2001) has subsequently been questioned (Zhai et al. 2002).

Atlantic-Style Passive Margins

Atlantic-style passive margins featuring widespread units of shallow-water carbonate and siliciclastic rocks do not exist in Archean granite–greenstone terranes. In the La Grande subprovince, lateral transitions over a distance of 5–8 km have been observed from shallow-water quartz arenites displaying cross-stratification and mud drapes, to submarine fans containing sheet sandstones (Goutier 2006). Sedimentary carbonate units in the Archean are rare and of limited lateral extent (Ojakangas 1985). However, Condie and Benn (2006) point to sequences such as the Moodies Supergroup of South Africa (Lowe et al. 1999) as possible analogues of Atlantic margins.

Deep-Water Sedimentary Rocks

Metasedimentary rocks, especially mudrocks, make up only a very small proportion of volcanic successions in Archean greenstone belts of most cratons, including the Superior Province (Williams et al. 1992), the Yilgarn craton (Myers and Swager 1997), the Pilbara craton (Barley 1997) and the West African craton (Attoh and Ekwueme 1997). Although wacke–pelite sequences are rare in greenstones of the Superior and Kaapvaal cratons, they do make up much of the sedi-

mentary subprovinces of the Superior craton (Williams et al. 1992) and the Limpopo belt of the Kaapvaal craton (Eglington and Armstrong 2004). In contrast, the Slave craton has areally extensive sediments overlying the greenstone belts (Bleeker and Hall 2007). In modern orogens, deep-water sedimentary rocks consist of ~70% mudstones (Aplin and Macquaker 2011).

Fold and Thrust Belts

There are numerous descriptions of thrusting within greenstone belts on most cratons (de Wit et al. 1987; Devaney and Williams 1989b; Van Kranendonk et al. 2002; Bleeker 2012; Furnes et al. 2013). The crucial question is whether the thrusting is local or larger in scale. Greenstone belts in the Superior craton (Williams et al. 1992), the Pilbara craton (Van Kranendonk et al. 2004), and in Zimbabwe (Prendergast 2004), as typical examples, feature upward-facing, upward-younging stratigraphy, and no major thrust-based stratigraphic duplication or long-distance tectonic transport by thrusts. Reflection seismic images (Goleby et al. 2004; Snyder et al. 2008) show that there is no kilometre-scale thrust transport of greenstone sequences, in contrast to the structural style of Phanerozoic accretionary orogens (Percival et al. 2004).

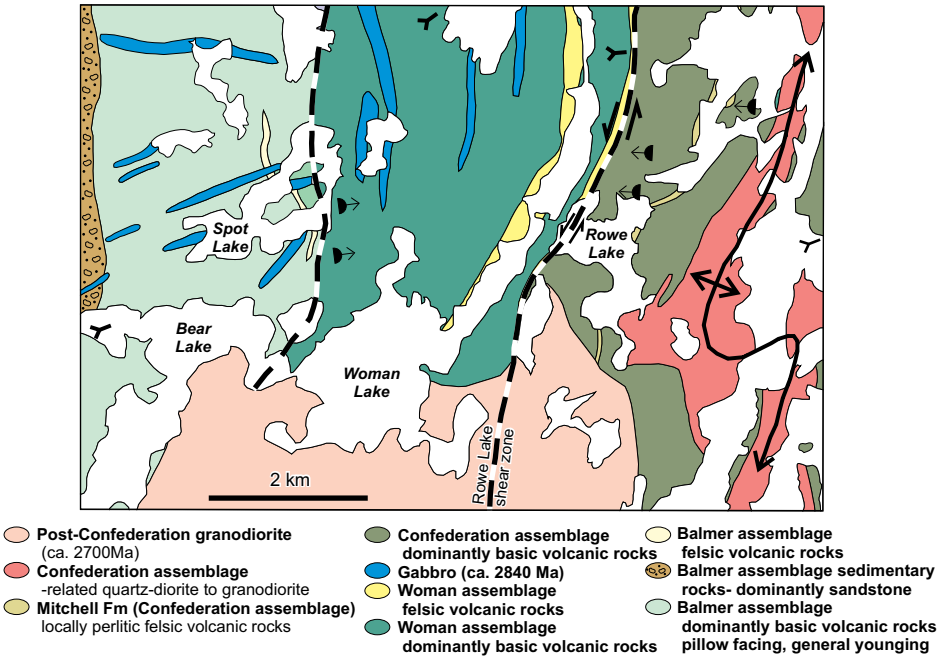

Figure 29. Dikes of 2832 Ma age (shown as 2840 Ma) cutting the basal ca. 2.9 Ga Balmer assemblage and the ca. 2.8 Ga Woman assemblage in the Confederation Lake greenstone belt east of Red Lake illustrating the autochthonous nature of the younger greenstones in this area (after Thurston et al. 2002 and Rogers et al. 2000). Location is number '3' on Figure 1.

Blueschists, Ultra-High-Pressure Rocks, and Paired Metamorphic Belts

Blueschist metamorphic rocks typical of subduction zones are not known in the Archean, probably because of higher thermal gradients (Hamilton 1998) and the difficulty of rapid exhumation (Ernst and Liou 1999). Likewise, ultra-high-pressure rocks of Archean age are rare (Brown 2007; Stern 2008), although they are found at Gridino on the White Sea in the Karelian craton (Perchuk and Morgunova 2014). Paired metamorphic belts consist of a trench-proximal, high pressure, low temperature belt succeeded inland by a low pressure, high temperature belt. Such pairings, typical of subduction settings (Miyashiro 1973), are not found in the Archean, again a likely function of the Archean thermal regime (Komiya et al. 2002).

Structural Style

The dome-and-keel structural style of Archean greenstone belts is unique and not repeated in subsequent earth history (Bédard et al. 2013). Although there is a southward younging of plutonism, volcanism, and shear zones in the Superior Province, each major terrane has a unique, specific assemblage of rock types and event ages (Percival 2007). These relationships have been interpreted in terms of a plate tectonic scenario (Percival 2007), but it must be borne in mind that these relationships are also consistent with simple lateral transport of individual terranes.

Autochthonous vs. Allochthonous Greenstone Belts

If greenstone belts are autochthonous, this would tend to support a non-plate tectonic origin; however, it is still possible to consider autochthonous greenstones to represent some sort of continental arc setting. Listed below are characteristics of greenstones supporting an autochthonous origin.

1) *Diking relationships* in the Abitibi greenstone belt (Ayer et al. 2005) and the Confederation Lake greenstone belt of the North Caribou terrane (Rogers et al. 2000) show that dikes cutting older units are feeders to overlying volcanic units (Fig. 29); thus, older units in two major Superior Province greenstone belts were present when younger units were deposited. This may represent a limited dataset, but it is in two critical areas for interpretation of Archean tectonics in the Superior Province: the North Caribou superterrane (see also Parks et al. 2006) respecting the superterrane as a whole, and the Abitibi greenstone belt.
2) *Isotopic inheritance* is seen in recent U–Pb zircon age determinations in about 15% of samples from the Abitibi greenstone belt. The xenocrystic zircon grains are found in younger greenstone units and represent the ages of underlying volcanic units (Ayer et al. 2005). Similar inheritance patterns are seen in the Marmion terrane (Buse et al. 2010) and in the North Caribou terrane (Parks et al. 2006) of the Superior Province. In the Murchison domain of the Yilgarn craton (Van Kranendonk et al. 2013), 39 of 117 U–Pb zircon ages (mainly of greenstone belt units) show xenocrystic zircons. Extensive isotopic inheritance is described in the Pilbara terrane (Van Kranendonk et al. 2007a). However, the Abitibi greenstone belt units are largely juvenile and gener-

ated in contemporaneous depleted mantle (Corfu and Noble 1992; Carignan et al. 1993; Vervoort et al. 1994). Nevertheless, Hf isotope data show that the western edge of the Abitibi greenstone belt was underlain by 2.8–2.9 Ga crust (Ketchum et al. 2008).

3) *Contamination* of Archean basalts, based on negative Ti, Nb and Ta anomalies, is postulated to represent contamination of basaltic magmas through contact with granitoid rocks (Thurston 2002, and references therein), although these features can also be explained by magma origins in subduction systems (Polat et al. 1998; Hollings and Kerrich 2000) or by melting of over-thickened mafic crust (Hoffmann et al. 2011).
4) *Basal unconformities* between basement and greenstone belt units imply either a continental arc setting for a given belt, or autochthonous development (Thurston 2002). Basal unconformities are widespread in the North Caribou terrane (Thurston et al. 1991), at Steeprock in the Marmion terrane of the Superior Province (Wilks and Nisbet 1988), in the Slave craton (Bleeker 2002), and in the Belingwe greenstone belt of Zimbabwe (Bickle et al. 1994). Subtle cryptic unconformities can be marked by leaching of underlying greenstones (Thurston and Kozhevnikov 2000).
5) *Stratigraphic patterns*: The volcanic units in most major greenstone belts worldwide display upward-facing sequences, along with the younging of volcanic units away from granitoid bodies, indicating that the batholiths and surrounding volcanic rocks represent a series of crustal sections (Van Kranendonk et al. 2002; Thurston et al. 2008). In the larger greenstone belts, some fundamental conundrums exist. For example, the seven volcanic assemblages of the Abitibi greenstone belt (Thurston et al. 2008) represent a total stratigraphic thickness of at least 45 km. However, the greenstone belt is at sub-greenschist to greenschist grade (Easton 2000), which is difficult to reconcile with an average geothermal gradient of 25–30°C/km. Have large greenstone belts (Fig. 2) undergone thrust-based condensation of stratigraphy? Is there some sort of volcanism-induced subsidence (Hargraves 1976), or is the stratigraphic thickness a function of onlapping stratigraphic lenses? In contrast to Phanerozoic orogens, most greenstone belts do not display evidence for large-scale horizontal tectonic transport. For example, in the Abitibi greenstone belt, Thurston et al. (2008) note a lack of evidence for large-scale thrusting, whereas in detailed seismic sections (Snyder et al. 2008), there are few out-of-sequence volcanic units (Ayer et al. 2005), and detailed structural studies (Benn and Peschler 2005) all indicate no large-scale thrusting. The stratigraphic map of the Abitibi greenstone belt (Thurston et al. 2008; Fig. 18) demonstrates off-lapping stratigraphic geometry. Similar patterns of upward-facing, upward-younging stratigraphy are seen in the North Caribou terrane (Thurston et al. 1991; Sanborn-Barrie et al. 2001), the Wabigoon subprovince (Sanborn-Barrie and Skulski 2006), and the Pilbara (Van Kranendonk et al. 2007a), Yilgarn (Van Kranendonk et al. 2013), and Zimbabwe (Bickle et al. 1994) cratons.

The stratigraphy of plume-related units in the Abitibi greenstone belt shows some interesting patterns involving potential structural controls. There are basically three plume events in the Abitibi greenstone belt: 1) the 2723–2720 Ma Stoughton–Roquemaure episode; 2) the 2719–2711 Ma Kidd–Munro episode (including the 2717–2714 Ma La-Motte–Vassan Group in Québec); and 3) the 2710–2704 Ma episode (Tisdale in Ontario and Jacola in Québec), collectively related to a single plume in which magma separation occurred at increasingly shallower depths (Sproule et al. 2002; Dostal and Mueller 2013). The komatiites occur along two crustal-scale fault zones, suggesting that the plume either created or followed these zones of weakness. Interdigitation of compositionally different komatiites and tholeiites in small-volume (1–10 km^3) flows suggests a compositionally heterogeneous plume; selective tapping of various plume zones would then explain this style of compositional variation. Dostal and Mueller (2013) compare this situation to the Yellowstone hotspot, which developed over ca. 17 m.y. and had a diameter of about 300 km.

Archean greenstone belts present a paradox, in that rocks of the komatiite–tholeiite association are of plume derivation and make up 80–90% of many greenstone belts (Ayer et al. 2005; Van Kranendonk et al. 2007a; Thurston et al. 2008; Barnes and Van Kranendonk 2014), whereas interbedded calc-alkaline units have been interpreted to represent convergent margin processes. Plume–arc interaction has been invoked (Kerrich et al. 1998; Wyman et al. 2002), but a scale problem and a mechanical problem both emerge when one observes that, in the Yilgarn (Barnes and Van Kranendonk 2014), extensive plume-related komatiites and tholeiites are accompanied by minor accumulations of calc-alkaline andesite to dacite/rhyolite. In the Abitibi greenstone belt there is a four-fold repetition of this pattern (Ayer et al. 2002b), requiring an appeal to multiple episodes of arc–plume interaction (Bédard 2013; Bédard et al. 2013). Wyman and Kerrich (2009) respond by proposing a subduction zone along the entire south margin of the Superior Province.

Evidence for Modern Plate Tectonic Interpretations

The term, 'oceanic domains,' is controversial. The 'oceanic domains' of Percival (2007) should display no isotopic inheritance; however, it must be borne in mind that an age difference between two units of at least 150 m.y. is necessary for discernible evidence of inheritance to be apparent in the Sm–Nd and Lu–Hf systems (Larbi et al. 1999). Second, the process of searching for datable zircon grains in a geochronological lab involves a general process of: 1) ignoring high-U grains, in that they are strongly discordant; and 2) concentration on one or two zircon populations in order to obtain a crystallization age. Thus, 20th century U–Pb zircon geochronology rarely found zircon xenocrysts. With the advent of single-grain dating, researchers have found xenocrystic zircons in multiple 'oceanic domains,' including modern oceanic crust (Pilot et al. 1998; Tapster et al. 2014) and in Archean settings such as the Abitibi

greenstone belt (Ayer et al. 2005) and the Marmion terrane (Tomlinson et al. 2003; Buse et al. 2010). Similar patterns of xenocrystic zircons representing subjacent units are now found in other cratons, such as the East Pilbara (Van Kranendonk 2012) and the Yilgarn (Claoué-Long et al. 1988).

Much of the evidence for any plate tectonic interpretation of granite–greenstone terranes lies in the geochemistry of the volcanic units and the post-TTG granitoid rocks. As described previously, geochemical signatures of 'arcs' are found both in the mafic and the felsic volcanic units within greenstone belts. The geochemical signature of modern arcs consists of: 1) enrichment of LILE (Sr, K, Rb, Ba) *vs.* HFSE (Th–Yb), which exhibit MORB-like concentrations. In addition, arc rocks show distinctive negative anomalies for Ti, Nb and Ta. However, the stratigraphic/tectonic location of Archean greenstones with the 'arc' signature is critical to their interpretation. 'Arc' rocks in greenstone belts occur mainly in the bimodal geochemical association in both the basaltic basal zones of these sequences and in the isolated felsic eruptive centres (Ayer et al. 2005) and, more rarely, in distinct tectonically-bounded zones of greenstone belts (Lodge et al. 2013).

There is evidence for large-scale tectonic transport of terranes (as distinct from stratigraphic units) in the Superior Province; this is seen in the uniform northward vergence of structures associated with terrane margins (White et al. 2001). In addition, the provenance of sedimentary rocks in the sedimentary subprovinces indicates derivation from terranes on the north margins of, for example, the English River (Breaks 1991; Hrabi and Cruden 2006) and the Quetico (Williams 1991) subprovinces. Inevitably, the margins of cratonic blocks in Archean orogens will demonstrate structural complexity. For example, Kusky and Polat (1999) describe the intercalation, along the south margin of the Wawa–Abitibi terrane, of tholeiitic to calc-alkaline basalts (island arc?) and metasedimentary rocks that are collectively interpreted to represent an accretionary collage. The thrust-telescoped transition along the south margin of the Wabigoon subprovince, from alluvial metasedimentary rocks and back arc basalts, through submarine fan sedimentary rocks and arc basalts, to abyssal wackes and oceanic basalts (Tomlinson et al. 1996), has been interpreted to record plate-related accretion (Devaney and Williams 1989).

Inconsistencies in the Plate Tectonic Model for Archean Greenstone Belts

In this section, the various inconsistencies in the plate tectonic model for Archean greenstone belts are enumerated, with emphasis on the Superior Province.

Geochemistry and Stratigraphy

Researchers of the Kerrich school (Kerrich, Wyman, Polat and Hollings) have found small volumes of unusual rock types such as boninites, adakites, Nb-enriched basalts and magnesian andesites within greenstone belts of the Superior Province, as described above. Similar features are found in the Pilbara craton (Smithies 2002; Smithies et al. 2005, 2007). Given the fact that approximately 90% of greenstone belt stratigraphic sections are plume-derived tholeiites and komatiites, arc–plume interaction (Wyman and Hollings 1998; Wyman and Kerrich 2009) is the conventional explanation for an apparent stratigraphic alternation of plume-derived units and units with an 'arc' signature. However, it is difficult to envision mechanisms for alternating between plumes and arcs on an erratic basis (Maurice et al. 2009; Leclerc et al. 2011); for example, a four-fold repetition of such a process is required, according to this model, to explain the stratigraphy of the Abitibi greenstone belt, although one can also appeal to the slab window hypothesis (Thorkelson 1996). It must be borne in mind that a subduction-related origin, proposed by some authors for the adakites, magnesian andesites and Nb-enriched basalts in Superior Province greenstones, can be explained by other processes.

The Andesite Problem

One of the more intriguing differences between Archean greenstones and modern orogens concerns the lack of andesites in the former. Classical fractional crystallization from basalt to granite should yield more andesites than are seen in greenstone belts (Thurston et al. 1985). Intermediate volcanic rocks in the andesite compositional range are scarce in komatiite–tholeiite geochemical associations of greenstone belts (Ayer et al. 2005) and are somewhat more abundant but still rather scarce in the bimodal geochemical association (Thurston et al. 1985). However, Archean andesites do not approach the nearly 40% abundance seen in the modern continental arc record and just slightly less in oceanic arcs (Winter 2001, p. 326). Archean andesites generally lack the diagnostic plagioclase and pyroxene phenocrysts of modern andesites (Thurston and Fryer 1983; Ayer et al. 2005). Leclerc et al. (2011) show that andesites in the Chibougamau area of the Abitibi greenstone belt occur as thin packages in a monotonous sequence of tholeiites and komatiites, and suggest that they are a mixing product. Some Archean andesites are products of fractionation from basaltic precursors (Thurston and Fryer 1983), some are produced by contamination of mafic magmas (Szilas et al. 2013; Barnes and Van Kranendonk 2014), and others are produced through what is considered to be an 'arc' petrogenesis (Polat et al. 1998; Polat and Kerrich 2002). The andesites in modern orogens are a product of the mixing of mantle-derived basaltic melts with fused granitoid material in the overlying continental crust (Gill 1981). Many Archean greenstones are either deposited on basement or have older granitoid rocks in the vicinity, indicating that granitoid material was available, if the Phanerozoic andesite petrogenetic model were found applicable to the Archean.

TTG Volumes and Their Production by Subduction-Related Melting

Archean TTGs make up as much as 90% of the presently exposed middle crust and deep crust of Archean cratons (Windley and Garde 2009; Bédard et al. 2013). However, Condie (1993) demonstrated, using the composition of Archean metasedimentary rocks, that, on average, Archean continental crust is more mafic than TTGs. Archean TTGs display steep REE patterns, considered by most researchers to be generated by anatexis of basic rocks, leaving behind garnet-bearing, feldspar-free residues. To explain the steep REE patterns, these rocks must either be products of small-degree melts, or have garnet in the residue (Martin 1987; Smithies and Champion 2000). Bédard et al. (2013) provide a series of argu-

ments to demonstrate the difficulty of generating the great volumes of TTGs in middle to deep crust by subduction processes. For example, given the 40 km thickness of northeastern Superior Province crust and its width of 500 km, some 20,000 km^3 of TTG/km of strike length must be generated in the 300 m.y. interval from 3.0 to 2.7 Ga. Furthermore, when the 2740–2720 Ma actual range of TTG ages in the northeastern Superior Province is factored in, 10,000 km^3 of TTG/km of strike length must be generated in a 20 m.y. period. If this is accomplished by 10% melting of a 10 km thick slab moving at 1.2 cm/year, then only 3600 km^3 of TTGs are generated in 300 m.y. In short, to generate the observed volume of TTGs in the northeastern Superior Province, six subduction zones operating an order of magnitude faster is required. These calculations assume melting of the entire 10 km thickness of the oceanic slab, which is also not realistic.

Role for Lateral Accretion?

Early investigators (Langford and Morin 1976; Card 1990) interpreted the southward younging of the ages of volcanic rocks, granitoid rocks, and terrane-bounding shear zones in the Superior Province in terms of plate tectonic processes. The argument can also be advanced that the southward-younging ages of shear zones, in particular, can be explained by lateral accretion of terranes onto an older (~3 Ga) central nucleus, the North Caribou Terrane, without requiring subduction (Bédard et al. 2013). In fact, the detritus in the sedimentary accumulations on the margins of granite–greenstone terranes (e.g. the English River and Quetico terranes in the Superior Province) are derived from the adjacent granite–greenstone terranes to the north of these metasedimentary subprovinces (Davis 1990, 1993).

Other Models

The geochemical arguments about rutile retention and production of the observed large volumes of TTGs in granite–greenstone terranes suggest that a serious re-examination of alternatives is required. Bédard et al. (2013) support a so-called 'mantle wind' model involving mantle currents laterally displacing oceanic plateaux. In this model, there would be contractional structures and accreted terranes at the leading edge of cratons, strike-slip and oblique extensional structures at the sides, and major shear zones in the cratonic interiors.

CONCLUSIONS

Secular Variation

In the Archean Earth, radioactive heat production was concentrated in the crust, given the greater concentration of K, U, and Th in the crust compared to the mantle. With heat production concentrated in the crust, the crust became strong. The temperature of the Archean asthenosphere was not uniform; rather, it was concentrated in mantle plumes (Kamber 2015). The proportion of komatiites was higher, and these rocks were distinctly different from their modern analogues (Arndt et al. 2008). TTGs were more abundant, and the high-Al type was more abundant than the low-Al type (Martin 1987; Bradley 2011).

Additional Constraints on Archean Tectonic Regimes

Condie and Benn (2006) provide an elegant summary of constraints on Archean tectonic regimes that forms the basis for the following analysis. Although the dome-and-keel structural style of Archean greenstone belts is more readily attributed to vertical tectonics (Van Kranendonk et al. 2004), the upright regional-scale folds and transpressive shear zones are more easily explained by rigid lithospheric plates (Choukroune et al. 1997). The large volume of Archean crust produced at ~2.7 Ga is not an artefact of preservation, in that it is mirrored by: 1) the abundance of komatiites and changes in shale geochemistry, a proxy for a major change in crustal composition (Taylor and McLennan 1985); and 2) variations in the compositon of sub-continental lithospheric mantle (Griffin et al. 2003). Archean cratons have unusually thick, depleted lithosphere that formed at about the same time as the overlying crust (Begg et al. 2009) and the buoyant oceanic plates beneath the continent, yet Archean eclogitic and granulite xenoliths are not common on Archean cratons (Condie and Benn 2006). Many Archean greenstones contain rocks with 'arc-like' geochemistry, a key indicator of plate tectonics. Plume-derived greenstones form up to 80% of Archean greenstone belts (Condie and Benn 2006), which is greater than the proportion seen in younger orogenic systems. Paleomagnetic data from the Kaapvaal craton (Layer et al. 1989) and Superior craton (Hale and Lloyd 1989) indicate that there was significant polar wandering in the Archean.

In the face of these factors, how is a definitive conclusion reached with respect to the operative processes in Archean tectonics? The modern style of plate tectonics requires the Earth to have cooled sufficiently to generate decompression melting at mid-ocean ridges, in turn allowing oceanic lithosphere to develop sufficient negative buoyancy after a few tens of millions of years to initiate subduction. A conservative point of view states that unequivocal plate tectonics did not begin until ca. 1.9 Ga (Lucas et al. 1996) or perhaps 1 Ga (Condie et al. 2006; Stern 2008). More moderate points of view (Dhuime et al. 2012; Laurent et al. 2014) would have plate tectonics begin at some point between 3.0 and 2.5 Ga. In reality, plate tectonics probably made a few 'false starts' prior to becoming the prevailing system we know today (Silver and Behn 2008).

At this time there are few explanations for the absence of key rock types such as andesites that are indicative of plate tectonics. Although some may not agree with the discussion of TTG generation and volumes of TTGs presented by Bédard et al. (2013), this author prefers to conclude that, while there are geochemical features interpreted as evidence of subduction, the missing rock types are a powerful argument for the 'mantle wind' hypothesis. Modifications of that hypothesis are contained in the work of Kamber (2015).

ACKNOWLEDGEMENTS

Aspects of this paper have been aided by a recent review of Archean greenstones concentrating largely on the Kaapvaal craton (Anhaeusser 2014) and an interesting review of Precambrian geodynamics (Kamber 2015). This review came about through an invitation from Jarda Dostal, an associate editor of Geoscience Canada. My knowledge of granite–greenstone terranes has benefited from my experience with the Ontario Geological Survey, as well as my subsequent tenure in the Department of Earth Sciences at Laurentian University. At Laurentian, I was aided by NSERC Discovery Grants to pursue various topics centred on greenstone belt geology. This contribution was improved by early reviews from colleagues Harold Gibson and Matt Leybourne, and by the work of journal referees Pierre-Simon Ross and

Pete Hollings. Drafting was done by Lorraine Dupuis, Sara-Jane McIlraith and Julie Chartrand.

REFERENCES

Abouchami, W., Boher, M., Michard, A., and Albarede, F., 1990, A major 2.1 Ga event of mafic magmatism in west Africa: An early stage of crustal accretion: Journal of Geophysical Research, v. 95, p. 17605–17629, http://dx.doi.org/10.1029/JB095iB11p17605.

Allard, G.O., 1976, Doré Lake Complex and its importance to Chibougamau geology and metallogeny: Ministère des Richesses naturelles du Québec, 487 p.

Allen, R.L., Weihed, P., Blandell, D., Crawford, T., Davidson, G., Galley, A., Gibson, H., Hannington, M., Herrington, R., Herzig, P., Large, R., Lentz, D., Maslennikov, V.V., McCutcheon, S., Peter, J., and Tornos, F., 2002, Global comparisons of volcanic-associated massive sulphide districts, *in* Blundell, D.J., Neubauer, F., Von Quadt, E.-Z., *eds.,* The timing and location of major ore deposits in an evolving orogen: Geological Society, London, Special Publications, v. 204, p. 13–37, http://dx.doi.org/10.1144/GSL.SP.2002.204.01.02.

Allibone, A.H., McCuaig, T.C., Harris, D., Etheridge, M., Munroe, S., Byrne, D., Amanor, J., and Gyapong, W., 2002, Structural controls on gold mineralization at the Ashanti Deposit, Obuasi, Ghana, *in* Goldfarb, R.J., and Nielsen, R.L., *eds.*, Integrated methods for discovery: global exploration in the twenty-first century: Society of Economic Geologists, Special Publication, v. 9, p. 65–93.

Alvarez, W., 2010, Protracted continental collisions argue for continental plates driven by basal traction: Earth and Planetary Science Letters, v. 296, p. 434–442, http://dx.doi.org/10.1016/j.epsl.2010.05.030.

Angerer, T., Duuring, P., Lascelles, D.F., and Hagemann, S.G., 2010, BIF-related iron ore in the Yilgarn Craton, Western Australia: Geological Setting and ore forming Processes (Abstract): Fifth International Archean Symposium Abstracts, Geological Survey of Western Australia, p. 277–280.

Angerer, T., Kerrich, R., and Hagemann, S.G., 2013, Geochemistry of a komatiitic, boninitic, and tholeiitic basalt association in the Mesoarchean Koolyanobbing greenstone belt, Southern Cross Domain, Yilgarn Craton: Implications for mantle sources and geodynamic setting of banded iron formation: Precambrian Research, v. 224, p. 110–128, http://dx.doi.org/10.1016/j.precamres.2012.09.012.

Anhaeusser, C.R., 1984, Structural elements of Archaean granite-greenstone terranes as exemplified by the Barberton Mountain Land, southern Africa, i*n* Kroener, A., and Greiling, R., *eds.,* Precambrian tectonics illustrated: E. Schweizerbart'sche Verlagsbuchhandl, (Naegele u. Obermiller), Stuttgart, Federal Republic of Germany, p. 57–78.

Anhaeusser, C.R., 2014, Archaean greenstone belts and associated granitic rocks - A review: Journal of African Earth Sciences, v. 100, p. 684–732, http://dx.doi.org/10.1016/j.jafrearsci.2014.07.019.

Ansdell, K.M., Connors, K.A., Stern, R.A., and Lucas, S.B., 1999, Coeval sedimentation, magmatism, and fold-thrust belt development in the Trans-Hudson Orogen: geochronological evidence from the Wekusko Lake area, Manitoba, Canada: Canadian Journal of Earth Sciences, v. 36, p. 293–312, http://dx.doi.org/10.1139/e98-082.

Aplin, A.C., and Macquaker, J.H.S., 2011, Mudstone diversity: Origin and implications for source, seal, and reservoir properties in petroleum systems: American Association of Petroleum Geologists Bulletin, v. 95, p. 2031–2059, http://dx.doi.org/10.1306/03281110162.

Arias, Z.G., deKemp, E.A., and Donaldson, J.A., 1986, Shallow-marine Archean stromatolites in the Eyapamikama Lake area, Superior Province, Canada (Abstract): Society of Economic Paleontologists Mineralogists, Annual Midyear Meeting, Raleigh, North Carolina, Abstracts, v. 3, p. 3.

Arndt, N.T., 1991, High Ni in Archean tholeiites: Tectonophysics, v. 187, p. 411–419, http://dx.doi.org/10.1016/0040-1951(91)90479-C.

Arndt, N.T., and Nesbitt, R.W., 1982, Geochemistry of Munro Township basalts, *in* Arndt, N.T., and Nisbet, E.G., *eds.,* Komatiites: George Allen and Unwin, London, UK, p. 309–329.

Arndt, N.T., Lesher, C.M., and Barnes, S.J., 2008, Komatiite: Cambridge University Press, New York, NY, 468 p., http://dx.doi.org/10.1017/CBO9780511535550.

Ashwal, L.D., Morrison, D.A., Phinney, W.C., and Wood, J., 1983, Origin of Archean anorthosites: Evidence from the Bad Vermilion Lake anorthosite complex, Ontario: Contributions to Mineralogy and Petrology, v. 82, p. 259–273, http://dx.doi.org/10.1007/BF01166620.

Attoh, K., and Ekwueme, B.N., 1997, The West African Shield: Oxford Monographs on Geology and Geophysics, v. 35, p. 517–528.

Ayer, J., and Davis, D.W., 1997, Neoarchean evolution of differing convergent margin assemblages in the Wabigoon Subprovince: geochemical and geochronogical evidence from the Lake of the Woods greenstone belt, Superior Province, Northwestern Ontario: Precambrian Research, v. 81, p. 155–178, http://dx.doi.org/10.1016/S0301-9268(96)00033-2.

Ayer, J., Berger, B., Johns, G., Trowell, N.F., Born, P., and Mueller, W.U., 1999, Late Archean Rock types and Controls on Gold Mineralization in the southern Abitibi Greenstone Belt of Ontario (Abstract): Geological Association of Canada Joint Annual Meeting May 1999, Sudbury, ON.

Ayer, J., Amelin, Y., Corfu, F., Kamo, S., Ketchum, J., Kwok, K., and Trowell, N., 2002a, Evolution of the Abitibi greenstone belt based on U–Pb geochronology: autochthonous volcanic construction followed by plutonism, regional deformation and sedimentation: Precambrian Research, v. 115, p. 63–95, http://dx.doi.org/10.1016/S0301-9268(02)00006-2.

Ayer, J.A., Ketchum, J.W.F., and Trowell, N.F., 2002b, New geochronological and neodymium isotopic results from the Abitibi greenstone belt, with emphasis on the timing and the tectonic implications of Neoarchean sedimentation and volcanism: Ontario Geological Survey, Open File Report 6100, p. 5-1–5-16.

Ayer, J., Thurston, P.C., Bateman, R., Dubé, B., Gibson, H.L., Hamilton, M.A., Hathway, B., Hocker, S.M., Houlé, M., Hudak, G.J., Ispolatov, V., Lafrance, B., Lesher, C.M., MacDonald, P.J., Péloquin, A.S., Piercey, S.J., Reed, L.E., and Thompson, P.H., 2005, Overview of results from the Greenstone Architecture Project: Discover Abitibi Initiative, Ontario Geological Survey, Open File Report 5984, 125 p.

Ayer, J., Goutier, J., Thurston, P., Dubé, B., and Kamber, B.S., 2010, Tectonic and metallogenic evolution of the Abitibi and Wawa Subprovinces, *in* Ayer, J., Easton, R.M., Beakhouse, G., Stott, G., Kelly, R.I., Debicki, E., Parker, J., and Brown, T., *eds.,* Summary of Field Work and other Activities: Ontario Geological Survey, Sudbury, p. 41–46.

Ayres, L.D., and Thurston, P.C., 1985, Archean supracrustal sequences in the Canadian Shield: An overview, *in* Ayres, L.D., Thurston, P.C., Card, K.D., and Weber, W., *eds.,* Evolution of Archean Supracrustal Sequences: Geological Association of Canada, Special Paper 28, p. 343–380.

Baadsgaard, H., Nutman, A.P., Bridgwater, D., Rosing, M., McGregor, V.R., and Allaart, J.H., 1984, The zircon geochronology of the Akilia association and Isua supracrustal belt, West Greenland: Earth and Planetary Science Letters, v. 68, p. 221–228, http://dx.doi.org/10.1016/0012-821X(84)90154-7.

Bagas, L., Smithies, R.H., and Champion, D., 2003, Geochemistry of the Corunna Downs Granitoid Complex, East Pilbara Granite-Greenstone Terrane, Western Australia: Western Australia Geological Survey, Annual Review, p. 61–69.

Baldwin, G.J., 2009, The sedimentology and geochemistry of Banded Iron Formations of the Deloro Assemblage, Bartlett Dome area, Abitibi greenstone belt, Ontario, Canada: Implications for BIF deposition and greenstone belt formation: Unpublished MSc thesis, Laurentian University, Sudbury, ON, 116 p.

Barker, F., and Arth, J.G., 1976, Generation of trondhjemitic-tonalitic liquids and Archean bimodal trondhjemite-basalt suites: Geology, v. 4, p. 596–600, http://dx.doi.org/10.1130/0091-7613(1976)4<596:GOTLAA>2.0.CO;2.

Barley, M.E., 1992, A Review of Archean volcanic-hosted massive sulfide and sulfate mineralization in Western Australia: Economic Geology, v. 87, p. 855–872, http://dx.doi.org/10.2113/gsecongeo.87.3.855.

Barley, M.E., 1997, The Pilbara Craton, *in* de Wit, M.J., and Ashwal, L.D., *eds.,* Greenstone Belts: Clarendon Press, Oxford, UK, p. 657–664.

Barnes, S.J., and Van Kranendonk, M.J., 2014, Archean andesites in the east Yilgarn craton, Australia: Products of plume-crust interaction?: Lithosphere, v. 6, p. 80–92, http://dx.doi.org/10.1130/L356.1.

Barrett, T.J., and MacLean, W.H., 1999, Volcanic sequences, lithogeochemistry, and hydrothermal alteration in some bimodal volcanic-associated massive sulfide systems: Reviews in Economic Geology, v. 8, p. 101–131.

Barrie, C.T., Naldrett, A.J., and Davis, D., 1990, Geochemical constraints on the genesis of the Montcalm gabbroic complex and Ni–Cu deposit, western Abitibi Subprovince, Ontario: Canadian Mineralogist, v. 28, p. 451–474.

Barrie, C.T., Ludden, J.N., and Green, T.H., 1993, Geochemistry of volcanic rocks associated with Cu–Zn and Ni–Cu deposits in the Abitibi subprovince: Economic Geology, v. 88, p. 1341–1358, http://dx.doi.org/10.2113/gsecongeo.88.6.1341.

Beakhouse, G., 2013, Western Wabigoon Synthesis Project: Ontario Geological Survey, Open File Report 6290, Sudbury, ON, p. 5-1–5-7.

Beakhouse, G.P., Lin, S., and Kamo, S.L., 2011, Magmatic and tectonic emplacement of the Pukaskwa batholith, Superior Province, Ontario, Canada: Canadian Journal of Earth Sciences, v. 48, p. 187–204, http://dx.doi.org/10.1139/E10-048.

Bédard, J.H., 2006, A catalytic delamination-driven model for coupled genesis of Archaean crust and sub-continental lithospheric mantle: Geochimica et Cosmochimica Acta, v. 70, p. 1188–1214, http://dx.doi.org/10.1016/j.gca.2005.11.008.

Bédard, J.H., 2013, How many arcs can dance on the head of a plume? A 'Comment' on: A critical assessment of Neoarchean 'plume only' geodynamics: Evidence from the Superior Province, by Derek Wyman, Precambrian Research, 2012: Precambrian Research, v. 229, p. 189–197, http://dx.doi.org/10.1016/j.precamres.2012.05.004.

Bédard, J.H., Brouillette, P., Madore, L., and Berclaz, A., 2003, Archaean cratonization and deformation in the northern Superior Province, Canada: an evaluation of plate tectonic versus vertical tectonic models: Precambrian Research, v. 127, p. 61–87, http://dx.doi.org/10.1016/S0301-9268(03)00181-5.

Bédard, J.H., Harris, L.B., and Thurston, P.C., 2013, The hunting of the snArc: Precambrian Research, v. 229, p. 20–48, http://dx.doi.org/10.1016/j.precamres.2012.04.001.

Begg, G.C., Griffin, W.L., Natapov, L.M., O'Reilly, S.Y., Grand, S.P., O'Neill, C.J., Hronsky, J.M.A., Poudjom Djomani, Y., Swain, C.J., Deen, T., and Bowden, P., 2009, The lithospheric architecture of Africa: Seismic tomography, mantle petrology, and tectonic evolution: Geosphere, v. 5, p. 23–50, http://dx.doi.org/10.1130/GES00179.1.

Benn, K., and Peschler, A.P., 2005, A detachment fold model for fault zones in the Late Archean Abitibi greenstone belt: Tectonophysics, v. 400, p. 85–104, http://dx.doi.org/10.1016/j.tecto.2005.02.011.

Berger, B.R., 2001, Variation in styles of gold mineralization along the Porcupine-Destor deformation zone in Ontario: An Exploration Guide: Summary of Field Work and other Activities: Ontario Geological Survey, Open File report 6070, p. 9-1 to 9-13.

Bickle, M.J., Bettenay, L.F., Boulter, C.A., Groves, D.I., and Morant, P., 1980, Horizontal tectonic interaction of an Archean gneiss belt and greenstones, Pilbara block, Western Australia: Geology, v. 8, p. 525–529, http://dx.doi.org/10.1130/0091-7613(1980)8<525:HTIOAA>2.0.CO;2.

Bickle, M.J., Arndt, N.T., Nisbet, E.G., Orpen, J.L., Martin, A., Keays, R.R., and Renner, R., 1993, Geochemistry of the igneous rocks of the Belingwe greenstone belt, Zimbabwe, *in* Bickle, M.J., and Nisbet, E.G., *eds.,* The geology of the Belingwe greenstone belt, Zimbabwe, a study of the evolution of Archean continental crust: A.A. Balkema, Rotterdam, p. 175–214.

Bickle, M.J., Nisbet, E.G., and Martin, A., 1994, Archean greenstone belts are not oceanic crust: The Journal of Geology, v. 102, p. 121–137, http://dx.doi.org/10.1086/629658.

Blackburn, C.E., Johns, G.W., Ayer, J.A., and Davis, D.W., 1991, Wabigoon Subprovince, *in* Thurston, P.C., Williams, H.R., Sutcliffe, R.H., and Stott, G.M., *eds.,* Geology of Ontario: Ontario Geological Survey, Special Volume 4, pt. 1, p. 303–381.

Bleeker, W., 1999, Structure, Stratigraphy, and Primary Setting of the Kidd Creek Volcanogenic Massive Sulfide Deposit: A Semi-quantitative Reconstruction, *in* Hannington, M.D., and Barrie, C.T., *eds.,* The Giant Kidd Creek Volcanogenic Massive Sulfide Deposit, Western Abitibi Subprovince, Canada: Economic Geology Monograph 10, p. 71–123.

Bleeker, W., 2002, Archaean tectonics: a review, with illustrations from the Slave craton, *in* Fowler, C.M.R., Ebinger, C.J., and Hawkesworth, C.J., *eds.,* The Early Earth: Physical, Chemical and Biological Development: Geological Society, London, Special Publications, v. 199, p. 151–181, http://dx.doi.org/10.1144/gsl.sp.2002.199.01.09.

Bleeker, W., 2003, The late Archean record: A puzzle in ca. 35 pieces: Lithos, v. 71, p. 99–134, http://dx.doi.org/10.1016/j.lithos.2003.07.003.

Bleeker, W., 2012, Lode gold deposits in Deformed and metamorphosed terranes: The role of Extension in the Formation of Timiskaming Basins and Large Gold Deposits, Abitibi Greenstone Belt–A Discussion, *in* Parker, J., *ed.*, Summary of Field Work and Other Activities 2012: Ontario Geological Survey, Open File Report 6280, p. 47-41 to 47-12.

Bleeker, W., and Hall, B., 2007, The Slave Craton: Geological and metallogenic evolution, *in* Goodfellow, W.D., *ed.,* Mineral Deposits of Canada: A synthesis of major Deposit-types, District Metallogeny, the Evolution of Geological Provinces, and Exploration Methods: Geological Association of Canada, Mineral Deposits Division, Special Publication 5, p. 849–879.

Bleeker, W., and Van Breemen, O., 2011, New geochronological, stratigraphic, and structural observations on the Kidd–Munro assemblage and the terrane architecture of the south- central Abitibi greenstone belt, Superior craton, Canada: Results from the Targeted Geoscience Initiative III Kidd–Munro Project: Ontario Geological Survey, Open File Report 6258, 142 p.

Blenkinsop, T., Fedo, C.M., Bickle, M.J., Eriksson, K.A., Martin, A., Nisbet, E.G., and Wilson, J.F., 1993, Ensialic origin for the Ngezi Group, Belingwe greenstone belt, Zimbabwe: Geology, v. 21, p. 1135–1138, http://dx.doi.org/10.1130/0091-7613(1993)021<1135:EOFTNG>2.3.CO;2.

Blenkinsop, T., Martin, A., Jelsma, H.A., and Vinyu, M.L., 1997, The Zimbabwe craton, *in* de Wit, M.J., and Ashwal, L.D., *eds.,* Greenstone Belts: Clarendon Press, Oxford, UK, p. 567–580.

Blewett, R.S., 2002, Archaean tectonic processes: A case for horizontal shortening in the North Pilbara Granite-Greenstone Terrane, Western Australia: Precambrian Research, v. 113, p. 87–120, http://dx.doi.org/10.1016/S0301-9268(01)00204-2.

Blewett, R.S., Champion, D.C., Whitaker, A.J., Bell, B., Nicoll, M., Goleby, B.R., Cassidy, K.F., and Groenewald, P.B., 2002, Three dimensional (3D) model of the Leonora-Laverton transect area: implications for Eastern Goldfields tectonics and mineralisation, *in* Cassidy, K.F., *ed.,* Geology, geochronology and geophysics of the north eastern Yilgarn Craton, with an emphasis on the Leonora-Laverton transect area: Geoscience Australia, p. 83–100.

Bloem, E.J.M., Dalstra, H.J., Ridley, J.R., and Groves, D.I., 1997, Granitoid diapirism during protracted tectonism in an Archaean granitoid-greenstone belt, Yilgarn Block, Western Australia: Precambrian Research, v. 85, p. 147–171, http://dx.doi.org/10.1016/S0301-9268(97)00034-X.

Boily, M., and Dion, C., 2002, Geochemistry of boninite-type volcanic rocks in the Frotet-Evans greenstone belt, Opatica subprovince, Quebec: implications for the evolution of Archaean greenstone belts: Precambrian Research, v. 115, p. 349–371, http://dx.doi.org/10.1016/S0301-9268(02)00016-5.

Bolhar, R., Van Kranendonk, M.J., and Kamber, B.S., 2005, A trace element study of siderite-jasper banded iron formation in the 3.45 Ga Warrawoona Group, Pilbara Craton—Formation from hydrothermal fluids and shallow seawater: Precambrian Research, v. 137, p. 93–114, http://dx.doi.org/10.1016/j.precamres.2005.02.001.

Bouma, A.H., 2000, Fine-grained, mud-rich turbidite systems: model and comparison with coarse-grained, sand-rich systems: American Association of Petroleum Geologists Memoir 72, SEPM Special Publication 68, p. 9–20.

Bradley, D.C., 2011, Secular trends in the geologic record and the supercontinent cycle: Earth-Science Reviews, v. 108, p. 16–33, http://dx.doi.org/10.1016/j.earscirev.2011.05.003.

Breaks, F.W., 1991, English River Subprovince: Ontario Geological Survey Special Volume 4, p. 239–277.

Breaks, F.W., and Moore, J.M., Jr., 1992, The Ghost Lake Batholith, Superior Province of Northwestern Ontario: a fertile peraluminous S-Type granite rare element pegmatite system: Canadian Mineralogist, v. 30, p. 835–875.

Breaks, F.W., Osmani, I.A., and deKemp, E.A., 2001, Geology of the North Caribou Lake area, north-western Ontario: Ontario Geological Survey, Open File Report 6023, 70 p.

Brooks, C., Ludden, J., Pigeon, Y., and Hubregtse, J.J.M.W., 1982, Volcanism of shoshonite to high-K andesite affinity in an Archean arc environment, Oxford Lake, Manitoba: Canadian Journal of Earth Sciences, v. 19, p. 55–67, http://dx.doi.org/10.1139/e82-005.

Brown, G.H., 1995, Precambrian Geology, Oliver and Ware Townships: Ontario Geological Survey, Geological Report 294, 48 p.

Brown, M., 2006, Duality of thermal regimes is the distinctive characteristic of plate tectonics since the Neoarchean: Geology, v. 34, p. 961–964, http://dx.doi.org/10.1130/G22853A.1.

Brown, M., 2007, Metamorphic conditions in orogenic belts: A record of secular change: International Geology Review, v. 49, p. 193–234, http://dx.doi.org/10.2747/0020-6814.49.3.193.

Brown, S.J.A., Barley, M.E., Krapež, B., and Cas, R.A.F., 2002, The Late Archaean Melita Complex, Eastern Goldfields, Western Australia: shallow submarine bimodal volcanism in a rifted arc environment: Journal of Volcanology and Geothermal Research, v. 115, p. 303–327, http://dx.doi.org/10.1016/S0377-0273(01)00314-6.

Buick, R., Thornett, J.R., McNaughton, N.J., Smith, J.B., Barley, M.E., and Savage, M., 1995, Record of emergent continental crust ~3.5 billion years ago in the Pilbara craton of Australia: Nature, v. 375, p. 574–577, http://dx.doi.org/10.1038/375574a0.

Buse, S., Lewis, D., Davis, D.W., and Hamilton, M.A., 2010, U–Pb geochronological results from the Lumby Lake greenstone belt, Wabigoon Subprovince, Northwestern Ontario: Summary of Field work and other Activities, 2010: Ontario Geological Survey, Open File Report 6260, p. 12-1 to12-9.

Calvert, A.J., and Ludden, J.N., 1999, Archean continental assembly in the southeastern Superior Province of Canada: Tectonics, v. 18, p. 412–429, http://dx.doi.org/10.1029/1999TC900006.

Calvert, A.J., Sawyer, E.W., Davis, W.J., and Ludden, J.N., 1995, Archaean subduction inferred from seismic images of a mantle suture in the Superior Province: Nature, v. 375, p. 670–674, http://dx.doi.org/10.1038/375670a0.

Calvert, A.J., Cruden, A.R., and Hynes, A., 2004, Seismic evidence for preservation of the Archean Uchi granite-greenstone belt by crustal-scale extension: Tectonophysic, v. 388, p. 135–143, http://dx.doi.org/10.1016/j.tecto.2004.07.043.

Campbell, I.H., Franklin, J.M., Gorton, M.P., Hart, T.R., and Scott, S.D., 1981, The role of subvolcanic sills in the generation of massive sulfide deposits: Economic Geology, v. 76, p. 2248–2253, http://dx.doi.org/10.2113/gsecongeo.76.8.2248.

Campbell, I.H., Coad, P., Franklin, J.M., Gorton, M.P., Scott, S.D., Sowa, J., and Thurston, P.C., 1982, Rare earth elements in volcanic rocks associated with Cu–Zn massive sulphide mineralization: a preliminary report: Canadian Journal of Earth Sciences, v. 19, p. 619–623, http://dx.doi.org/10.1139/e82-049.

Campbell, I.H., Griffiths, R.W., and Hill, R.I., 1989, Melting in an Archaean mantle plume: heads it's basalts, tails it's komatiites: Nature, v. 339, p. 697–699, http://dx.doi.org/10.1038/339697a0.

Capdevila, R., Goodwin, A.M., Ujike, O., and Gorton, M.P., 1982, Trace-element geochemistry of Archean volcanic rocks and crustal growth in southwestern Abitibi Belt, Canada: Geology, v. 10, p. 418–422, http://dx.doi.org/10.1130/0091-7613(1982)10<418:TGOAVR>2.0.CO;2.

Card, K.D., 1990, A review of the Superior Province of the Canadian Shield, a product of Archean accretion: Precambrian Research, v. 48, p. 99–156, http://dx.doi.org/10.1016/0301-9268(90)90059-Y.

Carignan, J., Gariépy, C., Machado, N., and Rive, M., 1993, Pb isotopic geochemistry of granitoids and gneisses from the late Archean Pontiac and Abitibi Subprovinces of Canada: Chemical Geology, v. 106, p. 299–315, http://dx.doi.org/10.1016/0009-2541(93)90033-F.

Carmichael, I.S.E., 1964, The petrology of Thingmuli, a Tertiary volcano in eastern Iceland: Journal of Petrology, v. 5, p. 435–460, http://dx.doi.org/10.1093/petrology/5.3.435.

Carson, H.J.E., Lesher, C.M., Houlé, M.G., Weston, R.J., and Shinkle, D.A., 2013, Stratigraphy, Geochemistry and Petrogenesis of the Black Thor Intrusive Complex and Associated Chromium and Ni–Cu–PGE Mineralization, McFaulds Lake Greenstone belt, Ontario: Summary of Field work and other Activities: Ontario Geological Survey, Open File Report 6290, p. 52-51 to 52-15.

Carter, M.W., 1993, The geochemical characteristics of Neoarchean alkalic magmatism in the central Superior Province: Ontario Geological Survey, Miscellaneous Paper 162, p. 13–19.

Champion, D.C., and Smithies, R.H., 2007, Geochemistry of Paleoarchean granites of the East Pilbara Terrane, Pilbara Craton, Western Australia: implications for early Archean crustal growth: Developments in Precambrian Geology, v. 15, p. 369–409.

Chardon, D., Choukroune, P., and Jayananda, M., 1996, Strain patterns, décollement and incipient sagducted greenstone terrains in the Archaean Dharwar Craton (South India): Journal of Structural Geology, v. 18, p. 991–1004, http://dx.doi.org/10.1016/0191-8141(96)00031-4.

Choukroune, P., Ludden, J.N., Chardon, D., Calvert, A.J., and Bouhallier, H., 1997, Archaean crustal growth and tectonic processes: a comparison of the Superior Province, Canada and the Dharwar Craton, India, *in* Gurg, J.-P., and Ford, M., Orogeny Through Time: Geological Society, London, Special Publications, v. 121, p. 63–98, http://dx.doi.org/10.1144/GSL.SP.1997.121.01.04.

Claoué-Long, J.C., Compston, W., and Cowden, A., 1988, The age of the Kambalda greenstones resolved by ion-microprobe: implications for Archaean dating methods: Earth and Planetary Science Letters, v. 89, p. 239–259, http://dx.doi.org/10.1016/0012-821X(88)90175-6.

Condie, K.C., 1981, Archean Greenstone Belts: Elsevier, Amsterdam, 433 p.

Condie, K.C., 1986, Origin and early growth rate of continents: Precambrian Research, v. 32, p. 261–278, http://dx.doi.org/10.1016/0301-9268(86)90032-X.

Condie, K.C., 1993, Chemical composition and evolution of the upper continental crust: Contrasting results from surface samples and shales: Chemical Geology, v. 104, p. 1–37, http://dx.doi.org/10.1016/0009-2541(93)90140-E.

Condie, K.C., and Benn, K., 2006, Archean geodynamics: Similar to or different from modern geodynamics?, *in* Benn, K., Mareschal, J.-C., and Condie, K.C., *eds.,* Archean Geodynamics and Environments: American Geophysical Union Monograph Series, v. 164, p. 47–59, http://dx.doi.org/10.1029/164gm05.

Condie, K.C., Kröner, A., and Stern, R.J., 2006, Penrose conference report: When did plate tectonics begin?: GSA Today, v. 16, p. 40–41.

Cooke, D.L., 1966, The Timiskaming Volcanics and Associated Sediments of the Kirkland lake Area: Unpublished PhD thesis, University of Toronto, Toronto, ON, 147 p.

Corcoran, P.L., and Mueller, W.U., 2007, Time-transgressive Archean unconformities underlying molasse basin-fill successions of dissected oceanic arcs, Superior Province, Canada: The Journal of Geology, v. 115, p. 655–674, http://dx.doi.org/10.1086/521609.

Corfu, F., and Noble, S.R., 1992, Genesis of the southern Abitibi greenstone belt, Superior Province, Canada: Evidence from zircon Hf isotope analyses using a single filament technique: Geochimica et Cosmochimica Acta, v. 56, p. 2081–2097, http://dx.doi.org/10.1016/0016-7037(92)90331-C.

Corfu, F., and Stone, D., 1998, Age structure and orogenic significance of the Berens River composite batholiths, western Superior Province: Canadian Journal of Earth Sciences, v. 35, p. 1089–1109, http://dx.doi.org/10.1139/e98-056.

Cousens, B.L., 2000, Geochemistry of the Archean Kam Group, Yellowknife greenstone belt, Slave Province, Canada: The Journal of Geology, v. 108, p. 181–197, http://dx.doi.org/10.1086/314397.

Crawford, A.J., Falloon, T.J., and Green, D.H., 1989, Classification, petrogenesis and tectonic setting of boninites, *in* Crawford, A.J., *ed.,* Boninites: Unwin Hyman, London, UK, p. 1–49.

D'Orazio, M., Agostini, S., Mazzarini, F., Innocenti, F., Manetti, P., Haller, M.J., and Lahsen, A., 2000, The Pali Aike Volcanic Field, Patagonia: Slab-window magmatism near the tip of South America: Tectonophysics, v. 321, p. 407–427, http://dx.doi.org/10.1016/S0040-1951(00)00082-2.

Daigneault, R., and Allard, G.O., 1990, Le Complexe du Lac Doré et son environnement géologique: Ministère de l'Eneregie et des Ressources du Québec, DPV 368, 275 p.

Dann, J.C., 2001, Vesicular komatiites, 3.5-Ga Komati Formation, Barberton Greenstone Belt, South Africa: Inflation of submarine lavas and origin of spinifex zones: Bulletin of Volcanology, v. 63, p. 462–481, http://dx.doi.org/10.1007/s004450100164.

Davis, D.W., 1990, The Seine-Coutchiching problem reconsidered: U–Pb geochronological data concerning the source and timing of Archean sedimentation in the western Superior Province (Abstract): Institute on Lake Superior Geology, Abstracts, v. 36, p. 19–21.

Davis, D.W., 1993, Report on U–Pb geochronology in the Atikokan area, Wabigoon subprovince: Royal Ontario Museum Report, Toronto, ON, p. 9.

Davis, D.W., and Edwards, G.R., 1986, Crustal evolution of Archean rocks in the Kakagi Lake area, Wabigoon Subprovince, Ontario, as interpreted from high-precision U–Pb geochronology: Canadian Journal of Earth Sciences, v. 23, p. 182–192, http://dx.doi.org/10.1139/e86-021.

Davis, D.W., Pezzutto, F., and Ojakangas, R.W., 1990, The age and provenance of metasedimentary rocks in the Quetico Subprovince, Ontario, from single zircon analyses: implications for Archean sedimentation and tectonics in the Superior Province: Earth and Planetary Science Letters, v. 99, p. 195–205, http://dx.doi.org/10.1016/0012-821X(90)90110-J.

Davis, W.J., Lacroix, S., Gariépy, C., and Machado, N., 2000, Geochronology and radiogenic isotope geochemistry of plutonic rocks from the central Abitibi subprovince: significance to the internal subdivision and plutono-tectonic evolution of the Abitibi belt: Canadian Journal of Earth Sciences, v. 37, p. 117–133, http://dx.doi.org/10.1139/e99-093.

de Rosen-Spence, A.F., 1976, Stratigraphy, development and petrogenesis of the central Noranda volcanic pile, Noranda, Quebec: Unpublished PhD thesis, University of Toronto, Toronto, ON, 439 p.

de Rosen-Spence, A.F., Provost, G., Dimroth, E., Gochnauer, K., and Owen, V., 1980, Archean subaqueous felsic flows, Rouyn-Noranda, Quebec, Canada, and their Quaternary equivalents: Precambrian Research, v. 12, p. 43–77, http://dx.doi.org/10.1016/0301-9268(80)90023-6.

de Wit, M.J., Hart, R.A., and Hart, R.J., 1987, The Jamestown Ophiolite Complex, Barberton mountain belt: a section through 3.5 Ga oceanic crust: Journal of African Earth Sciences, v. 6, p. 681–730, http://dx.doi.org/10.1016/0899-5362(87)90007-8.

Defant, M.J., and Drummond, M.S., 1990, Derivation of some modern arc magmas by melting of young subducted lithosphere: Nature, v. 347, p. 662–665, http://dx.doi.org/10.1038/347662a0.

Defant, M.J., and Drummond, M.S., 1993, Mount St. Helens: Potential example of the partial melting of the subducted lithosphere in a volcanic arc: Geology, v. 21, p. 547–550, http://dx.doi.org/10.1130/0091-7613(1993)021<0547:MSH-PEO>2.3.CO;2.

Defant, M.J., Jackson, T.E., Drummond, M.S., De Boher, J.Z., Bellon, H., Feigenson, M.D., Maury, R.C., and Stewart, R.H., 1992, The geochemistry of young volcanism throughout western Panama and southeastern Costa Rica: an overview: Journal of the Geological Society, v. 149, p. 569–579, http://dx.doi.org/10.1144/gsjgs.149.4.0569.

Depaolo, D.J., 1981, Trace element and isotopic effects of combined wallrock assimilation and fractional crystallization: Earth and Planetary Science Letters, v. 53, p. 189–202, http://dx.doi.org/10.1016/0012-821X(81)90153-9.

Devaney, J.R., and Williams, H.R., 1989, Evolution of an Archean subprovince boundary: a sedimentological and structural study of part of the Wabigoon-Quetico boundary in northern Ontario: Canadian Journal of Earth Sciences, v. 26, p. 1013–1026, http://dx.doi.org/10.1139/e89-082.

Dhuime, B., Hawkesworth, C.J., Cawood, P.A., and Storey, C.D., 2012, A change in the Geodynamics of Continental Growth 3 Billion Years ago: Science, v. 335, p. 1334–1336, http://dx.doi.org/10.1126/science.1216066.

Dilek, Y., and Polat, A., 2008, Suprasubduction zone ophiolites and Archean tectonics: Geology, v. 36, p. 431–432, http://dx.doi.org/10.1130/Focus052008.1.

Dimroth, E., and Lichtblau, A.P., 1979, Metamorphic evolution of Archean hyaloclastites, Noranda area, Quebec, Canada. Part I: Comparison of Archean and Cenozoic sea-floor metamorphism: Canadian Journal of Earth Sciences, v. 16, p. 1315–1340, http://dx.doi.org/10.1139/e79-120.

Dimroth, E., and Rocheleau, M., 1979, Volcanology and sedimentology of the Rouyn-Noranda area, Quebec: Geological Association of Canada Field Trip A-1 Guide Book, Université Laval, Quebec, 193 p.

Dimroth, E., Côté, R., Provost, G., Rocheleau, M., Tassé, N., and Trudel, P., 1974, Third progress report on the stratigraphy, volcanology, sedimentology and structure of the Rouyn-Noranda area, counties of Rouyn-Noranda, Abitibi-west and Temiskamingue: Ministère des Richesses naturelles (Québec), 64 p.

Dimroth, E., Imreh, L., Rocheleau, M., and Goulet, N., 1982, Evolution of the south-central part of the Archean Abitibi Belt, Quebec. Part 1: Stratigraphy and paleogeographic model: Canadian Journal of Earth Sciences, v. 19, p. 1729–1758, http://dx.doi.org/10.1139/e82-154.

Dimroth, E., Imreh, L., Goulet, N., and Rocheleau, M., 1983, Evolution of the south-central segment of the Archean Abitibi Belt, Quebec. Part III: Plutonic and metamorphic evolution and geotectonic model: Canadian Journal of Earth

Sciences, v. 20, p. 1374–1388, http://dx.doi.org/10.1139/e83-125.
Dimroth, E., Imreh, L., Cousineau, P., Leduc, M., and Sanschagrin, Y., 1985, Paleogeographic analysis of mafic submarine flows and its use in the exploration for Massive Sulphide Deposits, *in* Ayres, L.D., Thurston, P.C., Card, K.D., and Weber, W., *eds.,* Evolution of Archean Supracrustal Sequences: Geological Association of Canada, Special Paper 28, p. 203–222.
Donaldson, J.A., and de Kemp, E.A., 1998, Archaean quartz arenites in the Canadian Shield: examples from the Superior and Churchill Provinces: Sedimentary Geology, v. 120, p. 153–176, http://dx.doi.org/10.1016/S0037-0738(98)00031-1.
Dostal, J., and Mueller, W., 1992, Archean shoshonites from the Abitibi greenstone belt, Chibougamau (Québec, Canada): geochemistry and tectonic setting: Journal of Volcanology and Geothermal Research, v. 53, p. 145–165, http://dx.doi.org/10.1016/0377-0273(92)90079-S.
Dostal, J., and Mueller, W.U., 1997, Komatiite flooding of a rifted Archean rhyolitic arc complex: geochemical signature and tectonic significance of the Stoughton-Roquemaure Group, Abitibi Greenstone Belt, Canada: The Journal of Geology, v. 105, p. 545–563, http://dx.doi.org/10.1086/515956.
Dostal, J., and Mueller, W.U., 2013, Deciphering an Archean mantle plume: Abitibi greenstone belt, Canada: Gondwana Research, v. 23, p. 493–505, http://dx.doi.org/10.1016/j.gr.2012.02.005.
Dostal, J., Mueller, W.U., and Murphy, J.B., 2004, Archean molasse basin evolution and magmatism, Wabigoon Subprovince, Canada: The Journal of Geology, v. 112, p. 435–454, http://dx.doi.org/10.1086/421073.
Drummond, B.J., 1988, A review of crust/upper mantle structure in the Precambrian areas of Australia and implications for Precambrian crustal evolution: Precambrian Research, v. 40–41, p. 101–116, http://dx.doi.org/10.1016/0301-9268(88)90063-0.
Drummond, M.S., and Defant, M.J., 1990, A model for trondhjemite-tonalite-dacite genesis and crustal growth via slab melting: Archean to modern comparisons: Journal of Geophysical Research, v. 95, p. 21503–21521, http://dx.doi.org/10.1029/JB095iB13p21503.
Drury, S.A., 1977, Structures induced by granite diapirs in the Archaean greenstone belt at Yellowknife, Canada: Implications for Archaean geotectonics: The Journal of Geology, v. 85, p. 345–358, http://dx.doi.org/10.1086/628304.
Dubé, B., Williamson, K., McNicoll, V., Malo, M., Skulski, T., Twomey, T., and Sanborn-Barrie, M., 2004, Timing of gold mineralization at Red Lake, Northwestern Ontario, Canada: New constraints from U–Pb geochronology at the Goldcorp high-grade zone, Red lake Mine, and the Madsen Mine: Economic Geology, v. 99, p. 1611–1641, http://dx.doi.org/10.2113/99.8.1611.
Easton, R.M., 2000, Metamorphism of the Canadian Shield, Ontario, Canada. I. The Superior Province: The Canadian Mineralogist, v. 38, p. 287–317, http://dx.doi.org/10.2113/gscanmin.38.2.287.
Eglington, B.M., and Armstrong, R.A., 2004, The Kaapvaal Craton and adjacent orogens, southern Africa: a geochronological database and overview of the geological development of the craton: South African Journal of Geology, v. 107, p. 13–32, http://dx.doi.org/10.2113/107.1-2.13.
Eriksson, K.A., and Soegaard, K., 1985, The petrography and geochemistry of Archaean and Early Proterozoic sediments: implications for crustal compositions and surface processes (South Africa, Australia, USA): Bulletin - Geological Survey of Finland, v. 331, p. 7–32.
Ernst, W.G., and Liou, J.G., 1999, Overview of UHP metamorphism and tectonics in well-studied collisional orogens: International Geology Review, v. 41, p. 477–493, http://dx.doi.org/10.1080/00206819909465153.
Ewart, A., 1982, The mineralogy and petrology of Tertiary-Recent orogenic volcanic rocks: with special reference to the andesitic-basaltic compositional range, *in* Thorpe, R.S., *ed.,* Andesites: orogenic andesites and related rocks: John Wiley and Sons, Chichester, UK, p. 25–95.
Farquhar, J., and Wing, B.A., 2003, Multiple sulfur isotopes and the evolution of the atmosphere: Earth and Planetary Science Letters, v. 213, p. 1–13, http://dx.doi.org/10.1016/S0012-821X(03)00296-6.
Feng, R., and Kerrich, R., 1992, Geodynamic evolution of the southern Abitibi and Pontiac terranes: evidence from geochemistry of granitoid magma series (2700–2630 Ma): Canadian Journal of Earth Sciences, v. 29, p. 2266–2286, http://dx.doi.org/10.1139/e92-178.
Ferguson, I.J., Craven, J.A., Kurtz, R.D., Boerner, D.E., Bailey, R.C., Wu, X., Orellana, M.R., Spratt, J., Wennberg, G., and Norton, M., 2005, Geoelectric response of Archean lithosphere in the western Superior Province, central Canada: Physics of the Earth and Planetary Interiors, v. 150, p. 123–143, http://dx.doi.org/10.1016/j.pepi.2004.08.025.
Flint, D.J., 2010, REE, lithium, potash, and phosphate mineralization in Western Australia: Record - Geological Survey of Western Australia, p. 33–34.
Fralick, P., and Pufahl, P.K., 2006, Iron formation in Neoarchean deltaic successions and the microbially mediated deposition of transgressive systems tracts: Journal of Sedimentary Research v. 76, p. 1057–1066, http://dx.doi.org/10.2110/jsr.2006.095.
Fralick, P., Hollings, P., and King, D., 2008, Stratigraphy, geochemistry, and depositional environments of Mesoarchean sedimentary units in western Superior Province: Implications for generation of early crust, *in* Condie, K.C., and Pease, V., *eds.,* When Did Plate Tectonics Begin on Planet Earth?: Geological Society of America, Special Papers, v. 440, p. 77–96, http://dx.doi.org/10.1130/2008.2440(04).
Francis, D., Ludden, J., Johnstone, R., and Davis, W., 1999, Picrite evidence for more Fe in Archean mantle reservoirs: Earth and Planetary Science Letters, v. 167, p. 197–213, http://dx.doi.org/10.1016/S0012-821X(99)00032-1.
Franklin, J.M., Gibson, H.L., Jonasson, I.R., and Galley, A.G., 2005, Volcanogenic Massive sulfide Deposits: Economic Geology 100th Anniversary Volume, p. 523–560.
Fumerton, S.L., Stauffer, M.R., and Lewry, J.F., 1984, The Wathaman batholith: largest known Precambrian pluton: Canadian Journal of Earth Sciences, v. 21, p. 1082–1097, http://dx.doi.org/10.1139/e84-113.
Furnes, H., de Wit, M., and Robins, B., 2013, A review of new interpretations of the tectonostratigraphy, geochemistry and evolution of the Onverwacht Suite, Barberton Greenstone Belt, South Africa: Gondwana Research, v. 23, p. 403–428, http://dx.doi.org/10.1016/j.gr.2012.05.007.
Fyon, J.A., Breaks, F.W., Heather, K.B., Jackson, S.L., Muir, T.L., Stott, G., and Thurston, P.C., 1992, Metallogeny of Metallic Mineral Deposits in the Superior Province of Ontario, *in* Thurston, P.C., Williams, H.R., Sutcliffe, H.R., and Stott, G.M., *eds.,* Geology of Ontario: Ontario Geological Survey, Special Volume 4, p. 1091–1174.
Gaál, G., and Gorbatschev, R., 1987, An outline of the Precambrian evolution of the Baltic Shield: Precambrian Research, v. 35, p. 15–52, http://dx.doi.org/10.1016/0301-9268(87)90044-1.
Gaillard, N., Williams-Jones, A.E., Salvi, S., Beziat, D., Perrouty, S., Van Hinsberg, V., Linnen, R., Olivo, G.r., Piercey, S.J., and Wares, R.P., 2014, Canadian Malartic gold deposit footprint: Preliminary investigation of geological, geochemical and mineralogical features (Abstract): GAC–MAC Annual Meeting, Fredericton, NB, Abstracts, v. 37, p. 97.
Galley, A.G., Hannington, M.D., and Jonasson, I.R., 2007a, Volcanogenic Massive Sulphide Deposits, *in* Goodfellow, W., *ed.,* Mineral Deposits of Canada: A Synthesis of Major Deposit-types, District Metallogeny, the Evolution of Geological Provinces, and Exploration Methods: Geological Associaton of Canada, Mineral Deposits Division, Special Publication 5, p. 141–162.
Galley, A.G., Syme, R., and Bailes, A., 2007b, Metallogeny of thePpaleoproterozoic Flin Flon belt, Manitoba and Saskatchewan, *in* Goodfellow, W., *ed.,* Mineral Deposits of Canada: A Synthesis of Major Deposit-types, District Metallogeny, the Evolution of Geological Provinces, and Exploration Methods: Geological Associaton of Canada, Mineral Deposits Division, Special Publication 5, p. 509–531.
Gee, R.D., Baxter, J.L., Wilde, S.A., and Williams, I.R., 1981, Crustal development in the Archaean Yilgarn block, western Australia: Geological Society of Australia, Special Publication, v. 7, p. 43–56.
Gélinas, L., Brooks, C., and Trzcienski, W.E., Jr., 1976, Archean variolites - quenched immiscible liquids: Canadian Journal of Earth Sciences, v. 13, p. 210–230, http://dx.doi.org/10.1139/e76-024.
Gélinas, L., Brooks, C., Perrault, G., Carignan, J., Trudel, P., and Grasso, F., 1977, Chemostratigraphic divisions within the Abitibi volcanic belt, Rouyn-Noranda, Québec, *in* Baragar, W.R.A., Coleman, L.C., and Hall, J.M., *eds.,* Volcanic Regimes in Canada: Geological Association of Canada, Special Paper 16, p. 265–295.
Gibson, H.L., and Watkinson, D.H., 1990, Volcanogenic massive sulphide deposits of the Noranda Cauldron and shield Volcano, Quebec, *in* Rive, M., Verpaelst, P., Gagnon, Y., Lulin, J.-M., Riverin, G., and Simard, A., *eds.,* The Northwestern Quebec Polymetallic Belt: A summary of 60 years of mining exploration: Canadian Institute of Mining and Metallurgy, p. 119–132.
Gibson, H.L., Pehrsson, S., Thurston, P., and Lafrance, B., 2011, Volcanogenic Massive sulphide Deposits of the Paleoproterozoic Trans-Hudson Orogen and the Archean Abitibi subprovince: Characteristics and Metallogeny (Abstract): GAC–MAC Annual Meeting, Ottawa, ON, Abstracts v. 34, p. 75.
Gill, J.B., 1981, Orogenic Andesites and Plate Tectonics: Minerals and Rocks, v. 16, Springer-Verlag Berlin Heidelberg, 392 p., http://dx.doi.org/10.1007/978-3-642-68012-0.
Gleason, J.D., Moore, T.C., Jr., Johnson, T.M., Rea, D.K., Owen, R.M., Blum, J.D., Pares, J., and Hovan, S.A., 2004, Age calibration of piston core EW9709-07 (equatorial central Pacific) using fish teeth Sr isotope stratigraphy: Palaeogeography, Palaeoclimatology, Palaeoecology, v. 212, p. 355–366, http://dx.doi.org/10.1016/S0031-0182(04)00366-9.
Goldfarb, R.J., Baker, T., Dubé, B., Groves, D.I., Hart, C.J.R., and Gosselin, P., 2005, Distribution, character, and genesis of gold geposits in metamorphic terranes, *in* Hedenquist, J.W., Thompson, J.F.H., Goldfarb, R.J., and Richards, J.P., *eds.,* Economic Geology 100th Anniversary Volume, Society of Economic Geologists, p. 407–450.

Goldstein, S.B., and Francis, D., 2008, The petrogenesis and mantle source of Archaean ferropicrites from the Western Superior Province, Ontario, Canada: Journal of Petrology, v. 49, p. 1729–1753, http://dx.doi.org/10.1093/petrology/egn044.

Goleby, B.R., Blewett, R.S., Korsch, R.J., Champion, D.C., Cassidy, K.F., Jones, L.E.A., Groenewald, P.B., and Henson, P., 2004, Deep seismic reflection profiling in the Archaean northeastern Yilgarn Craton, Western Australia: implications for crustal architecture and mineral potential: Tectonophysics, v. 388, p. 119–133, http://dx.doi.org/10.1016/j.tecto.2004.04.032.

Goleby, B.R., Blewett, R.S., Fomin, T., Fishwick, S., Reading, A.M., Henson, P.A., Kennett, B.L.N., Champion, D.C., Jones, L., Drummond, B.J., and Nicoll, M., 2006, An integrated multi-scale 3D seismic model of the Archaean Yilgarn Craton, Australia: Tectonophysics, v. 420, p. 75–90, http://dx.doi.org/10.1016/j.tecto.2006.01.028.

Goscombe, B., Blewett, R., Foster, D., and Wade, B., 2012, Thermobarometric evolution of subdomains within the western Yilgarn Craton: Record - Geological Survey of Western Australia, p. 6–9.

Goutier, J., 2006, Géologie de la région du lac au Goéland (32F/15): Ministère des Ressources Naturelles et de la Faune, Québec, Rapport Géologique RG 2005-05, p. 44.

Goutier, J., Dion, C., Ouellet, M.-C., David, J., and Parent, M., 2000, Géologie de la région des lacs Guillaumat et Sakami (33F/002 et 33F/07): Géologie Québec, Rapport Géologique, 99-05, p. 40.

Gray, R., and Pysklywec, R.N., 2010, Geodynamic models of Archean continental collision and the formation of mantle lithosphere keels: Geophysical Research Letters, v. 37, L19301, http://dx.doi.org/10.1029/2010gl043965.

Green, J.C., and Schulz, K.J., 1977, Iron-rich basaltic komatiites in the early Precambrian Vermilion District, Minnesota: Canadian Journal of Earth Sciences, v. 14, p. 2181–2192, http://dx.doi.org/10.1139/e77-188.

Griffin, W.L., O'Reilly, S.Y., Abe, N., Aulbach, S., Davies, R.M., Pearson, N.J., Doyle, B.J., and Kivi, K., 2003, The origin and evolution of the Archean lithospheric mantle: Precambrian Research, v. 127, p. 19–41, http://dx.doi.org/10.1016/S0301-9268(03)00180-3.

Gromet, L.P., and Silver, L.T., 1987, REE variations across the Peninsular Ranges batholith: Implications for batholithic petrogenesis and crustal growth in magmatic arcs: Journal of Petrology, v. 28, p. 75–125, http://dx.doi.org/10.1093/petrology/28.1.75.

Grove, T.L., and Parman, S.W., 2004, Thermal evolution of the Earth as recorded by komatiites: Earth and Planetary Science Letters, v. 219, p. 173–187, http://dx.doi.org/10.1016/S0012-821X(04)00002-0.

Gunning, H.C., and Ambrose, J.W., 1939, The Timiskaming-Keewatin problem in the Rouyn-Harricanaw Region, Northwestern Quebec: Transactions of the Royal Society of Canada, Series 3, v. 33, p. 19–49.

Gupta, V.K., 1991, Shaded image of total magnetic field of Ontario: Maps 2585-88: Ontario Geological Survey, scale 1:1,000,000.

Gupta, V.K., Thurston, P.C., and Dusanowskyj, T.H., 1982, Constraints upon models of greenstone belt evolution by gravity modelling, Birch-Uchi greenstone belt, northern Ontario: Precambrian Research, v. 16, p. 233–255, http://dx.doi.org/10.1016/0301-9268(82)90062-6.

Hale, C.J., and Lloyd, P., 1989, Grant 342: Paleomagnetic analysis of regional and contact strains: Ontario Geological Survey, Miscellaneous Paper 143, p. 199–209.

Hallberg, J.A., 1986, Archaean basin development and crustal extension in the northeastern Yilgarn Block, Western Australia: Precambrian Research, v. 31, p. 133–156, http://dx.doi.org/10.1016/0301-9268(86)90071-9.

Hamilton, W.B., 1998, Archean magmatism and deformation were not products of plate tectonics: Precambrian Research, v. 91, p. 143–179, http://dx.doi.org/10.1016/S0301-9268(98)00042-4.

Hamilton, W.B., 2007, Driving mechanism and 3-D circulation of plate tectonics, *in* Sears, J.W., Harms, T.A., and Evenchick, C.A., *eds.,* Whence the Mountains? Inquiries into the Evolution of Orogenic Systems: A Volume in Honor of Raymond A. Price: Geological Society of America, Special Papers, v. 433, p. 1–25, http://dx.doi.org/10.1130/2007.2433(01).

Hamilton, W.B., 2011, Plate tectonics began in Neoproterozoic time, and plumes from deep mantle have never operated: Lithos, v. 123, p. 1–20, http://dx.doi.org/10.1016/j.lithos.2010.12.007.

Hannington, M.D., de Ronde, C.E.J., and Petersen, S., 2005, Sea-Floor tectonics and submarine hydrothermal systems, *in* Hedenquist, J.W., Thompson, J.F.H., Goldfarb, R.J., and Richards, J.P., *eds.,* Economic Geology 100th Anniversary Volume, Society of Economic Geologists, p. 111–141.

Hanski, E., Huhma, H., Rastas, P., and Kamenetsky, V.S., 2001, The Palaeoproterozoic komatiite-picrite association of Finnish Lapland: Journal of Petrology, v. 42, p. 855–876, http://dx.doi.org/10.1093/petrology/42.5.855.

Hanski, E.J., and Smolkin, V.F., 1989, Pechenga ferropicrites and other early Proterozoic picrites in the eastern part of the Baltic Shield: Precambrian Research, v. 45, p. 63–82, http://dx.doi.org/10.1016/0301-9268(89)90031-4.

Hargraves, R.B., 1976, Precambrian Geologic History: Science, v. 193, p. 363–371, http://dx.doi.org/10.1126/science.193.4251.363.

Hart, T.R., 1984, The geochemistry and petrogenesis of a metavolcanic and intrusive sequence in the Kamiskotia area; Timmins, Ontario: Unpublished MSc thesis, University of Toronto, Toronto, ON, 179 p.

Hart, T.R., Gibson, H.L., and Lesher, C.M., 2004, Trace element geochemistry and petrogenesis of felsic volcanic rocks associated with volcanogenic massive Cu–Zn–Pb sulfide deposits: Economic Geology, v. 99, p. 1003–1013, http://dx.doi.org/10.2113/gsecongeo.99.5.1003.

Heather, K.B., 2001, The Geological Evolution of the Archean Swayze Greenstone Belt, Superior Province, Canada: Unpublished PhD thesis, Keele University, Keele, UK, 370 p.

Helmstaedt, H., Padgham, W.A., and Brophy, J.A., 1986, Multiple dikes in Lower Kam Group, Yellowknife greenstone belt: Evidence for Archean sea-floor spreading?: Geology, v. 14, p. 562–566, http://dx.doi.org/10.1130/0091-7613(1986)14<562:MDILKG>2.0.CO;2.

Henry, P., Stevenson, R.K., and Gariépy, C., 1998, Late Archean mantle composition and crustal growth in the western Superior Province of Canada: Neodymium and lead isotopic evidence from the Wawa, Quetico, and Wabigoon Subprovinces: Geochimica et Cosmochimica Acta, v. 62, p. 143–157, http://dx.doi.org/10.1016/S0016-7037(97)00324-4.

Herzberg, C., 1992, Depth and degree of melting of Komatiites: Journal of Geophysical Research, v. 97, p. 4521–4540, http://dx.doi.org/10.1029/91JB03066.

Hessler, A.M., and Lowe, D.R., 2006, Weathering and sediment generation in the Archean: An integrated study of the evolution of siliciclastic sedimentary rocks of the 3.2 Ga Moodies Group, Barberton Greenstone Belt, South Africa: Precambrian Research, v. 151, p. 185–210, http://dx.doi.org/10.1016/j.precamres.2006.08.008.

Hildreth, W., 1981, Gradients in silicic magma chambers: Implications for lithospheric magmatism: Journal of Geophysical Research, v. 86, p. 10153–10192, http://dx.doi.org/10.1029/JB086iB11p10153.

Hildreth, W., and Moorbath, S., 1988, Crustal contributions to arc magmatism in the Andes of Central Chile: Contributions to Mineralogy and Petrology, v. 98, p. 455–489, http://dx.doi.org/10.1007/BF00372365.

Hill, R.E.T., 2001, Komatiite volcanology, volcanological setting and primary geochemical properties of komatiite-associated nickel deposits: Geochemistry: Exploration, Environment, Analysis, v. 1, p. 365–381, http://dx.doi.org/10.1144/geochem.1.4.365.

Hill, R.E.T., Barnes, S.J., Perring, C.S., Gole, M.J., and Dowling, S.E., 1994, The physical volcanology of komatiites in the Archaean Yilgarn Block, Western Australia: Australian research on Ore genesis symposium, Proceedings, Australian Mineral Foundation, Glenside, South Australia, AU, p. 4.1–4.5.

Hoffman, P.F., and Ranalli, G., 1988, Archean oceanic flake tectonics: Geophysical Research Letters, v. 15, p. 1077–1080, http://dx.doi.org/10.1029/GL015i010p01077.

Hoffmann, J.E., Münker, C., Næraa, T., Rosing, M.T., Herwartz, D., Garbe-Schönberg, D., and Svahnberg, H., 2011, Mechanisms of Archean crust formation inferred from high-precision HFSE systematics in TTGs: Geochimica et Cosmochimica Acta, v. 75, p. 4157–4178, http://dx.doi.org/10.1016/j.gca.2011.04.027.

Hofmann, A.W., 1988, Chemical differentiation of the Earth: The relationship between mantle, continental crust, and oceanic crust: Earth and Planetary Science Letters, v. 90, p. 297–314, http://dx.doi.org/10.1016/0012-821X(88)90132-X.

Hofmann, H.J., and Masson, M., 1994, Archean stromatolites from Abitibi greenstone belt, Quebec, Canada: Geological Society of America Bulletin, v. 106, p. 424–429, http://dx.doi.org/10.1130/0016-7606(1994)106<0424:ASFAGB>2.3.CO;2.

Hofmann, H.J., Sage, R.P., and Berdusco, E.N., 1991, Archean Stromatolites in Michipicoten Group siderite ore at Wawa, Ontario: Economic Geology, v. 86, p. 1023–1030, http://dx.doi.org/10.2113/gsecongeo.86.5.1023.

Hofmann, H.J., Thurston, P.C., and Wallace, H., 1985, Archean stromatolites from Uchi greenstone belt, northwestern Ontario, *in* Ayres, L.D., Thurston, P.C., Card, K.D., and Weber, W., *eds.,* Evolution of Archean Supracrustal sequences: Geological Association of Canada, Special Paper 28, p. 125–132.

Hollings, P., 2002, Archean Nb-enriched basalts in the northern Superior Province: Lithos, v. 64, p. 1–14, http://dx.doi.org/10.1016/S0024-4937(02)00154-8.

Hollings, P., and Kerrich, R., 1999, Trace element systematics of ultramafic and mafic volcanic rocks from the 3 Ga North Caribou greenstone belt, northwestern Superior Province: Precambrian Research, v. 93, p. 257–279, http://dx.doi.org/10.1016/S0301-9268(98)00088-6.

Hollings, P., and Kerrich, R., 2000, An Archean arc basalt–Nb-enriched basalt–adakite association: the 2.7 Ga Confederation assemblage of the Birch–Uchi greenstone belt: Contributions to Mineralogy and Petrology, v. 139, p. 208–226, http://dx.doi.org/10.1007/PL00007672.

Hollings, P., and Wyman, D., 1999, Trace element and Sm–Nd systematics of vol-

canic and intrusive rocks from the 3 Ga Lumby Lake Greenstone belt, Superior Province: evidence for Archean plume-arc interaction: Lithos, v. 46, p. 189–213, http://dx.doi.org/10.1016/S0024-4937(98)00062-0.

Hollings, P., Wyman D., and Kerrich, R., 1999, Komatiite–basalt–rhyolite volcanic associations in northern Superior Province greenstone belts: significance of plume-arc interaction in the generation of the proto-continental Superior Province: Lithos, v. 46, p. 137–161, http://dx.doi.org/10.1016/S0024-4937(98)00058-9.

Hollings, P., Stott, G., and Wyman, D., 2000, Trace element geochemistry of the Meen-Dempster greenstone belt, Uchi subprovince, Superior Province, Canada: back-arc development on the margins of an Archean protocontinent: Canadian Journal of Earth Sciences, v. 37, p. 1021–1038, http://dx.doi.org/10.1139/e00-007.

Hooper, P.R., Binger, G.B., and Lees, K.R., 2002, Ages of the Steens and Columbia River flood basalts and their relationship to extension-related calc-alkalic volcanism in eastern Oregon: Geological Society of America Bulletin, v. 114, p. 43–50, http://dx.doi.org/10.1130/0016-7606(2002)114<0043:AOTSAC>2.0.CO;2.

Houlé, M., Lesher, C.M., Gibson, H.L., Fowler, A.D., and Sproule, R.A., 2001, Physical volcanology of komatiites in the Abitibi Greenstone Belt: Ontario Geological Survey, Summary of Field Work and other Activities, Open File Report 6070, p. 13–11 to 13–17.

Houlé, M., Gibson, H.L., Lesher, C.M., Davis, P.C., Cas, R.A.F., Beresford, S.W., and Arndt, N.T., 2008a, Komatiitic Sills and Multi-Generational Peperite at Dundonald Beach, Abitibi Greenstone Belt, Ontario: Volcanic architecture and nickel sulfide distribution: Economic Geology, v. 103, p. 1269–1284, http://dx.doi.org/10.2113/gsecongeo.103.6.1269.

Houlé, M.G., Ayer, J.A., Baldwin, G., Berger, B., Dinel, E., Fowler, A.D., Moulton, B., Saumur, B.-M., and Thurston, P., 2008b, Stratigraphy and volcanology of supracrustal assemblages hosting base metal and gold mineralization in the Abitibi Greenstone Belt: Geological Association of Canada, Mineralogical Association of Canada, Field Trip B4, Quebec, 84 p.

Houlé, M.G., Préfontaine, S., Fowler, A.D., and Gibson, H.L., 2009, Endogenous growth in channelized komatiite lava flows: evidence from spinifex-textured sills at Pyke Hill and Serpentine Mountain, Western Abitibi Greenstone Belt, Northeastern Ontario, Canada: Bulletin of Volcanology, v. 71, p. 881–901, http://dx.doi.org/10.1007/s00445-009-0273-y.

Houlé, M.C., Lesher, C.M., Metsaranta, R.T., Goutier, J., Gilbert, H.P., and McNicoll, V., 2012, Temporal and spatial distribution of magmatic Ni, Cu, PGE, Cr and Fe,Ti, V deposits in the Bird River–Uchi–Oxford Stull, La Grande Eastmain superdomain: A new metallotect within the Superior Province: Society for Geology Applied to Minerals, 12th SGA Biennial Meeting, Uppsala, Sweden, p. 1009–1012.

Hrabi, R.B., and Cruden, A.R., 2006, Structure of the Archean English River subprovince; implications for the tectonic evolution of the western Superior Province, Canada: Canadian Journal of Earth Sciences, v. 43, p. 947–966, http://dx.doi.org/10.1139/e06-023.

Hudak, G.J., Morton, R.L., Franklin, J.M., and Peterson, D.M., 2003, Morphology, distribution, and estimated eruption volumes for intracaldera tuffs associated with volcanic-hosted massive sulfide deposits in the Archean Sturgeon Lake Caldera Complex, northwestern Ontario, *in* White, J.D.L., Smellie, J.L., and Clagur, D.A., *eds.,* Explosive Subaqueous Volcanism: American Geophysical Union, Monograph 140, p. 345–360, http://dx.doi.org/10.1029/140gm23.

Hunter, D.R., and Stowe, C.W., 1997, A historical review of the origin, composition, and setting of Archaean greenstone belts (pre-1980): Oxford Monographs on Geology and Geophysics, v. 35, p. 5–30.

Ishikawa, Y., Sawaguchi, T., Iwaya, S., and Horiuchi, M., 1976, Delineation of prospecting targets for Kuroko deposits based on modes of volcanism of underlying dacite and alteration halos: Mining Geology, v. 26, p. 105–117.

Jackson, S.L., and Fyon, J.A., 1991, The Western Abitibi Subprovince in Ontario, *in* Thurston, P.C., Williams, H.R., Sutcliffe, R.H., and Stott, G.M., *eds.,* Geology of Ontario: Ontario Geological Survey, Special Volume 4, Pt. 1, p. 405–482.

Jahn, B.M., 1997, Géochimie des granitoïdes archéens et de la croûte primitive, *in* Hagemann, R., and Treuil, M., *eds.,* Introduction à la géochimie et ses applications: Commissariat a l'énergie atomique, Université Pierre et Marie Curie, Paris.

Jelsma, H.A., van der Beek, P.A., and Vinyu, M.L., 1993, Tectonic evolution of the Bindura-Shamva greenstone belt (northern Zimbabwe): Progressive deformation around diapiric batholiths: Journal of Structural Geology, v. 15, p. 163–176, http://dx.doi.org/10.1016/0191-8141(93)90093-P.

Jensen, L.S., 1985, Stratigraphy and Petrogenesis of Archean Metavolcanic Sequences, Southwestern Abitibi subprovince, Ontario, *in* Ayres, L.D., Thurston, P.C., Card, K.D., and Weber, W., *eds.,* Evolution of Archean supracrustal Sequences: Geological Association of Canada, Special paper 28, p. 65–87.

Johnson, T.E., Brown, M., Kaus, B.J.P., and VanTongeren, J.A., 2014, Delamination and recycling of Archaean crust caused by gravitational instabilities: Nature Geoscience, v. 7, p. 47–52, http://dx.doi.org/10.1038/ngeo2019.

Jolly, W.T., 1978, Metamorphic history of the Archean Abitibi Belt, *in* Fraser, J.A., and Heywood, W.W., *eds.,* Metamorphism in the Canadian Shield: Geological Survey of Canada, Paper 78-10, p. 63–78.

Kamber, B.S., 2010, Archean mafic-ultramafic volcanic landmasses and their effect on ocean-atmosphere chemistry: Chemical Geology, v. 274, p. 19–28, http://dx.doi.org/10.1016/j.chemgeo.2010.03.009.

Kamber, B.S., 2015, The evolving nature of terrestrial crust from the Hadean, through the Archaean, into the Proterozoic: Precambrian Research, v. 258, p. 48–82, http://dx.doi.org/10.1016/j.precamres.2014.12.007.

Kamber, B.S., Bolhar, R., and Webb, G.E., 2004, Geochemistry of late Archaean stromatolites from Zimbabwe: evidence for microbial life in restricted epicontinental seas: Precambrian Research, v. 132, p. 379–399, http://dx.doi.org/10.1016/j.precamres.2004.03.006.

Katz, L.R., Kontak, D., Dubé, B., and McNicoll, V.J., 2015, The Archean Côté gold intrusion-related Au (–Cu) deposit, Ontario: a large tonnage, low-grade deposit centered on a magmatic-hydrothermal breccia, *in* Dubé, B., and Mercier-Langevin, P., *eds.*, Targeted Geoscience Initiative 4: Contributions to the understanding of Archean lode gold deposits and implications for exploration: Geological Survey of Canada Open File Report 7852, p. 139–155.

Keleman, P.B., 1995, Genesis of high Mg# andesites and the continental crust: Contributions to Mineralogy and Petrology, v. 120, p. 1–19, http://dx.doi.org/10.1007/BF00311004.

Kepezhinskas, P.K., Defant, M.J., and Drummond, M.S., 1995, Na-metasomatism in the island-arc mantle by slab melt–peridotite interaction: Evidence from mantle xenoliths in the North Kamchatka arc: Journal of Petrology, v. 36, p. 1505–1527.

Kerr, A.C., Marriner, G.F., Arndt, N.T., Tarney, J., Nivia, A., Saunders, A.D., and Duncan, R.A., 1996, The petrogenesis of Gorgona komatiites, picrites and basalts: new field, petrographic and geochemical constraints: Lithos, v. 37, p. 245–260, http://dx.doi.org/10.1016/0024-4937(95)00039-9.

Kerrich, R., and Fryer, B.J., 1979, Archean precious-metal hydrothermal systems, Dome Mine, Abitibi greenstone belt: II. REE and oxygen isotope relations: Canadian Journal of Earth Sciences, v. 16, p. 440–458, http://dx.doi.org/10.1139/e79-041.

Kerrich, R., and Manikyamba, C., 2012, Contemporaneous eruption of Nb-enriched basalts – K-adakites - Na-adakites from the 2.7 Ga Penakacherla terrane: Implications for subduction zone processes and crustal growth in the eastern Dharwar craton, India: Canadian Journal of Earth Sciences, v. 49, p. 615–636, http://dx.doi.org/10.1139/e2012-005.

Kerrich, R., and Wyman, D.A., 1996, The trace element systematics of igneous rocks in mineral exploration: An overview, *in* Wyman, D.A., *ed.,* Trace Element Geochemistry of Volcanic Rocks: Applications for Massive Sulphide Exploration: Geological Association of Canada, Short Course Notes 12, p. 1–50.

Kerrich, R., Wyamn, D., Fan, J., and Bleeker, W., 1998, Boninite series: low Ti-tholeiite associations from the 2.7 Ga Abitibi greenstone belt: Earth and Planetary Science Letters, v. 164, p. 303–316, http://dx.doi.org/10.1016/S0012-821X(98)00223-4.

Kerrich, R., Polat, A., Wyman, D., and Hollings, P., 1999, Trace element systematics of Mg- to Fe-tholeiitic basalt suites of the Superior Province: implications for mantle reservoirs and greenstone belt genesis: Lithos, v. 46, p. 163–187, http://dx.doi.org/10.1016/S0024-4937(98)00059-0.

Ketchum, J.W.F., Ayer, J.A., van Breemen, O., Pearson, N.J., and Becker, J.K., 2008, Pericontinental crustal growth of the southwestern Abitibi Subprovince, Canada — U–Pb, Hf, and Nd isotopic evidence: Economic Geology, v. 103, p. 1151–1184.

Kiyokawa, S., and Taira, A., 1998, The Cleaverville Group in the West Pilbara Coastal Granitoid-Greenstone terrain of Western Australia: an example of a Mid-Archaean immature oceanic island-arc succession: Precambrian Research, v. 88, p. 109–142, http://dx.doi.org/10.1016/S0301-9268(97)00066-1.

Komiya, T., Hayashi, M., Maruyama, S., and Yurimoto, H., 2002, Intermediate-P/T type Archean metamorphism of the Isua supracrustal belt: Implications for secular change of geothermal gradients at subduction zones and for Archean plate tectonics: American Journal of Science, v. 302, p. 806–826, http://dx.doi.org/10.2475/ajs.302.9.806.

Korja, A., Lahtinen, R., Heikkinen, P., Kukkonen, I.T., Ekdahl, E., Nironen, M., Kontinen, A., Paavola, J., Lukkarinen, H., Ruotsalainen, A., Lehtimaki, J., Forss, H., Lanne, E., Salmirinne, H., Pernu, T., Turunen, P., Ruokanen, E., Tiira, T., Keskinen, J., Hjelt, S.-E., Tiikkainen, J., Yliniemi, J., Jalkanen, E., Berzin, R., Suleimanov, A., Zamoshnyaya, N., Moissa, I., Kostyuk, A., and Litvinenko, V., 2006, A geological interpretation of the upper crust along FIRE 1: Geological Survey of Finland, Special Paper 43, p. 45–76.

Kositcin, N., Brown, S.J.A., Barley, M.E., Krapež, B., Cassidy, K.F., and Champion, D.C., 2008, SHRIMP U–Pb zircon age constraints on the Late Archaean tectonostratigraphic architecture of the Eastern Goldfields Superterrane, Yilgarn Craton, Western Australia: Precambrian Research, v. 161, p. 5–33,

http://dx.doi.org/10.1016/j.precamres.2007.06.018.
Kozhevnikov, V.N., 1992, Ggeology and geochemistry of Archean greenstone structures in North Karelia (in Russian): Karelian Branch Russian Academy of Sciences, Petrozavodsk, 199 p.
Krapez, B., and Barley, M.E., 1987, Archaean strike-slip faulting and related ensialic basins: evidence from the Pilbara Block, Australia: Geological Magazine, v. 124, p. 555–567, http://dx.doi.org/10.1017/S0016756800017386.
Krapez, B., and Eisenlohr, B., 1998, Tectonic settings of Archaean (3325–2775 Ma) crustal-supracrustal belts in the West Pilbara Block: Precambrian Research, v. 88, p. 173–205, http://dx.doi.org/10.1016/S0301-9268(97)00068-5.
Krogh, T.E., and Davis, G.L., 1971, Zircon U–Pb Ages of Archean Metavolcanic Rocks in the Canadian Shield: Carnegie Institution of Washington Yearbook 70, p. 241–242.
Kröner, A., 1991, Tectonic evolution in the Archaean and Proterozoic: Tectonophysics, v. 187, p. 393–410, http://dx.doi.org/10.1016/0040-1951(91)90478-B.
Kuiper, D., 2010, Geology, geochemistry and geochronology of the Dufault, Séguin, and Horseshoe gabbroic-dioritic intrusions, Blake River Group (2704–2695 Ma), Abitibi Subprovince, Québec: Unpublished MSc thesis, Laurentian University, ON, 88 p.
Kusky, T.M., 1998, Tectonic setting and terrane accretion of the Archean Zimbabwe craton: Geology, v. 26, p. 163–166, http://dx.doi.org/10.1130/0091-7613(1998)026<0163:TSATAO>2.3.CO;2.
Kusky, T.M., and Kidd, W.S.F., 1992, Remants of an Archean oceanic plateau, Belingwe greenstone belt, Zimbabwe: Geology, v. 20, p. 43–46, http://dx.doi.org/10.1130/0091-7613(1992)020<0043:ROAAOP>2.3.CO;2.
Kusky, T.M., and Polat, A., 1999, Growth of granite-greenstone terranes at convergent margins, and stabilization of Archean cratons: Tectonophysics, v. 305, p. 43–73, http://dx.doi.org/10.1016/S0040-1951(99)00014-1.
Kusky, T.M., Li, J.-H., and Tucker, R.D., 2001, The Archean Dongwanzi Ophiolite Complex, North China Craton: 2.505–Billion-Year-Old oceanic crust and mantle: Science, v. 292, p. 1142–1145, http://dx.doi.org/10.1126/science.1059426.
Laflèche, M.R., Dupuy, C., and Bougault, H., 1992, Geochemistry and petrogenesis of Archean mafic volcanic rocks of the southern Abitibi Belt, Québec: Precambrian Research, v. 57, p. 207–241, http://dx.doi.org/10.1016/0301-9268(92)90003-7.
Lafrance, B., Mueller, W.U., Daigneault, R., and Dupras, N., 2000, Evolution of a submerged composite arc volcano: volcanology and geochemistry of the Normétal volcanic complex, Abitibi greenstone belt, Québec, Canada: Precambrian Research, v. 101, p. 277–311, http://dx.doi.org/10.1016/S0301-9268(99)00092-3.
Lambert, M.B., Burbidge, G., Jefferson, C.W., Beaumont-Smith, C., and Lustwerk, R., 1990, Stratigraphy, facies and structure in volcanic and sedimentary rocks of the Archean Back River volcanic complex, NWT: Geological Survey of Canada, Current Research Paper 90-1C, p. 151–165, http://dx.doi.org/10.4095/131253.
Lambert, M.B., Ernst, R.E., and Dudás, F.O.L., 1992, Archean mafic dyke swarms near the Cameron River and Beaulieu River volcanic belts and their implications for tectonic modelling of the Slave Province, Northwest Territories: Canadian Journal of Earth Sciences, v. 29, p. 2226–2248, http://dx.doi.org/10.1139/e92-176.
Langford, F.F., and Morin, J.A., 1976, The development of the Superior Province of northwestern Ontario by merging island arcs: American Journal of Science, v. 276, p. 1023–1034, http://dx.doi.org/10.2475/ajs.276.9.1023.
Larbi, Y., Stevenson, R., Breaks, F., Machado, N., and Gariépy, C., 1999, Age and Isotopic composition of late Archean leucogranites: implications for continental collision in the western Superior Province: Canadian Journal of Earth Sciences, v. 36, p. 495–510, http://dx.doi.org/10.1139/e98-113.
Large, R.R., Gemmell, J.B., Paulick, H., and Huston, D.L., 2001, The alteration box plot: a simple approach to understanding the relationship between alteration mineralogy and lithogeochemistry associated with volcanic-hosted massive sulfide deposits: Economic Geology, v. 96, p. 957–971, http://dx.doi.org/10.2113/gsecongeo.96.5.957.
Large, R.R., Bull, S.W., and Maslennikov, V.V., 2011, A carbonaceous sedimentary source-rock model for Carlin-type and orogenic gold deposits: Economic Geology, v. 106, p. 331–358, http://dx.doi.org/10.2113/econgeo.106.3.331.
Larson, J.E., and Hutchinson, R.W., 1993, Selbaie Zn–Cu–Ag deposits, Quebec, Canada. An example of evolution from subaqueous to subaerial volcanism and mineralization in an archean caldera environment: Economic Geology, v. 88, p. 1460–1460, http://dx.doi.org/10.2113/gsecongeo.88.6.1460.
Laurent, O., Martin, H., Moyen, J.F., and Doucelance, R., 2014, The diversity and evolution of late-Archean granitoids: Evidence for the onset of "modern-style" plate tectonics between 3.0 and 2.5 Ga: Lithos, v. 205, p. 208–235, http://dx.doi.org/10.1016/j.lithos.2014.06.012.
Layer, P.W., Kröner, A., McWilliams, M., and York, D., 1989, Elements of the Archean thermal history and apparent polar wander of the eastern Kaapvaal Craton, Swaziland, from single grain dating and paleomagnetism: Earth and Planetary Science Letters, v. 93, p. 23–34, http://dx.doi.org/10.1016/0012-821X(89)90181-7.
Le Maitre, R.W., *editor,* 1989, A Classification of igneous rocks and glossary of terms: Recommendations of the International Union of Geological Sciences subcommission on the systematics of Igneous Rocks: Blackwell Scientific Publishing, Oxford, v. 193.
Leclerc, F., Bédard, J.H., Harris, L.B., McNicoll, V.J., Goulet, N., Roy, P., and Houlé, P., 2011, Tholeiitic to calc-alkaline cyclic volcanism in the Roy Group, Chibougamau area, Abitibi Greenstone Belt — revised stratigraphy and implications for VHMS exploration: Canadian Journal of Earth Sciences, v. 48, p. 661–694, http://dx.doi.org/10.1139/E10-088.
Legault, M., Gauthier, M., Jébrak, M., Davis, D.W., and Baillargeon, F., 2002, Evolution of the subaqueous to near-emergent Joutel volcanic complex, Northern Volcanic zone, Abitibi subprovince, Quebec, Canada: Precambrian Research, v. 115, p. 187–221, http://dx.doi.org/10.1016/S0301-9268(02)00010-4.
Lentz, D.R., 1998, Mineralized intrusion-related skarn systems: Mineralogical Association of Canada, Ottawa, ON, Canada, Short Course Handbook, 664 p.
Lesher, C.M., 1989, Komatiite-associated nickel sulfide deposits: Reviews in Economic Geology, v. 4, p. 44–101.
Lesher, C.M., 2007, Ni–Cu–(PGE) Deposits in the Raglan Area, Cape Smith Belt, New Quebec, *in* Goodfellow, W., *ed.,* Mineral Deposits of Canada: A Synthesis of Major Deposit-types, District Metallogeny, the Evolution of Geological Provinces, and Exploration Methods: Geological Association of Canada, Mineral Deposits Division, Special Publication 5, p. 351–385.
Lesher, C.M., and Keays, R.R., 2002, Komatiite-associated Ni–Cu–(PGE) deposits; geology, mineralogy, geochemistry and genesis, *in* Cabri, L.J., *ed.,* The geology, geochemistry, mineralogy and mineral beneficiation of platinum-group elements: Canadian Institute of Mining and Metallurgy, p. 579–617.
Lesher, C.M., Goodwin, A.M., Campbell I.H., and Gorton, M.P., 1986, Trace-element geochemistry of ore-associated and barren, felsic metavolcanic rocks in the Superior Province, Canada: Canadian Journal of Earth Sciences, v. 23, p. 222–237, http://dx.doi.org/10.1139/e86-025.
Lodge, R.W.D., Gibson, H.L., Stott, G.M., Hudak, G.J., Jirsa, M.A., and Hamilton, M.A., 2013, New U–Pb geochronology from Timiskaming-type assemblages in the Shebandowan and Vermilion greenstone belts, Wawa subprovince, Superior Craton: Implications for the Neoarchean development of the southwestern Superior Province: Precambrian Research, v. 235, p. 264–277, http://dx.doi.org/10.1016/j.precamres.2013.06.011.
London, D., and Morgan, G.B.,VI, 2012, The pegmatite puzzle: Elements, v. 8, p. 263–268, http://dx.doi.org/10.2113/gselements.8.4.263.
Lowe, D.R., Byerly, G.R., and Heubeck, C., 1999, Structural divisions and development of the west-central part of the Barberton Greenstone Belt, *in* Lowe, D.R., and Byerly, G.R., *eds.,* Geologic Evolution of the Barberton Greenstone Belt, South Africa: Geological Society of America, Special Papers, v. 329, p. 37–82, http://dx.doi.org/10.1130/0-8137-2329-9.37.
Lucas, S.B., Stern, R.A., Syme, E.C., Reilly, B.A., and Thomas, D.J., 1996, Intraoceanic tectonics and the development of continental crust: 1.92–1.84 Ga evolution of the Flin Flon belt, Canada: Geological Society of America Bulletin, v. 108, p. 602–629, http://dx.doi.org/10.1130/0016-7606(1996)108<0602:ITATDO>2.3.CO;2.
Ludden, J., Hubert, C., and Gariépy, C., 1986, The tectonic evolution of the Abitibi greenstone belt of Canada: Geological Magazine, v. 123, p. 153–166, http://dx.doi.org/10.1017/S0016756800029800.
Macgregor, A.M., 1951, Some milestones in the Precambrian of Southern Rhodesia [presidential address]: Proceedings of the Geological Society of South Africa, v. 54, p. 27–71.
Maier, W.D., Barnes, S.-J., and Pellet, T., 1996, The economic significance of the Bell River complex, Abitibi subprovince, Quebec: Canadian Journal of Earth Sciences, v. 33, p. 967–980, http://dx.doi.org/10.1139/e96-073.
Manikyamba, C., and Naqvi, S.M., 1998, Archaean oceanic ridge and floor basalt: an example and implications from Sandur greenstone belt, Dharwar Craton: Geological Survey of Finland, Special Paper 26, 36 p.
Manikyamba, C., Naqvi, S.M., Subba Rao, D.V., Ram Mohan, M., Khanna, T.C., Rao, T.G., and Reddy, G.L.N., 2005, Boninites from the Neoarchaean Gadwal Greenstone belt, Eastern Dharwar Craton, India: Implications for Archaean subduction processes: Earth and Planetary Science Letters, v. 230, p. 65–83, http://dx.doi.org/10.1016/j.epsl.2004.06.023.
Manikyamba, C., Kerrich, R., Khanna, T.C., Satyanarayanan, M., and Krishna, A. K., 2009, Enriched and depleted arc basalts, with Mg-andesites and adakites; A potential paired arc–back-arc of the 2.6 Ga Hutti greenstone terrane, India: Geochimica et Cosmochimica Acta, v. 73, p. 1711–1736, http://dx.doi.org/10.1016/j.gca.2008.12.020.
Manikyamba, C., Kerrich, R., Polat, A., Raju, K., Satyanarayanan, M., and Krishna, A.K., 2012, Arc picrite-potassic adakitic-shoshonitic volcanic association of the Neoarchean Sigegudda greenstone terrane, western Dharwar craton: Transition from arc wedge to lithosphere melting: Precambrian Research, v. 212–213, p.

207–224, http://dx.doi.org/10.1016/j.precamres.2012.05.006.
Martin, A., Nisbet, E.G., Bickle, M.J., and Orpen, J.L., 1993, Rock units and stratigraphy of the Belingwe greenstone belt: the complexity of the tectonic setting, *in* Bickle, M.J., and Nisbet, E.G., *eds.*, The Geology of the Belingwe Greenstone Belt, Zimbabwe: A study of the Evolution of Archaean Continental Crust: A.A. Balkema, Rotterdam, p. 13–37.
Martin, H., 1987, Evolution in compositon of granitic rocks controlled by time-dependent changes in petrogenetic processes: Examples from the Archaean of eastern Finland: Precambrian Research, v. 35, p. 257–276, http://dx.doi.org/10.1016/0301-9268(87)90058-1.
Martin, H., 1993, The mechanisms of petrogenesis of the Archeaean continental crust—Comparison with modern processes: Lithos, v. 30, p. 373–388, http://dx.doi.org/10.1016/0024-4937(93)90046-F.
Martin, H., 1999, Adakitic magmas: modern analogues of Archaean granitoids, Lithos, v. 46, p. 411–429, http://dx.doi.org/10.1016/S0024-4937(98)00076-0.
Martin, H., Smithies, R.H., Rapp, R., Moyen, J.-F., and Champion, D., 2005, An overview of adakite, tonalite-trondhjemite-granodiorite (TTG), and sanukitoid: relationships and some implications for crustal evolution: Lithos, v. 79, p. 1–24, http://dx.doi.org/10.1016/j.lithos.2004.04.048.
Maurice, C., David, J., Bédard, J.H., and Francis, D., 2009, Evidence for a widespread mafic cover sequence and its implications for continental growth in the Northeastern Superior Province: Precambrian Research, v. 168, p. 45–65, http://dx.doi.org/10.1016/j.precamres.2008.04.010.
McCall, G.J.H., 2003, A critique of the analogy between Archaean and Phanerozoic tectonics based on regional mapping of the Mesozoic–Cenozoic plate convergent zone in the Makran, Iran: Precambrian Research, v. 127, p. 5–17, http://dx.doi.org/10.1016/S0301-9268(03)00178-5.
McCarron, J.J., and Smellie, J.L., 1998, Tectonic implications of fore-arc magmatism and generation of high-magnesian andesites: Alexander Island, Antarctica: Journal of the Geological Society, v. 155, p. 269–280, http://dx.doi.org/10.1144/gsjgs.155.2.0269.
McCulloch, M.T., and Gamble, J.A., 1991, Geochemical and geodynamical constraints on subduction zone magmatism: Earth and Planetary Science Letters, v. 102, p. 358–374, http://dx.doi.org/10.1016/0012-821X(91)90029-H.
McDonough, W.F., and Ireland, T.R., 1993, Intraplate origin of komatiites inferred from trace elements in glass inclusions: Nature, v. 365, p. 432–434, http://dx.doi.org/10.1038/365432a0.
Migdisov, A.A., Bredanova, N.V., Rozen, O.M., and Abbyasov, A.A., 2003, Evolution of the mineral composition of pelitic and psammitic rocks in the geologic history of continents: Geochemistry International, v. 41, p. 959–978.
Miyashiro, A., 1973, Paired and unpaired metamorphic belts: Tectonophysics, v. 17, p. 241–254, http://dx.doi.org/10.1016/0040-1951(73)90005-X.
Morin, J.A., 1973, Geology of the Lower Shebandowan Lake area, District of Thunder Bay: Ontario Department of Mines, Geological Report 110, 45 p.
Morris, J.D., and Hart, S.R., 1983, Isotopic and incompatible element constraints on the genesis of island arc volcanics from Cold Bay and Amak Island, Aleutians, and implications for mantle structure: Geochimica et Cosmochimica Acta, v. 47, p. 2015–2030, http://dx.doi.org/10.1016/0016-7037(83)90217-X.
Mortensen, J.K., 1993, U–Pb Geochronology of the eastern Abitibi Subprovince. Part 2: Noranda – Kirkland Lake area: Canadian Journal of Earth Sciences, v. 30, p. 29–41, http://dx.doi.org/10.1139/e93-003.
Morton, R.L., Walker, J.S., Hudak, G.J., and Franklin, J.M., 1991, The early development of an Archean submarine caldera complex with emphasis on the Mattabi ash-flow tuff and its relationship to the Mattabi massive sulfide deposit: Economic Geology, v. 86, p. 1002–1011, http://dx.doi.org/10.2113/gsecongeo.86.5.1002.
Moyen, J.-F., and Stevens, G., 2006, Experimental constraints on TTG petrogenesis: Implications for Archean geodynamics, *in* Benn, K., Mareschal, J.-C., and Condie, K.C., *eds.,* American Geophysical Union, Monograph 164, p. 149–175, http://dx.doi.org/10.1029/164gm11.
Mueller, W., and Corcoran, P.L., 1998, Late-orogenic basins in the Archean Superior Province, Canada: characteristics and inferences: Sedimentary Geology, v. 120, p. 177–203, http://dx.doi.org/10.1016/S0037-0738(98)00032-3.
Mueller, W., and Corcoran, P.L., 2001, Volcano-sedimentary processes operating on a marginal continental arc: the Archean Raquette Lake Formation, Slave Province, Canada: Sedimentary Geology, v. 141–142, p. 169–196, http://dx.doi.org/10.1016/S0037-0738(01)00074-4.
Mueller, W., and Dimroth, E., 1987, A terrestrial-shallow marine transition in the Archean Opemisca Group east of Chapais, Quebec: Precambrian Research, v. 37, p. 29–55, http://dx.doi.org/10.1016/0301-9268(87)90038-6.
Mueller, W., and Pickett, C., 2005, Relative sea level change along the Slave craton coastline: Characteristics of Archean continental rifting: Sedimentary Geology, v. 176, p. 97–119, http://dx.doi.org/10.1016/j.sedgeo.2004.12.015.
Mungall, J.E., Harvey, J.D., Balch, S.J., Azar, B., Atkinson, J., and Hamilton, M.A., 2010, Eagle's Nest: A magmatic Ni–Cu–PGE deposit in the James Bay Lowlands, Ontario, Canada: Society of Economic Geologists, Special Publication, v. 15, p. 539–557.
Myers, J.S., and Swager, C., 1997, The Yilgarn Craton, Australia, *in* de Wit, M.J., and Ashwal, L.D., *eds.,* Greenstone Belts: Clarendon Press, Oxford, p. 640–656.
Naqvi, S.M., 2008, Geochemical indicators of the Neoarchaean subduction-accretion related magmatism: a global perspective with special reference to the Dharwar Craton: Geological Society of India, Memoir, v. 73, p. 1–20.
Naqvi, S.M., Khan, R.M.K., Manikyamba, C., Mohan, M.R., and Khanna, T.C., 2006, Geochemistry of the NeoArchaean high-Mg basalts, boninites and adakites from the Kushtagi-Hungund greenstone belt of the Eastern Dharwar craton (EDC): implications for the tectonic setting: Journal of Asian Earth Sciences, v. 27, p. 25–44, http://dx.doi.org/10.1016/j.jseaes.2005.01.006.
Nehring, F., Foley, S.F., Höltta, P., and Van Den Kerkhof, A.M., 2009, Internal differentiation of the Archean continental crust: Fluid-controlled partial melting of granulites and TTG - Amphibolite associations in Central Finland: Journal of Petrology, v. 50, p. 3–35, http://dx.doi.org/10.1093/petrology/egn070.
O'Neil, J., Maurice, C., Stevenson, R.K., Larocque, J., Cloquet, C., David, J., and Francis, D., 2008, The Geology of the 3.8 Ga Nuvvuagittuq (Porpoise Cove) Greenstone Belt, Northeastern Superior Province, Canada, *in* Van Kranendonk, M.J., Smithies, R.H., and Bennett, V.C., *eds.*, Earth's Oldest Rocks: Elsevier, Amsterdam, p. 219–250.
Ojakangas, R.W., 1985, Review of Archean clastic sedimentation, Canadian shield: major felsic volcanic contributions to turbidite and alluvial fan-fluvial facies associations, *in* Ayres, L.D., Thurston, P.C., Card, K.D., and Weber, W., *eds.*, Evolution of Archean Supracrustal Sequences: Geological Association of Canada, Special Paper 28, p. 23–47.
Othman, D.B., Arndt, N.T., White, W.M., and Jochum, K.P., 1990, Geochemistry and age of Timiskaming alkali volcanics and the Otto syenite stock, Abitibi, Ontario: Canadian Journal of Earth Sciences, v. 27, p. 1304–1311, http://dx.doi.org/10.1139/e90-140.
Palme, H., and Jones, A., 2004, Solar system abundances of the elements, *in* Holland, H.D., and Turekian, K.K., *eds.*, Treatise on Geochemistry: Elsevier Amsterdam, p. 41–61.
Parks, J., Lin, S., Davis, D., and Corkery, T., 2006, New high-precision U–Pb ages for the Island Lake greenstone belt, northwestern Superior Province: implications for regional stratigraphy and the extent of the North Caribou terrane: Canadian Journal of Earth Sciences, v. 43, p. 789–803, http://dx.doi.org/10.1139/e06-044.
Parman, S.W., Grove, T.L., and Dann, J.C., 2001, The production of Barberton komatiites in an Archean subduction zone: Geophysical Research Letters, v. 28, p. 2513–2516, http://dx.doi.org/10.1029/2000GL012713.
Pawley, M.J., Van Kranendonk, M.J., and Collins, W.J., 2004, Interplay between deformation and magmatism during doming of the Archaean Shaw Grantioid Complex, Pilbara Craton, Western Australia: Precambrian Research, v. 131, p. 213–230, http://dx.doi.org/10.1016/j.precamres.2003.12.010.
Pearce, J.A., and Peate, D.W., 1995, Tectonic implications of the composition of volcanic arc magmas: Annual Review of Earth and Planetary Sciences, v. 23, p. 251–285.
Perchuk, A.L., and Morgunova, A.A., 2014, Variable *P–T* paths and HP-UHP metamorphism in a Precambrian terrane, Gridino, Russia: Petrological evidence and geodynamic implications: Gondwana Research, v. 25, p. 614–629, http://dx.doi.org/10.1016/j.gr.2012.09.009.
Percival, J.A., 2007, Geology and Metallogeny of the Superior Province, Canada, *in* Goodfellow, W., *ed.*, Mineral Deposits of Canada: A Synthesis of Major Deposit Types, District Metallogeny, the Evolution of Geological Provinces and Exploration Methods: Geological Association of Canada, Mineral Deposits Division, Special Publication 5, p. 903–928.
Percival, J.A., and Helmstaedt, H., 2006, The western Superior Province Lithoprobe and NATMAP Transects: Introduction and summary: Canadian Journal of Earth Sciences, v. 43, p. 743–747, http://dx.doi.org/10.1139/e06-063.
Percival, J.A., and Stott, G.M., 2010, Superior Province: overview, update and reflections: Geological Survey of Western Australia, Record 2010/18, p. 4–6.
Percival, J.A., Stern, R.A., Skulski, T., Card, K.D., Mortensen, J.K., and Bégin, N.J., 1994, Minto Block, Superior Province: Missing link in deciphering assembly of the craton at 2.7 Ga: Geology, v. 22, p. 839–842, http://dx.doi.org/10.1130/0091-7613(1994)022<0839:MBSPML>2.3.CO;2.
Percival, J.A., Stern, R.A., and Rayner, N., 2003, Archean adakites from the Ashuanipi complex, eastern Superior Province, Canada: geochemistry, geochronology and tectonic significance: Contributions to Mineralogy and Petrology, v. 145, p. 265–280, http://dx.doi.org/10.1007/s00410-003-0450-5.
Percival, J.A., Bleeker, W., Cook, F.A., Rivers, T., Ross, G., and van Staal, C.R., 2004, PanLITHOPROBE workshop IV: Intra-orogen correlations and comparative orogenic anatomy: Geoscience Canada, v. 31, p. 23–39.
Percival, J.A., Sanborn-Barrie, M., Skulski, T., Stott, G.M., Helmstaedt, H., and White, D.J., 2006, Tectonic evolution of the western Superior Province from NATMAP and Lithoprobe studies: Canadian Journal of Earth Sciences, v. 43, p. 1085–1117, http://dx.doi.org/10.1139/e06-062.

Perring, C.S., Barnes, S.J., and Hill, R.E.T., 1994, Direct evidence for thermal erosion and related nickel-sulfide mineralisation at the base of a komatiite lava channel: Exploration and Mining Research News 2, p. 7–11.

Peschler, A.P., Benn, K., and Roest, W.R., 2004, Insights on Archean continental geodynamics from gravity modelling of granite–greenstone terranes: Journal of Geodynamics, v. 38, p. 185–207, http://dx.doi.org/10.1016/j.jog.2004.06.005.

Pettigrew, N.T., and Hattori, K.H., 2006, The Quetico intrusions of western Superior Province: Neo-Archean examples of Alaskan/Ural-type mafic-ultramafic intrusions: Precambrian Research, v. 149, p. 21–42, http://dx.doi.org/10.1016/j.precamres.2006.06.004.

Phinney, W.C., Morrison, D.A., and Maczuga, D.E., 1988, Anorthosites and related megacrystic units in the evolution of Archean Crust: Journal of Petrology, v. 29, p. 1283–1323, http://dx.doi.org/10.1093/petrology/29.6.1283.

Pilot, J., Werner, C-D., Haubrich, F., and Baumann, N., 1998, Palaeozoic and Proterozoic zircons from the Mid-Atlantic Ridge: Nature, v. 393, p. 676-679, http://dx.doi.org/10.1038/31452.

Polat, A., and Kerrich, R., 2001, Magnesian andesites, Nb-enriched basalt-andesites, and adakites from late-Archean 2.7 Ga Wawa greenstone belts, Superior Province, Canada: implications for late Archean subduction zone petrogenetic processes: Contributions to Mineralogy and Petrology, v. 141, p. 36–52, http://dx.doi.org/10.1007/s004100000223.

Polat, A., and Kerrich, R., 2002, Nd-isotope systematics of ~2.7 Ga adakites, magnesian andesites, and arc basalts, Superior Province: Evidence for shallow crustal recycling at Archean subduction zones: Earth and Planetary Science Letters, v. 202, p. 345–360, http://dx.doi.org/10.1016/S0012-821X(02)00806-3.

Polat, A., Kerrich, R., and Wyman, D.A., 1998, The late Archean Schreiber–Hemlo and White River–Dayohessarah greenstone belts, Superior Province: collages of oceanic plateaus, oceanic arcs, and subduction–accretion complexes: Tectonophysics, v. 289, p. 295–326, http://dx.doi.org/10.1016/S0040-1951(98)00002-X.

Poulsen, K.H., Robert, F., and Dubé, B., 2000, Geological classification of Canadian gold deposits: Geological Survey of Canada, Bulletin 540, 106 p., http://dx.doi.org/10.4095/211094.

Powell, W.G., Carmichael, D.M., and Hodgson, C.J., 1995, Conditions and timing of metamorphism in the southern Abitibi greenstone belt, Quebec: Canadian Journal of Earth Sciences, v. 32, p. 787–805, http://dx.doi.org/10.1139/e95-067.

Prendergast, M.D., 2004, The Bulawayan Supergroup: a late Archaean passive margin-related large igneous province in the Zimbabwe craton: Journal of the Geological Society, v. 161, p. 431–445, http://dx.doi.org/10.1144/0016-764902-092.

Prendergast, M.D., and Wingate, M.T.D., 2013, Zircon geochronology of late Archean komatiitic sills and their felsic country rocks, south-central Zimbabwe: A revised age for the Reliance komatiitic event and its implications: Precambrian Research, v. 229, p. 105–124, http://dx.doi.org/10.1016/j.precamres.2012.02.004.

Pyke, D.R., Naldrett, A.J., and Eckstrand, O.R., 1973, Archean ultramafic flows in Munro Township, Ontario: Geological Society of America Bulletin, v. 84, p. 955–978, http://dx.doi.org/10.1130/0016-7606(1973)84<955:AUFIMT>2.0.CO;2.

Rajamani, V., Shivkumar, K., Hanson, G.N., and Shirey, S.B., 1985, Geochemistry and petrogenesis of amphibolites, Kolar Schist Belt, south India: evidence for komatiitic magma derived by low percentages of melting of the mantle: Journal of Petrology, v. 26, p. 92–123, http://dx.doi.org/10.1093/petrology/26.1.92.

Reubi, O., and Blundy, J., 2009, A dearth of intermediate melts at subduction zone volcanoes and the petrogenesis of arc andesites: Nature, v. 461, p. 1269–1273, http://dx.doi.org/10.1038/nature08510.

Richards, J.P., and Kerrich, R., 2007, Special Paper: Adakite-like rocks: their diverse origins and questionable role in metallogenesis: Economic Geology, v. 102, p. 537–576, http://dx.doi.org/10.2113/gsecongeo.102.4.537.

Robert, F., and Poulsen, K.H., 1997, World-class Archaean gold deposits in Canada: An overview: Australian Journal of Earth Sciences, v. 44, p. 329–351, http://dx.doi.org/10.1080/08120099708728316.

Robert, F., Poulsen, K.H., and Dubé, B., 1997, Gold Deposits and their Geological Classification, *in* Gubins, A.G., *ed.,* Geophysics and Geochemistry at the Millenium: Prospectors and Developers Association of Canada, Toronto, p. 209–220.

Robin, C.M.I., and Bailey, R.C., 2009, Simultaneous generation of Archean crust and subcratonic roots by vertical tectonics: Geology, v. 37, p. 523–526, http://dx.doi.org/10.1130/G25519A.1.

Robinson, P.T., Malpas, J., Dilek, Y., and Zhou, M.-F., 2009, The significance of sheeted dike complexes in ophiolites: GSA Today, v. 18, p. 4–10, http://dx.doi.org/10.1130/GSATG22A.1.

Rogers, N., McNicoll, V., van Staal, C.R., and Tomlinson, K.Y., 2000, Lithogeochemical studies in the Uchi-Confederation greenstone belt, northwestern Ontario: implications for Archean tectonics: Geological Survey of Canada, Current Research Part C, p. 1–11, http://dx.doi.org/10.4095/211161.

Ross, P.-S., and Mercier-Langevin, P., 2014, Igneous Rock Associations 14. The volcanic setting of VMS and SMS deposits: A review: Geoscience Canada, v. 41, p. 365–377, http://dx.doi.org/10.12789/geocanj.2014.41.045.

Ross, P.-S., Goutier, J., McNicoll, V.J., and Dubé, B., 2008, Volcanology and geochemistry of the Monsabrais area, Blake River Group, Abitibi greenstone belt, Quebec: implications for volcanogenic massive sulphide exploration: Geological Survey of Canada, Current Research, p. 1–18, http://dx.doi.org/10.4095/224804.

Ross, P.-S., McNicoll, V.J., Debreil, J.-A., and Carr, P., 2014, Precise U–Pb geochronology of the Matagami mining camp, Abitibi greenstone belt, Quebec: stratigraphic constraints and implications for volcanogenic massive sulfide exploration: Economic Geology v. 109, p. 89–101, http://dx.doi.org/10.2113/econgeo.109.1.89.

Sajona, F.G., Maury, R.C., Bellon, H., Cotten, J., and Defant, M., 1996, High field strength element enrichment of Pliocene–Pleistocene Island Arc Basalts. Zomboanga Peninsula, western Mindanao (Philippines): Journal of Petrology, v. 37, p. 693–726, http://dx.doi.org/10.1093/petrology/37.3.693.

Sanborn-Barrie, M., and Skulski, T., 2006, Sedimentary and structural evidence for 2.7 Ga continental arc–oceanic-arc collision in the Savant–Sturgeon greenstone belt, western Superior Province, Canada: Canadian Journal of Earth Sciences, v. 43, p. 995–1030, http://dx.doi.org/10.1139/e06-060.

Sanborn-Barrie, M., Skulski, T., and Parker, J., 2001, Three hundred million years of tectonic history recorded by the Red Lake greenstone belt, Ontario: Geological Survey of Canada, Current Research 2001-C19, p. 1–14.

Sanschagrin, Y., 1982, La Transition entre les Faciès Massifs et Coussinés d'un Ensemble de Coulées Basaltiques, Canton d'Aiguebelle, Québec: Mémoire de Maitrise, Université de Québec à Chicoutimi, QC.

Sappin, A.-A., Houlé, M.G., Lesher, C.M., and McNicoll, V., 2013, Overview of the Mafic and Ultramafic Intrusions in the Eastern Uchi Domain of the Superior Province, Northern Ontario: Ontario Geological Survey, Open File Report 6290, p. 51–51 to 51–16.

Saunders, A.D., Norry, M.J., and Tarney, J., 1991, Fluid influence on the trace element compositions of subduction zone magmas: Philosophical Transactions of the Royal Society London, Series A, v. 335, p. 377–392, http://dx.doi.org/10.1098/rsta.1991.0053.

Sawyer, E.W., and Barnes, S.-J., 1994, Thrusting, magmatic intraplating, and metamorphic core complex development in the Archaean Belleterre-Angliers greenstone belt, Superior Province, Quebec, Canada: Precambrian Research, v. 68, p. 183–200, http://dx.doi.org/10.1016/0301-9268(94)90029-9.

Scarrow, J.H., Molina, J.F., Bea, F., and Montero, P., 2009, Within-plate calc-alkaline rocks: Insights from alkaline mafic magma-peraluminous crustal melt hybrid appinites of the Central Iberian Variscan continental collision: Lithos, v. 110, p. 50–64, http://dx.doi.org/10.1016/j.lithos.2008.12.007.

Schmitz, M.D., Bowring, S.A., de Wit, M.J., and Gartz, V., 2004, Subduction and terrane collision stabilize the western Kaapvaal craton tectosphere 2.9 billion years ago: Earth and Planetary Science Letters, v. 222, p. 363–376, http://dx.doi.org/10.1016/j.epsl.2004.03.036.

Schwerdtner, W.M., 1984, Foliation patterns in large gneiss bodies of the Archaean Wabigoon Subprovince, southern Canadian Shield, *in* Kröner, A., and Zwart, H.J., *eds.,* Precambrian Crustal Evolution: Journal of Geodynamics, v. 1, p. 313–337.

Scoates, J.S., and Scoates, R.F.J., 2013, Age of the Bird River Sill, southeastern Manitoba, Canada, with implications for the secular variation of layered intrusion-hosted stratiform chromite mineralization: Economic Geology, v. 108, p. 895–907, http://dx.doi.org/10.2113/econgeo.108.4.895.

Scott, C.R., Mueller, W.U., and Pilote, P., 2002, Physical volcanology, stratigraphy and lithogeochemistry of an Archean volcanic arc: evolution from plume-related volcanism to arc rifting of SE Abitibi Greenstone Belt, Val d'Or, Canada: Precambrian Research, v. 115, p. 223–260, http://dx.doi.org/10.1016/S0301-9268(02)00011-6.

Sensarma, S., and Palme, H., 2013, Silicate liquid immiscibility in the ~2.5 Ga Fe-rich andesite at the top of the Dongargarh large igneous province (India): Lithos, v. 170–171, p. 239–251, http://dx.doi.org/10.1016/j.lithos.2013.03.004.

Shchipansky, A.A., Samsonov, A.V., Bibikova, E.V., Babarina, I.I., Konilov, A.N., Krylov, K.A., Slabunov, A.I., and Bogina, M.M., 2004, 2.8 Ga boninite-hosting partial suprasubduction zone ophiolite sequences from the North Karelian greenstone belt, NE Baltic Shield, Russia: Developments in Precambrian Geology, v. 13, p. 425–486.

Shegelski, R.J., 1980, Archean cratonization, emergence and red bed development, Lake Shebandowan area, Canada: Precambrian Research, v. 12, p. 331–347, http://dx.doi.org/10.1016/0301-9268(80)90034-0.

Shibuya, T., Tahata, M., Kitajima, K., Ueno, Y., Komiya, T., Yamamoto, S., Igisu, M., Terabayashi, M., Sawaki, Y., Takai, K., Yoshida, N., and Maruyama, S., 2012, Depth variation of carbon and oxygen isotopes of calcites in Archean altered upperoceanic crust: implications for the CO_2 flux from ocean to oceanic crust in the Archean: Earth and Planetary Science Letters, v. 321–322, p. 64–73,

http://dx.doi.org/10.1016/j.epsl.2011.12.034.
Shirey, S.B., and Hanson, G.N., 1986, Mantle heterogeneity and crustal recycling in Archean granite-greenstone belts: Evidence from Nd isotopes and trace elements in the Rainy Lake area, Superior Province, Ontario, Canada: Geochimica et Cosmochimica Acta, v. 50, p. 2631–2651, http://dx.doi.org/10.1016/0016-7037(86)90215-2.
Silver, P.G., and Behn, M.D., 2008, Intermittent plate tectonics?: Science, v. 319, p. 85–88, http://dx.doi.org/10.1126/science.1148397.
Silver, P.G., and Chan, W.W., 1991, Shear wave splitting and subcontinental mantle deformation: Journal of Geophysical Research, v. 96, p. 16429–16454, http://dx.doi.org/10.1029/91JB00899.
Simard, M., Gaboury, D., Daigneault, R., and Mercier-Langevin, P., 2013, Multistage gold mineralization at the Lapa Mine, Abitibi Subprovince: insights into auriferous hydrothermal and metasomatic processes in the Cadillac–Larder Lake fault zone: Mineralium Deposita, v. 48, p. 883–905, http://dx.doi.org/10.1007/s00126-013-0466-3.
Slabunov, A.I., Lobach-Zhuchenko, S.B., Bibikova, E.V., Balagansky, V.V., Sorjonen-Ward, P., Volodichev, O.I., Shchipansky, A.A., Svetov, S.A., Chekulaev, V.P., Arestova, N.A., and Stepanov, V.S., 2006, The Archean of the Baltic Shield: geology, geochronology, and geodynamic settings: Geotectonics, v. 40, p. 409–433, http://dx.doi.org/10.1134/S001685210606001X.
Sleep, N.H., and Windley, B.F., 1982, Archean plate tectonics: Constraints and inferences: The Journal of Geology, v. 90, p. 363–379, http://dx.doi.org/10.1086/628691.
Smith, T.E., and Longstaffe, F.J., 1974, Archean rocks of shoshonitic affinities at Bijou Point, northwestern Ontario: Canadian Journal of Earth Sciences, v. 11, p. 1407–1413, http://dx.doi.org/10.1139/e74-135.
Smithies, R.H., 2002, Archaean boninite-like rocks in an intracratonic setting: Earth and Planetary Science Letters, v. 197, p. 19–34, http://dx.doi.org/10.1016/S0012-821X(02)00464-8.
Smithies, R.H., and Champion, D.C., 1999, Late Archaean felsic alkaline igneous rocks in the Eastern Goldfields, Yilgarn Craton, Western Australia; a result of lower crustal delamination?: Journal of the Geological Society, v. 156, p. 561–576, http://dx.doi.org/10.1144/gsjgs.156.3.0561.
Smithies, R.H., and Champion, D.C., 2000, The Archaean High-Mg diorite suite: Links to Tonalite-Trondhjemite-Granodiorite magmatism and implications for early Archaean crustal growth: Journal of Petrology, v. 41, p. 1653–1671, http://dx.doi.org/10.1093/petrology/41.12.1653.
Smithies, R.H., Champion, D.C., Van Kranendonk, M.J., Howard, H.M., and Hickman, A.H., 2005, Modern-style subduction processes in the Mesoarchaean: Geochemical evidence from the 3.12 Ga Whundo intra-oceanic arc: Earth and Planetary Science Letters, v. 231, p. 221–237, http://dx.doi.org/10.1016/j.epsl.2004.12.026.
Smithies, R.H., Champion, D.C., and Van Kranendonk, M.J., 2007, The oldest well preserved felsic volcanic rocks on Earth: geochemical clues to the early evolution of the Pilbara Supergroup and implications for the growth of a Paleoarchean protocontinent: Developments in Precambrian Geology, v. 15, p. 339–367.
Snyder, D.L., Bleeker, W., Reed, L.E., Ayer, J.A., Houlé, M.G., and Bateman, R., 2008, Tectonic and metallogenic implications of regional seismic profiles in the Timmins Mining Camp: Economic Geology, v. 103, p. 1135–1150, http://dx.doi.org/10.2113/gsecongeo.103.6.1135.
Sproule, R.A., Lesher, C.M., Ayer, J.A., Thurston, P.C., and Herzberg, C.T., 2002, Spatial and temporal variations in the geochemistry of komatiites and komatiitic basalts in the Abitibi Greenstone belt: Precambrian Research, v. 115, p. 153–186, http://dx.doi.org/10.1016/S0301-9268(02)00009-8.
Sproule, R.A., Lesher, C.M., Houlé, M.G., Keays, R.R., Ayer, J.A., and Thurston, P.C., 2005, Chalcophile element geochemistry and metallogenesis of komatiitic rocks in the Abitibi Greenstone Belt, Canada: Economic Geology, v. 100, p. 1169–1190, http://dx.doi.org/10.2113/gsecongeo.100.6.1169.
Stern, R.J., 2005, Evidence from ophiolites, blueschists, and ultrahigh-pressure metamorphic terranes that the modern episode of subduction tectonics began in Neoproterozoic time: Geology, v. 33, p. 557–560, http://dx.doi.org/10.1130/G21365.1.
Stern, R.J., 2008, Modern-style plate tectonics began in Neoproterozoic time: An alternative interpretation of Earth's tectonic history, *in* Condie, K.C., and Pease, C., *eds.,* When Did Plate Tectonics Begin on Planet Earth?: Geological Society of America, Special Papers, v. 440, p. 265–280, http://dx.doi.org/10.1130/2008.2440(13).
Stone, D., 1998, Precambrian Geology of the Berens River area, northwestern Ontario: Ontario Geological Survey, Open File Report 5963, 116 p.
Stone, D., 2005, Geology of the northern Superior area, Ontario: Ontario Geological Survey, Open File Report 6140, 94 p.
Stone, D., 2010, Precambrian Geology of the Central Wabigoon Subprovince area, northwestern Ontario: Ontario Geological Survey, Open File Report 5422, 130 p.
Stone, D., Kamineni, D.C., and Jackson, M.C., 1992, Precambrian Geology of the Atikokan Area, Northwestern Ontario: Geological Survey of Canada, Bulletin 405, 106 p.
Stone, W.E., 1990, Archean volcanism and sedimentation in the Bousquet gold district, Abitibi greenstone belt, Quebec: Implications for stratigraphy and gold concentration: Geological Society of America Bulletin, v. 102, p. 147–158, http://dx.doi.org/10.1130/0016-7606(1990)102<0147:AVASIT>2.3.CO;2.
Stone, W.E., Crocket, J.H., Dickin, A.P., and Fleet, M.E., 1995, Origin of Archean ferropicrites: geochemical constraints from the Boston Creek Flow, Abitibi greenstone belt, Ontario, Canada: Chemical Geology, v. 121, p. 51–71, http://dx.doi.org/10.1016/0009-2541(94)00126-S.
Storey, M., Mahoney, J.J., Kroenke, L.W., and Saunders, A.D., 1991, Are oceanic plateaus sites of komatiite formation?: Geology, v. 19, p. 376–379, http://dx.doi.org/10.1130/0091-7613(1991)019<0376:AOPSOK>2.3.CO;2.
Stott, G., 1986, A structural analysis of the central part of the Archean Shebandowan Greenstone belt and a crescent-shaped granitoid pluton, northwestern Ontario: Unpublished PhD thesis, University of Toronto, Toronto, ON, 285 p.
Stott, G.M., and Corfu, F., 1991, Uchi subprovince, *in* Thurston, P.C., Williams, H.R., Sutcliffe, R.H., and Stott, G.M., *eds.,* Geology of Ontario: Ontario Geological Survey, p. 145–238.
Sun, S.-s. and McDonough, W.F., 1989, Chemical and isotopic systematics of oceanic basalts; implications for mantle composition and processes, *in* Saunders, A.D., and Norry, M.J., *eds.,* Magmatism in the Ocean Basins: Geological Society, London, Special Publications, v. 42, p. 313–345, http://dx.doi.org/10.1144/GSL.SP.1989.042.01.19.
Sun, S.-S., and Nesbitt, R.W., 1978, Petrogenesis of Archaean ultrabasic and basic volcanics: Evidence from rare earth elements: Contributions to Mineralogy and Petrology, v. 65, p. 301–325, http://dx.doi.org/10.1007/BF00375516.
Sun, S.-S., Nesbitt, R.W., and McCulloch, M.T., 1989, Geochemistry and petrogenesis of Archaean and early Proterozoic siliceous high-magnesian basalts, *in* Crawford, A.J., *ed.,* Boninites: University of Tasmania, Hobart, Tasmania, p. 148–173.
Sutcliffe, H.R., Sweeny, J.M., and Edgar, A.D., 1989, The Lac des Iles Complex, Ontario: Petrology and platinum-group-elements mineralization in an Archean mafic intrusion: Canadian Journal of Earth Sciences, v. 26, p. 1408–1427, http://dx.doi.org/10.1139/e89-120.
Sutcliffe, H.R., Barrie, C.T., Burrows, D.R., and Beakhouse, G.P., 1993, Plutonism in the southern Abitibi Subprovince: A tectonic and petrogenetic framework: Economic Geology, v. 88, p. 1359–1375, http://dx.doi.org/10.2113/gsecongeo.88.6.1359.
Svetov, S.A., 2001, Archean high-MgO volcanism in East Fennoscandia (Abstract), *in* Cassidy, K.F., Dunphy, J.M., and Van Kranendonk, M.J., *eds.,* 4th International Archean Symposium Extended Abstracts: Geoscience Australia, p. 199–200.
Svetov, S.A., Huhma, H., Svetova, A.I., and Nazarova, T.N., 2004, The oldest adakites in the Fennoskandian shield: Doklady Akademii Nauk 397, p. 810–814.
Swager, C., Witt, W.K., Griffin, T.J., Ahmat, A.L., Hunter, W.M., McGoldrick, P.J., and Wyche, S., 1990, A Regional Overview of the Late Archaean Granite-Greenstones of the Kalgoorlie Terrane, *in* Ho, S.E., Glover, J.E., Myers, J.S., and Muhling, J.R., *eds.,*Third International Archaean Symposium, Perth 1990 Excursion Guidebook, University of Western Australia, Perth, AU, p. 205–303.
Sylvester, P.J., Harper, G.D., Byerly, G.R., and Thurston, P.C., 1997, Volcanic Aspects, *in* de Wit, M.J., and Ashwal, L.D., *eds.,* Greenstone Belts: Clarendon Press, Oxford, UK, p. 55–90.
Szilas, K., Hoffmann, J.E., Scherstén, A., Kokfelt, T.F., and Münker, C., 2013, Archaean andesite petrogenesis: Insights from the Grædefjord Supracrustal Belt, southern West Greenland: Precambrian Research, v. 236, p. 1–15, http://dx.doi.org/10.1016/j.precamres.2013.07.013.
Taner, M.F., Gault, R.A., and Scott, E.T., 2000, Vanadium mineralization and its industry in Canada: The Gangue 65, p. 1–9.
Tapster, S., Roberts, N.M.W., Petterson, M.G., Saunders, A.D., and Naden, J., 2014, From continent to intra-oceanic arc: Zircon xenocrysts record the crustal evolution of the Solomon island arc: Geology, v. 42, p. 1087–1090, http://dx.doi.org/10.1130/G36033.1.
Tatsumi, Y., 2005, The subduction factory: How it operates in the evolving Earth: GSA Today, v. 15, p. 4–10, http://dx.doi.org/10.1130/1052-5173(2005)015[4:TSFHIO]2.0.CO;2.
Taylor, S.R., and Hallberg, J.A., 1977, Rare-earth elements in the Marda calc-alkaline suite: An Archaean geochemical analogue of Andean type volcanism: Geochimica et Cosmochimica Acta, v. 41, p. 1125–1129, http://dx.doi.org/10.1016/0016-7037(77)90107-7.
Taylor, S.R., and McLennan, S.M., 1985, The continental crust: its composition and evolution: Blackwell Scientific, Oxford, 312 p.
Taylor, W.R., Rock, N.M.S., and Groves, D.I., 1990, The gold-shoshonitic lamprophyre association: new geochemical data and the tectonic context of Archaean lamprophyres from the Yilgarn Block, Western Australia (Abstract): Geological Society of Australia, Abstracts, 28, p. 2.

Terabayashi, M., Masada, Y., and Ozawa, H., 2003, Archean ocean-floor metamorphism in the North Pole area, Pilbara Craton, Western Australia: Precambrian Research, v. 127, p. 167–180, http://dx.doi.org/10.1016/S0301-9268(03)00186-4.

Thomson, J.E., 1946, The Keewatin-Timiskaming unconformity in the Kirkland lake District: Royal Society of Canada, Transactions, IV, p. 113–124.

Thorkelson, D.J., 1996, Subduction of diverging plates and the principles of slab window formation: Tectonophysics, v. 255, p. 47–63, http://dx.doi.org/10.1016/0040-1951(95)00106-9.

Thurston, P., 2012, Archean sedimentary rocks: record of a different world OR Where's the mud (Abstract): Geological Association of Canada–Mineralogical Association of Canada, Annual Meeting St. John's, NL, p. 140.

Thurston, P., Ayer, J.A., Goutier, J., and Hamilton, M.A., 2008, Depositional Gaps in Abitibi Greenstone Belt Stratigraphy: A key to exploration for syngenetic mineralization: Economic Geology, v. 103, p. 1097–1134, http://dx.doi.org/10.2113/gsecongeo.103.6.1097.

Thurston, P., Kamber, B.S., and Whitehouse, M., 2012, Archean cherts in banded iron formation: Insight into Neoarchean ocean chemistry and depositional processes: Precambrian Research, v. 214–215, p. 227–257, http://dx.doi.org/10.1016/j.precamres.2012.04.004.

Thurston, P.C., 1980, Subaerial volcanism in the Archean Uchi-Confederation Volcanic Belt: Precambrian Research, v. 12, p. 79–98, http://dx.doi.org/10.1016/0301-9268(80)90024-8.

Thurston, P.C., 1981, The Volcanology and Trace Element Geochemistry of Cyclical Volcanism in the Archean Confederation lake Area, Northwestern Ontario: Unpublished PhD thesis, University of Western Ontario, London, ON, 553 p.

Thurston, P.C., 1991, Archean Geology of Ontario: Introduction, *in* Thurston, P.C., Williams, H.R. Sutcliffe, R.H., and Stott, G.M., *eds.,* Geology of Ontario: Ontario Geological Survey, p. 73–80.

Thurston, P.C., 2002, Autochthonous development of Superior Province greenstone belts?: Precambrian Research, v. 115, p. 11–36, http://dx.doi.org/10.1016/S0301-9268(02)00004-9.

Thurston, P.C., 2003, The balance between autochthonous and allochthonous development of Superior Province Greenstones (Abstract): GAC–MAC, Annual Meeting Vancouver, BC, Abstracts 28, p. 170.

Thurston, P.C., and Ayres, L.D., 2004, Archaean and Proterozoic greenstone belts: Setting and Evolution, *in* Eriksson, P.G., Altermann, W., Nelson, D.R., Mueller, W., and Catuneanu, O., *eds.,* The Precambrian Earth: Tempos and Events: Elsevier, Amsterdam, p. 311–333.

Thurston, P.C., and Breaks, F.W., 1978, Metamorphic and tectonic evolution of the Uchi–English River Subprovince: Geological Survey of Canada, Paper 78-10, p. 49–62.

Thurston, P.C., and Carter, M.W., 1970, Operation Fort Hope: Ontario Division of Mines, Toronto, ON, 60 p.

Thurston, P.C., and Chivers, K.M., 1990, Secular variation in greenstone sequence development emphasizing Superior Province, Canada: Precambrian Research, v. 46, p. 21–58, http://dx.doi.org/10.1016/0301-9268(90)90065-X.

Thurston, P.C., and Fryer, B.J., 1983, The geochemistry of repetitive cyclical volcanism from basalt through rhyolite in the Uchi-Confederation greenstone belt, Canada: Contributions to Mineralogy and Petrology, v. 83, p. 204–226, http://dx.doi.org/10.1007/BF00371189.

Thurston, P.C., and Kozhevnikov, V.N., 2000, An Archean quartz arenite-andesite association in the eastern Baltic Shield, Russia: implications for assemblage types and shield history: Precambrian Research, v. 101, p. 313–340, http://dx.doi.org/10.1016/S0301-9268(99)00093-5.

Thurston, P.C., and Sutcliffe, R.H., 1986, The Archean crust as a density filter (Abstract): Geological Association of Canada–Mineralogical Association of Canada–Canadian Geophysical Union Abstracts, Joint Annual Meeting 11, p. 136.

Thurston, P.C., Ayres, L.D., Edwards, G.R., Gélinas, L., Ludden, J.N., and Verpaelst, P., 1985, Archean bimodal volcanism: Geological Association of Canada, Special Paper 28, p. 7–21.

Thurston, P.C., Osmani, I.A., and Stone, D., 1991, Northwestern Superior Province: review and terrane analysis, *in* Thurston, P.C., Williams, H.R., Sutcliffe, R.H., and Stott, G.M., *eds.,* Geology of Ontario: Ontario Geological Survey, p. 81–142.

Tipper, H.W., Woodsworth, G.J., and Gabrielse, H., 1981, Tectonic assemblage map of the Canadian Cordillera: Geological Survey of Canada, Map 1505A, scale: 1:2,000,000.

Tomlinson, K.Y., Hall, R.P., Hughes, D.J., and Thurston, P.C., 1996, Geochemistry and assemblage accretion of metavolcanic rocks in the Beardmore-Geraldton greenstone belt, Superior Province: Canadian Journal of Earth Sciences, v. 33, p. 1520–1533, http:dx.doi.org/10.1139/e96-115.

Tomlinson, K.Y., Davis, D.W., Stone, D., and Hart, T.R., 2003, U–Pb age and Nd isotopic evidence for Archean terrane development and crustal recycling in the south-central Wabigoon subprovince, Canada: Contributions to Mineralogy and Petrology, v. 144, p. 684–702, http://dx.doi.org/10.1007/s00410-002-0423-0.

Tormanen, T., and Karinen, T., 2011, Chrome and PGE deposits associated with the 2.45 Ga layered intrusions of northern Finland: Excursion Guide, 24 August 2011, Vuorimiesyhdistys, Outokumpu, Finland.

Ujike, O., Goodwin, A.M., and Shibata, T., 2007, Geochemistry and origin of Archean volcanic rocks from the Upper Keewatin assemblage (*ca* 2.7 Ga), Lake of the Woods Greenstone Belt, Western Wabigoon Subprovince, Superior Province, Canada: Island Arc, v. 16, p. 191–208, http://dx.doi.org/10.1111/j.1440-1738.2007.00566.x.

van der Velden, A.J., and Cook, F.A., 2005, Relict subduction zones in Canada: Journal of Geophysical Research, v. 110, B08403, http://dx.doi.org/10.1029/2004JB003333.

Van Kranendonk, M.J., 2000, Geology of the North Shaw 1:100,000 Sheet, Geological Survey of Western Australia, 86 p.

Van Kranendonk, M.J., 2012, A chronostratigraphic Division of the Precambrian: Possibilities and Challenges, *in*: Gradstein, F.M., Ogg, J.G., Schmitz, M.D., and Ogg, G.M., *eds.,* The Geologic Time Scale 2012. Vol. 1, p. 299–392.

Van Kranendonk, M.J., Hickman, A.H., Smithies, R.H., and Nelson, D.R., 2002, Geology and tectonic evolution of the Archean North Pilbara Terrain, Pilbara Craton, Western Australia: Economic Geology, v. 97, p. 695–732.

Van Kranendonk, M.J., Collins, W.J., Hickman, A.H., and Pawley, M.J., 2004, Critical tests of vertical *vs.* horizontal tectonic models for the Archaean East Pilbara Granite-Greenstone Terrane, Pilbara Craton, Western Australia: Precambrian Research, v. 131, p. 173–211, http://dx.doi.org/10.1016/j.precamres.2003.12.015.

Van Kranendonk, M.J., Smithies, R.H., Hickman, A.H., and Champion, D.C., 2007a, Paleoarchean development of a continental nucleus: the East Pilbara Terrane of the Pilbara Craton, Western Australia: Developments in Precambrian Geology, v. 15, p. 307–337.

Van Kranendonk, M.J., Smithies, R.H., Hickman, A.H., and Champion, D.C., 2007b, Review: secular tectonic evolution of Archean continental crust: interplay between horizontal and vertical processes in the formation of the Pilbara Craton, Australia: Terra Nova, v. 19, p. 1–38, http://dx.doi.org/10.1111/j.1365-3121.2006.00723.x.

Van Kranendonk, M.J., Ivanic, T.J., Wingate, M.T.D., Kirkland, C.L., and Wyche, S., 2013, Long-lived, autochthonous development of the Archean Murchison domain, and implications for Yilgarn craton tectonics: Precambrian Research, v. 229, p. 49–92, http://dx.doi.org/10.1016/j.precamres.2012.08.009.

Vervoort, J.D., White, W.M., and Thorpe, R.I., 1994, Nd and Pb isotope ratios of the Abitibi greenstone belt: new evidence for very early differentiation of the Earth: Earth and Planetary Science Letters, v. 128, p. 215–229, http://dx.doi.org/10.1016/0012-821X(94)90146-5.

Wang, Z., Wilde, S.A., Wang, K., and Yu, L., 2004, A MORB-arc basalt–adakite association in the 2.5 Ga Wutai greenstone belt: late Archean magmatism and crustal growth in the North China Craton: Precambrian Research, v. 131, p. 323–343, http://dx.doi.org/10.1016/j.precamres.2003.12.014 .

Whalen, J.B., Percival, J.A., McNicoll, V.J., and Longstaffe, F.J., 2004, Geochemical and isotopic (Nd–O) evidence bearing on the origin of late- to post-orogenic high-K granitoid rocks in the Western Superior Province: Implications for late Archean tectonomagmatic processes: Precambrian Research, v. 132, p. 303–326, http://dx.doi.org/10.1016/j.precamres.2003.11.007.

White, D., Musacchio, G., Helmstaedt, H., Harrap, R., Thomson, C., Sol, S., and Thurston, P.C., 2001, Remnants of Archean Subduction in the Western Superior Province: Results from combined LITHOPROBE Deep Seismic Studies (Abstract): Lithoprobe Superior Transect, Abstracts.

White, D.J., Musacchio, G., Helmstaedt, H.H., Harrap, R.M., Thurston, P.C., van der Velden, A., and Hall, K., 2003, Images of a lower-crustal oceanic slab: Direct evidence for tectonic accretion in the Archean Western Superior Province: Geology, v. 31, p. 997–1000, http://dx.doi.org/10.1130/G20014.1.

Whittaker, P.J., 1986, Chromite deposits in Ontario: Ontario Geological Survey, Resources, Toronto, ON.

Wilks, M.E., and Nisbet, E.G., 1988, Stratigraphy of the Steep Rock Group, northwest Ontario: a major Archaean unconformity and Archaean stromatolites: Canadian Journal of Earth Science, v. 25, p. 370–391, http://dx.doi.org/10.1139/e88-040.

Willbold, M., Hegner, E., Stracke, A., and Rocholl, A., 2009, Continental geochemical signatures in dacites from Iceland and implications for models of early Archaean crust formation: Earth and Planetary Science Letters, v. 279, p. 44–52, http://dx.doi.org/10.1016/j.epsl.2008.12.029.

Williams, H.R., 1991, Quetico Subprovince: Ontario Geological Survey, Special Volume 4, p. 383–403.

Williams, H.R., Stott, G.M., and Thurston, P.C., 1992, Tectonic evolution of Ontario: summary and synthesis. Part 1: Revolution in the Superior Province, *in* Thurston, P.C., Williams, H.R., Sutcliffe, R.H., and Stott, G.M., *eds.,* Geology of Ontario: Geological Survey of Ontario, p. 1255–1294.

Wilson, A.H., 2002, Early Archaean highly-depleted ultramafic boninitic lavas in the

southern Kaapvaal Craton, South Africa (Abstract): Geochimica et Cosmochimica Acta, Abstracts of the 12th annual Goldschmidt Conference, v. 66, p. 839.

Windley, B.F., and Garde, A.A., 2009, Arc-generated blocks with crustal sections in the North Atlantic Craton of West Greenland; crustal growth in the Archean with modern analogues: Earth-Science Reviews, v. 93, p. 1–30, http://dx.doi.org/10.1016/j.earscirev.2008.12.001.

Winter, J.D., 2001, An Introduction to igneous and Metamorphic Petrology: Prentice Hall, Upper Saddle River, NJ, 697 p.

Wray, N., 2014, Evidence for a younger Porcupine age komatiitic volcanism in the Abitibi greenstone belt, Ontario: Unpublished BSc thesis, Laurentian University, Sudbury, ON, 45 p.

Wyman, D., and Hollings, P., 1998, Long-lived mantle-plume influence on an Archean protocontinent; geochemical evidence from the 3 Ga Lumby Lake greenstone belt, Ontario, Canada: Geology, v. 26, p. 719–722, http://dx.doi.org/10.1130/0091-7613(1998)026<0719:LLMPIO>2.3.CO;2.

Wyman, D., and Kerrich, R., 1989, Archean shoshonitic lamprophyres associated with Superior Province gold deposits, distribution, tectonic setting, noble metal abundances, and significance for gold mineralization: Economic Geology Monographs, v. 6, p. 651–667.

Wyman, D., and Kerrich, R., 2009, Plume and arc magmatism in the Abitibi Subprovince: implications for the origin of Archean continental lithospheric mantle: Precambrian Research, v. 168, p. 4–22, http://dx.doi.org/10.1016/j.precamres.2008.07.008.

Wyman, D.A., and Kerrich, R., 2012, Geochemical and isotopic characteristics of Youanmi terrane volcanism: The role of mantle plumes and subduction tectonics in the western Yilgarn Craton: Australian Journal of Earth Sciences, v. 59, p. 671–694, http://dx.doi.org/10.1080/08120099.2012.702684.

Wyman, D.A., Ayer, J.A., and Devaney, J.R., 2000, Niobium-enriched basalts from the Wabigoon Subprovince, Canada: evidence for adakitic metasomatism above an Archean subduction zone: Earth and Planetary Science Letters, v. 179, p. 21–30, http://dx.doi.org/10.1016/S0012-821X(00)00106-0.

Wyman, D.A., Kerrich, R., and Polat, A., 2002, Assembly of Archean cratonic mantle lithosphere and crust; plume-arc interaction in the Abitibi-Wawa subduction-accretion complex: Precambrian Research, v. 115, p. 37–62, http://dx.doi.org/10.1016/S0301-9268(02)00005-0.

Wyman, D.A., Hollings, P., and Biczok, J., 2011, Crustal evolution in a cratonic nucleus: Granitoids and felsic volcanic rocks of the North Caribou Terrane, Superior Province Canada: Lithos, v. 123, p. 37–49, http://dx.doi.org/10.1016/j.lithos.2010.07.025.

Xie, Q., Kerrich, R., and Fan, J., 1993, HFSE/REE fractionations recorded in three komatiite-basalt sequences, Archean Abitibi greenstone belt: Implications for multiple plume sources and depths: Geochimica et Cosmochimica Acta, v. 57, p. 4111–4118, http://dx.doi.org/10.1016/0016-7037(93)90357-3.

Yogodzinski, G.M., Kay, R.W., Volynets, O.N., Koloskov, A.V., and Kay, S.M., 1995, Magnesian andesite in the western Aleutian Komandorsky region: Implications for slab melting and processes in the mantle wedge: Geological Society of America Bulletin, v. 107, p. 505–519, http://dx.doi.org/10.1130/0016-7606(1995)107<0505:MAITWA>2.3.CO;2.

Zegers, T.E., White, S.H., de Keijzer, M., and Dirks, P., 1996, Extensional structures during deposition of the 3460 Ma Warrawoona Group in the eastern Pilbara Craton, Western Australia: Precambrian Research, v. 80, p. 89–105, http://dx.doi.org/10.1016/S0301-9268(96)00007-1.

Zhai, M., Zhao, G., and Zhang, Q., 2002, Is the Dongwanzi complex an Archean ophiolite?: Science, v. 295, p. 923a, http://dx.doi.org/10.1126/science.295.5557.923a.

Received August 2014
Accepted as revised May 2015

REVIEW

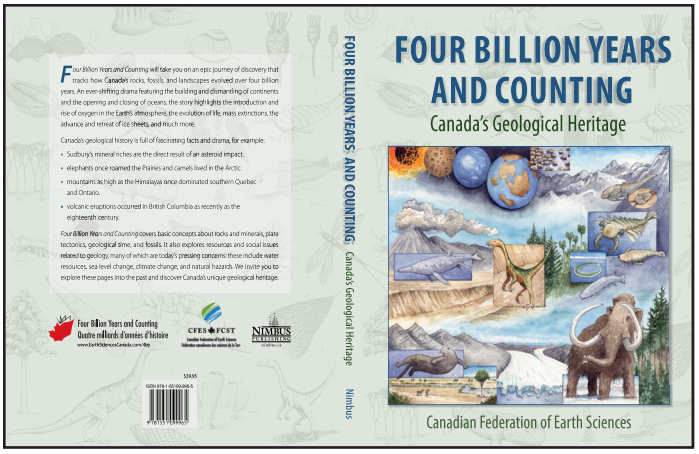

Four Billion Years and Counting: Canada's Geological Heritage[1]

Robert Fensome, Graham Williams, Aïcha Achab, John Clague, David Corrigan, Jim Monger, and Godfrey Nowlan (*editors*)

Co-publishers: Nimbus Publishing and the Canadian Federation of Earth Sciences (CFES)
Website: www.fbycbook.com
Published: 2014; 402 p.
Orders online: $39.95 (CND); Softcover
Discounts for bulk purchases, and GAC member discount through the GAC Bookstore

Reviewed by Brian J. Skinner
Yale University
Department of Geology and Geophysics
New Haven, Connecticut, 06520, USA
E-mail: brian.skinner@yale.edu

A hundred authors crafted this delightful volume. It is one of Canada's contributions to the United Nations-initiated 2008 program, *The Year of Planet Earth*. One might wonder how the editors managed to smooth the inevitable prose bumps with such a large authorship, but they have done so very effectively. The book reads smoothly and engagingly. And what a topic they discuss—the geology of one of Earth's most geologically diverse and intriguing land masses.

To fully appreciate geology some background scientific introduction is needed. The first section of the book, "Foundations," provides the necessary introduction in a succinct, four-chapter treatment of physical geology, how surface and subsurface maps are prepared, and the importance of fossils in understanding Earth's history. The second section, "The Evolution of Canada" is a six-chapter discussion of the formation and growth of Canada as a continental land mass and the life forms that have been its inhabitants through time. The final section, "Wealth and Health" is a ten-chapter introduction to the economic and social issues that both support and challenge the human population that inhabits Canada today.

The great ice sheets that covered Canada in recent geological times have exposed a wealth of evidence by clearing and polishing ancient rock surfaces. Our understanding of the geological evolution of Earth rests heavily on glacially exposed evidence from Canada. For example, how and when the cratons in the cores of today's continents were assembled is best understood from Canadian evidence. And much of our knowledge of the diversity and uniqueness of the earliest forms of macroscopic life comes from evidence discovered in Canadian rocks. These stories and many more are related in "The Evolution of Canada." I particularly like the human touches added through vignettes of early Canadian scientists, and stories of discovery by those who first saw and realized the importance of the evidence in Canadian rocks. One story concerns Stanley Tyler. As a graduate student, I happened to be at the 1953 Geological Society of America meeting in Boston when Tyler presented his evidence of possible microscopic fossils in the 1.9 billion year old Gunflint Formation from Ontario. He created quite a buzz, though no one knew just how important his epochal discovery really was. The discoveries by pioneers such as Billings, Logan, the Dawsons, Coleman and many others make clear just how important the roles played by Canadian scientists have been in the development of geology as a science.

For the past 150 years, Canada has played a world-leading role in the discovery and exploitation of natural resources, particularly gold, ferrous and non-ferrous metals, coal, petroleum, fertilizers, and most recently, diamonds. The resource story is succinctly related in Chapter 13. The final short chapters of this engrossing volume cover topics that are all too often overlooked in geological discussions. Chapter 14, "Building Canada" discusses the stones with which dwellings and many iconic public buildings in the older cities are constructed. Chapter 15 covers Canada's abundant water supplies, and Chapter 16,

[1] "Four Billion Years and Counting" is a project of the Canadian Federation of Earth Sciences (CFES). The book's website (www.fbycbook.com) provides information not only about the project, but also about the authors, organizers and sponsors. For those interested in the potential of the book for education and outreach, many figures, maps and photographs are available for direct download for such use, as long as the sources are duly acknowledged. The book is also available in French, and is entitled "Quatre milliards d'année's d'histoire."

"At the Beach," discusses shoreline erosion, the tides, and the effects of rising sea level. Chapter 17 concerns a topic that is becoming increasingly important as the population density increases—natural hazards and natural disasters, such as floods, landslides, tsunamis, and even meteorite impacts. Chapter 18 addresses the environmental challenges facing Canada's growing population as it moves from a rural base to an urban base—another issue concerned with population density. Chapter 19 concerns a topic that has only recently demanded attention of the geological community, though it has always been there—geology and health—which is discussed in "Toxins in the Rocks."

The final chapter of this ambitious volume is titled "Canada's Geological Heritage." It is a tightly written summary of the key steps along the way as separate fragments of crust aggregated to form the proto-continent Laurentia, the subsequent history of Laurentia, and the final steps in the assembly of North America and Canada's importance in unravelling the story.

The authors are all geologists and experts in their respective areas of expertise. They clearly had a diverse readership in mind as they wrote their chapters and they have been very successful. This is a volume that, once opened, is difficult to put down—it is a pleasure to read and beautifully illustrated with clearly drawn maps and striking photos. The writing is smooth and always clear and balanced. Short of a continent-wide field trip to actually see all the evidence, I can't imagine a better way to introduce a Canadian citizen to the geology of his or her fascinating country.

EDUCATION MATTERS

The Teachers' Mining Tour in Ontario – A Professional Development Program for Educators

Lesley Hymers[1], Bill Steer[2], and Janice Williams[3]

[1]Ontario Mining Association
5775 Yonge Street, Toronto
Ontario, M2M 4J1, Canada
Email:lhymers@oma.on.ca

[2]Canadian Ecology Centre
6905 Ontario 17, Mattawa
Ontario, P0H 1V0, Canada

[3]Mining Matters
904-1200 Eglinton Avenue East
Toronto, Ontario, M3C 1H9, Canada

SUMMARY

The Teachers' Mining Tour is a professional development program for educators hosted at the Canadian Ecology Centre (CEC) located near Mattawa, Ontario. Each year in late summer for three years (2010–2012) approximately thirty Ontario teachers participated in a five day program that included presentations by mineral industry professionals, site visits to mines and mine manufacturing operations, and educational resource workshops. In 2013, to meet demand, the Tour program was expanded to include two tours, annually.

The goal of the Tour is to provide teachers with the information and resources that they need to become more proficient Earth Science teachers and to educate their students about the mining industry and, through this increased knowledge and experience, to encourage their students to pursue post-secondary education and careers in Earth Sciences and mining-related disciplines. Additional objectives are to create and cultivate a network of teachers using mining as a theme in their classrooms, and to promote informed opinions amongst participants with regard to the economic, social and environmental aspects of mining. The Tour content focuses on modern mining techniques and technology, environmental responsibility, workplace safety, and mining careers.

Tours consistently receive favourable reviews from teachers, industry participants and representatives from sponsor organizations. In addition to the feedback sought through evaluation forms at the conclusion of each Tour program, additional feedback is sought from participants in the following spring of each academic year. A formal survey is circulated, providing teachers with the opportunity to report back about how their Tour experience is influencing their teaching. Respondents report that they are satisfied with the information and resources that they received during the Tour, that the program is directly applicable to the subjects that they are teaching, and that their perceptions about mining changed because of their experience.

RÉSUMÉ

Le *Teachers' Mining Tour* est un programme de formation pour enseignants qui se tient au Centre écologique du Canada (CEC) situé à Mattawa, Ontario. Chaque année à la fin de l'été depuis trois ans (2010–2012) une trentaine d'enseignants d'Ontario ont participé à ce programme de cinq jours de présentations par des professionnels de l'industrie minérale, de visites de sites miniers et d'usines de transformation, et d'ateliers sur les moyens éducatifs. En 2013, pour répondre à la demande, le programme du *Tour* a été porté à deux sessions par année.

L'objectif de ce *Tour* est de fournir aux enseignants les informations et les moyens éducatifs requis pour devenir des enseignants en sciences de la Terre mieux qualifiés pour instruire leurs élèves sur la réalité de l'industrie minière et, par là, d'encourager leurs élèves à poursuivre une formation postsec-

ondaire et opter pour des carrières en sciences de Terre ou dans les disciplines de l'industrie minière. Ce programme vise aussi d'autres objectifs dont ceux de créer et promouvoir un réseau d'enseignants qui utilisent le thème minier dans leur enseignement, et faire en sorte que les participants en ressortent avec des opinions mieux éclairés sur les aspects économiques, sociaux et environnementaux de l'exploitation minière. Le contenu du *Tour* porte surtout sur les processus et la technologie de l'exploitation minière moderne, l'éco-responsabilité, la sécurité du milieu de travail et les opportunités de carrière dans l'industrie minière.

Ce programme d'activités est systématiquement louangé par les enseignants, les participants d'industrie et les représentants des organismes de parrainage. Le niveau de satisfaction est établi par l'administration de formulaires d'évaluation à la fin de chaque session du programme d'activités, et par les réactions colligées auprès des participants au printemps suivant l'année scolaire. Un sondage formel est soumis aux enseignants dans le but d'évaluer l'impact des activités du *Tour* sur leur enseignement. Les répondants se disent satisfaits des informations reçues et des moyens éducatifs enseignés pendant le *Tour*, confirment que le programme d'activités est directement applicable aux sujets qu'ils enseignent, et que leurs perceptions de l'exploitation minière en ont été changées.

Traduit par le Traducteur

INTRODUCTION

The Canadian Earth Science education and outreach community, and the mining industry share a collective concern with regard to the limited number of students choosing to pursue post-secondary education in Earth Science or mining-related disciplines. These groups have been working separately and collectively toward addressing this concern. One approach is to provide instructional development opportunities to educators so that they are able to teach about Earth Science or the mining industry more effectively, or integrate these themes into other subject areas. The Teachers' Mining Tour in Ontario, a professional development program for educators, is an example of such an opportunity.

The Tour is hosted at the Canadian Ecology Centre (CEC), a non-profit environmental science education facility located in Samuel De Champlain Provincial Park, near Mattawa, Ontario. The Centre provides environmental education to elementary, secondary and post-secondary students and the public, and delivers professional development programs to teachers.

BACKGROUND

Acknowledging the shift in the natural resources sector from forestry toward mining, the CEC became interested in developing and delivering a professional development program for teachers around mining sector themes. The program was modeled after the successful Canadian Institute of Forestry Teachers' Tour that had been delivered by the CEC for many years. Sponsors were approached and in-kind contributions were received, and the proposal was approved. For three years (2010–2012) approximately thirty Ontario teachers participated in a five day program during late summer. The program included presentations by mineral industry professionals, site visits to mines and mine manufacturing operations, and educational resource workshops. The Tour program expanded to include two Tours annually from 2013, reflecting increased demand.

The goal of the Tour is to expose teachers to mining and to provide them with additional information and resources that help them to become more proficient Earth Science teachers. The knowledge and experience gained are passed on to students, encouraging them to pursue post-secondary education and careers in Earth Sciences and mining. Additional objectives are to provide teachers with the opportunity to learn about modern mining, to emphasize the roles that environmental stewardship, sustainability and occupational health and safety play in the sector, and to inform about the wide variety of careers that the sector provides.

The Tour is fully sponsored and available at no cost to teachers. Sponsors include the Ontario Mining Association (OMA), the Canadian Institute of Mining & Metallurgy, Gateway and Sudbury Chapters, and EdGEO. Many OMA member companies contribute content to the Tour, provide access to their operations, and also encourage participation by their professional staff.

TOUR ITINERARY

Since the inception of the Tour, the CEC has worked collectively with sponsors and industry representatives to develop the Tour education program. Although the content varies from year to year, the core theme remains the same: providing educators with the opportunity to learn about mining by participating in a variety of activities including discussions, site visits and hands-on learning. The Tour content and schedules have changed in response to evaluations by participating teachers and comments from other participants and sponsors. An overnight camping trip was added to the program in 2011 and, in 2013, responding to demand and interest from sponsors, the program was expanded to include two annual Tours. Participation was also expanded, making the second Tour available to teachers from across Canada. The content of each Tour differs but includes some common elements. The first Tour continues to focus on operators, mines and manufactures in the Sudbury and North Bay areas, whereas the second Tour focuses on operations in the Timmins area.

Opening Day

The opening day of the program for both Tours starts in the late afternoon at the CEC. It includes an introduction to the facility, the staff and Tour participants, followed by presentations from industry and sponsoring organization representatives which focus on setting the groundwork and context for the Tour. The next two days of the Tour program involve field trips to the Sudbury or Timmins areas.

Sudbury Field Trip

First Day

Morning site visits hosted by Vale include presentations, followed by visits to the Copper Cliff smelter and refinery (Fig. 1). The afternoon has included: a site visit to a small-scale dimension stone operation at the McLaren's Bay Mica Stone Quarry; a geological excursion around the Sudbury Basin, facilitated by the Ministry of Northern Development and Mines, for the purpose of setting the geological context for the

Figure 1. Sudbury reclamation tour in Copper Cliff.

Tour; and an excursion facilitated by Laurentian University professors and members of VETAC, the Vegetation Enhancement Technical Advisory Committee. VETAC is an organization whose focus is the Sudbury Re-greening Program, and this excursion includes visits to sites of historical importance and research re-vegetation plots. In 2014, a site visit to Dynamic Earth, a Sudbury science centre, was added to the program. There, teachers toured mining and geology exhibits and met with a geologist to discuss the formation of the Sudbury Basin and the Sudbury mining camp. Teachers were also provided with an opportunity to learn about the Centre's Education Programming, including school visits and outreach programs, and the role that a science centre can play in support of their teaching. The first day concludes with an overnight camp at Windy Lake Provincial Park.

Second Day

The morning involves a site visit to Glencore's Nickel Rim South Mine (Fig. 2), the most modern mine in the Sudbury Basin, and includes both surface and underground visits. Before returning to the CEC for the evening, the afternoon is spent with a Prospector and Industrial Mineral Consultant at a North Bay sand and gravel pit, where teachers 'stake a claim' and learn about the role government regulations play in mineral resource development.

Timmins Field Trip

First Day

Site visits on the way to Timmins have included stops in New Liskeard, Cobalt and Haileybury, and are followed by a detailed regional geological excursion in the vicinity of Timmins (Fig. 3). The day is capped off with an overnight camp at Kettle Lakes Provincial Park.

Second Day

Site visits include an underground visit to Goldcorp's Dome Mine and a tour of their Coniaurum and Hollinger tailings reclamation sites. The evening of the third day involves travel back to the Canadian Ecology Centre.

Final Two Days

For both Tours, the final full day of the program features hands-on learning training workshops using "Deeper and

Figure 2. Timmins area geology tour.

Figure 3. Going underground at the Nickel Rim South Mine.

Figure 4. Teachers participating in an EdGEO workshop at the Canadian Ecology Centre, 2013.

Deeper" and "Discovering Diamonds" resources (from 'Mining Matters'), and "Bringing Earth Science to Life" and "Putting the Earth into Science" resources (from EdGEO) (Fig. 4). Site visits to North Bay mining manufacturers, includ-

ing Redpath, Cementation, Boart Longyear and Atlas Copco, and a geologically-themed canoe trip on the Mattawa River, a Canadian Heritage River, are also included. Presentations by a non-governmental organization, an environmental scientist or another representative who has worked in aboriginal engagement in the sector also form part of the program.

The final half day of the program is held at the CEC and focuses on the mineral resource development cycle, careers in mining, and innovation in exploration and development. Each of these topics is highlighted by presentations and opportunities for discussion. For example, in 2011 teachers participated in a focus group for the purpose of gathering feedback about education, and outreach resources and needs.

EVALUATIONS

Comprehensive feedback is sought from program participants immediately following the conclusion of each Tour. Teachers are asked to complete detailed evaluation forms that seek feedback about whether the Tour met their expectations, which components of the program they most enjoyed, what new perceptions they gained, how they will use the knowledge that they acquired, and how the Tour could be improved, adapted, or changed to enhance their experience. Opinions are also sought about the specific sites and speakers included in the program. The majority of participants reported that Tours exceeded their expectations and that they provide a thorough introduction to the mining sector. The comments included in evaluations influence the future content of Tour programs.

Follow-up Surveys

Tour sponsors and facilitators became interested in collecting additional feedback from teachers. Of particular interest was to ascertain if teachers were using what they had learned during their Tour in their classrooms, and how. Were they staying connected to the network of teachers and colleagues that they had met on the Tour? As a means of gathering this feedback a comprehensive follow-up survey was designed to be sent out, electronically, in the Spring following the year in which a teacher participated in a Tour. The first survey was issued in Spring 2011 to teachers who had participated in the inaugural Tour program. This survey was revised and expanded and forwarded to teachers who had participated in subsequent Tours. In 2012, a second follow-up survey was forwarded to the 2010 Tour participants. As with the evaluation forms distributed at the conclusion of Tours, the survey feedback would be used to influence the content of future Tours. The surveys consisted of 12–15 questions designed to gather feedback from respondents with regard to several criteria, including:

1) The grade level they are currently teaching;
2) The applicability of the Tour curriculum to their teaching;
3) Their level of satisfaction with the Tour information and resources;
4) Whether or not they have shared their Tour experience, information and resources, including videos and photos with colleagues and/or administration;
5) How their opinion of modern mining had changed because of what they learned on the Tour; and
6) Their greatest change in perception.

Results

The response rates of teachers to the 2010–2013 follow-up surveys were 50%, 36%, 16% and 18%, respectively. The second follow-up survey issued to the 2010 teachers in 2012 had a very low response rate and therefore was not representative and results are not included here. Although the 2012 and 2013 response rates were low, they are included in this discussion because they reflect existing trends. Taking into consideration the trend in response rate, the decision was taken not to proceed with collection in 2014.

Responses received indicate that although Tour participants teach in many levels of the education system most of the participants to date have been secondary school teachers (Table 1). Outdoor education, science outreach education, and teacher professional development instructors have also been participants. At the time of each survey, the majority of teachers who responded indicated that the Tour content directly applied to subject areas that they were currently teaching including: Geography, Canadian and World Studies, Environmental Science, Rocks and Minerals, and Biodiversity and Natural Resources.

Table 1. Teaching level of participants.

Year	2010	2011	2012	2013
Total Number of Respondents	14	14	5*	13*
Elementary	3	1	1	4
Middle	2	0	1	2
Secondary	7	8	3	9
Alternative	0	1	0	1
Other	2	4	1	1

* respondent teaches more than one level of education

When asked whether aspects of Tour content were directly applicable to their classrooms, Teachers' responses ranked 'Mining Matters' resources as the most applicable, followed by educational resources from other organizations like the Ontario Mining Association, the information shared by guest speakers and via presentations, and the experiences of mine and reclamation site visits, respectively (Table 2).

Table 2. Tour content that was found to be directly applicable to the classroom.

Year	2010	2011	2012	2013
Total Number of Respondents	14*	14*	5	13*
Speakers and Presentations	4	5	1	4
Site Visits	2	4	0	3
Mining Matters Resources	6	12	3	10
Other Resources	3	6	1	4

*multiple aspects applied to the classroom

Teachers ranked their greatest change in perception about mining as better understanding the role that environmental stewardship and sustainability play in the industry, followed by occupational health and safety, the role that mining plays in

their daily lives, and the variety of careers available in the sector (Table 3). Overall, teachers were satisfied with the information and resources they received on the Tour, most have shared their Tour experience, information and resources with their colleagues and administration, and most continued to network with the other teachers and tour participants

Table 3. Teachers' greatest change in perception about mining at the conclusion of Tours.

Year	2010	2011	2012	2013
Total Number of Respondents	14	14	5	13
Environmental Stewardship and Sustainability	8	4	3	6
Occupational Health and Safety	4	3	0	1
Mining Industry Careers	0	2	0	4
Mining in Our Daily Lives	2	5	2	2

CONCLUSIONS

The Teachers' Mining Tour provides teachers with the opportunity to learn about all aspects of the mineral resources development cycle, from prospecting to reclamation. The Tour experience provides education about the geology of important mining regions in Ontario, and allows participants to tour operating and reclaimed mine sites and mine manufacturing facilities. Teachers are familiarized with the variety of careers available in the sector and with Earth Science teaching resources for use in the classroom. Follow-up survey results indicate that into the academic year, teachers in a variety of educational settings continue to benefit from their participation in the Teachers' Mining Tour. Teachers indicate that they continue to find what they learned during the Tour to be an asset in the classroom. This is not only an excellent outcome for teachers and their students but a meaningful endorsement of the program for sponsors, industry participants and facilitators.

Corporate Members

Platinum

Memorial University

Gold

Anglo American Exploration (Canada) Ltd.
Newfoundland and Labrador Department of Natural Resources
Northwest Territories Geological Survey

Silver

British Columbia Geological Survey
IBK Capital Corp.
Royal Tyrrell Museum of Palaeontology
Yukon Geological Survey

Nickel

Acadia University

GEOLOGICAL ASSOCIATION OF CANADA (2015-2016)

OFFICERS

President
Victoria Yehl
Vice-President
Graham Young
Past President
Brian Pratt
Secretary-Treasurer
James Conliffe

COUNCILLORS

Alwynne Beaudoin
Oliver Bonham
James Conliffe
David Corrigan
Lori Kennedy
Andy Kerr
Brad McKinley
David Pattison
Sally Pehrsson
Brian Pratt
Dène Tarkyth
Chris White
Victoria Yehl
Graham Young

STANDING COMMITTEES

Communications: TBA
Finance: Dène Tarkyth
Publications: Chris White
Science Program: David Corrigan

GEOSCIENCE CANADA

JOURNAL OF THE GEOLOGICAL ASSOCIATION OF CANADA
JOURNAL DE L'ASSOCIATION GÉOLOGIQUE DU CANADA

Column **373**
The Tooth of Time: J. O. Wheeler
P.F. Hoffman

Andrew Hynes Series: Tectonic Processes **383**
Tectonic Consequences of a Uniformly Hot Backarc and Why is the Cordilleran Mountain Belt High?
R.D. Hyndman

Post-peak Evolution of the Muskoka Domain, Western Grenville Province: Ductile Detachment Zone in a Crustal-scale Metamorphic Core Complex **403**
T. Rivers and W. Schwerdtner

Series **437**
Igneous Rock Associations 19.
Greenstone Belts and Granite−Greenstone Terranes: Constraints on the Nature of the Archean World
P.C. Thurston

Review **485**
Four Billion Years and Counting: Canada's Geological Heritage
B.J. Skinner

Education Matters **487**
The Teachers' Mining Tour in Ontario – A Professional Development Program for Educators
L. Hymers, B. Steer, and J. Williams

2015 VOLUME 42 GSCNA7 42 373-492
PRINT EDITION ISSN 0315-0941
ONLINE EDITION ISSN 1911-4850